ISSN: 1715-9997
Vol. 4, No. 2, June 2010

Canadian Journal of pure & applied sciences

an International Journal

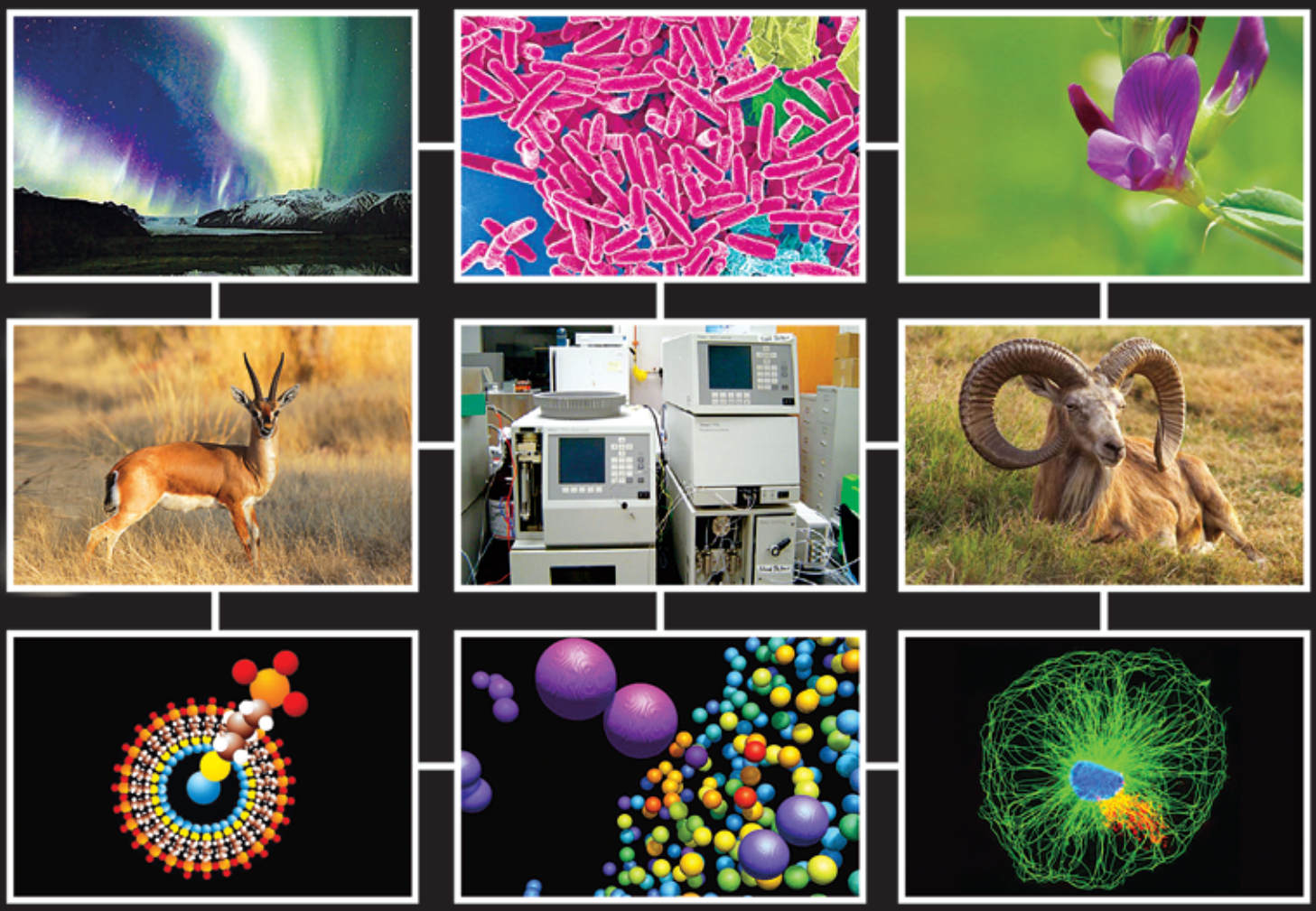

SENRA
Academic Publishers
Burnaby, British Columbia

Print ISSN 1715-9997
Online ISSN 1920-3853

Volume 4, Number 2
June 2010

CANADIAN JOURNAL OF PURE AND APPLIED SCIENCES

The Canadian Journal of Pure and Applied Sciences (CJPAS-ISSN 1715-9997) is a peer reviewed multi-disciplinary specialist journal aimed at promoting research worldwide in Agricultural Sciences, Biological Sciences, Chemical Sciences, Computer and Mathematical Sciences, Engineering, Environmental Sciences, Medicine and Physics (all subjects).

Editorial Office
E-mail: editor@cjpas.ca
: editor@cjpas.net

SENRA Academic Publishers
7845 15th Street Burnaby
British Columbia V3N 3A3 Canada
www.cjpas.net
E-mail: senra@cjpas.ca

Board of Editorial Advisors

Canadian Journal of pure & applied sciences

Volume 4, Number 2
June 2010

CONTENTS

LIFE SCIENCES

PHYSICAL SCIENCES

SENRA Academic Publishers, Burnaby, British Columbia
Vol. 4, No. 2, pp. 1127-1131, June 2010
ISSN: 1715-9997

Canadian Journal of pure&applied sciences

FUNGAL PROTEIN ESTIMATION OF *ASPERGILLUS ORYZAE* GROWING IN SOLID STATE CULTIVATION CONDITIONS

Zhongping Chen, Zhisheng Wang and *Anguo Zhou
Institute of Animal Nutrition, Sichuan Agricultural University, 46 Xinkang Road, Yaan 625 014, Sichuan, China

ABSTRACT

The estimation of fungal protein is an essential parameter for nitrogen metabolism studies and evaluating the biological efficiency of fungal protein synthesis during fermented soybean meal processing. The aim of this study was to validate the fungal protein of *Aspergillus oryzae* SICC 3.302 measurement in solid state cultivation conditions using glucosamine content. Factors influencing the correlation between the glucosamine amount and fungal protein content, including incubation time, culture conditions (liquid or solid medium), carbon and nitrogen source, have been measured. Results suggest that the correlation of the glucosamine level and fungal protein content, regardless of incubation time and culture conditions, was a nearly constant. The influence of the medium composition, in particular the nitrogen source on the correlation has occurred. Collectively, these results indicated that glucosamine could be considered as reliable fungal protein indicator under the same nitrogen source.

Keywords: Glucosamine, fungal protein, *Aspergillus oryzae*, solid state cultivation.

INTRODUCTION

Soybean meal (SBM) is an important source of dietary protein in animal feed industry. However, variety of antinutritional factors, such as trypsin inhibitor, lectins and soya globulins, etc. contained in SBM limited the wide application of SBM in animal especially young animal feed (Dunsford *et al*., 1989; Li *et al*., 1990; Jiang *et al*., 2000). Fermentation with *Aspergillus oryzae,* a fungus widely used for hundreds of years in production of sake, miso, and soy sauce, could decrease antinutritional factors and improve the nutritional quality of SBM (Hong *et al*., 2004; Feng *et al*., 2007). Many biochemical reactions occurred during fermented SBM process involving substrate protein degradation and fungal protein synthesis, however, little is known about the method for distinguishing substrate protein and fungal protein when *A. oryzae* grow in solid state. The quantity of fungal protein is an essential parameter in nitrogen metabolism studies and for evaluating the biological efficiency of fungal protein synthesis during fermented SBM processing.

In the case of solid state fermentation, direct measurement of fungal protein is very difficult because fungi penetrate into and bind themselves tightly to the solid substrate particles (Desgranges *et al*., 1991). Many authors have described indirect methods to estimate biomass in solid state fermentation. These indirect methods are based on measuring the content of certain cell components such as glucosamine (Nahara *et al*., 1982; Sparringa and Owens, 1999; Wei *et al*., 2006), ergosterol (Nout *et al*., 1987; Wu *et al*., 2002), protein (Matcham *et al*., 1984; Córdova-López *et al*., 1996) and nucleic acids (Koliander *et al*., 1984; Wei *et al*., 2006), and measuring the biological activity like enzymatic activity (Barak and Chet, 1986) and respiration (Oriol *et al*., 1988), or measuring the consumption of some media components (Matcham *et al*., 1984). Meanwhile, previous studies have observed that the glucosamine content have a good correlations with sucrose consumption (Desgranges *et al*., 1991), amyloglucosidase and α-amylase level (Aidoo *et al*., 1981). These provide a possible indirect method to measure fungal protein, by determining the quantity of glucosamine in solid state cultivation conditions. However, less information is available on the correlation relationship between fungal protein and glucosamine level in solid state cultivation conditions.

Thus, the aim of the present work was to validate the fungal protein of *Aspergillus oryzae* measurement in solid state cultivation conditions using glucosamine content. As a fungal protein indicator, the relationship must ideally be constant throughout the fungal development. In the same way, culture conditions (liquid or solid medium) must not influence the relationship. If one of these two conditions is not fulfilled, this cell constituent cannot be considered as fungal protein indicator. In this study, agar plates covered with a membrane were used as a model system for solid state fermentation. This system prevents penetration of mycelium into the agar and allows the complete recovery of fungal biomass, so the content of glucosamine and fungal protein can be related to per gram dried biomass.

*Corresponding author email: zhouanguo02@yahoo.com.cn

MATERIALS AND METHODS

Microorganism

Aspergillus oryzae SICC 3.302, was maintained on potato dextrose agar (PDA) slants. After two days incubation at 30°C, the slants were stored at 4°C, for one month at most until use.

Preparation of spore suspension

Spore suspensions were prepared as previously (Córdova-López *et al*., 1996), the slants were suspended with 10ml 0.1% tween 80 sterile water and counted in blood counting chamber.

Submerged conditions

The liquid medium were formed by five carbon sources (glucose, sucrose, maltose, glycerol and sodium acetate) at 16g C/l, four nitrogen sources (bactopeptone, urea, $(NH_4)_2SO_4$ and $NaNO_3$) at 1.58g N/l and mineral element (0.1 g/l K_2HPO_4, 0.05 g/l KCl, 0.05 g/l $MgSO_4 \cdot 7H_2O$ and 0.001 g/l $FeSO_4$) in this experiment. Carbon, nitrogen and mineral element solutions were sterilized separately at 121°C for 30min.

The cultures were carried out in 250 ml Erlenmeyer flasks containing 95ml of different culture media. Each flask was inoculated with 5 ml of a spore suspension (Containing 10^6 spores ml^{-1}), and incubated at 30±0.5°C for 24, 48, 72, 96 and 120h. All cultures were incubated on an orbital shaker at 120rpm. The fungal were harvested by filtering through a weighed filter (Millipore HVLP 04700, porosity 0.45µm) and the cake was washed with distilled water. Then, the dry weight is measured after drying in an oven at 65°C for 48h. The mycelium was grounded in a mortar, redried at 65°C for 24h and stored in a desiccator until analysed.

Solid state conditions

Because of the difficulty, or impossibility, of separating mycelium from solid state fermentation, the fungi was grown on agar medium to imitate the solid state conditions. The composition of agar medium was the same as the liquid medium except that each agar medium contained purified agar (15g/l). The sterilized and weighed filter (Millipore HVLP 04700, porosity 0.45µm) was placed on each agar plate, and it was inoculated 0.2 ml spore suspension (Containing 10^6 spores ml^{-1}). The agar plates were incubated at 30±0.5°C in static conditions for 48h. The filter with the fungus was washed with distilled water and dried in an oven at 65°C for 48h. The pulverization and storage was the same as Submerged conditions.

Glucosamine determination

For fungal chitin hydrolysis into N-acetyl glucosamine, 20mg dried biomass was incubated with 2ml of H_2SO_4 (72%) in a test tube. After standing on a rotary shaker (130rpm) for 60min at 25°C, it was diluted with 3ml of distilled water and autoclaved at 121°C for 2h. The hydrolyzate was neutralized to pH 7.0 with 10M and then 0.5M NaOH using a pH meter, and diluted to 100ml. Finally, glucosamine was assayed by the colorimetric method described by Tsuji *et al*. (1969) and modified by Ride and Drysdale (1972). 1ml diluted hydrolysate was mixed with 1ml of $NaNO_2$ (5%) and 1ml of $KHSO_4$ (5%) in a centrifuge tube. After shaking occasionally for 15min, it was centrifuged at 3500rpm for 5min; 2ml of supernatant was mixed with 0.67ml of $NH_4SO_3NH_2$ (12.5%) and shaken for 3min. To the mixture was added 0.67ml of 3-methyl-2-benzothiazolinone hydrazone hydrochloride (MBTH; 0.5%, prepared daily), and then the mixture was boiled for 3min and immediately cooled to room temperature; 0.67ml of $FeCl_3$ (0.5%, prepared within 3 days) was added. After standing for 30min, the absorbance at 650nm was measured spectrophotometrically. The glucosamine content was calculated as milligrams per gram of fungal biomass according to the standard curve.

Protein assay

To determine the total protein of fungal cake, micro Kjeldahl method was used (AOAC, 1990). All reagents were of analytical grade, and determinations were conducted in triplicate unless stated otherwise. The total protein of fungal cake was expressed as milligrams per gram of fungal biomass.

RESULTS AND DISCUSSION

Effects of the age of the culture on fungal glucosamine and fungal protein content

Biomass, glucosamine and fungal protein were determined from *Aspergillus oryzae* grown in liquid medium (sucrose and $NaNO_3$) for 24, 48, 72, 96, 120h (Table 1). The fungal growth almost stopped after 48h cultivation and the biomass maintained at a relatively stable value. The glucosamine and fungal protein content of mycelium grown in liquid medium was 115 and 396 millgram per gram dried biomass respectively for 24h, and maintained at a nearly constant in the monitoring time. Scotti *et al*. (2001) and Desgranges *et al*. (1991) have obtained exactly the same results of the glucosamine respectively for *Cunninghamella elegans* and *Beauveria bassiana*. Moreover, the ratio of glucosamine and fungal protein was almost a constant too. It appears that the glucosamine, fungal protein content and the correlation of glucosamine and fungal protein of *Aspergillus oryzae* are constant during all cultivation time.

Effects of the culture conditions on fungal glucosamine and fungal protein content

To compare the culture condition on fungal glucosamine and fungal protein content, the nutrition was the same in submerged and solid state conditions, except containing

Table1. Evolution of glucosamine and fungal protein content during cultivation time.

Items	Cultivation time(hours)				
	24	48	72	96	120
Biomass(g)	0.17±0.02	0.60±0.06	0.65±0.02	0.64±0.06	0.65±0.06
Glucosamine (mg/g)[a]	115.07±2.27	119.98±3.27	116.92±8.37	117.69±3.35	119.29±4.09
Fungal protein (mg/g)[b]	396.18±17.85	391.43±8.34	398.22±6.49	400.92±3.97	398.33±9.61
a[c]	3.44±0.21	3.26±0.13	3.42±0.29	3.41±0.06	3.20±0.13

[a] Expresses in mg glucosamine per gram of biomass dry weight. [b] Expresses in mg fungal protein per gram of biomass dry weight. [c]Represents the correlation of fungal protein and glucosamine (expressed in mg fungal protein per millgram glucosamine). Data represents the means ± SEM, n=3.

Table 2. Effects of carbon source on glucosamine and protein content in submerged and in solid state conditions, with similar nutrients.

Culture conditions	Bactopeptone + carbon source	Glucosamine (mg/g)[a]	Fungal protein (mg/g)[b]	a[c]
Submerged conditions	Glucose	109.84±1.57	394.60±8.22	3.59±0.28
	Sucrose	109.85±12.42	395.39±9.42	3.60±0.07
	Maltose	111.80±2.81	401.09±2.73	3.59±0.07
	Glycerol	111.77±5.90	400.62±6.26	3.59±0.17
	Sodium Acetate	115.53±11.74	393.52±15.90	3.40±0.11
Solid state conditions	Glucose	84.10±3.43	305.03±11.09	3.63±0.27
	Sucrose	85.07±1.31	306.64±9.74	3.60±0.07
	Maltose	85.30±0.18	307.61±15.34	3.61±0.17
	Glycerol	84.32±0.59	296.62±48.25	3.52±0.57
	Sodium Acetate	86.70±2.71	309.25±5.92	3.57±0.10

[a] Expresses in mg glucosamine per gram of biomass dry weight. [b] Expresses in mg fungal protein per gram of biomass dry weight. [c]Represents the correlation of fungal protein and glucosamine (expressed in mg fungal protein per millgram glucosamine). Data represents the means ± SEM, n=3.

Table 3. Effects of nitrogen source on glucosamine and protein content in submerged and in solid state conditions, with similar nutrients.

Culture conditions	Sucrose + nitrogen source	Glucosamine (mg/g)[a]	Fungal protein (mg/g)[b]	a[c]
Submerged conditions	Bactopeptone	109.85±2.42	395.39±1.42	3.60±0.07
	Sodium nitrate	111.11±18.82	392.80±29.64	3.54±0.32
	Ammonium Sulfate	136.44±2.88	336.96±51.00	2.47±0.33
	Urea	135.10±5.74	321.39±36.31	2.39±0.36
Solid state conditions	Bactopeptone	85.07±1.31	306.64±9.74	3.60±0.07
	Sodium nitrate	84.99±1.37	303.75±20.43	3.57±0.24
	Ammonium Sulfate	93.11±5.56	226.30±13.31	2.43±0.13
	Urea	93.21±7.08	233.68±22.77	2.53±0.41

[a] Expresses in mg glucosamine per gram of biomass dry weight. [b] Expresses in mg fungal protein per gram of biomass dry weight. [c]Represents the correlation of fungal protein and glucosamine (expressed in mg fungal protein per millgram glucosamine). Data represents the means ± SEM, n=3.

15g/l agar in solid state condition. As shown in table 2 and table 3, the glucosamine and fungal protein content of mycelium grown in submerged medium were higher than those obtained in solid state conditions on the corresponding medium. But, the correlation of glucosamine and fungal protein were very close between submerged (3.57mg fungal protein per millgram glucosamine) and solid state conditions (3.59mg fungal protein per millgram glucosamine) on the corresponding medium. Contrary to the results obtained by Ride and Drysdale (1971) on *Fusarium oxysporum*, our results permit to deduce that for *Aspergillus oryzae*, the glucosamine content is not influenced by the culture conditions. Scotti *et al*. (2001) reported the same result on *Cunninghamella elegans*.

Effects of the medium composition on fungal glucosamine and fungal protein content

To show the influence of the medium composition on glucosamine and fungal protein content, two experiments were carried out in submerged and solid state conditions.

The results (Table 2) show that the glucosamine, fungal protein content and the ratio of glucosamine and fungal protein were not influenced by carbon sources, whether in submerged or solid state condition. Thus, *Aspergillus oryzae* cultivated on bactopeptone and different carbon sources had the same glucosamine (117.76mg glucosamine per gram of biomass dry weight) and fungal protein content (397.05mg fungal protein per gram of biomass dry weight) in submerged condition, whereas it contained only a mean value of 85.10mg glucosamine per gram of biomass dry weight and 305.03mg fungal protein per gram of biomass dry weight in solid state condition. Moreover, the correlation of glucosamine and fungal protein were almost the same value.

Consequently, within different carbon source, the glucosamine, fungal protein content can be considered as a good indicator of the biomass growth. Furthermore the glucosamine amount can be considered as a good indicator of fungal protein.

The glucosamine, fungal protein content and the ratio of glucosamine and fungal protein, grown on media containing different nitrogen sources and sucrose as carbon sources, were determined. As shown in table 3, the glucosamine, fungal protein content and the ratio of glucosamine and fungal protein varied according to the carbon source.

The results can be divided in two categories in submerged and solid state condition, respectively. Lowest glucosamine content and highest fungal protein content and the ratio of glucosamine and fungal protein values were obtained with bactopeptone and sodium nitrate, with a mean value of 110.48 and 85.03mg glucosamine per gram of biomass dry weight, 394.10 and 305.20mg fungal protein per gram of biomass dry weight and 3.57 and 3.59 mg fungal protein per millgram glucosamine in submerged and solid state condition respectively. Ammonium sulfate and urea media give around 135.77 and 93.16mg glucosamine per gram of biomass dry weight, 329.18 and 230.00mg fungal protein per gram of biomass dry weight and 2.43 and 2.48mg fungal protein per millgram glucosamine in submerged and solid state condition respectively.

Obviously, the glucosamine amount can be considered as a good indicator of the fungal protein within each category of carbon source, whatever the culture conditions may be. Our results can be compared with those results obtained by Ride and Drysdale (1971) concerning *Fusarium oxysporum* and Desgranges *et al*. (1991) with *Beauveria bassiana*. Indeed, glucosamine content of *Beauveria bassiana* varied according to the medium composition, between 43 and 71mg of glucosamine per gram of fungal dry weight. But in this paper, comparison of glucosamine content was done for media having different compositions, as well for carbon and nitrogen sources as concentrations. Moreover, these results also show that glucosamine amount can be very different according to the strain.

CONCLUSION

The results of the experiments show that the glucosamine measurement of *Aspergillus oryzae* can be considered as a reliable indirect method for estimating fungal protein. In fact, the correlation of glucosamine and fungal protein content is constant whatever the age of the cultivation and culture conditions may be. On the other hand, the correlation appears to depend on the medium composition. Indeed, it was affected by the nitrogen source, but not by the carbon source. However, when the medium is well defined, this study demonstrates that the established results permit a good estimation of the fungal protein.

ACKNOWLEDGEMENT

We are grateful to the Program for Changjiang Scholars and Innovative Research Team in the University, No. IRT0555, and the Double-funded for 211 Project of Sichuan Agricultural University.

REFERENCES

Aidoo, KE., Hendry, R. and Wood, BJB. 1981. Estimation of fungal growth in a solid state fermentation system. European Journal of Applied Microbiology and Biotechnology. 12:6-9.

AOAC. 1990. Official Methods of Analysis, 15th ed. Association of Official Analytical Chemists, Arlington, Virginia, VA, USA.

Barak, R. and Chet, I. 1986. Determination, by fluorescein diacetate staining, of fungal viability during mycoparasitism. Soil Biology and Biochemistry. 18(3): 315-319.

Córdova-López, J., Gutiérres-Rojas, M., Huerta, S., Saucedo-Castaneda, G. and Favela-Torres, E. 1996. Biomass estimation of *Aspergillus niger* growing on real and model supports in solid-state fermentation. Biotechnology Techniques. 10:1-6.

Desgranges, C., Vergoignan, C., Georges, M. and Durand, A. 1991. Biomass estimation in solid state fermentation. I. Manual biochemical methods. Applied Microbiology and Biotechnology. 35:200-205.

Dunsford, BR., Knabe, DA. and Hacnsly, WE. 1989. Effect of dietary soybean meal on the microscopic anatomy of the small intestine in the early-weaned pig. Journal of Animal Science. 67:1855-1864.

Feng, J., Liu, X., Liu, YY., Xu, ZR. and Lu, YP. 2007. Effects of *Aspergillus oryzae* 3.042 fermented soybean meal on growth performance and plasma biochemical parameters in broilers. Animal Feed Science and Technology. 134:235-242.

Hong, KJ., Lee, CH. and Kim, SW. 2004. *Aspergillus oryzae* GB-107 fermentation improves nutritional quality of food soybeans and soybean meal. Journal of Medicinal Food. 7(4):430-436.

Jiang, R., Chang, X., Stoll, B., Ellis, KJ., Shypallo, RJ., Weaver, E., Campbell, J. and Burrin, DG. 2000. Diatery plasma proteins used more efficiently than extruded soy protein for lean tissue growth in early-weaned pigs. Journal of Nutrition. 130:2016-2019.

Koliander, B., Hampel, W. and Roehr, M. 1984. Indirect estimation of biomass by rapid ribonucleic acid determination. Applied Microbiology and Biotechnology. 19:272-276.

Li, DF., Nelssen, JL., Reddy, PG., Blecha, F., Hancock, JD., Allee, G., Goodband, RD. and Klemm, RD. 1990. Transient hypersensitivity to soybean meal in the early weaned pig. Journal of Animal Science. 68: 1790-1799.

Matcham, SE., Jordan, BR. and Wood, DA. 1984. Methods for assessment of fungal growth on solid substrates. Society for Applied Bacteriology Technical Series. 19:5-18.

Nahara, H., Koyama, Y., Yoshida, T., Pichangkura, S., Ueda, R. and Taguchi, H. 1982. Growth and enzyme production in a solid-state culture of *Aspergillus oryzae*. Journal of fermentation technology. 60:311-319.

Nout, MJR., Bonants-van Laarhoven, TMG., de Jongh, P. and de Koster, PG. 1987. Ergosterol content of *Rhizopus oligosporus* NRRL5905 grown in liquid and solid substrates. Applied Microbiology and Biotechnology. 26: 456-461.

Oriol, E., Schetino, B., Viniegra-Gonzalez, G. and Raimbault, M. 1988. Solid-state culture of *Aspergillus niger* on support. Journal of Fermentation Technology. 66:57-62.

Ride, JP. and Drysdale, RB. 1971. A chemical method for estimating *Fusarium oxysporum* f. *lycopersici* in infected tomato plants. Physiological Plant Pathology. 1(4):409-420.

Ride, JP. and Drysdale, RB. 1972. A rapid method for the chemical estimation of filamentous fungi in plant tissue. Physiological Plant Pathology. 2:7-15.

Scotti, CT., Vergoignan, C., Feron, G. and Durand, A. 2001. Glucosamine measurement as indirect method for biomass estimation of *Cunninghamella elegans* grown in solid state cultivation conditions. Biochemical Engineering Journal. 7 (1):1-5.

Sparringa, RA. and Owens, JD. 1999. Glucosamine content of tempe mould, *Rhizopus oligosporus*. International Journal of Food Microbiology. 47(1-2):153-157.

Tsuji, A., Kinoshita, T. and Hoshino, M. 1969. Analytical chemical studies on amino sugar. II. Determination of hexosamines using 3-methyl-2-benzothiazolone hydrazone hydrochloride. Chemical and Pharmaceutical Bulletin. 17:1505-1510.

Wei, PL., Cen, PL. and Sheng, CQ. 2006. Comparison of three biomass estimation methods in solid state fermentation. Journal of Food Science and Biotechnology. 25(1):60-64.

Wu, K., Yang, BH., Zhang, J., Liu, B., Cai, JM., Pan, RR. and Marinus, M. 2002. *Trichoderma viride* biomass assay and its cellulase synthesis Characteristic. Food and Fermentation Industries. 28(8):9-12.

Received: Jan 19, 2010; Revised: April 26, 2010; Accepted: May 4, 2010

SENRA Academic Publishers, Burnaby, British Columbia
Vol. 4, No. 2, pp. 1133-1139, June 2010
ISSN: 1715-9997

Canadian Journal of pure&applied sciences

PSEUDOMONAS AERUGINOSA ASSOCIATED WITH NEGATIVE INTERACTIONS ON COLIFORM BACTERIA GROWTH

*Ulrich Vaconcelos[1], Maria Alice Gomes de Andrade Lima[2] and Glicia Maria Torres Calazans[1]
[1]Universidade Federal de Pernambuco, Centro de Ciências Biológicas, Departamento de Antibióticos, Av. Prof. Aurélio de Castro Cavalcanti, 79/104, CEP 51210-020, Recife-PE, Brazil
[2]Universidade Federal de Pernambuco, Centro de Tecnologia e Geociências
Departamento de Engenharia Química, Recife-PE, Brazil

ABSTRACT

Screening aquatic Pseudomonads which inhibit growth of *Escherichia coli* and *Enterobacter aerogenes* produced sixteen strains of pyocyanin-producing *Pseudomonas aeruginosa.* Cell enumeration was carried out by the Most-Probable-Number technique for 96h by using diluted Müeller-Hinton broth. Conditions favouring pyocyanin production resulted in reduced growth of coliform strains. Representative strains were resistant to ciprofloxacin, norfloxacin and imipenem. It was also verified that a high population of coliform strains was reached when grown individually. Results show that there was an antagonistic phenomenon provided by *Pseudomonas aeruginosa* against coliform bacteria when pyocyanin was formed. This paper highlights the risks for human and environmental health that this phenomenon represents.

Keywords: Pyocyanin-producing *Pseudomonas aeruginosa*, *Escherichia coli*, *Enterobacter aerogenes*, antagonism.

INTRODUCTION

Pseudomonas aeruginosa (Migula, 1894) is a formidable widespread organism occurring naturally in water and other environments (Trivedi *et al*., 2008; Shrivastava *et al*., 2004). However it is most often described as an opportunistic pathogen involved in nosocomial infections and episodic outbreaks (Bou *et al*., 2009; Corvec *et al*., 2008).

Pyocyanin (phenazine 5-methyl-1-hydroxy phenazinium betaine) is a pigment produced by over 90% of strains (Mavrodi *et al*., 2001; Reyes *et al*., 1981) and some authors suggest that pyocyanin is particularly responsible for the antagonistic phenomenon against other microorganisms through the generation of reactive oxygen species which would be expected to exert antimicrobial activity toward coliform bacteria (D'áquila *et al*., 2000; Guilherme and Silva, 2000; Duncan *et al*., 1999).

The coliform bacteria comprise more than 30 taxonomically different microorganisms. Genera *Escherichia* and *Enterobacter* are among the most important of the group. Since the 19th century, coliform bacteria have been considered effective indicators of recent fecal pollution in water and *E. coli* (Escherich, 1895) is the most important microorganism from this point of view (Foppen and Schijven, 2006).

There are several common laboratory methods used for estimating concentration of viable cells. Most-Probable-Number (MPN) is a rapid and simple method and important reasons for choosing this method can be listed: 1- when replacing a solid medium method due to the kinetic of growth of microorganisms that are highly variable and would obscure colonies of the organism of interest; 2- It is useful when microorganisms of interest produce some detectable product and cells can be estimated; 3- solid media may have factors such as heavy metals that alter the reliability of the count or interfere with the aim of the experimental plan and, 4- even if contaminating organisms overgrow the culture, the cells of interest can still be estimated (Gerhardt *et al*., 1994).

Coliform enumeration may be affected by several physical and chemical sources such as temperature, pH, chloride content, salinity and metals which could mask the analysis leading to false-negative results. In addition, biological agents also interfere by inhibiting coliform cell growth through various mechanisms which includes amensalism, pigment concentration and competition for nutrients between non-coliforms and coliforms (Spangenberg, 2007).

Several microorganisms may be antagonistic to the coliform group. Due to its opportunistic nature and metabolic versatility, *P. aeruginosa* strains are one of most important injury-promoting species of coliform bacteria inhibition in aquatic environments (Tamagnini and Gonzáles, 1997). Earlier data on negative interactions toward *E. coli* in water analysis identified some genera other than *Pseudomonas* may also be involved in this antagonistic phenomenon, such as Gram-positive

*Corresponding author email: ulvasco@gmail.com

Actinomyces, *Micrococcus* and *Sarcina*, Gram-negative *Flavobacterium* and yeasts (Hutchinson *et al*., 1943).

This paper reports a negative interaction of *P. aeruginosa* strains isolated from different aquatic sources against coliforms *E. coli* and *E. aerogenes* (Kruse, 1896). Tests were conducted to detect this phenomenon by measuring population of *P. aeruginosa* and coliform bacteria incubated simultaneously by simulating a recent coliform contamination in an environment where pyocyanin-producing *P. aeruginosa* strains were already established.

MATERIALS AND METHODS

Bacterial strains, media and identification methods

A total of sixteen aquatic strains of *P. aeruginosa* were investigated in this study. All strains were isolated from environmental and clinical water samples surrounding Recife, capital of the state of Pernambuco, Brazil and data are shown in Table 1. Representative *E. coli* EC-5 and *E. aerogenes* EA-1, respectively, were isolated from distinct well water samples where *P. aeruginosa* was absent. The reference type strains of *P. aeruginosa* ATCC 27853, *E. coli* ATCC 25922 and *E. aerogenes* ATCC 15012 were also included in the study.

All *P. aeruginosa* strains were identified by using asparagine and acetamide broth at 37±2°C for 24-48h of incubation, fluorescence at 360±20nm wavelength, growth on cetrimide Agar (Acumedia, Maryland, US) and enzymatic oxidase test (Probac do Brasil, São Paulo, Brazil). In order to guarantee conditions favouring the enhancement of pyocyanin, *P. aeruginosa* strains were grown on Pseudomonas P medium. During the tests, the presence of pyocyanin was verified by the discoloration of acidic $KMnO_4$ solution and by observing fluorescence at 360±20nm (Health Protection Agency, 2003; APHA *et al*., 1998).

E. coli and *E. aerogenes* strains were identified by using lactose broth and green brilliant bile broth at 37±2°C for 24-48h of incubation, and confirmed in EC broth and eosin-methylene-blue agar, respectively. Biochemical tests: indole production, methyl-red test, Vokes-Proskauer test and citrate utilization, were also performed (APHA *et al*., 1998).

Antibiotic sensitivity was assessed using Müeller-Hinton agar (Merk, Darmstadt, Germany) and antibiotic disks (Sensidisc-DME, São Paulo, Brazil).

Characterization of strains inhibitory to coliform

The assay was conducted as described by Ichikawa *et al*. (1971). *P. aeruginosa* strains were subcultured onto the surface of Müeller-Hinton agar disks and incubated in sterilized Petri dishes at 37±2°C for 48h. Then, coliforms were spread on the surface of Müeller-Hinton agar and disks containing grown *P. aeruginosa* were transferred onto the agar surface and incubated at 37±1°C overnight. Tests were carried out in triplicate. The inhibition zones formed were measured. A greater inhibition zone diameter indicated more coliform susceptibility to *P. aeruginosa*.

Table 1. The aquatic sources of *Pseudomonas aeruginosa* strains.

Strains	Source	Counts (MPN.100ml^{-1})	Multi-drug resistance (from 8 antibiotics tested)
PA1	Várzea Cemitery (well #1)	$\geq$ 1600	0
PA2	Várzea Cemitery (well #2)	$17x10^3$	2
PA3	Várzea Cemitery (well #3)	$\geq$ 1600	0
PA4	Tap (hospital)	$7x10^3$	0
PA5	Bottled water	$26x10^3$	0
PA6	Storage tank (hospital)	$17x10^4$	0
PA7	Well (domestic)	$11x10^2$	0
PA8	Water cooler (school)	ND	0
PA9	Tap (school)	ND	0
PA10	Tap (school's kitchen)	ND	0
PA11	Tap (kinder care's kitchen)	ND	0
PA12	Tap (hospital)	$23x10^4$	0
PA13	Tap (UFPE campus bathroom)	ND	0
PA14	Landfill (influent tank)	$6x10^5$	3
PA15	Landfill (facultative lagoon)	$2x10^4$	0
PA16	Well (industry plant)	ND	3

ND – not determined. Strain was isolated without quantification

Inhibitory activity test in liquid-state

The three most harmful strains in the selective inhibitory activity assay on solid medium were studied using diluted Müeller-Hinton Broth (Vetec, Rio de Janeiro, Brazil). The assay comprised the *P. aeruginosa* and coliform enumeration of the Most-Probable-Number for a period of 96h at intervals of 24h by using the multiple tube technique with 5 tubes per dilution: 10.0, 1.0 and 0.1mL. A sample from *P. aeruginosa* suspension (around 10^2 CFU/mL) was inoculated and incubated at 37±1°C for 72h, after which either EA-1 or EC-5 inoculation occurred by transferring their suspensions (around 10^2 CFU/mL) into the flask and re-incubating overnight. Tests were also conducted between reference type strains. Control tests with each strain grown individually were also carried out using the same conditions and time intervals.

RESULTS AND DISCUSSION

In this study we investigated the antagonistic interactions among pyocyanin-producing *P. aeruginosa* strains characterized by *in vitro* assays on solid and in liquid medium where the coliform bacteria represented a recent contamination in an environment where *P. aeruginosa* has already been established.

All *P. aeruginosa* strains previously confirmed their ability to produce pyocyanin and further showed antimicrobial activity against coliform bacteria, detected by measuring the inhibition zone diameters formed. Fluorescein production was also observed in five strains. Diameters from 9 to 17±0.1mm for EC-5 and from 7 to 29±0.1mm for EA-1 ($p<0.05$) were found and are summarized in Table 2.

Based on the inhibition zone size between reference type strains in the inhibitory activity assay performed on solid medium, six *P. aeruginosa* strains formed inhibition zones less than 11±0.1 mm and nine reached values more than 11±0.1 mm against EC-5 ($p<0.05$). Against EA-1, seven *P. aeruginosa* strains showed inhibition zone sizes of more than 16±0.1 mm and eight less than 16±0.1 mm ($p<0.05$). *P. aeruginosa* archived similar inhibition patterns for both coliforms despite the differences in inhibition zone sizes. Results based on the characterization of inhibitory activity were important for choosing the most suitable strains for the inhibitory activity test in liquid-state. It was established that the greater antimicrobial activity against *E. coli* would be tested further. Then, PA2, PA14 and PA16 were selected for the following investigation.

After the contact between the strains in liquid medium, the interval between 24 and 48h was decisive for *P. aeruginosa* to be successful. While coliform bacteria viable cells started to decay in number, *P. aeruginosa* strains increased and maintained their growth until 96h. Legnani *et al.* (1999) concluded in their study that when competing for nutrients, *P. aeruginosa* showed a faster initial growth within 48h, then, growth slowed in order to allow log phase to continue up to 7 days. Similar findings were also observed in the present study.

The percentage of reduction in number of coliform cells is

Table 2. Growth inhibition of coliform bacteria strains by *Pseudomonas aeruginosa* and by reference strain differing in pigment production.

P. aeruginosa strains	Pigment	Indicator coliform bacteria strains (inhibition zones)	
		Enterobacter aerogenes EA-1	*Escherichia coli* EC-5
PA1	Pyocyanin, Fluorescein	+	++
PA2	Pyocyanin	+++	+++
PA3	Pyocyanin, Fluorescein	+	++
PA4	Pyocyanin, Fluorescein	++	++
PA5	Pyocyanin	+++	++
PA6	Pyocyanin, Fluorescein	++	+
PA7	Pyocyanin	+	+
PA8	Pyocyanin	+++	++
PA9	Pyocyanin, Fluorescein	+	++
PA10	Pyocyanin	+++	++
PA11	Pyocyanin	+++	++
PA12	Pyocyanin	+	++
PA13	Pyocyanin	++	++
PA14	Pyocyanin	+++	+++
PA15	Pyocyanin	+++	++
PA16	Pyocyanin	++	+++

shown in figure 1. Among wild-type strains, reduction in number of cells ranged 18.3-29.8±0.1% for EA-1 and from 9.8 to 40.3±0.1% for EC-1 ($p<0.05$). Although the two coliform bacteria presented similar inhibition patterns in the presence of PA2 (21.3 and 21.1±0.1% for EA-1 and EC-5, respectively), they differed among the other *P. aeruginosa* strains in terms of inhibitory activity by developing a pronounced susceptibility toward PA14 and less susceptibility toward PA16. Many reasons may be hypothesized in order to elucidate these results, such as, pigment concentration or multi-drug resistance. In addition, environmental selective pressure found at isolation sites may explain the inhibitory pattern of the strains.

Disturbed environments such as leachate-contaminated waters tend to permit physiological evolution and increase of gene pool by mutation as well as limited selective pressure. In addition, genetic exchange between microorganisms and external stress may act as driving forces on microbial size and stability (Evans *et al*., 1981). To know that PA14 and PA16 strains were isolated from landfill's influent tank and industry well, respectively, it is clearly obvious that environmental stress exerted influence on pyocyanin-producing *P. aeruginosa* strains metabolic versatility and also may have contributed most to the antimicrobial activity toward coliforms.

This affirmation may be reinforced with results from the control test. Among type-strains, *E. aerogenes* proved to be more sensitive than *E. coli* toward type-strain *P. aeruginosa*. Selective pressure would be related to driving forces in order to enhance metabolic versatility and may permit *P. aeruginosa* to present antagonistic antimicrobial activity against non-caustic environmental isolates. The two type-strains *P. aeruginosa* and *E. coli* were originated from nosocomial environments and this would explain why *E. coli* showed more resistance than wild type-strain *E. aerogenes.*

In figures 2 and 3, inhibitory antagonistic phenomenon between EA-1 and EC-5 and pyocyanin-producing *P. aeruginosa* strains is detailed as the development of coliforms cell (increase and decrease) within 96h at intervals of 24h in the liquid-state test and for the control, i.e., EA-1 and EC-5 individually grown in diluted Müeller-Hinton broth.

Presence of pyocyanin-producing *P. aeruginosa* strains strongly disturbed the two coliforms' growth when they were inoculated into tubes of diluted Müeller-Hinton broth simultaneously. A decreasing of growth pattern was observed, and the first 24-48h was decisive for the event, possibly related to the physiological effects of injury stress during the coliforms' lag time. At the end of the assay, major decrease in growth of EA-1 and EC-5 (against PA14) reached 3 orders of magnitude. Moreover, reduction in growth has not been observed in control tubes and led us to confirm that pyocyanin-producing *P. aeruginosa* strains have acted as a biological interference on coliform analysis. We emphasize that though coliform bacteria were reduced in number of estimated cells in the present study, they still reached significant levels.

In order to elucidate if the detected antagonistic interaction corresponded to a bacteriostatic or bactericidal event, plating of serial dilutions of the coliform suspensions at time 0h and a sample from the tube 96h later revealed EA-1 and EC-5 to be recovered on eosin-methylene-blue agar. Furthermore, the number of colony forming units was apparently reduced by the presence of the antagonist.

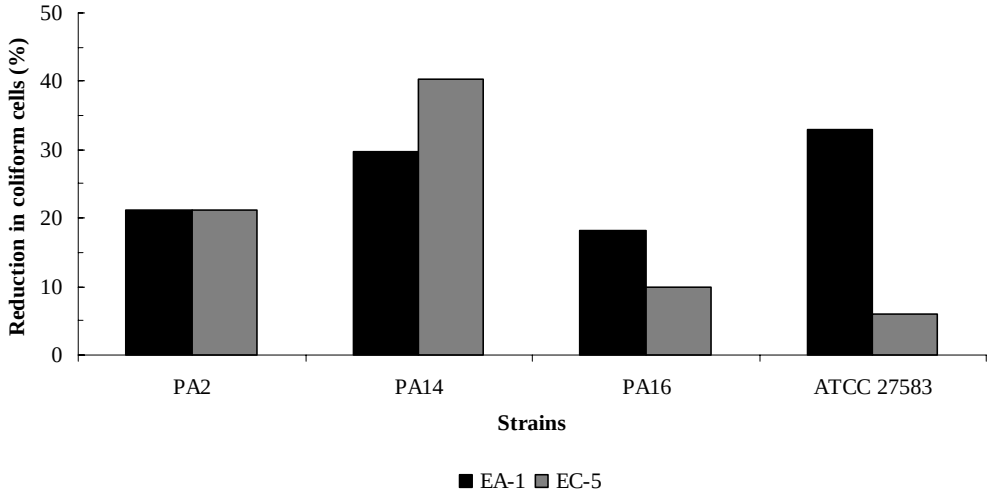

Fig. 1. Decrease in coliform growth after 96h.

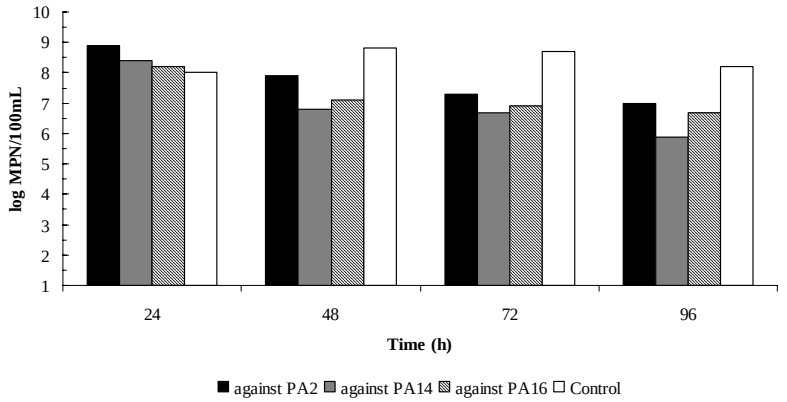

Fig. 2. Patterns of EA-1 growth inhibition in the presence of pyocyanin-producing *Pseudomonas aeruginosa* strains. Control refers to EA-1 grown individually. Single values from experiments repeated on at least two separate occasions.

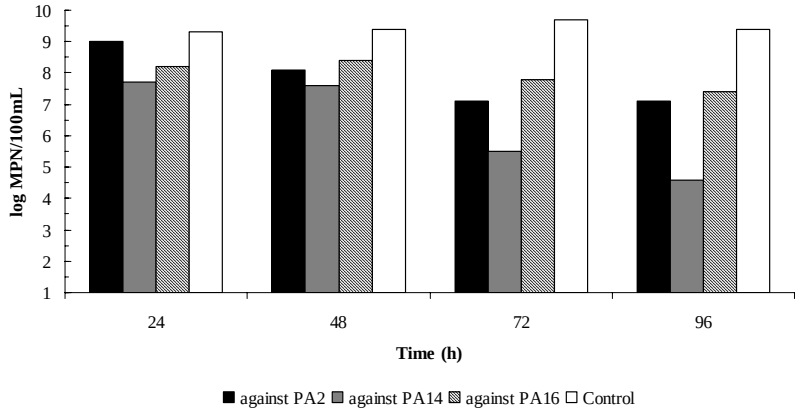

Fig. 3. Patterns of EC-5 growth inhibition in the presence of pyocyanin-producing *Pseudomonas aeruginosa* strains. Control refers to EC-5 grown individually. Single values from experiments repeated on at least two separate occasions.

Our findings were consistent to a classical study on the incidence and significance of microorganisms antagonistic to the coliform group which demonstrated a reduction of 28-97% when antagonist and *E. coli* were inoculated simultaneously (Hutchison *et al*., 1943). The lower reduction in percentage of coliforms found in this study was possibly caused by the different culture medium and initial cell concentrations used.

The use of diluted medium stimulated competition for carbon sources where coliform bacteria and *P. aeruginosa* were forced to overlap. Technically, coliform bacteria would have advantages due to shorter doubling-time when compared to *P. aeruginosa* (Tamagnani and Gonzáles, 1997; Camper *et al*., 1991). Nevertheless, pyocyanin-producing *P. aeruginosa* strains have proven to be more nutritionally versatile and capable of adaptation when competing with another microorganism. Moreover, literature reported that under competition for nutrients, coliform bacteria usually delay in lag time which would also explain the susceptibility of that group in the present study (Evans *et al*., 1981).

Although coliform bacteria are the universal indicators of fecal pollution in waters for human consumption, detection of *P. aeruginosa* as a complementary test is matter of concern because presence of *P. aeruginosa* and low coliform bacteria concentration would hide a major risk and would compromise the results from current methods used for water analysis.

P. aeruginosa creates an element of concern, as this species can cause nosocomial infections or multi-drug resistant strains which may be untreatable. The three most harmful strains in this study were also resistant to at least three important antibiotics used for the treatment of *P. aeruginosa* infections, as follows (concentration tested in $\mu g.ml^{-1}$): ciprofloxacine (5), norfloxacine (10) and imipenem (10), and were sensitive to amikacin (30), ceftazidime (30), gentamicin (10), ticarciline/clavulanate

(75/10) and tobramycin (10). The other thirteen remaining strains were sensitive to all antibiotics tested. Multi-drug resistance may also be related to selective pressures exerted by the environment influencing physiological evolution as discussed early.

Some authors have also discussed that *P. aeruginosa* tends to persist in water for a longer period of time and it is metabolically able to resist caustic agents in nature, as opposed to coliform survival which decreases with sunlight and allows opportunistic pathogens to grow (Schultz-Fademrecht *et al*., 2008; Ahlén *et al*., 1998). Guilherme and Silva (2000) affirmed that pyocyanin is accepted as the main factor in the antagonistic role of *P. aeruginosa*. Other mechanisms of action of pyocyanin have been discussed in literature, which include involvement with the redox reaction and formation of superoxide and hydrogen peroxide with further ATP depletion (O'Malley *et al*., 2003; Denning *et al*., 1998).

The *P. aeruginosa* bacteriocins suggest a potential role in environmental ecology, and further studies must be carried out to evaluate the effect of pyocyanin concentration in the process of coliform inhibition. The presence of pyocyanin-producing *P. aeruginosa* strains themselves would lead to inhibitory activity against coliform bacteria. If such microorganisms belong to the feacal coliform group, great attention must be given due to their epidemiological importance.

Reduction in coliform growth induced by *P. aeruginosa* may lead to situations where the drinking water would be considered potable, however, under favorable conditions, coliform re-growth may develop and interspecies equilibrium would re-establish within the environment. Hence, coliform bacteria activation even in the presence of Psedomonads may possibly portray a hazardous scenario and may lead to real human and environmental health risks.

This study also provided some contribution to the knowledge of the action of pyocyanin-producing *P. aeruginosa* related to environmental control of coliform bacteria. Although our findings do not represent a general rule and site specific studies are needed, the methodological approach used here can be a relevant support tool when designing water analysis strategies.

CONCLUSIONS

The results of the experimental work undertaken in the present study described one inhibitory activity of *P. aeruginosa* against coliform bacteria in solid and liquid media. This effect could lead to human and environmental health risks if, for example, total coliform concentrations in water samples were low or not detectable as a result of the presence of *P. aeruginosa*, but then subsequent favorable conditions allow for coliform re-growth, including potentially pathogenic strains.

REFERENCES

Ahlén, C., Mandal, LH. and Iversen, OJ. 1998. Identification of infectious *Pseudomonas aeruginosa* strains in an occupational saturation diving environment. Journal of Occupational and Environmental Medicine. 55:480-484.

APHA, AWWA, WEF. 1998. Standard methods for the examination of water and wastewater, (20th ed.). Washington, DC, USA.

Bou, R., Lorente, L., Aguilar, A., Perpiñán, J., Ramos, P., Peris, M. and Gonzáles, D. 2009. Hospital economic impact of an outbreak of *Pseudomonas aeruginosa* infections. Journal of Hospital Infection. 71:138-142.

Camper, AK., McFeters, GA., Characklis, WG. and Jones, WL. 1991. Growth kinetics of coliform bacteria under conditions relevant to drinking water distribution systems. Applied and Environmental Microbiology. 57:2233-2239.

Corvec, S., Poirel, L., Espaze, E., Giraudeau, C., Drugeon, H. and Nordmann, P. 2008. Long-term evolution of a nosocomial outbreak of *Pseudomonas aeruginosa* producing VIM-2 metallo-enzyme. Journal of Hospital Infection. 68:73-82.

D'áquila, PS., Roque, OCD., Miranda, CAS. and Ferreira, AP. 2000. Quality assessment of the public water supply in Nova Iguaçu, Rio de Janeiro. Public Health Report. 16:791-798.

Denning, GM., Wollenweber, LA., Railssback, MA., Cox, CD., Stoll, L. and Britigan, BE. 1998. *Pseudomonas* pyocyanin increases interleukin-8 expression by human airway epithelial cells. Infect Immunology. 66:5777-5784.

Duncan, SH., Doherty, CJ., Govan, JRW, Neogrady, S., Galfi, P. and Stewart, CS. 1999. Characteristics of sheep-rumen isolates of *Pseudomonas aeruginosa* inhibitory to the growth of *Escherichia coli* O157. FEMS Microbiology Letters. 180:305-310.

Evans, TM., Waarvick, CE., Seidler, RJ. and LeChevallier, MW. 1981. Failure of the Most-Probable-Number technique to detect coliforms in drinking water and raw water supplies. Applied and Environmental Microbiology. 41:130-138.

Foppen, JWA. and Shijven, JF. 2006. Evaluation of data from the literature on the transport and survival of *Escherichia coli* and thermotolerant coliforms in aquifers under saturated conditions. Water Research. 40:401-426.

Gerhardt, P., Murray, RGE., Wood, WA. and Krieg, NR. 1994. Methods for general and molecular bacteriology. American Society for Microbiology. Washington, DC, USA.

Guilherme, EFM. and Silva, JAM. 2000. *Pseudomonas aeruginosa* as an indicator of water pollution. Revista Higiene Alimentar. 14:43-47.

Heath Protection Agency. 2003. Enumeration of *Pseudomonas aeruginosa* by membrane filtration. National Standard Methods issue 2.3, *W6*i2.3. London, UK.

Hutchison, D., Weaver, RH. and Scherago, M. 1943. The incidence and significance of microorganisms antagonistic to *Escherichia coli.* Journal of Bacteriology. 45:29.

Ichikawa, T., Date, M., Ishikura, T. and Ozaki, A. 1971. Improvement of kasugamycin-producing strain by the agar piece method and the prototroph method. Folia Microbiologica. 16:218-224.

Legnani, P., Leoni, E., Rapuano, S., Turin, D. and Valenti, C. 1999. Survival and growth of *Pseudomonas aeruginosa* in natural mineral water: a 5-year study. International Journal of Food Microbiology. 53:153-158.

Mavrodi, DV., Bonsall, R., Delaney, SM., Soule, MJ., Phillips, G. and Thomashow, LS. 2001. Functional analysis of genes for biosynthesis of pyocyanin and phenazine-1-carboxamide from *Pseudomonas aeruginosa* PA01. Journal of Bacteriology. 183:6454-6465.

O'Malley, YQ., Abdalla, MY., McCormick, ML., Reszka, KJ., Denning, GM. and Britigan, BE. 2003. Subcelluar localization of *Pseudomonas aeruginosa* pyocyanin cytotoxicity in human lung epithelial cells. American Journal of Physiology: Lung Cell and Molecular Physiology. 284:L420-L430.

Reyes, EAP., Bale, MJ., Cannon, WH. and Matsen, JM. 1981. Identification of *Pseudomonas aeruginosa* by pyocynin production on Tech agar. Journal of Clinical Microbiology. 13:456-458.

Spangenberg, JH. Biodiversity pressure and driving forces behind. 2007. Ecological Economics. 61:146-158.

Schltz-Fademrecht, C., Wichern, M. and Horn, H. 2008. The impact of sunlight on inactivation of indicator microorganisms both in river water and benthic biofilms. Water Research. 42:4771-4779.

Shrivastava, R., Upreti, RK., Jain, SR., Prasad, KN., Seth, P. and Chaturvedi, UC. 2004. Suboptimal Chlorine treatment of drinking water leads to selection of mutidrug-resistent *Pseudomonas aeruginosa*. Ecotoxicology and Environmental Safety. 58:277-283.

Tamagnini, LM. and Gonzáles, RD. 1997. Bacteriological stability and growth kinetics of *Pseudomonas aerugiunosa* in bottled water. Journal of Applied Microbiology. 83:91-94.

Trivedi, P., Pandey, A. and Palni, LMS. 2008. *In vitro* evaluation of antagonistic properties of *Pseudomonas corrugata*. Microbiology Reviews. 163:329-336.

Received: April 10, 2010; Accepted: May 14, 2010

SENRA Academic Publishers, Burnaby, British Columbia
Vol. 4, No. 2, pp. 1141-1149, June 2010
ISSN: 1715-9997

Canadian Journal of pure&applied sciences

INHIBITORY EFFECTS OF RCG1, A β-GALACTOSIDE-BINDING LECTIN FROM *RANA CATESBEIANA* (AMERICAN BULLFROG) OOCYTES AGAINST HUMAN AND PHYTOPATHOGENS

*Sarkar MA Kawsar[1], Sarkar MA Mamun[2], Md S Rahman[3], Hidetaro Yasumitsu[1] and *Yasuhiro Ozeki[1]
[1]Laboratory of Glycobiology and Marine Biochemistry, Department of Genome System Sciences, Graduate School of Nano Biosciences, Yokohama City University, 22-2 Seto, Kanazawa-ku, Yokohama 236-0027, Japan
[2]Department of Botany, Faculty of Science, University of Chittagong, Chittagong-4331
[3]Department of Microbiology, Faculty of Science, University of Chittagong, Chittagong, Bangladesh

ABSTRACT

A β-galactoside-binding galectin-1 (RCG1) was purified from the oocytes of the American bullfrog, *Rana catesbeiana* by affinity column chromatography and was evaluated for its growth of inhibition effects on bacteria and fungi. Through SDS-PAGE and gel permeation chromatography, RCG1 was found to be a non-covalently-bonded dimeric protein that consisted of two 15 kDa polypeptide subunits. This lectin showed significant hemagglutinting activity against trypsinized human and rabbit erythrocytes and it was inhibited by asialofetuin, thiodigalactoside and lectose. RCG1 was screened for *in vitro* antibacterial activity against eleven human pathogenic bacteria and significantly inhibited the growth of gram-positive bacteria than the gram-negative bacteria. *Bacillus subtilis* (10±1 mm) and *Bacillus cereus* (8±1 mm) were exhibited the highest growth of inhibition by the lectin (250 µg/disc). At the same time, RCG1 showed good growth inhibition against the gram-negative bacterium, *Salmonella typhi* but not others such as, *Pseudomans* sp., *Escherichia coli* and *Vibrio cholerae*. Antifungal activity also was investigated against six phytopathogenic fungi based on a food poisoning technique. Among the test fungi, the maximum inhibition of mycelial growth were observed in *Fusarium equiseti* (18.4±1%) followed by *Colletotrichum corchori* (13.3±1%) and *Curvularia lunata* (8.4±1%) at a concentration of the RCG1 100 µg/ml. These results suggest that future findings of lectin applications obtained from bullfrog oocytes may be of importance to clinical microbiology and have potential drug-resistant agents.

Keywords: *Rana catesbeiana*, antibacterial, antifungal, inhibition zone, mycelial growth, lectin.

INTRODUCTION

Galectins, comprise S-type β-galactosyl binding proteins that are present in vertebrates and invertebrates and do not require divalent cations for their binding activity (Vasta, 2009). The galectin family has been subdivided in several subgroups; 'proto', 'tandem' and 'chimera' (Rabinovich *et al.*, 2007) and they are bind to lactose/*N*-acetyllactosamine (Ahmed and Vasta, 1994). Galectin has been found in many organs of many organisms including liver, placenta, lung, heart, spleen, testis, and even also electric organ of electric eel - however the physiological function of galectin is still unknown. Galectins have activity about apoptosis (Koh *et al.*, 2008), cell adhesion (Stowell *et al.*, 2008), immune response and cancer metastasis (Hernandez and Baum, 2002) *in vitr*o, all suggesting that the protein has highly potency for creatures. In amphibians, galectins have been purified from the genus *Rana* (Ozeki *et al.*, 1991[a]), *Bufo* (Ahmed *et al.*, 1996) and *Xenopus* (Shoji *et al.*, 2003) and proto type galectin (galectin-1) was isolated in abundance from oocytes of the American bullfrog *Rana catesbeiana* living in aqua (Ozeki *et al.*, 1991[a]) and found to exist free from the endogenous ligand and abundant in oocytes. American bullfrog oocytes galectin-1 is located in the yolk platelets and is distributed in the extracellular matrices of these organs after development into adults (Uchiyama *et al.*, 1997). It was also shown to have potential cell adhesive activity to human rhabdomyosarcoma cells (Ozeki *et al.*, 1991[b]) and tissue fibronectin was determined to be a putative endogenous ligand (Ozeki *et al.*, 1995).

Gram-positive bacteria are those that are stained blue or violet by gram staining. This is in contrast to gram-negative bacteria, which cannot retain the crystal violet stain, instead taking up the counterstain (safranin) and appearing red or pink. Gram-positive organisms are able to retain the crystal violet stain because of the high amount of peptidoglycan in the cell wall. Gram-positive cell walls typically lack the outer membrane found in gram-negative bacteria. The cell wall of virtually all bacteria consists of a rigid peptidoglycan layer that is either overlaid by an outer lipopolysaccharide (LPS) layer in gram-negative bacteria or remains exposed on the

*Corresponding author email: akawsarabe@yahoo.com

surface of gram-positive bacteria. Peptidoglycan is a polymer of alternating *N*-acetylglucosamine (GlcNAc or NAG) and *N*-acetylmuramic acid (NAM) units connected by short pentapeptides. The β-1,4-glycosidic bond of the *N*-acetylglucosamine-*N*-acetylmuramic acid peptide-glycan backbone can be hydrolyzed by lysozyme (muramidase; mucopeptide *N*-acetylmuramoylhydrolase), a ubiquitous enzyme involved in innate immune reaction of numerous animal species (Ito *et al.*, 1999). Galectins can interact directly with bacterial surface glycans. Furthermore, bacterial infection can modulate galectin expression, which in turn regulates leukocyte function and inflammatory responses. Both gram-positive bacteria, such as *Streptococcus pneumoniae* and gram-negative bacteria, such as *Klebsiella pneumoniae* display surface carbohydrate galectin ligands (Mey *et al.*, 1996; Mandrell *et al.*, 1994). Galectins can binds to bacterial lipopolysaccharides (LPSs) in a dual manner: the C terminus CRD binds to lactosyl moieties of *K. pneumoniae* LPS, whereas the non-carbohydrate-binding *N*-terminal domain of galectin-3 binds to the lipid A moiety of *Salmonella enterica* subsp *enterica* serovar Minnesota LPS (Mey *et al.*, 1996). Galectins also binds mycobacterial phosphatidylinositol mannosides, glycolipids that accumulate on the membrane of *Mycobacterium*-containing phagosomes during infections (Barboni *et al.*, 2005). The galectin BbtGal-L from the cephalochordate amphioxus (*Branchiostoma belcheri*) specifically recognizes *Vibrio vulnificus* but not *Vibrio parahaemolyticus* or *Staphylococcus aureus* and its expression is upregulated by bacterial challenge (Yu *et al.*, 2007). Galectins also can recognize surface glycans on the surface of saprophytic or pathogenic fungi and could function as a macrophage receptor for fungal pathogens (Fradin *et al.*, 2000). Interestingly, the selective binding of galectin-3 to the *Candida albicans* cell wall glycans is fungicidal (Kohatsu *et al.*, 2006) as function in innate immunity. It has been reported that many lectins from marine invertebrates show antibacterial activity. The lectin from the horse mussel *M. modiolus* exhibited strong antibacterial activity against tested *vibrio* strains (Tunkijjanukij and Olafsen, 1998). T-antigen binding lectin purified from sea cucumber showed strong broad spectrum antibacterial activity against both gram-positive and gram-negative bacteria (Gowda *et al.*, 2008).

We previously evaluated the cell adhesion activity by human rhabdomyosarcoma cells and determined the glycan-binding properties of the lectin by using frontal affinity chromatography technology (FACT) (Kawsar *et al.*, 2009). In this paper, we evaluate the antibacterial and antifungal activities by the determination of growth inhibitory effects of the purified lectin, RCG1 from the American bullfrog *Rana catesbeiana* oocytes against human and phytopathogens.

MATERIALS AND METHODS

Drugs and reagents

A lactosyl-agarose column was purchased from Seikagaku Kogyo Co. Ltd., Japan and standard protein marker mixture (Daiichi-III) for SDS-PAGE was purchased from Daiichi Pure Chem. Co. Ltd., Japan. A bicinchoninic acid (BCA) kit was purchased from Pierce Co. Ltd., USA. Superdex 75 and Sephadex G-75 were obtained from GE Healthcare, USA. Agar, dextrose, peptone, beef extract were purchased from Merck Ltd., India and BDH Ltd., Bangladesh and were of the highest purity grade. Female American bullfrogs (*Rana catesbeiana*) were purchased from an experimental animal company, Nippon Seibutsu Zairyo Co. Ltd., Tokyo, Japan. Eggs were stored at -80°C or used after collection according to the situation.

Purification of the lectin (RCG1)

RCG1, β-galactoside-binding lectin was purified from the oocytes of the American bullfrog (*Rana catesbeiana*) by affinity column chromatography (Ozeki *et al*., 1991[a]). Briefly, unfertilized oocytes (100 g w/v) were obtained from the abdominal cavity of a female by laparotomy, homogenized in a cooled pestle and frozen in 500 ml of acetone. During homogenization lipids located in the upper layer were discarded. After removal of lipids several times via frozen acetone, the precipitate was dried completely into powdered form by vacuum drying. Acetone-extracted oocyte powder (10 g) was homogenized with 20 times (w/v) TBS (10mM Tris(hydroxymethyl)aminomethane-HCl, pH 7.4, containing 150 mM NaCl) and centrifuged at 27,500 *g* for 1 h at 4°C and the supernatant was applied to an affinity column of lactosyl-agarose (5 ml) that was fitted with a Sephadex G-75 pre-column (5 ml). After application of extracts, the lactosyl-agarose column was extensively washed with TBS. The lectin was eluted with 100 mM lactose in TBS and each 1 ml of elution was collected in tubes with a fraction collector. The eluted fractions were analyzed by spectrophotometer at 280 nm. The fractions were dialyzed against 1,000 times volumes of TBS to remove free lactose.

Hemagglutinating activity

The hemagglutinating activity was performed using 1% (w/v) trypsinized and 0.25% glutaraldehyde-fixed rabbit and human erythrocytes as described previously (Matsui, 1984). Erythrocytes were suspended at a concentration of 1% (w/v) in TBS. In the general assay, 20 µl each of TBS, TBS containing 1% Triton X-100, and erythrocytes were added to 20 µl of the two times-serially-diluted lectin with TBS in 96 well V-shape titer plates for 1 h. The hemagglutination activity of the lectin was expressed as the titer defined as the reciprocal of the highest dilution giving positive hemagglutination.

Sodium dodecyl sulfate-polyacrylamide gel electrophoresis

The molecular mass of the polypeptide was determined by sodium dodecyl sulfate polyacrylamide gel electrophoresis (SDS-PAGE). Purified lectin was mixed with an equal amount of sample buffer (20 mM Tris-HCl, pH 6.8; 0.2% SDS, and 20% glycerol) and then heated at 70°C for 15 min. Aliquots of 30 µl were applied to the well of a mini-slab gel (gel size: 80mm × 100 mm with 1 mm thickness; 12% and 5% polyacrylamide were used in separation and upper gels, respectively, constant current at 30 mA for 1h) according to a previous report (Laemmli, 1970). The following polypeptides were used as molecular mass markers; phosphorylase b (M_r 94 kDa), bovine serum albumin (M_r 66 kDa), ovalbumin (M_r 42 kDa), carbonic anhydrase (M_r 30 kDa), trypsin inhibitor (M_r 20 kDa), and lysozyme (M_r 14 kDa). After SDS-PAGE, the gel was stained with 0.1% (w/v) Coomassie Brilliant Blue (CBB) R-250 in 40% (v/v) and 10% acetic acid (v/v) followed by discoloration by excessive staining with 40% methanol and 10% acetic acid.

Gel permeation chromatography

The purified lectin was dissolved in 2.5% glycerol and subjected to gel permeation chromatography (GPC) utilizing a Superdex 75 column (1.0 × 65 cm) connected to an FPLC system (GE Healthcare, USA) in the presence of 50 mM lactose containing TBS. The elution time of the lectin from the column was detected by UV at an absorbance of 280 nm. Bovine serum albumin (66 kDa), ovalbumin (43 kDa), carbonic anhydrase (30 kDa), myoglobin (17 kDa) ribonuclease (14 kDa) and cytochrome *c* (6; 12 kDa) were used as standard molecular marker.

Protein determination

Protein concentrations were determined using BCA protein assay kit (Smith *et al.*, 1985; Wiechelman *et al*., 1988) with bovine serum albumin as the standard by measuring absorbance at 562 nm with spectrophotometer ND-1000 (Nano Drop Tech. Inc., USA).

Tested pathogens

The bacterial and fungal pathogens used in this study were obtained from the Microbiology Laboratory, Department of Microbiology, University of Chittagong, Bangladesh. Gram-positive bacterial strains were *Bacillus subtilis* BTCC 17, *Bacillus cereus* BTCC 19, *Bacillus megaterium* BTCC 18 and *Staphylococcus aureus* ATCC 6538. Gram-negative bacterial strains were *Salmonella typhi* AE 14612, *Salmonella paratyphi* AE 146313, *Shigella dysenteriae* AE 14396, *Shigella sonnei* CRL (ICDDR,B), *Escherichia coli* ATCC 25922, *Vibrio cholerae* (CRL (ICDDR,B) and *Pseudomonas sp.* CRL (ICDDR,B). The fungal pathogens were *Alternaria alternata* (Fr.) Kedissler, *Botryodiplodia theobromae* Pat., *Curvularia lunata* (Wakker) Boedijin, *Colletotrichum corcori* Ikata (Yoshida), *Fusarium equiseti* (Corda) Sacc and *Macrophomina phaseolina* (Tassi) Goid.

Culture and media

Standard NA (Nutrient Agar) medium was used for growing bacterial strains throughout the work whereby 20 g of agar powder, 5 g of peptone, 3 g of beef extract and 0.5 g of NaCl were added per liter of water. The medium was autoclaved for 15 minutes at 121°C with 15 psi. Older cultures were transferred to freshly prepared NA slants separately for each species via sterilized bacterial loop. In such a way, four tubes were freshly prepared for each bacterial pathogen. These tubes of inoculated slants were incubated at 35±2°C in incubator for 18-24 hours and each culture was used throughout for antibacterial screening studies. For preservation of the stock culture, one set of culture slants were kept in polythene bag, properly tied and preserved at 10°C.

Antibacterial assay

The *in vitro* growth inhibition assay against bacteria by RCG1 was carried out by the disc diffusion method (Bauer *et al.,* 1966). In this method, sterilized paper discs of 4 mm in diameter and petridishes of 150 mm in diameter were used throughout the experiment. The autoclaved Mueller-Hinton agar medium, cooled to 45°C, was poured into sterilized petridishes to a depth of 3 to 4 mm and after solidification of the agar medium; the plates were transferred to an incubator at 37°C for 15 to 20 minutes to dry off the moisture that develops on the agar surface. The plates were inoculated with the standard bacterial suspensions (as of McFarland 0.5 standard) by help of sterilized glass and allowed to dry for three to five minutes. Dried and sterilized filter paper discs were treated separately with 20 µl (250 µg/disc) from 5% phosphate buffered saline (PBS, pH 7.4) solution of RCG1 using a micropipette, dried in air under aseptic condition and were placed at equidistance in a circle on the seeded plate. A control plate was also maintained in each case without any test material. These plates were kept for 4-6 hours at low temperature and the RCG1 diffused from disc to the surrounding medium by this time. The plates were then incubated at 35±2°C for 24 hours to allow maximum growth of the organisms. The antibacterial activity of the test agent was determined by measuring the mean diameter of zone of inhibitions in millimeter. Each experiment was repeated thrice. Galactose was used as negative control. All the results were compared with the standard antibacterial antibiotic ampicillin (20 µg/disc), (BEXIMCO Pharm., Bangladesh Ltd.).

Antifungal activity

The *in vitro* antifungal activity of the bullfrog oocytes lectin was determined by the poisoned food technique (Grover and Moore, 1962) with some modification (Miah *et al.*, 1990). Potato dextrose agar (PDA) medium was

used for the culture of fungi. A required amount of PDA was taken in conical flasks separately and was sterilized by autoclave (121°C, 15 psi) for 15 minutes. Purified lectin (in PBS solution) was mixed with sterilized melted PDA medium to have 100 µg/ml in PDA and this was poured (about 20 ml/plate) in sterilized petridishes. At the center of each plate, 5 days old fungal mycelial block (4 mm in diameter) was inoculated and incubated at 27°C. A control set was also maintained in each experiment. Linear mycelial growth of fungus was measured after 3-5 days of incubation in triplicate. The average of two measurements was taken as mycelial colony diameter of the fungus in milimeter. All the antifungal results were compared with the standard antifungal antibiotic nystatin (100 µg/ml) in PDA. Galactose was used as negative control. The percentage inhibition of radial mycelial growth of the test fungus was calculated as follows:

$$\% \text{ Inhibition} = (C\text{-}T/C) \times 100$$

Where, C = diameter of the fungal colony in the control petridish and T = diameter of the fungal colony in the treated petridish.

RESULTS AND DISCUSSION

The supernatant extract from acetone-powdered bullfrog oocytes showed strong hemagglutinating activity and the activity was cancelled by the co-presence of β-galactosides such as lactose but not by the α-galactose or melibiose and therefore it was applied to a lactosyl-agarose column. After column washing with TBS, the column bound lectin was specifically purified by the addition of 100 mM lactose in TBS (Fig. 1). Four milligrams of RCG1 was purified from 100g (wet weight) of unfertilized oocytes and it was concentrated approximately 410 fold by affinity chromatography (Table 1). The purified *Rana catesbeiana* oocyte galectin-1 (RCG1) showed strong hemagglutinating activity against trypsinized and glutaraldehyde-fixed human erythrocytes and was slightly more sensitive to human erythrocytes when compared to those from rabbit (Table

Table 1. Purification of galactose-binding lectin from bullfrog *Rana catesbeiana* oocytes.

Purification Steps	Titer (HU)	Volume (ml)	Total activity	Protein conc. (mg/ml)	Specific activity	Purification fold	Recovery of activity (%)
Crude extract obtained by acetone	512	100	51200	2.1	2.4	1	100
Purified lectin	4096	5	20480	0.83	987	411	40

Total activity is shown by Titer × volume
Specific activity was shown by titer/mg of protein.

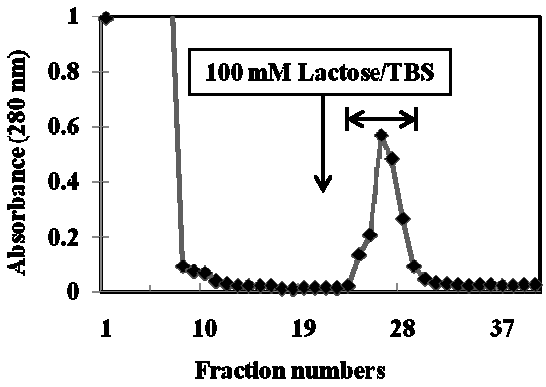

Fig. 1. Lactosyl-agarose affinity chromatography. Crude extract of *R. catesbeiana* oocytes were applied to an affinity column equilibrated with TBS. The column was extensively washed with TBS and the lectin was eluted with 100 mM lactose in TBS (arrow). The column bound fractions shown by the bar were collected and designated as purified lectin after dialysis against TBS.

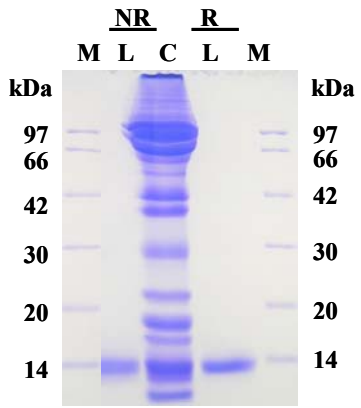

Fig. 2. SDS-polyacrylamide gel electrophoresis. C: crude extract of *R. catesbeiana* oocyte from acetone powdered; L: purified RCG1; NR: non-reducing and R: reducing conditions. 12% polyacrylamide was used as separating gel and the gels were stained with Coomassie brilliant blue. M: molecular weight markers (from top to bottom): phosphorylase b (97 kDa); bovine serum albumin (66 kDa); ovalbumin (42 kDa); carbonic anhydrase (30 kDa); trypsin inhibitor (20 kDa) and lysozyme (14 kDa).

2). RCG1 was purified as a single 15 kDa polypeptide under both reducing and non-reducing conditions by SDS-PAGE (Fig. 2, lane L). However, crude extract of the acetone powdered oocytes contained various proteins by SDS-PAGE (Fig. 2, lane C). On the other hand, RCG1 appeared to have a molecular mass at 30 kDa in GPC (Fig. 3A & B), indicating that the lectin was a non-covalent bound dimeric protein consisting of two 15 kDa polypeptide subunits. A partial primary structure analysis of the lectin showed that the amino acid sequence of the protein belonged to a superfamily of galectins (Ozeki *et al.*, 1991[c]) in addition to the carbohydrate binding specificity against β-galactoside.

Table 2. Hemagglutinating activity of RCG1 by human and rabbit erythrocytes.

Blood type*	Titer (HU)
Human (Type O)	2048
Human (Type A)	2048
Human (Type B)	1024
Rabbit	1024

*Trypsinzed and glutaraldehyde fixed erythrocytes were used.

Table 3. Antibacterial activity of RCG1 against gram-positive bacteria.

Name of bacteria	Diameter of zone of inhibition in milimeter	
	Lectin (250 µg/disc)	Ampicillin* (20 µg/disc)
Bacillus subtilis	10±1	20±1
Bacillus cereus	8±1	19±1
Bacillus megaterium	4±1	18±1
Staphylococcus aureus	0	21±1

Note: *Standard antibacterial antibiotic, Statistical analysis (RBD) at 1% level, organisms significant (F value 183.5), replica significant (F value 6.95).

The inhibitory effects of eleven human pathogenic bacteria to RCG1 was tested and compared to that of the antibacterial antibiotic, ampicilin. The results of the sensitivity test are presented in Tables 3 and 4. It was found that the RCG1 (250 µg/disc) gave promising inhibitory effects against gram-positive bacteria such as *Bacillus subtilis*. The diameter zone of inhibition by the

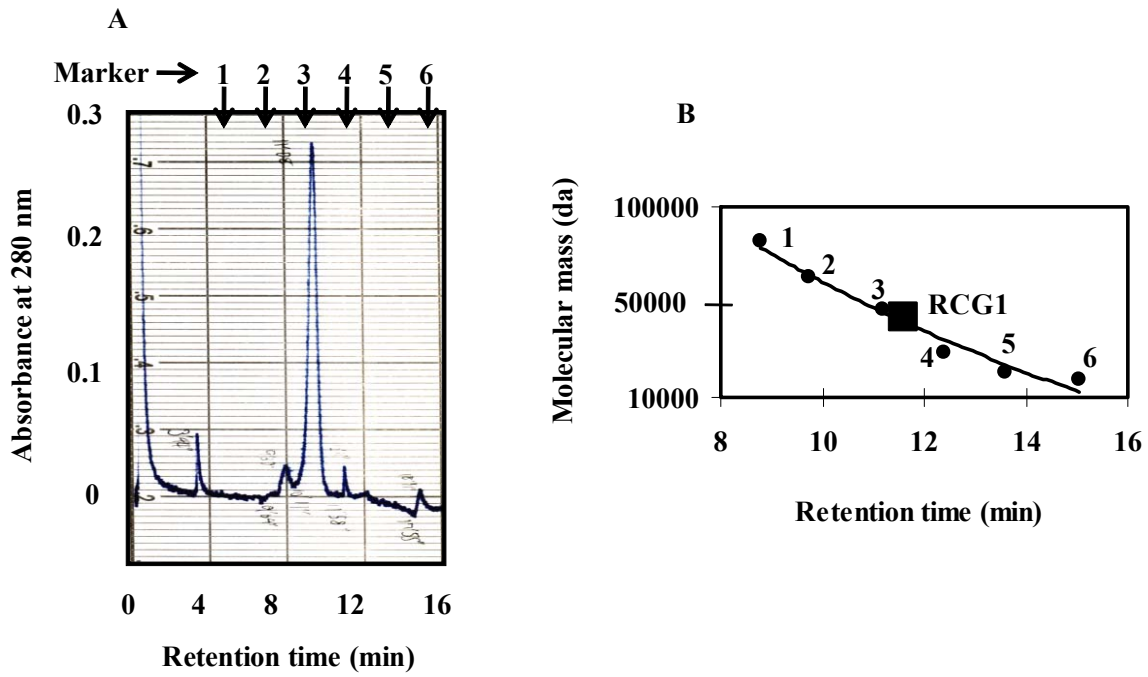

Fig. 3. Determination of the molecular weight by GPC. A: RCG1 (20 µg) was separated on a Superdex 75 column using FPLC system at a flow of 0.5 ml/min (chart speed is 0.5 cm/ml). B: Calibration line for the determination of molecular weight of RCG1 was determined using standard molecular mass marker proteins as; bovine serum albumin (1; 66 kDa), ovalbumin (2; 43 kDa), carbonic anhydrase (3; 30 kDa), myoglobin (4; 17 kDa), ribonuclease (5; 14 kDa) and cytochrome *c* (6; 12 kDa).

addition of RCG1 was significantly effective for *Bacillus subtilis* and *Bacillus cereus*; 10 and 8 mm, respectively (Table 3) although the growth inhibition of *Bacillus megaterium* was less effective. On the other hand, RCG1 showed good antibacterial activity against gram-negative bacterium *Salmonella typhi* but it did not inhibit the growth of other gram-negative bacteria such as *Pseudomonas* sp., *Escherichia coli* and *Vibrio cholerae* (Table 4), though the control antibiotic, ampicillin (20 µg/disc) inhibited the growth against all gram-negative bacteria. Amongst all bacterial strains, the gram-positive bacteria were more susceptible to the lectin as compared to gram-negative bacteria. This result suggested that the structure of surface-exposed carbohydrates on gram-positive bacteria were different even if they belong to the same genus within *Bacillus*.

Table 4. Antibacterial activity of RCG1 against gram-negative bacteria.

Name of bacteria	Diameter of zone of inhibition in milimeter	
	Lectin (250 µg/disc)	Ampicillin* (20 µg/disc)
Salmonella typhi	8±1	22±1
Salmonella paratyphi	6±1	19±1
Shigella sonnei	4±1	18±1
Shigella dysenteriae	3±1	20±1
Pseudomonas sp	0	19±1
Escherichia coli	0	17±1
Vibrio cholerae	0	18±1

Note: *Standard antibacterial antibiotic, Statistical analysis (RBD) at 1% level, organisms significant (F value 183.5), replica significant (F value 6.95).

A glycomics approach to determine the structure of surface glycans of bacteria may provide more useful clinical information to prevent disease using lectins. Indeed, galectins may be interesting candidates for interacting with bacteria owing to their specificity for β-galactosides in that they might be able to interact with some of the bacterial carbohydrates on the cell surface (Mandrell *et al.*, 1994). The glycan binding profile of RCG1 was analyzed by frontal affinity chromatography (Kawsar *et al.*, 2009) and it specifically recognizes branched complex type *N*-linked oligosaccharides having a lactosamine (Galβ1-4GlcNAc) structure. It seems reasonable that RCG1 may catch bacteria containing a lipopolysaccharide layer because the β-galactoside structure (Galβ1-4Glc) is contained in most of the major lipopolysaccharides at the non reducing terminal. In many galectins, a specific affinity moiety was reported against the *N*-acetyllactosamine and poly *N*-acetyllactosamine (Sharma *et al.*, 1992), indicating that galectin family is available as a candidate molecule to trap gram-positive bacteria by binding to lipopolysaccharides that express the "asialo-lactoneo-series" structure. Recently, a lipopolysaccharide-binding lectin purified from the seeds of *Eugenia uniflora* showed antibacterial activity similar to RCG1, as it effectively inhibited growth against gram-positive bacteria such as *Bacillus subtilis* (Oliveira *et al.*, 2008) and a β-galactoside binding pearl shell lectin purified from the marine bivalve, *Pteria penguin* showed antibacterial activity similar to RCG1 as well (Naganuma *et al.*, 2006). Rhamnose-binding steelhead trout (*Oncorhynchus mykiss*) egg lectin inhibited the growth of gram-positive and gram-negative bacteria by recognizing lipopolysaccharide or lipoteichoic acid (Tateno *et al.*, 2002) and in addition, galectin interactions with lipopolysaccharides in the gram-negative bacteria as *Salmonella minnesota* inhibited the growth of same genus *Salmonella* in a similar fashion to RCG1 (Mey *et al.*, 1996).

It has been reported (Yu *et al.*, 2007) that host galectins can bind directly to glycoconjugates on the surface of bacteria, either facilitating or inhibiting pathogen entry, followed by positive and negative regulation of host innate and adaptive immunity. The presence of the lectin in the oocytes of *R. catesbeiana* led us to consider its possible biological involvement in the defense mechanisms of the species. RCG1 is the first lectin from frog reported to exhibit microbial growth inhibition. This activity was previously postulated for invertebrates (Inamori *et al.*, 1999), which expressed soluble and bound membrane lectin forms that appeared to be one of the groups of molecules for recognition and defense. An instance of the above is provided by several types of hemocyte-derived lectins which may play a role of functional in the innate immunity. The same fact was suggested for mammalian lectins, such as mannose-binding lectins as collectin family, which play an important role in host-pathogen interactions by specific recognition of the cell surface substances of bacteria (Rabinovich and Gruppi, 2005). Some lectins seem to be useful for identification of pathogenic bacteria based on the specific binding moieties of lectins to the characteristic glycans on cell wall of such types of bacteria (Munoz-Crego *et al.*, 1999). The characterization of glycans that presented the cell walls of gram-positive and gram-negative bacteria was characterized by lectins, finding to their peptidoglycan and lipopolysaccharides (Doyle, 1994).

Contrastively, the interactions between lectins and glycans in fungi are not well known. In this study, we have found that RCG1 reduced the growth rate of some strains of fungi against six phytopathogenic strains by comparing with the antifungal antibiotic nystatin as positive control. The inhibition of fungal mycelial growth by RCG1 and nystatin are given in Table 5. From these results we observed that the mycelial growth of *Fusarium equiseti* was found to be inhibited (18.4±1%) by RCG1

(100 µg/ml), which showed highest inhibition towards the mycelial growth of all tested fungal strains, although the inhibition effect by the lectin was less than the case of bacteria. The growth of *Colletotrichum corchori* and *Curvularia lunata* (13.3-8.4±1%) was moderately inhibited but *Botryodiplodia theobromae* was least inhibited by RCG1. On the other hand, *Alternaria alternata* and *Macrophomina phaseolina* were never inhibited by the lectin, though the growth of all six fungi was totally inhibited by standard antibiotic, nystatin (100 µg/ml). By now, antifungal activity has been reported in many plant lectins (Broekaert *et al.*, 1989). Our results suggested that RCG1 has antifungal activity similarly to mannose-binding lectins from red cluster pepper (*Capsicum frutescens*) and *Pisum sativum* seeds that inhibited the growth of fungi *Fusarium moniliforme* and *Fusarium oxysporum, Aspergillus flavus* and *Trichoderma viride* (Nagi and Ng, 2007; Sitohy *et al.*, 2007).

Table 5. Antifungal activity of RCG1 from the bullfrog *R. catesbeiana* oocytes.

Name of fungi	Percentage inhibition of fungal mycelial growth	
	Lectin (100 µg/ml PDA)	Nystatin* (100 µg/ml PDA)
Fusarium equiseti	18.4±1	47.4±1
Colletotrichum corchori	13.3±1	50.3±1
Curvularia lunata	8.4±1	46.5±1
Botryodiplodia theobromae	4.6±1	40.4±1
Alternaria alternate	0	39.4±1
Macrophomina phaseolina	0	52.2±1

Note: *Standard antifungal antibiotic, Growth measured- radial growth in cm.

RCG1 has belongs to the galectin family. Many galectins were reported to have multivalent functions such as in cell adhesion and apoptosis through the carbohydrate-binding activity. In this study, we have found that the lectin possess antimicrobial activity in addition to cell adhesive activity (Kawsar *et al.*, 2009). Because the lectin is located on the outer membrane of frog eggs, it may play an integral role in defense against bacterial pathogens. Recently, a number of galactose-binding lectin were shown to act as host receptors for bacteria and fungi (Vasta, 2009; Ideo *et al.*, 2009) by apparent direct or indirect galectin-dependent specific host-pathogen interactions. Since RCG1 can be purified in large amounts from bullfrog eggs, it may be a potential drug discovery target for both anti-cancer and anti-inflammatory agents.

CONCLUSION

The present study showed that RCG1 displayed significant growth inhibition effects against selected human and phytopathogens. American bullfrog *Rana catesbeiana* oocytes galectin-1 (RCG1) was screened for the first time for antibacterial and antifungal activities and these antimicrobial activities may provide an effective defense capability against invading microbes in the amphibian *Rana catesbeiana*.

ACKNOWLEDGEMENTS

We are grateful to the Chairman of the Department of Microbiology, University of Chittagong, Bangladesh to give us the opportunity to carry out the microbiology work. We are also thankful to Dr. Robert A. Kanaly (USA & YCU) for improving our manuscript. This work was supported by Grants-in Aid for Scientific Research from JSPS (Japan Society for the Promotion of Science).

REFERENCES

Ahmed, H., Vasta, GR. 1994. Galectins: conservation of functionally and structurally relevant amino acid residues defines two types of carbohydrate recognition domains. Glycobiology. 4(5): 545-548.

Ahmed, H., Pohl, J., Fink, NE., Strobel, F. and Vasta, GR. 1996. The primary structure and carbohydrate specificity of a β-galactosyl-binding lectin from toad (*Bufo arenarum* Hensel) ovary reveal closer similarities to the mammalian galectin-1 than to the galectin from the clawed frog *Xenopus laevis*. The Journal of Biological Chemistry. 271(51): 33083-33094.

Barboni, E., Coade, S. and Fiori, A. 2005. The binding of mycolic acids to galectin-3: a novel interaction between a host soluble lectin and trafficking mycobacterial lipids?. FEBS Letters. 579(30): 6749-6755.

Bauer, AW., Kirby, MM., Sherris, JC. and Turck M. 1966. Antibiotic susceptibility testing by a standardized single disc method. American Journal of Clinical Pathology. 45: 493-496.

Broekaert, WF., Van, PJ., Leyn, F., Joos, H. and Peumans, W. 1989. A chitin-binding lectin from stinging nettle rhizomes with antifungal properties. Science. 245(4922): 1100-1102.

Doyle, RJ. 1994. Introduction to lectins and their interactions with microorganisms. In Lectin-microorganism Interactions ed. Doyle RJ, Slifkin MV, New York, Marcel Dekker, Inc. 1-65.

Fradin, C., Poulain, D. and Jouault, T. 2000. β-1,2-linked oligomannosides from *Candida albicans* bind to a 32-kilodalton macrophage membrane protein homologous to

the mammalian lectin galectin-3. Infection and Immunity. 68(8): 4391-4398.

Gowda, NM., Goswami. U. and Khan, MI. 2008. T-antigen binding lectin with antibacterail activity from marine invertebrate, sea cucumber (*Holothuria scabra*): possible involvment in differential recognition of bacteria. Journal of Invertebrate Pathology. 99(2): 141-145.

Grover, RK. and Moore, JD. 1962. Toximetric studies of fungicides against the brown rot organisms, *Sclerotinia fructicola* and *S. laxa.* Phytopathology. 52: 876-880.

Hernandez, JD. and Baum, LG. 2002. Ah, sweet mystery of death! galectins and control of cell fate. Glycobiology. 12(10): 127-136.

Ideo, H., Fukushima, K., Ando, KG., Mitani, S., Dejima, K., Nomura, K. and Yamashita, K. 2009. A *Caenorhabditis elegans* glycolipid-binding galectin functions in host defense against bacterial infection. The Journal of Biological Chemistry. 284(39): 26493-26501.

Inamori, K., Saito, T., Iwaki, D., Nagira, T., Iwanaga, S., Arisaka, F. and Kawabata, S. 1999. A newly identified horseshoe crab lectin with specificity for blood group A antigen recognizes specific O antigens of bacterial lipopolysaccharides. The Journal of Biological Chemistry. 274(6): 3272-3278.

Ito, Y., Yoshikawa, A., Hotani, T., Fukuda, S., Sugimura, K. and Imoto T. 1999. Amino acid sequences of lysozymes newly purified from invertebrates imply wide distribution of a novel class in the lysozyme family. European Journal of Biochemistry. 259(1-2): 456-461.

Kawsar, SMA., Matsumoto, R., Fuji, Y., Yasumitsu, H., Uchiyama, H., Hosono M., Nitta, K., Hamako, J., Matsui T., Kojima, N. and Ozeki, Y. 2009. Glycan-binding profile and cell adhesion activity of American bullfrog (*Rana catesbeiana*) oocyte galectin-1. Protein & Peptide Letters. 16(7): 677-684.

Koh, HS., Lee, C., Lee, KS., Ham, CS., Seong, RH., Kim, SS. and Jeon, SH. 2008. CD7 expression and galectin-1-induced apoptosis of immature thymocytes are directly regulated by NF-κB upon T-cell activation. Biochemical Biophysical Research Communications. 370(1): 149-153.

Kohatsu, L., Hsu, DK., Jegalian, AG., Liu, FT. and Baum, LG. 2006. Galectin-3 induces death of *Candida* species expressing specific β-1,2-linked mannans. The Journal of Immunology. 177 (7): 4718-4726.

Laemmli, UK. 1970. Cleavage of structural proteins during the assembly of the head of bacteriophage T4. Nature. 227(5259): 680-685.

Mandrell, RE., Apicella, MA., Lindstedt, R. and Leffler, H. 1994. Possible interaction between animal lectins and bacterial carbohydrates. Methods in Enzymology. 236: 231-254.

Matsui, T. 1984. D-galactoside specific lectins from coelomocytes of the echiuran, *Urechis unicinctus*. The Biological Bulletin. 166(1): 178-188.

Mey, A., Leffler, H., Hmama, Z., Normier, G. and Revillard, JP. 1996. The animal lectin galectin-3 interacts with bacterial lipopolysaccharides via two independent sites. The Journal of Immunology. 156(4): 1572-1577.

Miah, MAT., Ahmed, HU., Sharma, NR., Ali, A. and Miah, SA. 1990. Antifungal activity of some plant extracts. Bangladesh Journal of Botany. 19: 5-10.

Munoz-Crego A., Alvarez O., Alonso B., Rogers DJ. and Lvovo J. 1999. Lectin as diagnostic probes in clinical bacteriology-an overview. In: Lectins, Biology, Biochemistry, Clinical Biochemistry (Vol. 13th ed.) Eds. Van Driessche, E, Beeckmans, S. and Bøg-Hansen, TC. Lemchesvej, Hellerup, Denmark: TEXTOP. http://plab.ku.dk/tcbh/Lectins12/Calderon/paper.htm.

Naganuma, T., Ogawa, T., Hirabayashi, J., Kasai, K., Kamiya, H. and Muramoto, K. 2006. Isolation, characterization and molecular evolution of a novel pearl shell lectin from a marine bivalve, *Pteria penguin*. Molecular Diversity. 10(4): 607-618.

Nagi, PHK. and Ng, TB. 2007. A lectin with antifungal and mitogenic activities from red cluster pepper (*Capsicum frutescens*) seeds. Applied Microbiology and Biotechnology. 74(2): 366-371.

Oliveira, MDL., Andrade, CAS., Magalhaes, NSS., Coelho, LCBB., Teixeira, JA., Cunha, MGC. and Correia, MTS. 2008. Purification of a lectin from *Eugenia uniflora* L. seeds and its potential antibacterial activity. Applied Microbiology. 46(3): 371-376.

Ozeki, Y., Matsui, T., Suzuki, M. and Titani, K. 1991c. Amino acid sequence and molecular characterization of a D-galactoside-specific lectin purified from sea urchin (*Anthocidaris crassispina*) eggs. Biochemistry. 30(9): 2391-2394.

Ozeki, Y., Matsui, T., Nitta, K., Kawauchi, H., Takayanagi, Y. and Titani, K. 1991a. Purification and characterization of β-galactoside binding lectin from frog (*Rana catesbeiana*) eggs. Biochemical Biophysical Research Communications. 178(1): 407-413.

Ozeki, Y., Matsui, T. and Titani, K. 1991b. Cell adhesive activity of two animal lectins through different recognition mechanisms. FEBS Letters. 289(2): 145-147.

Ozeki, Y., Matsui, T., Yamamoto, Y., Funahashi, M., Hamako, J. and Titani, K. 1995. Tissue fibronectin is an endogenous ligand for galectin-1. Glycobiology. 5(2): 255-261.

Rabinovich, GA., Toscano, MA., Jackson, SS. and Vasta, GR. 2007. Functions of cell surface galectin-glycoprotein lattices. Curr. Opin. Struct. Biol. 17(5): 513-520.

Rabinovich, GA. and Gruppi, A. 2005. Galectins as immunoregulators during infectious processes: from microbial invasion to the resolution of the disease. Parasite Immunology. 27(4): 103-114.

Sharma, A., DiCioccio, RA. and Allen, HJ. 1992. Identification and synthesis of a novel 15 kDa β-galactoside-binding lectin in human leukocytes. Glycobiology. 2(4): 285-292.

Shoji, H., Nishi, N., Hirashima, M. and Nakamura, T. 2003. Characterization of the *Xenopus* galectin family: Three structurally different types as in mammals and regulated expression during embryogenesis. The Journal of Biological Chemistry. 278(14): 12285-12293.

Sitohy, M., Doheim, M. and Badr, H. 2007. Isolation and characterization of a lectin with antifungal activity from Egyptian *Pisum sativum* seeds. Food Chemistry. 104(3): 971–979.

Stowell, SR., Arthur, CM., Slanina, KA., Horton, JR., Smith, DF. and Cummings, RD. 2008. Dimeric galectin-8 induces phosphatidylserine exposure in leukocytes through polylactosamine recognition by the C-terminal domain. The Journal of Biological Chemistry. 283(29): 20547-20559.

Smith, PK., Krohn, RI., Hermanson, GT., Mallia, AK., Gartner, FH., Provenzano, MD., Fujimoto, EK., Goeke, NM., Olson, BJ. and Klenk, DC. 1985. Measurement of protein using bicinchoninic acid. Analytical Biochemistry. 150(1): 76-85.

Tateno, H., Ogawa, T., Muramoto, K., Kamiya, H. and Saneyoshi, M. 2002. Rhamnose-binding lectins from steelhead trout (*Oncorhynchus mykiss*) eggs recognize bacterial lipopolysaccharides and lipoteichoic acid. Bioscience Biotechnology and Biochemistry. 66(3): 604-612.

Tunkijjanukij, S. and Olafsen, JA. 1998. Sialic acid-binding lectin with antibacterial activity from the horse mussel: further characterization and immunolocalization. Developmental & Comparative Immunology. 22(2): 139-150.

Uchiyama, H., Komazaki, S., Oyama, M., Matsui, T. and Ozeki, Y. 1997. Distribution and localization of galectin purified from *Rana catesbeiana* oocytes. Glycobiology. 7(8): 1159-1165.

Vasta, GR. 2009. Roles of galectins in infection. Nat. Rev. Microbiol. 7(6): 424-438.

Wiechelman, KJ., Braun, RD. and Fitzpatrick, JD. 1988. Investigation of the bicinchoninic acid protein assay: identification of the groups responsible for color formation. Analytical Biochemistry. 175(1): 231-237.

Yu, Y., Yuan, S., Yu, Y., Huang, H., Feng, K., Pan, M., Huang, S., Dong, M., Chen, S. and Xu, A. 2007. Molecular and biochemical characterization of galectin from amphioxus: primitive galectin of chordates participated in the infection processes. Glycobiology. 17(7): 774-783.

Received: March 1, 2010; Revised: May 22, 2010; Accepted: May 24, 2010

SENRA Academic Publishers, Burnaby, British Columbia
Vol. 4, No. 2, pp. 1151-1162, June 2010
ISSN: 1715-9997

Canadian Journal of pure&applied sciences

VERTEBRATE BIODIVERSITY AND KEY MAMMALIAN SPECIES STATUS OF HINGOL NATIONAL PARK

M Zaheer Khan, Afsheen Zehra, Syed Ali Ghalib, Saima Siddiqui and Babar Hussain
Department of Zoology (Wildlife & Fisheries) University of Karachi, Karachi-75270

ABSTRACT

Pakistan has recognized three categories of protected areas: National Parks, Wildlife Sanctuaries, and Game Reserves. Currently Pakistan has 22 National Parks of which Hingol National Park is the most unique and important because it consists of six ecosystems including Arabian Sea, Rugged Mountains, Desert, River, Estuary, and open plains. The park has rich biodiversity and diversified fauna of terrestrial, marine, and freshwater ecosystems. The park has many important mammals, birds, fish, reptiles and amphibian species, including Ibex (C*apra aegagrus*), Urial (*Ovis vignei*), Chinkara (*Gazella bennettii)*, Dalmatian Pelican (*Pelecanus crispus*), Spotted-billed Pelican (*Pelecanus philippinus*), Houbara Bustard (*Chlamydotis undulat*), Imperial Eagle (*Aquila heliaca*), Sooty Falcon (*Falco concolor*), Flamingo (*Phoenicopterus roseus*), fish Mahsheer (*Tor putitora*), Marsh Crocodile (*Crocodylus palustris*), Green Sea Turtle (*Chelonia mydas*), Skittering frog (*Rana cyanophlyctis*) etc. During the study 2005 to 2009, 165 bird species (75 resident and 90 migratory species), and 16 mammalian species were recorded. While Ibex, Urial and Chinkara are the key species of the park. Jungle Cat (*Felis chaus*), Desert Cat (*Felis libyca*), Desert Fox (*Vulpes vulpes*), Wolf (*Canis lupus*), and Asiatic Jackal (*Canis aureus*) have been observed. Due to aesthetic reason, and venues like mountains, wetlands, river, estuary, sea beach, mud volcano and sand dunes, the park has a potential to be developed as Eco-tourist Park.

Keywords: Unique park, Hingol River, vertebrate biodiversity, green turtle, key mammalian species.

INTRODUCTION

Protected Areas are recognized as an important tool in conserving animal and plant species and ecosystems. These systems vary considerably from country to country, depending on priorities, and national needs, and on differences in institutional, legislative and financial support (Khan, 2004). Pakistan has 235 protected areas including 22 national parks (Table 1), 99 wildlife sanctuaries, 100 game reserves and 14 unclassified areas. Hingol National Park is located in the Province of Balochistan and covers an area of 619,043 hectares. This area falls at coordinates 26°00' and 25°17' North and 65°10' and 65° 55' East. Hingol National Park is named after the Hingol River, which flows through the center of the Park and empties into the Arabian Sea.

In 2005, 600 km long Mekran Coastal Highway was built along most of the Southern Coastal Area of Balochistan, that runs for some 109 km through the HN Park area (Management Plan of HNP, 2006). Hingol National Park comprises the area from the Arabian Sea up to 5 fathom depth to the Dhrun Mountain with the Shak top at 1580 m above sea level.

There are a number of plain valleys between hills in the HN park. The park area can be divided into areas West and East of Hingol River. The parallel mountain ranges West of the Hingol River follow an EW direction, including the Shur Mountain Range, Hinglaj-Nani Mountains, Gurangatti and Rodaini - Kacho – Dhrun area. The mountain ranges East of Hingol River follow a more SSW-NNE direction including the Tranche Block and the Deo-Beharo Block. Further East, the mountain ranges show a NS direction including the Hala Range (Shir and Nawar Mountains) and the Haro Range, which flanks the Phore Valley respectively at the West and the East side. Between the large mountains blocks are small valleys including the Sham Valley located between Sangal-Kund Malir Range and the Shur Mountain Range, the Kundrach Valley between Shur and Hinglaj, the Harian-Maneji Valley between Hinglaj and Gurangatti (Zehra, 2009). The drainage of the park area is mainly to the Hingol River. The main rivers from the North are the Nal-Hingol River entering the park at the NW boundary, the Arra River entering the park between the Dhrun Mountains and the Washiaab, the Babro River entering the park at the NE boundary, North of Tranch. The drainage of Dhrun Mountain is to all directions. The major drainage, from the high plateau is in Eastern direction emptying in the Ara River South of Kukeri Bhent. The largest part of the Southern slopes drains into the Rodaini Kacho Valley and then to the Daraj-Kacho gorge into the Northern Plains and its Ara River (Management Plan of HNP, 2006; Zehra, 2009).

In the HNP, 150 plant species have been reported (Zehra,

*Corresponding author email: zaheerkhan67@yahoo.ca

Table 1. Current List of the National Parks of Pakistan (Khan and Siddiqui, 2005; Ahmad, 2009).

Name of National Park	Location	Year of establishment	Name of National Park	Location	Year of establishment
Ayubia	NWFP	1984	Kala Chitta	Punjab	2009
Central Karakoram	Northern Areas	1995	Khirthar	Sindh	1974
Chinji	Punjab	1987	Khunjerab	Northern Areas	1975
Chitral Gol	NWFP	1984	Lal Suhanra	Punjab	1972
Deosai	Northern Areas	1993	Lulusar	NWFP	2003
Deva Vatala	AJK	2009	Machiara	AJK	1996
Ghamot	AJK	2004	Margalla Hills	Fed. Capital Territory	1980
Gurez	AJK	2009	Pir Lasora	AJK	2005
Handrap Shandoor	Northern Areas	1993	Saif-ul-muluk	NWFP	2003
Hazarganji Chiltan	Balochistan	1980	Sheikh Budin	NWFP	1993
Hingol	Balochistan	1997	Toh Pir	AJK	2005

2009). The main vegetated areas are in the small zones of the valleys, the floodplains, riverbeds, and more extensive area of the coastal plains. Most ecological units are bare or almost bare including the mud flats, the salt plains, the clay Mountains and mud vent areas, the stone rippled terraces, and the smooth slopes of brown clay rock, mountains ridges, the steep mountain walls and the crusted valley floor and the active flood bank areas. The park is represented by six ecosystems including Arabian Sea, Rugged Mountains, River, Desert, Estuary, and open plains. The wildlife of the coastal area of HNP is diverse due to a combination of habitats found together at several areas. The coastal plains show rocky hill areas (Sappat Mountains, Agor Hills, Jabal Haro-Kund Malir), sand dunes, agricultural fields and river beds.

The Arabian Sea, including the area bordering national park, is known to be highly productive. Nesting of Green turtle has been reported from the coastal area of HNP. A variety of water birds occurs at the coast line. Estuarine area of the River Hingol, supports a variety of resident and migratory water birds. Adjacent to coastline there is a large desert with prominent sand dunes. These sand dunes may be categorized as stable or fixed sand dunes. The desert area of the park has diversified biodiversity including birds, small mammals and reptiles. Occurrence of Houbara Bustard in winter is also reported in the dune areas (Azam, 2004).

The objective of the present study was to record the vertebrate biodiversity and population status of three key mammalian species (Ibex, Urial and Chinkara) of Hingol National Park in the selected areas during 2005-2009.

MATERIALS AND METHODS

Based on preliminary studies in the Hingol National Park, Nani Mandir Complex, Rodaini Kacho, Harian Valley, Dhrun, Machii, Maneji, Ara Kaur, Babro Kaur , Agor, Kundrach, Qasim Goth, Wadh Bundar, Maneji, Nani Mandir/Nani Bent, Nala Jhakee, Kashee Goth, Kund Malir, Kalair Goth, Nokoo Goth, Allah Buksh Goth, and Sanguri area were selected for the study of key mammalian and other vertebrate biodiversity (Table 2, Fig. 1, 2). The following methods and surveys techniques were employed for the observation, census and documentation of key mammalian species.

1. Track Counts
2. Point Surveys
3. Roadside Counts
4. Line Transects or Strip Census
5. Pellet Counts

Track Counts

Tracks can be the first indication of the presence of animals in an area. Track counts especially after rain are useful in identifying different animals especially for nocturnal and secretive ones. A fresh rain eliminates the previous tracks, and the recent tracks of animals entering or leaving the study areas can be used as a measure of their abundance. During all studies the track count technique was applied at selected areas of HNP and this was more effective compare to other methods.

Point Surveys

In this method, observation points are established along roads, edges of ponds or marshes, at a higher place and other locations suitable for viewing the habitat. For a period of 1 to 5 hours at each observation point, the observer records all sightings of the mammals at that site and then an index of abundance of each species is expressed as the number of animals seen per hour of observations (Brower *et al.*, 1990). Point surveys were conducted twice daily, first during early morning, i.e. one hour before sunrise until dawn and second, in the evening, i.e., begins one-half an hour before the sunset until dark.

Roadside Counts

Usually it is difficult to locate a mammal especially a large mammal by walking in its habitat, because it smells

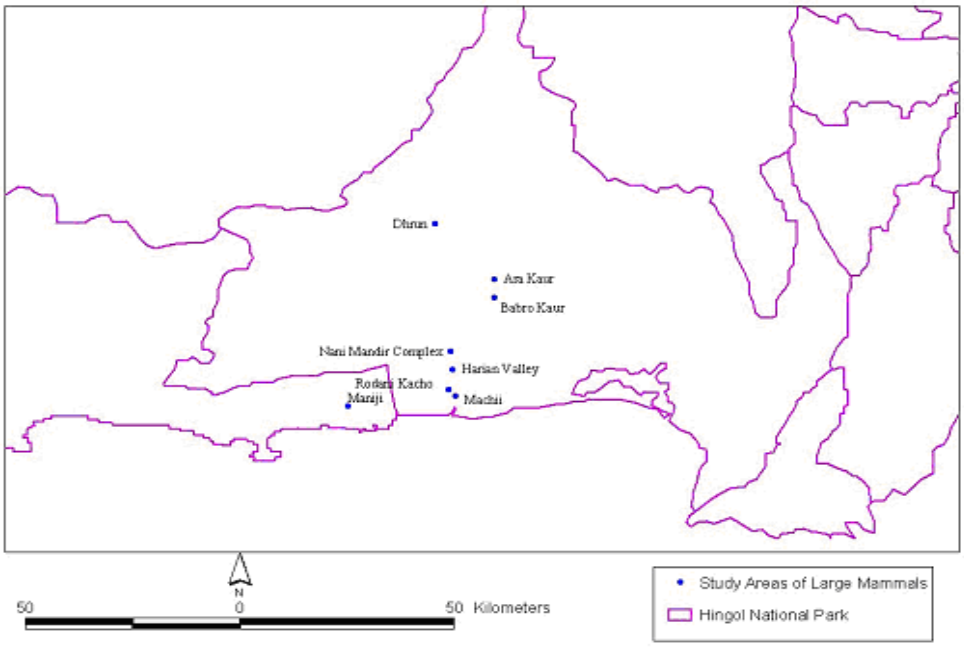

Fig. 1. Study areas of key mammalian species and birds of Hingol National Park.

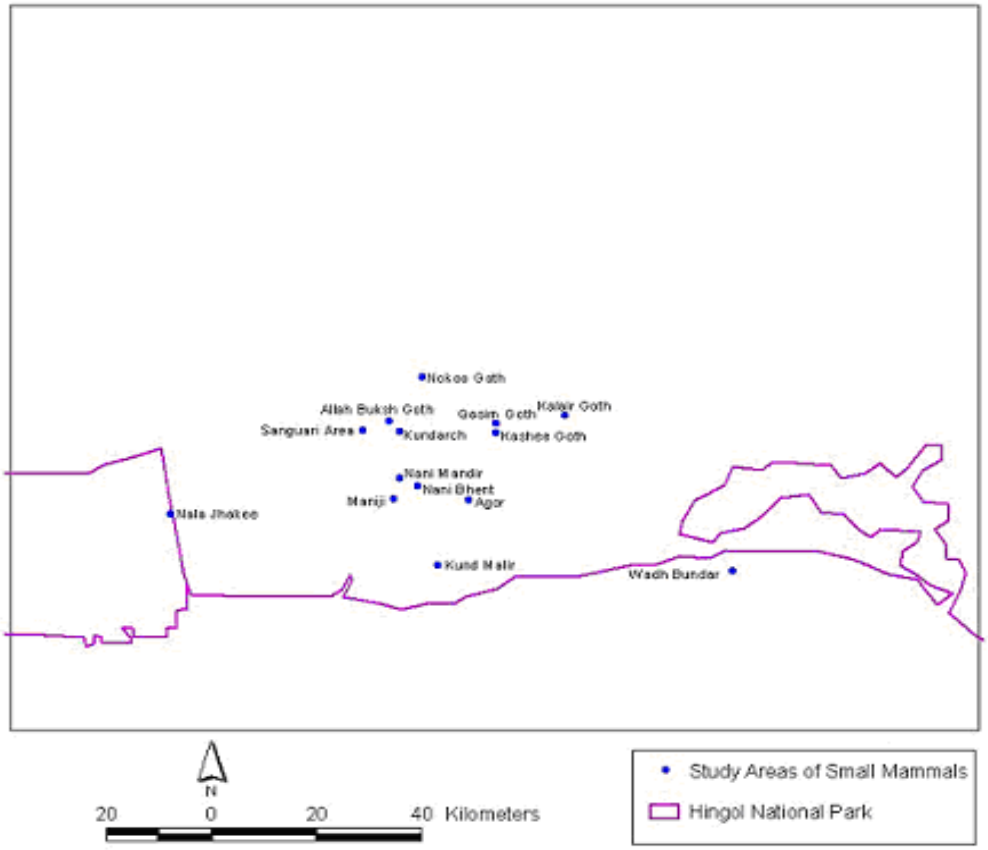

Fig. 2. Study areas of small mammals and birds of Hingol National Park.

human presence from a long distance. Hence, the method of roadside counts was applied to locate and estimate the population of different mammalian species. In this method, the observer travels by motor vehicle along roads and trails while the sighted number of individuals of the species being estimated is tallied and related to the number of km travelled (Brower *et al.*, 1990). This method has some advantages such as; travelling by

vehicle disturbs the animals and there is always a chance to observe the animals along the road / track from a distance of few meters. Secondly, by this method large areas can be covered quickly and easily by only two persons. The roadside counts technique was applied during survey along the coastal highway, mostly for nocturnal mammals like foxes, jackals, cats as well as for the diurnal mammals e.g., mongoose. For this purpose, 4 x 4 vehicles were driven at a slow speed (7km/h) on inter-compartmental tracks, sandy plains river bank (4km/h) and on rough tracks along water channels at Hingol River (3km/h) in the park. These roadside counts were carried out during early morning, at dusk and during night by using search lights on top of the vehicle.

Line Transects

The line transect or strip census method of population estimation involves counting the animals seen by an observer traversing a predetermined transect line and recording the distances at which they were seen or flushed. The average of the flushing distance is determined and used to calculate the effective width of the strip covered by the observer. The population for the entire area is then considered to be the number of animals flushed, divided by the area of the strip and multiplied by the total area (Schemnitz, 1980).

$$P = AZ / 2XY$$

Where P = population
A = total area of study
Z =number of animals flushed
Y =average flushing distance
X =length of strip

Line transects or strip census method is particularly a useful technique when animals are difficult to see and must be flushed to be counted. This methodology was applied in HNP for estimating large mammals eg., Ibex, Urial, Chinkara etc. The transect method was also used for surveys of marine mammals in HNP. The transect was randomly selected from the chart prior to leaving shore. Large and medium sized boats were used during the survey. The boat speed was maintained below 12 knots and the width of transect was 25 m on either side of the boat. Two observers and one recorder worked at a time. Each observer watched 90^0 in an arc sweeping one quarter on front view from mid boat. The auto focus binoculars were used for observations.

Pellet Counts

Fecal material such as pellets counted in a specific area is a good technique for locating large mammals and assessing their population. This technique involves removing all pellet groups from plots and then estimating from subsequent observations on those plots the number of groups per hectare to compare animal use of areas between sampling periods. In some cases it is not possible to remove all the pellet groups from an area. Therefore, under such circumstances; an observer with a little practice can identify the fresh pellets depending on the color and dryness of the pellets. Ten to fifteen 100 sq. m plots (7.07 X 14.14) can be used for this purpose. These plots should be checked every three to seven days and the periods between sampling should not be so long that feces will decompose or be destroyed by weather or insects. A random selection of plots in the study area and the number of pellets groups in each plot were tallied and summed (Brower *et al*., 1990).

The number of pellet group per unit area is determined as an index of density (ID) and determined as:

$$ID = n / A$$

where, n is the sum of pellet group counted over all plots and A is the total area sampled (i.e., the sum of the areas of all the plots).

This method is effective in habitats with dry weather and little or no dung beetle activity where pellets groups remain preserved between sampling periods. After counting pellets, one must be assured that they will not be counted on successive sampling periods so they should be removed by the observer if they will not disappear by natural processes. Defecation rates for the species under the study are estimated if it is desired to convert pellet counts to number of animals.

Techniques and tools for survey of small mammals

Trapping

Sherman Traps were used to collect the live specimens. Traps were set on a line approx 500 m long and approx 10 m apart. Each trap was marked by a colored ribbon to locate the traps easily. The traps were set in the afternoon and checked early morning. The trapped animals were each carefully transferred into an already weighed transparent polythene bag. The species and sex of the trapped animals were noted. Other data for each trap, such as date of trap setting, date of data collection, habitat, location, elevation and weather conditions were recorded on a data sheet. After recording the data, the animals were released. Specimens with some doubt in identification were preserved in 10% formalin and brought to laboratory and identified. Specimens of each species were preserved as voucher specimens.

A mixture of different food grains mixed with fragrant seeds was used as bait to attract small mammals. Wheat and rice were used as food grains while peanut butter coriander, oats and honey were used for fragrance. This bait was very successful in the study area probably due to overall food shortage and also because four ingredients were used for fragrance. Freshly prepared

bait was used on every trapping day. Only a small amount of bait was put on the platform near the traps. Because of limited time for surveys, trapping was done only at night at each of the sites and for best results trapping continued at least for 3 nights. To supplement low intensity trapping during field surveys, other data collection procedures such as active searching (day and night), spot light search, and interviews of local peoples, visible signs and literature review were also adopted.

Spot Light Method

This method is used at night for locating small and large mammals such as Hare, Porcupine, Hedgehog, Fox, Wild Cat, Jackal etc. because all these nocturnal animals move for food. In this way the populations of different species at different localities were estimated.

Counting of Fresh Holes and Tracks

According to Brower *et al*. (1990) the holes and tracks method can be used to determine the population range and status of small mammals. Fresh holes and tracks were counted in the study area of one sq. km, which provided population estimate.

Several bird surveys were undertaken during the study. For bird identification, field guides such as Grimmett *et al*. (1988) and Khanum *et al*. (1980) were used.

RESULTS AND DISCUSSION

In this study, vertebrate biodiversity and key mammalian species status of Hingol National Park was determined for the selected sites, using several methods and survey techniques for the observation, census and documentation of the mammalian fauna, and other vertebrate biodiversity from 2005 to 2009. During the study, 16 mammalian species have been recorded including three large and 13 small mammal species

Population and Status of Key Mammalian Species

Three key mammalian species have been recorded during 2005 to 2007. Ibex (*Capra aegagrus*) was rated common, while Urial (*Ovis vignei*), and Chinkara (*Gazella bennettii)* less common. In 2005, Ibex was rated 79.64%, Urial 10.32%, and Chinkara 10.02% (Table 3). In 2006, Ibex was rated 78.53%, Urial 11.12%, and Chinkara 10.34% (Table 4). In 2007, Ibex was rated 78.29%, Urial 11.18%, and Chinkara 10.51% (Table 5). During 2008 and 2009, Wild goat (*Capra aegagrus*) was rated as common, while Urial (*Ovis vignei*), and Chinkara (*Gazella bennettii*) less common. In 2008, Wild goat was rated 79.16%, Urial 11.45 %, and Chinkara 9.37% (Table 6). In 2009, Wild goat was rated 80%, Urial as 11.6%, and Chinkara 8.4% (Table 7). The population of key species at Nani Mandir Complex, Rodaini Kacho, Harian Valley, Dhrun, Machii, Maneji, Ara Kaur, and Babro Kaur areas has also been summarized in tables 8-10.

Ibex (*Capra aegagrus*)

There are three key mammalian species in HNP, and *Capra aegagrus* (Ibex) is one of them. The estimated population of Ibex was observed was 540 in 2005, 600 in 2006, 700 in 2007, 760 in 2008 and 800 in 2009 in different areas of the park (Table 8). Males, females, yearlings and young ones were also included in count. During the study period 2005 – 2009, the habitat conditions are better as both feed and shelter are in plenty in HNP. Even though the Ibex has to face the hunting pressure from different sources and disturbance at different times of the year from the pilgrims to Nani Mandir area and from the livestock herders, its population is still good. Livestock pressure in the area is the deciding factor in the distribution of the Ibex. In the face of competition with the livestock, Ibex either leave the area or their visitation is reduced.

Urial (*Ovis vignei*)

During the study period, *Ovis vignei* (Urial) was rated as less common. The estimated population of Urial was observed was 70 in 2005, 85 in 2006, 100 in 2007, 110 in 2008 and 116 in 2009 in different areas of the park (Table 9). The Urial population has faced the hunting pressure due to easy access to its habitat and the competition with the livestock. However, during our study, no direct evidence of hunting pressure on Urial was found. The reason for the decline could be the deterioration in habitat conditions and competition with livestock. (Scanty population demands further studies and adoption of conservation measures). Urial habitat was observed in the foothill areas, close to the mountains where a reasonably good shelter may be available.

Chinkara (*Gazella bennettii*)

Gazella bennettii (Chinkara) was also rated as less common. Chinkara being distributed in the plain area is susceptible to hunting pressure as these areas are easily approachable even on motor cycles. This was evident by the presence of signs of motor cycles in many areas. The condition of the animals seen was good and did not suggest that they were not reproducing. The habitat conditions in the area were suitable. There was no indication of a competition with the livestock as no interaction was witnessed. Chinkara was observed in specific habitat *viz*., large plain areas in the valley bottoms and vast nullah beds. They move to the mountains or even to the foothill. Low population of Chinkara needs immediate attention and further studies especially into the population structure and non-recruitment to the population are required. The estimated population of Chinkara was observed to be 68 in 2005, 79 in 2006, 94 in 2007, 90 in 2008 and 84 in 2009 in different areas of the park (Table 10).

Table 3. Population of key Mammalian Species of Hingol National Park in 2005.

S. No	Study Area	Ibex (*Capra aegagrus*)	Urial (*Ovis vignei*)	Chinkara (*Gazella bennettii*)	Total	%
1.	NaniMandir Complex	325	-	-	325	47.93
2.	Rodaini Kacho	110	11	10	131	19.32
3.	Harian Valley	40	09	13	62	9.14
4.	Dhrun	18	-	-	18	2.65
5.	Machii	25	14	-	39	5.75
6.	Maneji	22	15	12	49	7.22
7.	Ara Kaur	-	11	17	28	4.12
8.	Babro Kaur	-	10	16	26	3.83
	Total	540	70	68	678	
	%	79.64	10.32	10.02		

Table 4. Population of key Mammalian Species of Hingol National Park in 2006.

S. No	Study Area	Ibex (*Capra aegagrus*)	Urial (*Ovis vignei*)	Chinkara (*Gazella bennettii*)	Total	%
1.	NaniMandir Complex	360	-	-	360	47.12
2.	Rodaini Kacho	120	13	12	145	18.97
3.	Harian Valley	44	10	16	70	9.16
4.	Dhrun	20	-	-	20	2.61
5.	Machii	30	17	-	47	6.15
6.	Maneji	26	18	12	56	7.32
7.	Ara Kaur	-	15	21	36	4.71
8.	Babro Kaur	-	12	18	30	3.92
	Total	600	85	79	764	
	%	78.53	11.12	10.34		

Table 5. Population of key Mammalian Species of Hingol National Park in 2007.

S. No	Study Area	Ibex (*Capra aegagrus*)	Urial (*Ovis vignei*)	Chinkara (*Gazella bennettii*)	Total	%
1.	NaniMandir Complex	415	-	-	415	46.42
2.	Rodaini Kacho	140	14	15	169	18.90
3.	Harian Valley	50	12	20	82	9.17
4.	Dhrun	29	-	-	29	3.24
5.	Machii	36	20	-	56	6.26
6.	Maneji	30	20	16	66	7.38
7.	Ara Kaur	-	18	22	40	4.47
8.	Babro Kaur	-	16	21	37	4.13
	Total	700	100	94	894	
	%	78.29	11.18	10.51		

Population and Status of Small Mammals

From 2005 – 2009, thirteen species of small mammals have been recorded. Based on the data, House Mouse (*Mus musculus*), Balochistan Gerbil (*Gerbillus nanus*), Palm Squirrel (*Funambulus pennantii*), Afghan Hedgehog (*Hemiechinus auritus*), House Rat (*Rattus rattus*), Porcupine (*Hystrix cristatus*), Indian Gerbil (*Tatera* indica), and Grey Spiny Mouse (*Mus saxicola*) were rated as common, while Cairo Spiny Mouse (*Acomys cahirinus*), Cape Hare (*Lepus capensis*), Mouse like Hamster (*Callomyscus bailwardi*), and Indian Desert Jird (*Meriones hurrianae*) were rated as less common, and during 2006 – 2009, Persian Jird (*Meriones persicus*) was rated as rare.

In 2005, House Mouse was rated as 12.17%, Balochistan Gerbil 8.86%, Cairo Spiny Mouse 5.79%, Palm Squirrel 11.34%, Cape Hare 3.54%, Mouse like Hamster 4.49%,

Table 6. Population of key Mammalian species of Hingol National Park in 2008.

S. No	Study Area	Ibex (*Capra aegagrus*)	Urial (*Ovis vignei*)	Chinkara (*Gazella bennettii*)	Total	%
1.	Nani Mandir Complex	445	-	-	445	46.35
2.	Rodaini Kacho	148	16	14	178	18.54
3.	Harian Valley	56	14	19	89	9.27
4.	Dhrun	34	-	-	34	3.54
5.	Machii	42	22	-	64	6.66
6.	Maneji	35	22	16	73	7.60
7.	Ara Kaur	-	19	21	40	4.16
8.	Babro Kaur	-	17	20	37	3.85
	Total	760	110	90	960	
	%	79.16	11.45	9.37		

Table 7. Population of key Mammalian Species of Hingol National Park in 2009.

S. No	Study Area	Ibex (*Capra aegagrus*)	Urial (*Ovis vignei*)	Chinkara (*Gazella bennettii*)	Total	%
1.	NaniMandir Complex	467	-	-	467	46.7
2.	Rodaini Kacho	155	17	13	185	18.5
3.	Harian Valley	59	15	18	92	9.2
4.	Dhrun	38	-	-	38	3.8
5.	Machii	44	23	-	67	6.7
6.	Maneji	37	23	15	75	7.5
7.	Ara Kaur	-	20	20	40	4
8.	Babro Kaur	-	18	18	36	3.6
	Total	800	116	84	1000	
	%	80	11.6	8.4		

Table 8. Population of Ibex (*Capra aegagrus*) in HNP during 2005 to 2009.

S. No.	Study Area	2005	2006	2007	2008	2009
1.	Nani Mandir Complex	325	360	415	445	467
2.	Rodaini Kacho	110	120	140	148	155
3.	Harian Valley	40	44	50	56	59
4.	Dhrun	18	20	29	34	38
5.	Machii	25	30	36	42	44
6.	Maneji	22	26	30	35	37
	Total	540	600	700	760	800

Afghan Hedgehog 10.87%, House Rat 9.69%, Indian Desert Jird 6.38%, Porcupine 10.52%, Indian Gerbil 9.10%, and Grey Spiny Mouse 7.21%.

In 2006, House Mouse was rated as 11.12%, Balochistan Gerbil 10.01%, Cairo Spiny Mouse 6.06%, Palm Squirrel 11.12%, Cape Hare 5.35%, Mouse like Hamster 4.55%, Afghan Hedgehog 11.12%, House Rat 8.08%, Indian Desert Jird 4.85%, Porcupine 9.90%, Indian Gerbil 8.80%, Grey Spiny Mouse 7.88%, and Persian Jird 1.01%.

In 2007, House Mouse was rated as 13.64%, Balochistan Gerbil 9.93%, Cairo Spiny Mouse 6.14%, Palm Squirrel 6.50%, Cape Hare 4.06%, Mouse like Hamster 3.25%, Afghan Hedgehog 11.29%, House Rat 10.38%, Indian Desert Jird 6.05%, Porcupine 9.93%, Indian Gerbil 9.30%, Grey Spiny Mouse 8.58%, and Persian Jird 0.90% (Table 11).

In 2008, House Mouse was rated as 12.25%, Balochistan Gerbil 10.22%, Cairo Spiny Mouse 6.70%, Palm Squirrel 6.79%, Cape Hare 3.79%, Mouse like Hamster 3.08%, Afghan Hedgehog 11.37%, House Rat 9.96%, Indian Desert Jird 6.17%, Porcupine 10.40%, Indian Gerbil 8.73%, Grey Spiny Mouse 8.73%, and Persian Jird 1.76% (Table 11).

In 2009, House Mouse was rated as 12.33%, Balochistan Gerbil 10.42%, Cairo Spiny Mouse 6.68%, Palm Squirrel

Table 9. Population of Urial (*Ovis vignei*) in HNP during 2005 to 2009.

S. No.	Study Area	2005	2006	2007	2008	2009
1.	Rodaini Kacho	11	13	14	16	17
2.	Harian Valley	09	10	12	14	15
3.	Machii	14	17	20	22	23
4.	Maneji	15	18	20	22	23
5.	Ara Kaur	11	15	18	19	20
6.	Babro Kaur	10	12	16	17	18
	Total	70	85	100	110	116

Table. 10. Population of Chinkara (*Gazella bennettii*) in HNP during 2005 to 2009.

S. No.	Study Area	2005	2006	2007	2008	2009
1.	Rodaini Kacho	10	12	15	14	13
2.	Harian Valley	13	16	20	19	18
3.	Maneji	12	12	16	16	15
4.	Ara Kaur	17	21	22	21	20
5.	Babro Kaur	16	18	21	20	18
	Total	68	79	94	90	84

Table. 10. Population of Chinkara (*Gazella bennettii*) in HNP during 2005 to 2009.

S. No.	Study Area	2005	2006	2007	2008	2009
1.	Rodaini Kacho	10	12	15	14	13
2.	Harian Valley	13	16	20	19	18
3.	Maneji	12	12	16	16	15
4.	Ara Kaur	17	21	22	21	20
5.	Babro Kaur	16	18	21	20	18
	Total	68	79	94	90	84

Table 11. Population of Small Mammals in Hingol National Park 2005 to 2009.

S. No	Year	House Mouse	Baloch Gerbil	Cairo Spiny Mouse	Palm Squirrel	Cape Hare	Mouse like Hamster	Afghan Hedgehog	House Rat	Indian Desert Jird	Por-cupine	Indian Gerbil	Grey Spiny Mouse	Persian Jird	Total
1	2005	103	75	49	96	30	38	92	82	54	89	77	61	0	846
2	2006	110	99	60	110	53	45	110	88	48	98	80	78	10	989
3	2007	151	110	68	72	45	36	125	115	67	110	103	95	10	1107
4	2008	139	116	76	77	43	35	129	113	70	118	99	99	20	1134
5	2009	142	120	77	80	42	33	133	121	73	122	104	88	16	1151
Total		645	520	330	435	213	187	589	519	312	537	463	421	56	5227

6.95%, Cape Hare 3.64%, Mouse like Hamster 2.86%, Afghan Hedgehog 11.55%, House Rat 10.51%, Indian Desert Jird 6.34%, Porcupine 10.59%, Indian Gerbil 9.03%, Grey Spiny Mouse 7.64%, and Persian Jird 1.34% (Table 11).

Other Vertebrate Biodiversity

In the Hingol National Park the following vertebrates have been reported. However, none was seen during the study (Zehra, 2009):

Desert Wolf (*Canis lupus*)

The presence of Desert Wolf (*Canis lupus*) was reported in valleys viz Ara Kaur, Babro Kaur, adjoining Tranche valley, and Dhrun areas.

Caracal or Bashoshah (*Felis caracal*)

Caracal was reported only from Rodaini Kachho area.

Common Leopard (*Panthera pardus saxicolor*)
Common Leopard signs were reported from at least two valleys (between Dhrun and Rodaini Kacho). Local people also talked about the occurrence of this animal.

Asiatic Jackal (*Canis aureus*)
Asiatic Jackal footprints were seen in Pachree valley.

Pangolin or Scaly anteater (*Manis crassicaudata*)
Local people reported Pangolin occurrence in other valleys also but this could not be confirmed. Its footprints were seen in Pacchri valley only.

Wild Boar (*Sus scrofa davidi*)
Wild Boar was recorded through the footprints in Harian and Pachree valley areas.

Birds
In Pakistan, 666 bird species have been recorded, out of which 380 species have been recorded in Balochistan (Ghalib *et al*., 2004). Azam (2004) reported 108 species belonging to 68 genera 37 families and 14 orders from HNP. The avifauna of the HNP consists of resident as well as migratory bird species. During the study, we have observed many bird habitats including; coastal area, estuarine area, river, mangrove area, mountains and desert. During the study 165 bird species were recorded in which 75 were resident and 90 were migratory species (Table 12).

Table 12. Birds of Hingol National Park, observed during 2005-2009.

S. No.	Scientific name	Common name
1.	*Phalacrocorax carbo*	Large Cormorant
2.	*Phalacrocorax niger*	Little Cormorant
3.	*Pelecanus crispus*	Dalmatian Pelican
4.	*Pelecanus onocrotalus*	White or Rosy Pelican
5.	*Pelecanus philippensis*	Spotted billed Pelican
6.	*Dupetor flavicollis*	Yellow-throated black bittern
7.	*Egretta alba*	Large Egret or Great Egret
8.	*Egretta garzetta*	Little Egret
9.	*Egretta gularis*	Indian Reef Heron
10.	*Egretta intermedia*	Smaller or Median Egret
11.	*Ardea cinerea*	Grey Heron
12.	*Ardea goliath*	Giant Heron
13.	*Ardea purpurea*	Purple Heron
14.	*Ciconia nigra*	Black Stork
15.	*Psuedibis papillosa*	Black Ibis
16.	*Platalea leucoirodia*	Spoonbill
17.	*Phoenicopterus roseus*	Flamingo
18.	*Anas acuta*	Pintail
19.	*Anas crecca*	Common Teal
20.	*Anas clypeata*	Shoveller
21.	*Anas penelope*	Wigeon
22.	*Anas strepera*	Gadwall
23.	*Milvus migrans*	Black Kite
24.	*Haliastur indus*	Brahminy Kite
25.	*Haliaeetus leucoryphus*	Pallas's Fishing Eagle
26.	*Gypaetus barbatus*	Bearded Vulture
27.	*Neophron percnopterus*	Egyptian Vulture
28.	*Gyps fulvus*	Indian Griffon Vulture
29.	*Circus aeroginosus*	Marsh Harrier
30.	*Accipiter badius*	Central Asian Shikra
31.	*Accipiter nisus*	Eurasian Sparrow Hawk
32.	*Aquila heliaca*	Imperial Eagle
33.	*Aquila rapax*	Tawny Eagle
34.	*Pandion haliaeetus*	Osprey
35.	*Falco columbarius*	Pallid Merlin
36.	*Falco concolor*	Sooty Falcon
37.	*Falco jugger*	Lagger Falcon
38.	*Falco naumani*	Lesser Kestrel
39.	*Falco peregrinus*	Peregrine Falcon
40.	*Falco tinnunculus*	Kestrel
41.	*Ammoperdix griseogularis*	See-see Partridge
42.	*Francolinus pondicerianus*	Grey Patridge
43.	*Conturnix conturnix*	Common Quail
44.	*Gallinula chloropus*	Moorhen
45.	*Fulica atra*	Coot
46.	*Chlamydotis undulata*	Houbara Bustard
47.	*Himantopus ostralegus*	Oyster Catch or Sea-Pie
48.	*Himantopus himantopus*	Black-winged Stilt
49	*Dromas ardeola*	Crab Plover
50.	*Burhinus oedicnemus*	Stone curlew/ Eurasian Thick-Knee
51.	*Esacus recurvirostris*	Great Stone Plover/Thick-Knee
52.	*Charadrius alexandrinus*	Kentish Plover
53.	*Charadrius dubius*	Little Ringed Plover
54.	*Charadrius hiaticula*	Ringed Plover
55.	*Charadrius leschenaultii*	Large Sand Plover
56..	*Charadrius mongolus*	Lesser Sand Plover
57.	*Vanellus gregarious*	Sociable Lapwing
58.	*Vanellus indicus*	Red Wattled Lapwing
59.	*Vanellus leucurus*	White-tailed Lapwing

S. No.	Scientific name	Common name
60.	*Calidris alpinus*	Dunlin
61.	*Calidris minutus*	Little Stint
62.	*Calidris temminckii*	Temminck's Stint
63.	*Calidris testaceus/ferruginea*	Curlew-Sandpiper
64.	*Limicola falcinellus*	Broad billed Sandpiper
65.	*Philomachus pugnax*	Ruff
66.	*Capella gallinago*	Common or Fantail Snipe
67.	*Limosa lapponica*	Ber tailed Godwit
68.	*Limosa limosa*	Black tailed Godwit
69.	*Numenius arquata*	Curlew
70.	*Numenius phaeopus*	Whimbrel
71.	*Tringa hypoleucos*	Common Sandpiper
72.	*Tringa nebularia*	Greenshank
73.	*Tringa ochropus*	Green Sandpiper
74.	*Tringa stagnatilis*	Marsh Sandpiper
75.	*Tringa terek*	Terek Sandpiper
76.	*Tringa totanus*	Redshank
77.	*Larus argentatus*	Herring Gull
78.	*Larus brunnicephalus*	Brown-headed Gull
79.	*Larus cachinans*	Yellow-legged Gull
80.	*Larus fuscus*	Black-backed Gull
81.	*Larus genei*	Slender billed Gull
82.	*Larus ichthyaetus*	Great Black headed Gull or Pallas's Gull
83.	*Larus ridibundus*	Black-headed Gull
84.	*Gelochelidon nilotica*	Gull billed Tern
85.	*Hydroprogne caspia*	Caspian Tern
86.	*Sterna albifrons*	Little Tern
87.	*Sterna bengalensis*	Lesser Crested Tern
88.	*Sterna hirundo*	Common Tern
89.	*Sterna repressa*	White-cheeked Tern
90.	*Sterna sandvicensis*	Sandwich Tern
91.	*Chlidonias hybrida*	Whiskered Tern
92.	*Pterocles coronatus*	Caronetted Sandgrouse
93.	*Pterocles indicus*	Painted Sandgrouse
94.	*Pteroceles orientalis*	Imperial or Black-bellied Sandgrouse
95.	*Columba livia*	Blue Rock Pigeon
96.	*Streptopelia decaocto*	Ring Dove
97.	*Streptopelia senegalensis*	Little Brown or Senegal Dove
98.	*Psittacula krameri*	Rose Ringed Parakeet
99.	*Caprimulgus mahrattensis*	Syke's or Sind Nightjar
100.	*Athene brama*	Spotted Owlet
101.	*Apus affinis*	House Swift
102.	*Apus apus*	Common Swift
103	*Apus pallidus*	Pale Brown or Pallid Swift

S. No.	Scientific name	Common name
104.	*Alcedo atthis*	Common Small Blue Kingfisher
105.	*Halcyon smyrnensis*	White breasted Kingfisher
106.	*Merops orientalis*	Small Green Bee-eater
107.	*Merops superciliosus*	Blue-checked Bee-eater
108.	*Coracias bengalensis*	Ruller or Blue Jay
109.	*Upupa epops*	Hoopoe
110.	*Picoides assimilis*	Sind Pied Woodpecker
111.	*Eremopterix grisea*	Ashycrowned Finch-lark
112.	*Eremopterix nigriceps*	Blackcrowned Finch-lark
113.	*Ammomanes deserti*	Indian Desert Finch-lark
114.	*Alaemon alaudipes*	Hoopoe Lark / Bifasciated Lark
115.	*Calandrella acutirostris*	Hume's Short-toed Lark
116.	*Galerida cristata*	Crested Lark
117.	*Riparia paludicola*	Brown-throated Sand Martin
118	*Riparia riparia*	Collared Sand Martin
119.	*Delichon urbica*	Common House Martin
120.	*Hirundo daurica*	Redrumped Swallow
121.	*Hirundo rustica*	Barn Swallow
122.	*Hirundo smithi*	Wire-tailed Swallow
123.	*Motacilla alba*	White or Pied Wagtail
124.	*Motacilla cinerea*	Grey Wagtail
125.	*Motacilla flava*	Yellow Wagtail
125.	*Anthus trivialis*	Tree Pipit
127.	*Pycnonotus cafer*	Red-vented Bulbul
128.	*Pycnonotus leucogenys*	White-cheeked Bulbul
129.	*Lucsinia svecica*	Bluethroat
130.	*Oenanthe alboniger*	Hume's Chat or Wheatear
131.	*Oenanthe deserti*	Desert Chat or Desert Wheatear
132.	*Oenanthe isabellina*	Isabelline Wheatear
133.	*Oenanthe monacha*	Hooded Chat or Wheatear
134.	*Phoenicurus ochruros*	Black Redstart
135.	*Saxicola ferea*	Gray Bushchat
136.	*Saxicola torquata*	Collared Indian Bush Chat or Stone Chat
137.	*Acrocephalus dumetorumn*	Blyth's Reed Warbler

S. No.	Scientific name	Common name
138.	*Acrocephalus stantoreus*	Clamorous Warbler
139.	*Phylloscopus collibita*	Chiffchaff
140.	*Phylloscopus neglectus*	Plain Leaf Warbler
141.	*Prinia buchanani*	Rufous Fronted Wren Warbler
142.	*Sylvia curruca*	Lesser Whitethroat
143.	*Sylvia nana*	Desert Warbler
144.	*Ficedula parva*	Red throated Flycatcher
145.	*Rhipidura aureola*	White browed Flycatcher
146.	*Turdoides caudatus*	Common Babbler
147.	*Nectarinia asiatica*	Purple Sunbird
148.	*Lanius excubitor*	Grey Shrike
149.	*Lanius isabellinus*	Rufous-tailed or Isabelline Shrike
150.	*Lanius schach*	Rufous-backed Shrike
151.	*Lanius vittatus*	Baybacked Shrike
152.	*Dicrurus adsimilis*	Black Drongo or King Crow
153.	*Corvus corax*	Common Raven
154.	*Corvus ruficollis*	Dasert Raven
155.	*Corvus splendens*	Indian House Crow
156.	*Acridotheres tristis*	Indian Myna
157.	*Passer domesticus*	House Sparrow
158.	*Passer hispaniolensis*	Spanish Sparrow
159.	*Passer pyrrhonotus*	Sind Jungle Sparrow
160.	*Passer xanthocollis*	Sind Yellow throated Sparrow
161.	*Lonchura malabarica*	Common Silverbill or White throated Munia
162.	*Carpodacus erythrinus*	Common Rosefinch
163.	*Emberiza cia*	Rock Bunting
164.	*Emberiza melanocephala*	Black headed Bunting
165.	*Emberiza striolata*	Striped or House Bunting

Fish fauna

Following fourteen fish species have been recorded: *Cyprinion watsoni*, *Cyprinion microphthalmum*, *Cyprinion milesi*, *Schistura balochiorum*, *Tor pititora*, *Scaphiodom irregularis*, *Jalmius soldado*, *Pseudorhombus arsius*, *Mugil cascasia*, *Mugil cephalus*, *Scatophagus argus*, *Dastatis gugei*, *Aspidoparia morar* and *Crossocheilus diplocheilus*.

Amphibians and Reptiles

During the study, two species of amphibian *Rana cyanophlyctis* (Skittering Frog) and *Bufo stomaticus* (Indus Valley Toad) have been recorded. Nine species of reptiles including two species of turtle *Chelonia mydas* (Green turtle), *Eretmochelys imbricata* (Hawksbill Turtle), five species of lizards *Hemidactylus brooki*, (House Gecko), *Trapelus agilis* (Brilliant Agama), *Acanthodactylua cantrois* (Indian Fringed-toed Lizard), *Varanus griseus* (Desert Monitor), *Crossobamon orientalis* (Sand Sind Gecko), one species of *Crocodylus palustris* (Marsh Crocodile) and one snake species *Echis carinatus* (Saw Scaled Viper) have been observed.

Ecotourism and Hingol National Park

Tourism is a principal export for 83% of developing countries. For the world's poorest countries, tourism is the 2nd most important source of foreign exchange, after oil (Hospodarsky and Lee, 2007). Due to aesthetic venues like mountains, wetlands, river, estuary, sea beach, mud volcano, sand dunes, and cultural attractions, the HN park has the potential to be developed as Eco-tourist Park, and eco-tourism can increase local jobs, income and other benefits for local peoples. The Hingol National Park area also has the Nani Mandar, a popular sacred place for the Hindus.

ACKNOWLEDGMENTS

This paper was presented in the International Congress Healthy Parks Healthy People held at Melbourne Convention Centre, Australia, in April 2010, and for paper presentation, traveling grant was provided by the Higher Education Commission (HEC), for which the authors deeply thank the HEC. We also thank Prof. Jamil Kazmi, Department of Geography, University of Karachi for preparation of study areas map.

REFERENCES

Ahmad, W. 2009. National Parks in Pakistan. Natura. 33 (1):24-28.

Azam, MM. 2004. Avifaunal Diversity of Hingol National Park. Rec. Zool. Surv. Pakistan. 15:7-15.

Brower, J., Zar, J. and Ende, C. 1990. Field and laboratory methods for general ecology. Wm . C . Brown Publishers. 2460 Kerper Boulevard, Dubuque. A 52001.

Hospodarsky, D. and Lee, M. 2007. Ecotourism and Natural Resources Management. International Seminar on Forest Administration and Management, USA.

Ghalib, SA., Khan, MZ., Zehra, A. and Khan, AR. 2004. Current Population Status of the Birds of Balochistan, Pakistan. J. Nat. Hist. Wildlife. 3(2): 51-62.

Ghalib, SA., Jabbar, A., Khan, AR. and Zehra, A. 2007. Current status of the mammals of Balochistan. Pakistan J. Zool. 39(2):117-122.

Grimmett, R., Inskipp, C. and Inskipp, T. 1988. Birds of the Indian sub-continent. Oxford University Press, Mumbai.

Khanum, Z., Ahmed, MA. and Ahmed, M. 1980. A Check list of Birds of Pakistan with Illustrated Keys to their Identification. Rec. Zool. Surv. 9 (1&2):138pp.

Khan, MZ. 2004. Protected areas with reference to Pakistan. J. Nat. Hist. Wildlife 3(1): 7-2.

Khan, MZ. and Siddiqui, S. 2005. The Vertebrate biodiversity of Hazarganji Chiltan National Park, Balochistan. J. Nat. Hist. Wildlife. 4(1):93-99.

Management Plan HNP (draft). 2006. Balochistan Forest and Wildlife Department. pp 198.

Schemnitz, SD. 1980. Wildlife Management Techniques Manual. The Wildlife Society, Inc 5410 Grosvenor Lane, Bethesda, Maryland 20814.

Zehra, A. 2009. Current Status of the Mammals of Hingol National Park. Ph.D thesis, Department of Zoology, University of Karachi, Karachi.

Received: Jan 4, 2010; Revised: April 27, 2010; Accepted: May 17, 2010

SENRA Academic Publishers, Burnaby, British Columbia
Vol. 4, No. 2, pp. 1163-1168, June 2010
ISSN: 1715-9997

Canadian Journal of pure&applied sciences

EFFECT OF MAGNESIUM CHLORIDE AND SODIUM FLUORIDE ON VARIOUS HYDROXYPROLINE FRACTIONS IN RAT KIDNEYS

EA. Al Omireeni, *NJ Siddiqi and AS Alhomida
Department of Biochemistry, College of Science, PO Box 22452
King Saud University, Riyadh -11495, Saudi Arabia

ABSTRACT

Magnesium chloride ($MgCl_2$) has been reported to protect against sodium fluoride (NaF) induced toxicity. This study was undertaken to study the effect of $MgCl_2$ on NaF induced alteration in rat kidney hydroxyproline fractions and collagen. Four groups of rats were studied (each consisting of 4-6 rats) (i) normal rats: (ii) rats injected with $MgCl_2$: (iii) rats injected with NaF: (iv) rats injected with $MgCl_2$ followed by NaF. Results show that $MgCl_2$ and NaF treatment alone and together caused a significant ($p < 0.05$) decrease in kidney protein, free, peptide–bound, protein-bound, total hydroxyproline and soluble collagen hydroxyproline. Administration of $MgCl_2$ before NaF did not restore the altered parameters to normal levels. However administration of $MgCl_2$ before NaF restored insoluble collagen hydroxyproline which was altered by NaF to near normal levels. Though $MgCl_2$ has been reported to be protective against the toxic effect of NaF, it has no significant effect on NaF induced changes in kidney hydroxyproline/collagen except insoluble collagen Hyp.

Keywords: Sodium fluoride; hydroxyproline; collagen; magnesium chloride.

INTRODUCTION

Fluorine occurs in environment in combination with other elements as a fluoride compound (Manna *et al.*, 2007). Human beings are exposed to fluoride through food (Stannard *et al.*, 1991; Dabek and McKenzie, 1995), drinking water (Zhao, 1996) and inhalation (Gritsan *et al.*, 1995). Frequent absorption of the fluoride causes tooth decay (Neurath, 2005), damage of kidneys (Lantz *et al.*, 1987), bones (Bezerra de Menezes *et al.*, 2003), nerves (Shivarajashankara *et al.*, 2002) and muscles (Cicek *et al.*, 2005). The adverse toxic effects of fluoride arise due to a) enzyme inhibition, b) collagen break down, c) gastric damage and d) disruption of the immune system (Ahmad *et al.*, 2000). Magnesium is a mineral that is involved in over 300 reactions in the body. It is important for every organ in the body, particularly the heart, muscles, and kidneys. It also contributes to the composition of teeth and bones. Most importantly, it activates enzymes, contributes to energy production, and helps regulate the levels of other minerals in the body (Saris *et al.*, 2000).

The kidneys excrete waste products of metabolism and play an important role in maintaining the homeostasis by regulating the body water and solute balance. In addition to the excretory function, the kidneys also have an endocrine function producing hormones like renin, erythropoietin etc. The most commonly used medium for studying fluoride toxicity is urine. Acute exposure to high doses of fluoride damages renal tissue and causes renal dysfunction (Zabulyte *et al.*, 2007). In our previous studies (Al-Omireeni *et al.*, 2009) we have shown that different doses of NaF have profound effect on various hydroxyproline (Hyp) fractions in rat kidneys. Hyp is a component amino acid of collagen and has been used as an index of collagen turnover (Reddy and Enwemeka., 1996). Magnesium chloride ($MgCl_2$) has been reported to exert a protective effect on sodium fluoride (NaF) induced mortality in rats (Luoma *et al.*, 1984). The present study was carried out to study the effect of $MgCl_2$ on NaF induced changes in Hyp fractions and collagen content in rat kidneys.

MATERIALS AND METHODS

Chemicals

Chloramine-T, p-dimethylaminobenzaldeyde (Ehrlich's reagent), L-hydroxyproline, sodium acetate, citric acid, perchloric acid, n-propanol, sodium hydroxide, and acetic acid were purchased from Sigma Chemical Company, St Louis, MO, USA. Double distilled water was used throughout the study.

Animal Care

Healthy adult male Wister rats each weighting 150-200g (four to six weeks old) were obtained from Breeding Laboratory, King Saud University, Riyadh, Saudi Arabia. The animals were labeled by identifying ear notches,

*Corresponding author email: nikhat@ksu.edu.sa

housed in clean cages, and placed in the animal care room. Ethical guidelines for animal care were followed.

Effect of magnesium chloride and sodium fluoride on different Hyp fractions in rat kidneys

The following groups of rats were studied (each consisting of 4-6 rats) (i) normal rats (Control group, n = 4 - 6 rats); (ii) rats injected with $MgCl_2$ through intraperitoneal route 30 mg/kg body weight dose ($MgCl_2$ treated group); (iii) rats injected with NaF through intraperitoneal route 10 mg/kg body weight dose (NaF treated group); (iv) rats injected with $MgCl_2$ through intraperitoneal route 30 mg/kg body weight followed by NaF 10 mg/kg body weight through intraperitoneal route 30 minutes after $MgCl_2$ injection ($MgCl_2$ + NaF treated group).

Preparation of the sample

Rats were killed by carbon dioxide asphyxiation 24 hours after the final injection. The kidneys were dissected out, cleared of adhering tissues and weighed. The kidneys were then homogenized in normal saline (10% W/V) and the homogenate was used for Hyp determination as described below.

Extraction of Free, Peptide- and Protein-bound Hydroxyproline

Free and protein-bound Hyp was extracted by the method of Varghese *et al*. (1981) with slight modification. Briefly, 0.5ml of the homogenate was treated with 3 X 2 ml portion of re-rectified absolute alcohol and centrifuged at 3000rpm for 10min. The supernatants were pooled and evaporated to dryness. The residue was dissolved in suitable amount of distilled water and an aliquot of the extract was used for estimation of free Hyp. The peptide-bound Hyp was determined after alkaline hydrolysis of the ethanol extractable fraction. The pellets were dissolved in distilled water and an aliquot of the extract was used for determination of protein-bound Hyp. The free Hyp fraction was measured on an aliquot of the ethanol extracted residue without alkali hydrolysis, whereas the peptide-bound Hyp was measured after alkaline hydrolysis. The precipitate obtained on ethanol treatment of the homogenate was subjected to alkali hydrolysis to determine protein-bound Hyp. Further details about the extraction of Hyp fractions have been described previously (Siddiqi *et al*., 2000). Hyp was determined in different fractions as described in the later section.

Extraction of Soluble- and Insoluble-Collagen Hyp

Soluble- and insoluble-collagen Hyp were extracted by the method of Kivirikko *et al*. (1965). Briefly, the tissue samples were homogenized (4ml/g tissue) in a cold 0.45 M sodium chloride. The homogenate was extracted at 4^0C for 24 hours with occasional stirring, followed by centrifugation at 13000rpm for 1hour. The supernatants obtained were precipitated with 4 volumes of a cold ethanol and were centrifuged twice with 80% ethanol, twice with absolute alcohol, twice with ether and twice with warm ethanol-ether (1:2). The residues were gelatinized with distilled water at 120^0C for 3 hours and after filtration a sample of gelatine solution was used for soluble-collagen Hyp estimation as described below.

The precipitates obtained after the above centrifugation were washed 3 times with 0.45 M NaCl and twice with distilled water, after which they were extracted with absolute ethanol, ether and ethanol-ether and gelatinized as above. A sample of gelatine solution was used for insoluble-collagen Hyp estimation as described in the following section.

Determination of Hydroxyproline Concentration

Hyp was measured by the modified alkaline hydrolysis method of Reddy and Enwemeka (1996). Briefly, an aliquot of the sample was added into NaOH (2 N final concentration) and the aliquot was hydrolyzed by heating in a boiling water bath for about 3-4 hours. An aliquot of 56 mM chloramine-T reagent was added to the hydrolyzed sample and oxidation was allowed to proceed at room temperature for 25min. Then an aliquot of 1M Ehrlich's reagent (p-dimethylaminobenzaldehyde) was added to the oxidized sample and the chromophore was developed by incubating the samples at 65^0C for 20 minutes. The absorbance was read at 550 nm using an Ultrospec 2000 UV/visible spectrophotometer (Pharmcia Biotech Ltd, Science Park, Cambridge, England). The Hyp concentration in the samples was calculated from the standard curve of Hyp. Further details about the optimization, linearity, specificity, precision and reproducibility of the method have been described previously (Siddiqi *et al.,* 2000).

Determination of Total Collagen

Total collagen content was calculated from Hyp concentration assuming that Hyp constitutes 12.5% of total collagen (Edwards and O'Brien, 1980).

Statistical Analysis

Each sample was run in duplicate. The Hyp content was expressed as mean ± SD µg/gram wet tissue, for n = 4-6 rats. Hyp levels between groups were compared using one way ANOVA analysis followed by Tukey's for multiple comparison test. Values were considered significant if $p < 0.05$. Statistical analysis was performed by means of InStat® package for personal computers (GraphPad ™ Software, Inc., San Diego, USA).

RESULTS

Table 1 shows the effect of $MgCl_2$ and NaF on protein content of rat kidneys. $MgCl_2$ and NaF alone caused a significant decrease of 70% ($p<0.001$) and 24% ($p<0.01$) respectively in kidney protein content when compared to control rats. Combined treatment of $MgCl_2$ and NaF also caused a decrease of 63% ($p<0.001$) in the kidney protein content when compared to control group of rats.

Table 1. Effect of $MgCl_2$ and NaF treatment on protein content of rat kidneys.

Experimental groups	Kidney protein (mg/gram tissue)
Control	150.1 ± 37.5
$MgCl_2$	45.61 ± 2.04***
NaF	113.7 ± 22.64*
$MgCl_2$ + NaF	54.93 ± 2.88***

Rats were injected sodium fluoride (10 mg/kg body weight) and magnesium chloride (30 mg/kg body weight) through intraperitoneal route.
The rats were injected with sodium fluoride 30 minutes after magnesium chloride administration.
The animals were sacrificed 24 hours after the sodium fluoride treatment.
*P<0.05 as compared to control group (Tukey's multiple comparison test).
***P<0.001 as compared to control group (Tukey's multiple comparison test).

Table 2 shows the effect of $MgCl_2$ and NaF on various Hyp fractions in rat kidneys. $MgCl_2$ treatment of control rats caused a significant decrease of all the Hyp fractions of rat kidneys ($p < 0.001$) except protein-bound Hyp. NaF treatment also caused a significant decrease in free, peptide- bound and total Hyp concentration in rat kidneys ($p <0.001$). NaF treatment however caused no significant change ($P > 0.05$) in protein bound Hyp fractions in rat kidneys. Administration of $MgCl_2$ before NaF resulted in a tendency towards restoration of parameters altered by $MgCl_2$ or NaF towards normal level but did not completely restore them to normal levels.

Figure 1 shows the effect of $MgCl_2$ and NaF on total collagen in rat kidneys. $MgCl_2$ and NaF alone caused a significant decrease in total collagen ($p < 0.001$) in rat kidneys when compared to control rats. $MgCl_2$ injection before NaF injection caused an increase in total collagen when compared to $MgCl_2$ and NaF alone but it did not restore total collagen to normal level.

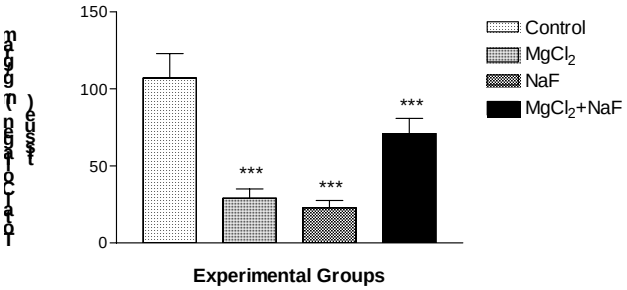

Fig. 1. Effect of magnesium chloride and sodium fluoride on total collagen content of rat kidneys.

Rats were injected magnesium chloride (30 mg/kg body weight) and sodium fluoride (10mg/kg body weight) through intraperitoneal route.
The rats were injected with sodium fluoride 30 minutes after magnesium chloride administration.
The animals were sacrificed 24 hours after the sodium fluoride treatment.
***P<0.01 as compared to 5 mg/kg body weight group (Tukey's multiple comparision test).

Figure 2 shows the effect of $MgCl_2$ and NaF on soluble collagen Hyp in rat kidneys. There was a significant decrease ($p < 0.001$) in soluble collagen Hyp in the

Table 2. Effect of $MgCl_2$ and NaF treatment on various hydroxyproline fractions in rat kidneys.

Experimental Groups	Free Hyp (µg/gm fresh tissue)	Hydroxyproline Fractions		Total Hyp (mg/gm fresh tissue)
		Peptide –bound Hyp (mg/gm fresh tissue)	Protein-bound Hyp (mg/gm fresh tissue)	
Control	329.3 ± 54.65	11.29 ± 0.88	1.04 ± 0.15	12.67 ± 0.96
$MgCl_2$	149.6 ± 22.77***	1.99 ± 0.47***	1.73 ± 0.17***	3.87 ± 0.48***
NaF	125.3± 15.94***	1.61 ± 0.91***	1.26 ± 0.23 ^{ns}	3.44 ± 0.79 ***
$MgCl_2$ + NaF	218.1 ± 11.16***	6.67 ± 1.23***	2.41 ± 0.33***	9.19 ± 1.21***

Rats were injected sodium fluoride (10 mg/kg body weight) and magnesium chloride (30 mg/kg body weight) through intraperitoneal route.
The rats were injected with sodium fluoride 30 minutes after magnesium chloride administration.
The animals were sacrificed 24 hours after the sodium fluoride treatment.
^{ns} Not siginificant as compared to control group (Tukey's multiple comparision test).
***P <0.001 as compared to control group (Tukey's multiple comparision test).

kidneys of all the experimental groups viz., $MgCl_2$ alone, NaF alone and $MgCl_2$ plus NaF treated groups when compared to control rats.

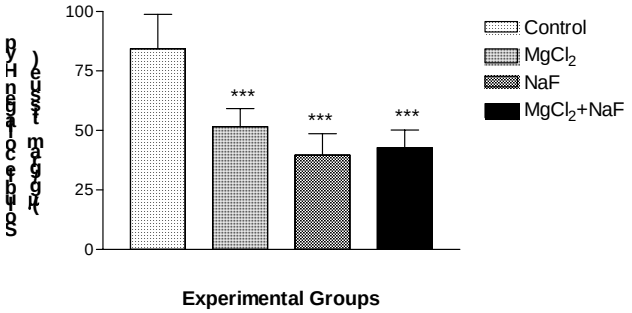

Fig. 2. Effect of magnesium chloride and sodium fluoride on soluble collagen hydroxyproline in rat kidneys.

Rats were injected sodium fluoride (10mg/kg body weight) and magnesium chloride (30mg/kg body weight) through intraperitoneal route.
The rats were injected with sodium fluoride 30 minutes after magnesium chloride administration.
The animals were sacrificed 24 hours after the sodium fluoride treatment.
***P<0.01 as compared to 5mg/kg body weight group (Tukey's multiple comparison test).

Figure 3 shows the effect of $MgCl_2$ and NaF on insoluble collagen Hyp in rat kidneys. Among all the groups studied only in the group of rats treated with NaF alone, there was a significant ($p < 0.01$) decrease in insoluble collagen Hyp in the kidneys when compared to control rats. $MgCl_2$ alone or with NaF caused no significant change ($p>0.05$) in insoluble collagen Hyp in rat kidneys.

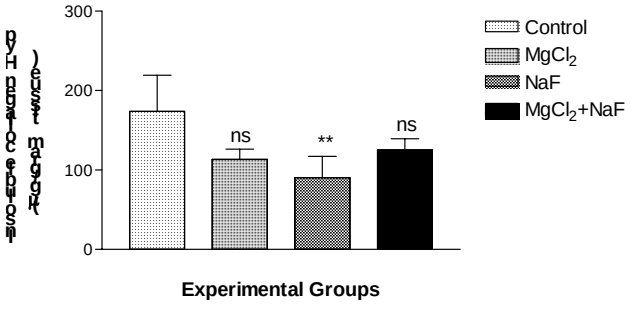

Fig. 3. Effect of magnesium chloride and sodium fluoride on insoluble collagen hydroxyproline in rat kidneys.

Rats were injected sodium fluoride and magnesium chloride through intraperitoneal route.
The rats were injected with sodium fluoride 30 minutes after magnesium chloride administration.
The animals were sacrificed 24 hours after the sodium fluoride treatment.
[ns]Not significant as compared to control group (Tukey's multiple comparison test);
**P<0.01 as compared to 5mg/kg body weight group (Tukey's multiple comparision test).

DISCUSSION

Fluoride is useful in preventing dental caries but excessive intake of fluoride can be toxic. The first noticeable signs of excessive exposure to fluoride are discoloration of the enamel. Abnormalities in mineralization processes affect by and large the osteoarticular system and are associated with changes in the density and structure of the bone presenting as irregular mineralization of the osteoid. Fluorine compounds also act on the organic part of supporting tissues, including collagen and other proteins, and on cells of the connective tissue. These interactions reduce the content of collagen proteins, modify the structure and regularity of collagen fibers and induce mineralization of collagen (Machoy-Makrzynska, 2004).

The kidneys are paired bean-shaped organs located on both sides of the spinal column. The kidneys perform a variety of functions for the body, the most important being removal of unwanted substances from the plasma, homeostasis of the body's water, electrolyte and acid/base status and participation in endocrine regulation. The amount of collagen in the kidney depends on factors like the species of the animal, its age and the presence of disease. In general collagen forms only a small proportion of the renal mass about 2% of the dry weight of renal cortex of adult rats (Weiss and Jayson, 1982) and this may be due to the presence of an active collagenolytic mechanism in the kidney (Weiss and Jayson, 1982). Nevertheless, collagen is of great physiological importance as a support for the renal parenchyma and as a component of the basement membrane. Magnesium chloride administered thirty minutes before sodium fluoride has been shown to increase the LD_{50} for fluoride from 76 to 104 mg/kg body weight (Luoma *et al.*, 1984). In the present study both $MgCl_2$ as well as NaF were found to decrease the protein content in the kidneys. Earlier studies of Birkner *et al.* (2000) have found disturbance in protein metabolism after acute dose of sodium fluoride. Though the most common medium used to study fluoride toxicity is urine, fluoride has been reported to cause renal tissue damage and disrupt renal function (Zabulyte *et al.*, 2007). Oxidative stress has been reported to be one of the factors in the pathogenesis of sodium fluoride (Ranjan *et al.*, 2009). Doses of NaF and $MgCl_2$ caused a decrease in peptide- bound Hyp. Hyp is excreted by the kidneys as small peptides (Adams and Frank, 1980). In the present study NaF treatment caused a decrease in total collagen. The degraded collagen may be excreted in the form of peptide-bound Hyp causing a decrease in peptide-bound Hyp fraction. These results are in agreement with earlier studies (Sharma, 1982[a]) which have demonstrated that fluoride interferes with the collagen biosynthesis resulting in decreased collagen content (in terms of hydroxyproline). Therefore the decrease in collagen content of kidneys of NaF treated

animals may be either due to decreased synthesis or increased degradation by collagenase (Machoy – Mokrzynska, 2004).

In the present study soluble collagen Hyp was found to be more susceptible to the effects of both $MgCl_2$ as well as NaF. Both $MgCl_2$ and NaF caused a decrease in soluble collagen Hyp in rat kidneys. Earlier studies of Prockop (1964) have shown that there exists at least 3 pools of body collagen with half lives of about 1day, 5days and 50-100 days. The first two of these represent the soluble collagen fractions, i.e. fractions containing collagen not yet aggregated to insoluble-collagen fiber and the third pool, the insoluble collagen. In the present study the soluble collagen Hyp appeared to be susceptible to degradation by $MgCl_2$ and NaF. This may be due to the fact that it has still not aggregated to form insoluble collagen fibers. Studies of Sharma (1982[b]) have shown that fluoride interferes with collagen crosslinking. Studies by the same author have also demonstrated that NaF interferes with maturation and normal metabolism of tissue collagen. The insoluble collagen Hyp was affected only by NaF treatment alone. Administration of $MgCl_2$ before NaF restored the altered insoluble collagen Hyp to near normal levels. This appears to be the only protective effect of $MgCl_2$ on NaF induced change in kidney collagen.

CONCLUSION

Therefore the present study concludes that though $MgCl_2$ has been reported to be protective against the toxic effect of NaF it has no significant effect on NaF induced changes in kidney Hyp/collagen. However administration of $MgCl_2$ before NaF restored insoluble collagen hydroxyproline which was altered by NaF to near normal levels.

ACKNOWLEDGEMENTS

The authors would like to thank the Research Center, Center for Scientific and Medical Female Colleges, King Saud University, Riyadh and King Abdul Aziz City for Science and Technology (Grant Number 098-17 AT), Riyadh for financial support to EAA.

REFERENCES

Adams, E. and Frank, L. 1980. Metabolism of proline and hydroxyprolines. Annual Reviews of Biochemistry. 49:1005 -1061.

Ahmad, S., Hiyasat, A., Elbetieha, AM. and Darmani, H. 2000. Reproductive toxic effects of ingestion of sodium fluoride in female rats. Fluoride. 33:279-284.

Al-Omireeni, E.A., Siddiqi, NJ. and Alhomida, AS. 2009. Effect of different doses of sodium fluoride on various hydroxyproline fractions in rat kidneys. Kidney research Journal. http://scialert.net/abstract/?doi= krj.0000.13409.13409. ISSN 1819-3374.

Bezerra de Menezes, LM., Volpato, MC., Rosalen, PL. and Cury, JA. 2003. Bone as a biomarker of acute fluoride toxicity. Forensic Science International. 137: 209-214.

Birkner, E., Grucka-Mamczar, E., Machoy, Z., Tarnawski, R., Polaniaka, R., Katowice. and Szczecin. 2000. Disturbance of protein metabolism in rats after acute poisoning with sodium fluoride. Fluoride. 33 (4): 182- 186.

Cicek, E., Aydin, G., Akdogan, M. and Okutan, H. 2005. Effects of chronic ingestion of sodium fluoride on myocardium in a second generation of rats. Human and Experimental Toxicology. 24:79-87.

Dabek, AWD. and McKenzie, AD. 1995. Survey of lead, cadmium, fluoride, nickel, and cobalt in food composites and estimation of dietary intakes of these elements by Canadians in 1986-1988. Journal of AOAC International. 78: 897-909.

Edwards, CA. and O'Brien, WD Jr. 1980. Modified assay for determination of hydroxyproline in a tissue hydrolyzate. Clinica chimica acta. 104:161-167.

Gritsan, NP., Miller, GW. and Schumatkov, GG. 1995. Correlation among heavy metals and fluoride in soil, air and plants in relation to environmental damage. Fluoride. 28:180- 188.

Kivirikko, KI., Laitinen, O., Aer, J. and Halme, J. 1965. Studies with ^{14}C – proline on the action of cortisone on metabolism of collagen in rat. Biochemical Pharmacology. 14 (10):1445-1451.

Lantz, O., Jouvin, MH., De Vemejoul, MC. and Druet, P. 1987. Fluoride-induced chronic renal failure. American Journal of Kidney Diseases. 10:136-139.

Luoma., H, Koskinen. M., Tuomisto, J. and Collan, Y. 1984. Reduction in the lethality and the nephrocalcinotic effect of single fluoride doses by magnesium in rats. Magnesium. 3 (2):81- 87.

Machoy-Mokrzynska, A. 2004. Fluorine as a factor in premature aging. Annales Academiae Medicae Stetinensis. 50: Suppl 1, 9 -13.

Manna, P., Sinha, M. and Sil, PC. 2007. A 43 kD protein isolated from the herb *Cajanus indicus L* attenuates sodium fluoride-induced hepatic and renal disorders in vivo. Jounal of Biochemistry and Molecular Biology. 40: 382-395.

Neurath, C. 2005. Tooth decay trends for 12 year old in nonfluoridated and fluoridated countries. Fluoride. 38: 324-325.

Prockop, DJ. 1964. Isotopic studies on collagen degradation and the urinary excretion of hydroxyproline. Journal of Clinical Investigation. 43(3):453-460.

Ranjan, R., Swarup, D. and Patra, RC. 2009. Oxidative stress indices in the erythrocytes, liver and kidneys of fluoride exposed rats. Fluoride. 42 (2):88-93.

Reddy, G.K. and Enwemeka, CS. 1996. A simplified method for the analysis of hydroxyproline in biological tissues. Clinical Biochemistry. 29(3):225- 229.

Saris, NL., Mervaala, E., Karppanen, H., Khawaja, JA. and Lewenstam, A. 2000. Magnesium An update on physiological, clinical and analytical aspects. Clinica chimica acta. 294:1-26.

Sharma, YD. 1982[a]. Effect of Sodium fluoride on collagen cross-link precursors. Toxicology Letters. 10: 97 -100.

Sharma, YD. 1982[b]. Variations in the metabolism and maturation of collagen after fluoride ingestion. Biochimica et Biophysica Acta. 715 (1): 137-141.

Shivarajashankara, YM., Shivashankara, AR., Gopalakrishna Bhat, P. and Hanumanth Rao, S. 2002. Brain lipid peroxidation and antioxidant systems of young rats in chronic fluoride intoxication. Fluoride. 35:197-203.

Siddiqi, N.J, Al-Jafari, AA. and Alhomida, AS. 2000. Investigation of total, free, peptide-bound, protein-bound, soluble- and insoluble-collagen hydroxyproline content in tissues from the Arabian camel (*Camelus dromadarius*). Cell Biochemistry and Function. 18:243-248.

Stannard, JG., Skim, YS., Kirtsineli, M., Labropoulou, P. and Tsamtsouris, A. 1991. Fluoride Levels and Fluoride Contamination of Fruit Juices. The Journal of clinical pediatric dentistry. 16:38-40.

Varghese, Z., Moorhead, JF. and Wills, MR. 1981. Plasma hydroxyproline fractions in patients with dialysis osteodystrophy. Clinica Chimica Acta. 110:105-111.

Weiss, JB. and Jayson, MIV. 1982. in Collagen in Health and Disease, Churchill Livingstone, New York, USA. pp 404-405.

Zabulyte, D., Uleckiene, S., Kalibatas, J., Viciene, AP., Jascaniniene, N. and Stosik M, 2007. Experimental studies on effect of sodium fluoride and nitrate on biochemical parameters in rats. Bull. Vet. Inst. Pulawy. 51:79-82.

Zhao, LB., Liang, D. and Liang, WWL. 1996. Effects of a high fluoride water supply on children's intelligence. Fluoride. 29:190-192.

Received: Jan 26, 2010: Revised: April 21, 2010; Accepted: April 29, 2010

SENRA Academic Publishers, Burnaby, British Columbia
Vol. 4, No. 2, pp. 1169-1178, June 2010
ISSN: 1715-9997

Canadian Journal of pure&applied sciences

SYNTHESIS, CHARACTERISATION AND IN-VITRO BIOLOGICAL ACTIVITIES OF SOME METAL(II) COMPLEXES OF 3-(-1-(4-METHYL-6-CHLORO)-2-PYRIMIDINYLIMINO)METHYL-2-NAPTHOL

*A A Osowole[1], R Kempe[2], R Schobert [3] and S A Balogun[4]
[1]Department of Chemistry, University of Ibadan, Ibadan, Nigeria
[2]Anorganische Chemie II, Universität Bayreuth, D-95440 Bayreuth, Germany
[3]Organische Chemie I, Universität Bayreuth, D-95440 Bayreuth, Germany
[4]Department of Microbiology, Adekunle Ajasin University Akungba–Akoko, PMB 001
Akungba–Akoko, Ondo state, Nigeria

ABSTRACT

Synthesis, spectroscopic characterisation and in-vitro antibacterial and anticancer studies were done on the neutral bidentate (NO) Schiff base, 3-(-1-(4-methyl-6-chloro)-2-pyrimidinyl imino)methyl-2-napthol and its Mn(II), Co(II), Ni(II), Pd(II), Cu(II) and Zn(II) complexes. These complexes assumed a 4-coordinate tetrahedral /square-planar geometry as corroborated by room temperature magnetic data, IR and electronic spectral measurements. The conductance data confirmed their covalent nature while mass spectra and TGA data affirmed the proposed structure. The ligand was not sensitive to HL 60 (leukaemia) but resistant to 518A2 (melanoma) carcinomas. The Pd(II) complex had the best cytotoxic activities against HL 60 (Leukemia) and Melanoma (518A2) carcinomas with IC_{50} of 11.89 and 9.11 µm at 48 and 72 h respectively, which was a third as, and four times more sensitive than CDDP (Cis-platin). The complexes generally exhibited good antibacterial activities against five Gram negative (*E. cloacae, S. arizona, Serratia sp, E. Coli*) and three Gram positive (*C. violaceum, S. aureus, Bacillus sp*) bacteria with inhibitory zones range of 7-19 mm. Similar to gentamycin, the Cu(II) and Zn(II) complexes had broad-spectrum activity against the bacteria used, although much lower.

Keywords: Antibacterial and anticancer activities, cis-platin –sensitive and –resistant cell lines, Schiff base.

INTRODUCTION

The interest in metal complexes as drugs has increased in the last decade due to the search for drugs with an enhanced therapeutic effect in combination with decreased toxicity (Zhaohua *et al.,* 2001; Zhong *et. al*., 2006). It has been documented that drugs containing pyrimidine moiety are more prominent in treating solid tumours and cancers due to their good anti-proliferation activity and low toxicity e.g. bevacizumab in combination with 5-fluoro uracil is used in treatment of metastatic colorectal cancer (Ramaling and Belani, 2007) while sorafenib and sunitinib, which are small-molecule multikinase inhibitors are used for the treatment of advanced renal-cell carcinoma (Atkins *et al*., 2006; Wilhelm *et al*; 2006). Currently, the drug pazopanib (5-(4-[(2,3-dimethyl-2H-indazoyl-6-yl)methylamino]-2-pyrimidinyl]amino-2-methyl benzene sulfonamide) is undergoing clinical development for use in treating renal-cell cancer and other solid tumours (Harries *et al*., 2008). In addition, pyrimidinyl Schiff bases are widely studied due to their ease of preparation, coordination to many metal ions, and the stability of such oxidation states. Furthermore, their good solubility in DMSO and DMF makes them suitable for cell lines studies (Gorneva and Golovinsky, 2003; Shreelekha *et al*., 2006). In continuation of our studies on synthesis, characterisation and anticancer /antimicrobial properties of some metal(II) complexes of various pyrimidinyl Schiff bases (Osowole *et al*., 2009), we report our findings on anticancer and antibacterial properties of Mn(II), Ni(II), Co(II), Cu(II), Zn(II) and Pd(II) complexes of 3-(-1-(4-methyl-6-chloro-2-pyrimidinyl imino)methyl-2-napthol (derived from condensation of 2-amino-4-methyl-6-chloropyrimidine and 2-hydroxy-1-napthaldehyde) against cis-platin–sensitive (Leukemia) and –resistant (Melanoma) cell lines and, *E. cloacae, S. arizona, Serratia sp, E. Coli*) and three Gram positive (*C. violaceum, S. aureus, Bacillus sp*). Their spectroscopic, magnetic and thermal properties are also discussed. This ligand and its metal complexes are new, being reported here by our group for the first time.

MATERIALS AND METHODS

Chemicals and Instrumentation

All the chemicals used were of reagent grade. 2-amino-4-methyl-6-chloropyrimidine and 2-hydroxy-1-napthaldehyde (Across), palladium(II) chloride, hydrated manganese(II) nitrate, cobalt(II) nitrate, nickel(II) nitrate,

*Corresponding author email: aderoju30@yahoo.com

copper(II) nitrate and zinc(II) nitrate (Aldrich) were used as received. The solvents were purified using conventional methods. C, H and N analyses were carried out using a GmbH VarioEl analyser. Palladium, Manganese, cobalt, nickel, copper and zinc were determined titrimetrically (Bassett *et al*., 1978). The ^{1}H nmr spectra were recorded on a 300 MHz Oxford Varian NMR instrument in $CDCl_3$ at 295K. ^{1}H chemical shifts were referenced to the residual signals of the protons of $CDCl_3$ and are quoted in ppm. Magnetic susceptibilities were measured on Johnson Matthey magnetic susceptibility balance at room temperature (27^{o}C) all susceptibilities were corrected for the diamagnetic contributions using Pascal's constants (Earnshaw, 1980). The reflectance spectra were recorded on a Perkin-Elmer λ20 spectrophotometer equipped with an integrating sphere. The infrared spectra were measured as KBr discs on a Bruker-IFS 66V spectrometer in the range 4000-400 cm^{-1}. Thermogravimetric analyses were done in static air, using a T6 Linseis thermal analyser with a heating rate of 10°C/min in the range 30-700°C while electrolytic conductivities of the complexes (1 x 10^{-3} Mdm^{-3}) in nitromethane were determined using a Hanna HI 8828N conductometer and melting points (uncorrected) were done using a Stuart scientific melting point apparatus smp3.

Biological Studies

The human HL 60 leukaemia cells were obtained from the German National Resource Centre for Biological Materials (DSMZ), Braunschweig and the human 518A2 melanoma cells were cultured in the Department of Oncology and Hematology, medical faculty of the Martin-Luther University, Halle, Germany.

Cytotoxicity (MTT) Assay

MTT[3(4,5-dimethylthiazol-2-yl)-2,5-diphenyltetrazolium bromide] was used to identify viable cells which were capable of reducing it in their mitochondria by succinate dehydrogenase to a violet formazan product.

Cell lines and Culture condition

HL 60 (0.5 x 10^6 cells/mL) and 518A2 cells (1.7 x 10^5 cells/mL) were seeded out and cultured for 24h on 96-well microplates. Incubation (5% CO_2, 95% humidity, and 37°C) of cells following treatment with test compounds was continued for 24, 48 and 72h. Blank and solvent controls were incubated under identical conditions. A 5 mg/mL stock solution of MTT in phosphate-buffered saline (PBS) was then added to a final concentration of 0.05%. After 2 h the precipitate of formazan crystals was redissolved in a 10% solution of sodium dodecylsulfate (SDS) in DMSO containing 0.6% acetic acid in the case of the HL 60 cells. For the adherent melanoma (518A2) cells, the microplates were swiftly turned to discard the medium prior to adding the solvent mixture. The microplates were gently shaken in the dark for 30 min and left in the incubator overnight, to ensure a complete dissolution of the formazan. Finally the absorbance at wavelengths 570 and 630nm (background) was measured using an ELISA plate reader. All experiments were carried out in quadruplicate, and the percentage of viable cells quoted was calculated as the mean ± SD with respect to the controls set to 100%. Blank tests have shown that DMSO used in the preparation of the test compound does not have any effect on the cancer cell lines.

Antibacterial assay

The assay was carried out on the ligand and metal(II) complexes. The bacteria used were identified laboratory strains of *E. cloacae, S. arizona, Bacillus sp, S. liquefaciens, S. aureus, Klebsiella sp, Salmonella sp, Serratia sp, Pseudomonas sp, E. coli, C. violaceum*. The antibacterial susceptibility test was carried out using the Agar diffusion technique. The surface of the agar in a Petri dish was uniformly inoculated with 0.3 mL of 18 h old test bacteria culture. Using a sterile cork borer, 6 mm wells were bored into agar. Then 0.06 mL of 10 mg/mL concentration of each metal complex in DMSO was introduced into the wells and the plates were allowed to stand on bench for 30 min before incubation at 37^{0}C for 24 h after which inhibitory zones (in mm) were taken as a measure of antibacterial activity. The experiments were conducted in duplicates and gentamycin was used as a reference drug.

Synthesis

Preparation of Ligand

The ligand, {[$C_{10}H_6$(OH)CH:N($C_5H_4N_2$Cl)]} HL, was prepared by refluxing a mixture of 0.017 mol (2.50 g) of 2-amino-4-methyl-6-chloropyrimidine and 0.017 mol (3.00 g) of 2-hydoxy-1-napthaldehyde with 6 drops of acetic acid in 60 mL of absolute ethanol for 6 h. The yellow product, formed on cooling to room temperature, was filtered and recrystallized from ethanol and dried *in vacuo* over anhydrous calcium chloride. The yield of the resulting Schiff base was 3.62 g (70%). ^{1}H nmr (ppm) δ10.8 (s, OH), 9.38(s, 1H, HCN); δ 7.38-8.60 (m, 6H, $C_{10}H_6$); 6.70 (s, 1H, $CH_{pyrimidine}$); 2.50 (s, 3H, CH_3).

Preparation of the Metal(II) Complexes

A solution of the metal(II) nitrates (0.54 mmol, 0.10-0.16 g M = Mn, Co, Ni, Cu, Zn) in 20 mL ethanol was added to a stirring solution of the ligand (1.08 mmol, 0.32 g) in 30mL ethanol at room temperature (26°C), followed by gradual addition of triethylamine (1.08 mmol, 0.15 mL). The resulting homogeneous solution was refluxed for 6h, and the products formed were later filtered, washed with ethanol and dried in *vacuo* over anhydrous $CaCl_2$.

RESULTS AND DISCUSSIONS

The reactions of the ligand with the metal (II) nitrates (Mn, Co, Ni, Cu, and Zn) gave mononuclear complexes in moderate-good yields (50-70%). The physical and analytical data, colours, % yields, melting points/decomposition temperature and room temperature magnetic moments of the compounds are presented in Table 1 and the proposed structures are shown in figure 1. The complexes were all air stable but decomposed on programmed heating and were soluble in methylene chloride, nitromethane, dimethylfornamide and dimethylsulphoxide. The elemental analysis, showed the stoichiometry of the complexes as 2L:M and confirmed the suggested molecular formula of the complexes. The decomposition pattern obtained from TGA curve corroborates the proposed formulation of the complexes. All complexes isolated adopted $[ML_2]xH_2O$ stoichiometry {Mn, Pd: x = 2; Ni, Zn: x = 1} except, the Cu(II) complex which was anhydrous. The molar conductances of the complexes ranged between 12-20 Ω^{-1} cm^2 mol^{-1} in nitromethane, showing they were non-electrolytes. A value of 60-90 Ω^{-1} cm^2 mol^{-1} is expected for a 1:1 electrolyte (Osowole *et al*., 2009). Attempts to isolate suitable crystals for single X-ray structural determination have not yet been successful.

[1]Hnmr spectra

The ligand showed the napthyl ring protons as a multiplet at δ 6.94-9.45 ppm (m, 6H, $C_{10}H_6$). The phenolic proton was observed as a singlet at 10.8 ppm(s, 1H, OH) and the proton of the imine resonated as a singlet at δ 6.70 ppm (s,1H, H=CN) while that of the pyrimidine was seen as a singlet at δ 6.67 ppm(s, 1H, $CH_{pyrimidine}$). The methyl protons resonated as a singlet at 2.50ppm(s, 3H, CH_3). On coordination to Zn(II) ion, the napthyl ring protons were deshielded and resonated as a multiplet at δ 7.01-8.24 ppm (m, 6H, $C_{10}H_6$). The phenolic proton was conspicuously absent, indicating the involvement of OH in chelating. The HC=N and CH(pyrimidine) protons resonated as singlets at δ 6.79 and δ 6.56 ppm respectively, while the methyl protons singlet shifted to δ 2.36 ppm. These shifts indicate deshielding due to coordination of the imine nitrogen atom. Similarly, Pd(II) complex napthyl ring protons were deshielded and resonated as a multiplet at δ 7.24-9.33 ppm (m, 6H, $C_{10}H_6$). The phenolic proton was conspicuously absent, indicating the involvement of OH in chelating. The HC=N proton signet, appeared at δ 6.72 ppm, while the CH of the pyrimidine appeared at δ 6.69 ppm. The methyl protons singlet shifted to δ 2.51 ppm. These downfield shifts indicate coordination of the imine nitrogen atom.

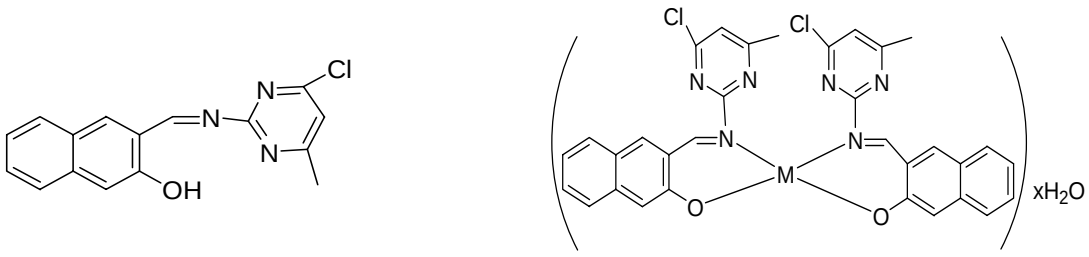

A, Schiff base; B, Metal(II) Schiff base complexes

Fig 1. Proposed structures for the ligand and its complexes.

Table 1. Analytical data for the compounds.

Compound (Empirical formula)	Formula mass	Color	μeff	% Yield	Λ_m^*	M.p (°C)	Analysis (Calculated)			
							%C	%H	%N	% M
HL ($C_{16}H_{12}N_3OCl$)	297.56	Yellow	-	70	-	188-189	64.53 (64.58)	4.13 (4.07)	13.89 (14.12)	-
$[MnL_2]2H_2O$ ($MnC_{32}H_{26}N_6O_4Cl_2$)	684.08	Brownish green	5.70	60	10.00	259-260	56.18 (56.19)	3.54 (3.83)	11.84 (12.29)	7.95 (8.03)
$[CoL_2]H_2O$ ($CoC_{32}H_{24}N_6O_3Cl_2$)	647.59	Brown	4.36	70	20.00	280-281	57.46 (57.36)	3.56 (3.61)	12.41 (12.54)	9.06 (9.10)
$[NiL_2]H_2O$ ($NiC_{32}H_{24}N_6O_3Cl_2$)	629.30	Dark Orange	3.41	70	25.00	283-284	57.16 (57.33)	3.55 (3.61)	12.51 (12.55)	9.20 (9.07)
$[CuL_2]$ ($CuC_{32}H_{22}N_6O_2Cl_2$)	616.70	Brown	1.91	70	18.00	238-239	58.67 (58.53)	3.40 (3.38)	12.50 (12.80)	10.25 (10.30)
$[ZnL_2]H_2O$ ($CuC_{32}H_{24}N_6O_3Cl_2$)	635.64	Orange	D	60	12.00	268-269	57.44 (56.90)	3.56 (3.58)	12.20 (12.40)	10.17 (10.23)
$[PdL_2]2H_2O$ ($PdC_{32}H_{26}N_6O_4Cl_2$)	733.14	Brown	D	50	15.00	183-184	52.67 (52.50)	3.40 (3.60)	11.57 (11.50)	14.24 (14.19)

D = diamagnetic; $^*\Omega^{-1}$ cm^2 mol^{-1}

Infrared spectra

The relevant infrared data are presented in table 2. The assignments of the infrared bands were made by comparing the spectra of the compounds with reported literature on similar systems (Abd El Wahab, 2008; Osowole *et al*., 2005; Osowole *et al*., 2008; Sonmez and Haciyusufoglu, 2006; Sonmez *et al*., 2004). The strong band in the ligand at 3425 cm^{-1}, which disappeared in the spectra of all the complexes, is assigned as νOH. This indicates the involvement of the enolic *O* in bonding to the metal ions. Furthermore, the ν(C-O) enolic band in the ligand at 1447 and 1360 cm^{-1} were bathochromic shifted to 1281-1192 cm^{-1} also corroborating enolic oxygen′s coordination. A new broad band, ν(OH) at 3500 cm^{-1}, in the hydrated complexes is assigned to coordinated water. The uncoordinated C=N and C=C stretching vibrations in the ligand were expectedly coupled and observed at 1631-1539 cm^{-1} (Osowole *et al*., 2005). These bands suffered bathochromic shifts to 1630-1522 cm^{-1} in the metal complexes, thus confirming the involvement of the imine *N* atom in coordination to metal(II) ion (Singh *et al*., 2001). The δC—H vibration of the ligand was observed at 967 cm^{-1} and it was bathochromic shifted to 897-776 cm^{-1} in the complexes due to the pseudo-aromatic nature of the chelates (Osowole *et al*., 2008). The bands due to ν(M—O) and ν(M—N) were observed at 499-417 and 585-501 cm^{-1} respectively in the complexes (Sonmez *et al*., 2004).

Electronic spectra and room temperature magnetic moments

In the UV region, the reflectance electronic spectra (Table 2) of all the complexes were similar, displaying strong absorption maxima between 26.50-50.00 kK, which are assigned to n- π*, π-π* and charge transfer transitions (Kwiatkowski and Kwiatkowski, 1980; Singh *et al*., 2001).

The Mn(II) complex showed two weak bands at 15.40 and 24.80 kK respectively, consistent with a four-coordinate, tetrahedral geometry and are assigned to $^6A_1 \rightarrow {}^4E_1$ (ν_1) and $^6A_1 \rightarrow {}^4A_1$ (ν_2) transitions. The effective magnetic moment of Mn(II) complexes are expected to be close to the spin-only value of 5.90 B.M. since the ground term is $^6A_{1g}$ and as such there is no orbital contribution. Consequently an observed moment of 5.70 B.M. for this complex indicates that it is high spin and complementary of tetrahedral geometry (Chohan, 2001).

The Co(II) complex exhibited two bands at 13.00 and 19.50 kK, typical of a 4-coordinate tetrahedral geometry and are assigned to $^4A_2 \rightarrow {}^4T_1(F)$, ($\nu_2$), and $^4A_2 \rightarrow {}^4T_1(P)$, ($\nu_3$), transitions. The transition, $^4A_2 \rightarrow {}^4T_2$, ($\nu_1$) in the range 5-7 KK was not observed, being outside the range covered by the instrument. An observed moment of 4.36 B.M is corroborative of tetrahedral geometry, since moments in the range 4.3-4.6 B.M are usually observed for tetrahedral Co(II) compounds (Singh *et al*., 2001; Sonmez and Haciyusufoglu, 2006; Sonmez *et al*., 2004).

The reflectance spectra of the Ni(II) complex showed absorption bands at 12.00 and 17.00 kK which are assigned to $^3T_1(F) \rightarrow {}^3T_2$,($\nu_2$) and $^3T_1(F) \rightarrow {}^3A_2$, ($\nu_3$) transitions, in a tetrahedral environment. Generally, square planar Ni(II) complexes are usually diamagnetic, while tetrahedral and octahedral complexes are paramagnetic with moments in the range 3.20-4.10 and 2.90-3.30 B.M respectively**.** This complex gave a moment of 3.41 B.M. and hence is tetrahedral (Abd El Wahab, 2008; Sonmez and Haciyusufoglu, 2006).

The observance of two bands at 15.70 and 24.40 kK in the Cu(II) complex indicates square planar geometry with the assignment of the bands as $^2B_{1g} \rightarrow {}^2A_{1g}$ and $^2B_{1g} \rightarrow {}^2E_{1g}$ transitions. A moment of 1.9-2.2 B.M. is usually observed for mononuclear copper(II) complexes, regardless of stereochemistry, expectedly higher than the spin only moment due to orbital contribution and spin-orbit

Table 2. Relevant infrared and electronic spectral data of the complexes

Compound	νOH	ν(C=N) + ν(C=C)	νPh/C—O	δC—H	ν(M—N)	ν(M—O)	Electronic spectral (kK)
[HL]	3425s	1631s 1572s 1539s	1447s 1360s	967s	-	-	28.00 32.00 39.00 42.00
$[Mn(L)_2]2H_2O$	3500b	1620s 1567s 1538s	1289s 1188s	897s 747s	537m 501m	486m 450s	15.40 24.80 27.20 31.70 44.10 47.40
$[Co(L)_2]\ H_2O$	3400b	1618s 1605s 1562s 1529s	1286m 1195m	832s 754s	568s 550m	481m 446m	11.00 17.50 29.20 34.51 42.30
$[Ni(L)_2]H_2O$	3500b	1623s 1577s 1551s	1290m 1190m	875s 786m	544m 518m	458m 423m	12.00 17.00 26.53 32.10 42.92 48.50
$[Cu(L)_2]$	-	1619s 1604s 1581s 1539s	1290m 1195m	833s 747s	525m 504m	461m 417m	15.70 24.40 26.50 30.40 42.00 50.00
$[Zn(L)_2]H_2O$	3500b	1620s 1605s 1579s 1522s	1281m 1196m	831s 755s	550m 544m	499m 456m	20.00 30.00 33.30 39.50 45.00
$[Pd(L)_2]2H_2O$	3500b	1615s 1600s 1575s 1522s	1291m 1192m	827s 749s	585m 559m	486m 452m	16.00 23.30 29.90 33.00 39.40 44.00

b = broad, s = strong, m = medium; 1kK = 1000 cm^{-1}.

coupling. [CuL_2] had a moment of 1.91 B.M. and is consequently mononuclear (Singh *et al*., 2001).

The Zn(II) complex showed only the CT transitions from M→L at 20.00 kK as no d-d transition is expected. The bands at 30.00, 33.30, 39.50 and 45.00 kK are assigned as π-π* and intraligand charge transfer transitions respectively. This complex is expectedly diamagnetic, confirming its tetrahedral geometry (Singh *et al*., 2001).

The Pd(II) complex showed absorption bands typical of a square-planar geometry at 16.00 and 23.25 kK, which are assigned to $^1A_{1g} \rightarrow {}^1B_{1g}$ and $^1A_{1g} \rightarrow {}^1E_{2g}$ transitions. Its diamagnetism is corroborative of square-planar geometry (Kwiatkowski and Kwiatkowski, 1980).

Mass spectroscopy and Thermal studies

The mass spectra of ligand and the complexes showed peaks attributed to the molecular ions m/z at 297 $[L]^+$; 647 $[MnL_2\text{-}2H]^+$; 651 $[CoL_2\text{-}3H]^+$; 652 $[NiL_2\text{-}2H]^+$; 655 $[CuL_2\text{-}3H]^+$; 658 $[ZnL_2\text{-}H]^+$ and 696 $[PdL_2\text{-}2H]^+$. The decomposition stages, temperature ranges, percentage losses in mass and assignment of decomposition moieties are given in table 3.

The ligand, HL, decomposed in three stages. Stage one was between 110-170°C and corresponds to the loss of the fragment C_2H_2N, with mass losses of (obs. = 14.00%, calc. = 13.46%). The second stage involved the loss of the fragment C_4H_4Cl, with mass losses of (obs. = 29.89%, calc. = 29.43%) within a temperature range of 170-380°C and the final stage was the loss of the organic moiety, $C_{10}H_6N_2$ at 380-700°C, with mass losses of (obs. = 58.94%, calc. = 57.19%).

The Mn(II) complex decomposed in six steps. The first

Table 3. Thermal data for the ligand and complexes.

Compound	Temperature range(°C)	TG weight loss(%) Calc.	Found	Assignments
HL ($C_{16}H_{12}N_3OCl$)	110-170	13.46	14.00	C_2H_2N
	170-380	29.43	29.89	C_4H_4Cl
	380-700	57.19	58.94	$C_{10}H_6N_2O$
[MnL_2]$2H_2O$ ($MnC_{32}H_{26}N_6O_4Cl_2$)	30-100	9.95	9.83	$2H_2O + O_2$
	100-160	1.02	1.05	¼N_2
	160-230	2.64	2.93	$CH_4 + H_2$
	230-300	6.45	6.41	C_3H_8
	300-410	7.69	7.72	C_3H_6N¾
	410-700	64.81	66.50	$C_{25}H_2N_5Cl_2$ Mn(residue)
[CoL_2]H_2O ($CoC_{32}H_{24}N_6O_3Cl_2$)	30-310	5.99	6.03	$CH_4 + 3H_2 + H_2O$
	310-410	8.37	8.41	$C_2H_4N_2$
	410-660	69.75	70.02	$C_{25}H_8N_4Cl_2O_2$ Co (residue)
[NiL_2]H_2O ($NiC_{32}H_{24}N_6O_3Cl_2$)	30-100	5.40	5.92	$CH_4 + 3H_2 + H_2O$
	100-200	10.60	10.57	Cl_2
	200-390	16.75	16.74	$C_6H_{12}N_2$
	390-700	58.57	65.68	$C_{25}H_4N_4O_2$ Ni(residue)
[CuL_2] ($CuC_{32}H_{22}N_6O_2Cl_2$)	30-170	21.05	21.24	$C_8H_{14}N_2$
	170-330	10.80	11.21	Cl_2
	330-700	58.53	66.26	$C_{24}H_8O_2N_4$ Cu(residue)
[ZnL_2]H_2O ($ZnC_{32}H_{24}N_6O_3Cl_2$)	50-100	14.62	14.72	$C_6H_6 + H_2O$
	100-230	22.54	23.23	Cl_2
	230-430	10.80	10.54	$C_{17}H_4O_2N_4$
	430-700	45.04	44.59	Zn(residue)
[PdL_2]$2H_2O$ ($PdC_{32}H_{26}N_6O_4Cl_2$)	30-80	10.66	10.72	$2H_2O + C_3H_6$
	130-360	16.53	16.71	$C_7H_9 + H_2$
	360-700	58.57	65.68	$C_{22}H_7N_4O_2Cl_2$ Pd(residue)

step was the loss of two molecules of water and oxygen with mass losses of (obs. = 9.95%, calc. = 9.83%) in the temperature range 30-100°C. The second step involved the loss of 0.25 mole N_2, with mass losses of (obs. = 1.05%, calc. = 1.02%) between 100-160°C. The third step corresponds to the loss of methane and hydrogen at 160-230°C with, mass losses of (obs. = 2.93%, calc. = 2.64%). The fourth step involved the loss of propane, with mass losses of (obs. = 6.41%, calc. = 6.45%) at 230-300°C. The fifth was the loss of the fragment $C_3H_6N_{¾}$ in the temperature range 300-410°C, with mass losses of (obs. = 7.72%, calc. = 7.69%). The final step involved loss of the organic moiety $C_{25}H_2N_5Cl_2$ at 410-700°C, with mass losses of (obs. = 66.50 %, calc. = 64.81%), leaving behind Mn as the residue.

The thermal degradation of the Co(II) complex occurred in three steps. The first step was within the temperature range of 30-310°C and corresponds to the loss of a molecule of water and methane, and three molecules of hydrogen with mass losses of (obs. = 6.03%, calc. = 5.99%). The second step occurred between 310-410°C and was characterized by loss of the fragment, $C_2H_4N_2$, with mass losses of (obs. = 8.41%, calc. = 8.37%). The final step involved the loss of the organic moiety $C_{25}H_8O_2N_4Cl_2$, within a temperature range of 410-700°C with corresponding mass losses of (obs. = 70.02 %, calc. = 69.75%). The final product was cobalt.

The Ni(II) complex decomposed in four steps. The first step was the loss of a molecule of water, methane and hydrogen at 30-100°C, with mass losses of (obs. = 5.92%, calc. = 5.40%). The second step was in the temperature range of 100-200 °C, and is attributed to the loss of Cl_2 (obs. = 10.57%, calc. = 10.60%). The third step involved the loss of the fragment $C_6H_{12}N_2$, at 200-390°C, with mass losses of (obs. = 16.74%, calc. = 16.75%). The final step was within the temperature range of 390-700°C and is assigned to the loss of the organic moiety $C_{25}H_4N_4O_2$, (obs. = 66.10%, calc. = 58.57%). The remaining residue was Ni.

The Cu(II) complex decomposed in three ways. The first decomposition, was the loss of the fragment, $C_8H_{14}N_2$ at 30-170°C, with mass losses of (obs. = 21.24%, calc. = 21.05 %). The second step occurred within a temperature range of 170-330°C and is attributed to the loss of Cl_2 (obs. = 11.21%, calc. = 10.80%). The final stage was within a temperature range of 460-700°C, assigned to the loss of the organic moiety $C_{24}H_8O_2N_4$ (obs. = 66.26%, calc. = 58.53%). The remaining fraction was Copper.

The Zn(II) complex decomposed in four stages. The stage one was between 50-100°C, which indicated the loss of a mole of water and benzene respectively, with mass losses of (obs. = 14.72%, calc. = 14.62%). The second stage was from 100-230 °C and is assigned to the loss of the fragment, $C_9H_{12}N_2$, with mass losses of (obs. = 23.32 %, calc. = 22.54%). The third stage involved the loss of a mole of chlorine at 230-430°C, with mass losses of (obs. = 10.54%, calc. = 10.80%). The final stage was within a temperature range of 430-700°C, attributed to the loss of the organic moiety $C_{17}H_4N_4O_2$, (obs. = 44.59%, calc. = 45.04%). The remaining residue was Zn.

The Pd(II) complex decomposed in three steps. The first step involved the loss of two molecules of water and a molecule of propene at 30-130°C, with mass losses of (obs. = 10.72%, calc. = 10.66 %). The second was within a temperature range of 130-360°C, which corresponds to the loss of the fragment, $C_7H_9N_2$ with mass losses of (obs. = 16.71%, calc. = 16.53%). The final stage was within a temperature range of 360-700°C and corresponds to the loss of the organic moiety $C_{22}H_7O_2N_4Cl_2$ with mass losses of (obs. = 65.68%, calc. = 58.70%). The remaining fraction was Pd. The high mass residue (~7%) observed in

Table 4. IC_{50} values of the ligand and its complexes against Melanonoma (518A2) and Leukemia (HL60) cells.

Compound	IC_{50} [µM] Melanoma cells(518A2)			IC_{50} [µM] Leukaemia cells (HL 60)		
	24h	48h	72h	24h	48h	72h
CDDP	35	-	-	3.5	-	-
H_2L	74.12±15.82	78.01±15.56	56.43 ±7.33	>100	>100	>100
$[Mn(L)_2]2H_2O$	>100	37.02±4.29	31.93±3.96	32.39	29.58	18.80
$[Co(L)_2]H_2O$	>100	>100	>100	>100	35.35	26.91
$[Ni(L)_2]H_2O$	>100	>100	>100	>100	16.43	28.48
$[Cu(L)_2]$	>100	>100	>100	14.04	75.33	39.29
$[Zn(L)_2]H_2O$	>100	>100	>100	>100	>100	>100
$[Pd(L)_2]2H_2O$	10.68±1.47	12.51±0.88	9.11±0.55	20.56	11.89	22.55

<5 µm = super active; 5-10µm = strongly active; 11-19µm = moderately active; 20-30µm = weakly active; >30µm = resistant; >100 µm = not active; CDDP = cis-platin; - = Not determined

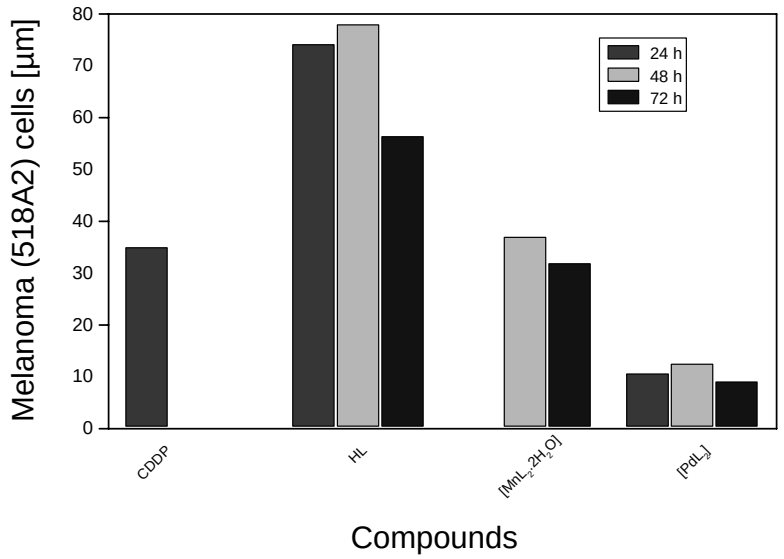

Fig 2. The inhibitory effect of the ligand, Mn(II) and Pd(II) complexes against Melanoma cells.

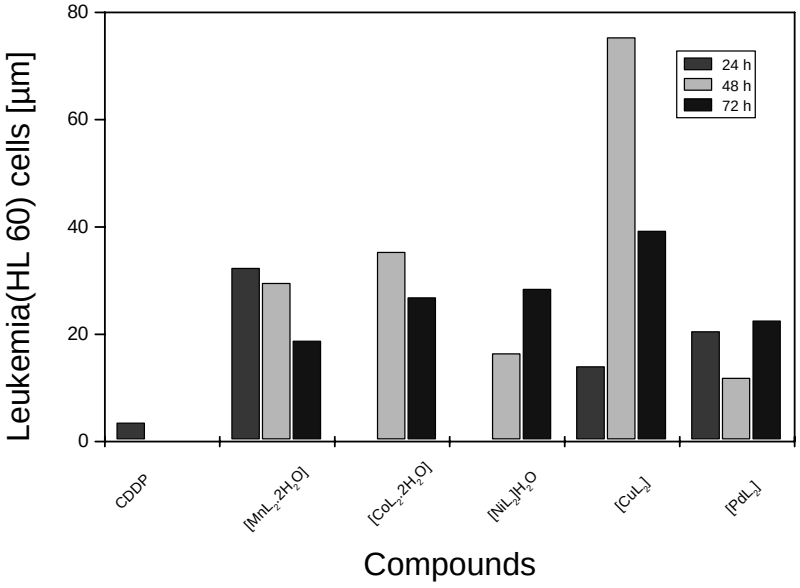

Fig 3. The inhibitory effect of some of the complexes against Leukemia cells.

the Ni(II), Cu(II) and Pd(II) complexes were attributed to carboneous material (Sharma and Srivastava, 2006).

Biological studies

The growth inhibitory effects of the ligand and its complexes on the cis-platin (CDDP) resistant 518A2 (Melanoma) and (CDDP) sensitive HL 60(Leukemia) cell lines are shown in table 4, figures 2 and 3. The ligand, HL (74.12-78.01µm) was about twice as resistant as CDDP (35.0µm) against Melanoma cells during the first 48h of experiment, while its resistance dropped by about 20% at 72 h of exposure. In contrast, the Co(II), Ni(II), Cu(II) and Zn(II) complexes showed no anti-tumor activity throughout the duration of experiment. It is important to

Table 5. Inhibitory zones(mm) of the ligand and complexes against various bacterial isolates.

Complexes	*E. Cloacae*	*S.arizona*	*Bacillus sp*	*S.Liquefaciens*	*S. aureus*	*Klebsiella sp*	*Serratia sp*	*Pseudomonas sp*	*E.Coli*	*C.violaceum*
HL	7.0±0.1	R	R	8.0±0.3	R	R	7.0±1.2	R	11.0±0	11.0±0
$[Mn(L)_2]2H_2O$	10.0±0.5	7.0±0.3	8.0±0.1	10.0±0.1	10.0±0.01	9.0±1.2	14.0±1.2	R	15.0±0	7.0±0.2
$[Co(L)_2]H_2O$	7.0±0.01	10.0±0.5	R	R	8.0±0.01	R	7.0±0.4	R	19.0±0.1	12.0±0.6
$[Ni(L)_2]H_2O$	8.0 ±0.03	15.0±0.2	8.0±0.01	R	8.0±0.1	R	9.0±2.0	R	18.0±0.2	8.0±0
$[Cu(L)_2]$	11.0±0.1	10.0±0.1	9.0±0.2	11.0±0.1	13.0±0.1	11.0±2.0	14.0±2.1	10.0±0.6	15.0±1.1	12.0±1.1
$[Zn(L)_2]H_2O$	12.0±0.3	12.0±0.1	7.0±1.0	13.0±0.1	7.0±0	9.0±0.6	15.0±1.1	7.0±0.3	19.0±0.1	7.0±1.2
$[Pd(L)_2]2H_2O$	8.0±0.1	10.0±0.4	13.0±1.1	13.0±0.2	9.0±0.3	7.0±2.1	19.0±1.4	R	16.0±0.3	10.0±0
DMSO*	R	R	R	R	R	R	R	R	R	R
Gentamycin$^+$	40.0±0.1	30.0±2.0	28.0±1.2	26.0±1.4	40.0±0.8	30.0±1.3	29.0±1.2	40.0±1.6	45.0±1.2	43.0±1.6

R = Resistant, * = Negative standard, $^+$ = Positive standard, *E. cloacae* = *Enterococcus cloacae*; *S. arizona* = *Salmonella arizona*; *S. liquefaciens* = *Serratia liquefaciens*; *S. aureus* = *Staphyloccus aureus*; *E. Coli* = *Escherichia coli*; *C. violaceum* = *Chromobacter violaceum*

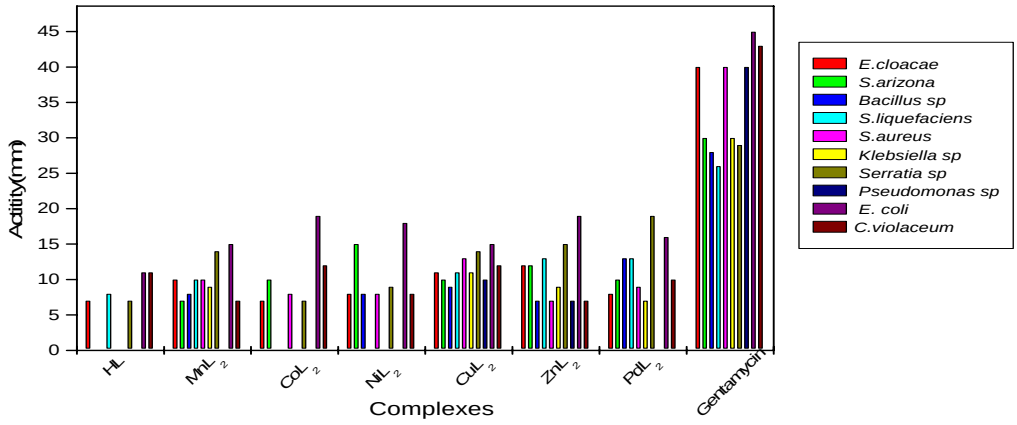

Fig. 4. The comparative activities of the complexes against bacteria strains and standard antibiotic.

note that though the Mn(II) complex does not show antitumor activity at 24 h, it exhibited comparable activity to CDDP (35.0µm) at 48 and 72 h, with IC_{50} values of 37.02 and 31.93µm respectively. Notably, $[PdL_2]$ was about three times more sensitive than CDDP with IC_{50} of 10.68 and 12.51 µm, at 24 and 48 h of experiment respectively. Further exposure of the cell line to the metal complex at 72 h, showed that the sensitivity increased to four times that of CDDP. Consequently, for further studies with the Pd(II) complex in drug development against melanoma cancers, the most effective time for exposure is 72 h.

The ligand and the Zn(II) complex were not sensitive to CDDP (3.5 µm) sensitive HL 60 Leukemia cells throughout the duration of experiment (Fig. 3). The Mn(II) complex was resistant with IC_{50} of 32.39 µm at 24 h. Further exposure at 48 and 72 h showed improved weak and moderate activity with IC_{50} of 29.58 and 18.80µm respectively. Similarly, the Co(II) complex had no activity at 24 h, but became resistant at 48 h (35.35 µm) and weakly active (26.91µm) at 72 h respectively. The Ni(II) complex was not effective at 24 h but showed moderate activity at 48 h (16.43 µm) and became weakly active at 72 h (28.48 µm). On the other hand, the Cu(II) complex exhibited moderate activity at 24 h (14.04 µm), which was a quarter of that of CDDP (3.5 µm). However it became resistant at 48 (75.33 µm) and 72 (39.29 µm) h respectively, with the latter having overcome the former's resistance by about 50 %. The Pd(II) complex was sensitive throughout the duration of the experiment. It was weakly active (20.56 µm) at 24 h. It then became moderately active (11.89 µm) at 48 h and finally at 72 h, activity dropped back to weakly active (22.55 µm). The activity at 48 h was a third of that of CDDP (3.5 µm).

It was evident from this cytotoxic studies, that the Pd(II) complex had the best anticancer activity against both

Melanoma (518A2) and HL60 (Leukemia) carcinomas in-vitro with IC_{50} values of 9.11 and 11.87 µm at 72 h and 48 h of exposure respectively, which was four times more sensitive than, and a third as sensitive as CDDP. The activities of the Cu(II) and Pd(II) complexes may be attributed to their planar structure. It has been documented that complexes with such geometry avoid possible steric hindrance during physiological actions, and are consequently more active than complexes of other geometries (Bolos *et al*., 1998).

Antibacterial studies

The results of the antibacterial activities of the compounds are presented in figure 4 and Table 5. Five organisms, *E. cloacae, S. liquefaciens, Serratia sp, E. coli, S. aureus* and *C. violaceum* were sensitive to the ligand with inhibitory zones range of 7-11 mm. The metal complexes are generally more active than the ligand against the organisms with the exception of $[CoL_2]H_2O$ which had the same activity (7 mm) as the ligand against *E. cloacae* and *Serratia sp*. $[MnL_2]2H_2O$, $[NiL_2]H_2O$ and $[ZnL_2]H_2O$ had lower activities (7<11 mm) against *C. violaceum*. Improved activities of the complexes were attributed to chelation, which reduced the polarity of the metal atom, mainly because of partial sharing of its positive charge with donor groups of the ligand and possible π-electron delocalisation on the aromatic rings. This increased the lipophilic character, favouring its permeation into the bacterial membrane, causing the death of the organisms (Thangadurai and Natarajan, 2001). Furthermore, *E. cloacae*, *S.arizona, S. aureus*, *Serratia sp*, *E. coli* and *C. violaceum* were sensitive to all the complexes with inhibitory zones in the range of 8-11, 7-15, 8-13, 9-15, 15-20 and 7-12 mm respectively. *Pseudomonas sp* was resistant to all the complexes except $[CuL_2]$ and $[ZnL_2]H_2O$ with inhibitory zones of 7 and 10 mm respectively. This was attributed to its very versatile nutritional capability and adaptability to various hydrocarbon rings, and the possession of pump mechanism which ejects metal complexes as soon as they enter the cell (Pelczar *et al*., 1996). It is not clear why *E. coli* showed a high sensitivity (15-19 mm) to the complexes. In addition, *Klebsiella sp* and *S.liquefaciens* were sensitive to all the complexes with the exception of $[CoL_2]H_2O$ and $[NiL_2]H_2O$ with inhibitory zones of 7-11 and 10-13 mm respectively. A look at the antibiotic, gentamycin, activities (26-45 mm) against the various bacterial isolates relative to the metal complexes (7-19 mm) showed that the activities of the latter were much lower, with optimum activity being about half of gentamycin with *Serratia sp*{$[ZnL_2]H_2O$}, *S. liquefaciens* {$[ZnL_2]H_2O$}, {$[PdL_2]2H_2O$}, *S. arizona* {$[NiL_2]H_2O$} and *Bacillus sp,* {$[PdL_2]2H_2O$}. The complexes, $[CuL_2]$ and $[ZnL_2]H_2O$ had broad-spectrum activities like gentamycin against the organisms used, although much lower.

CONCLUSION

The coordination of the Schiff base, 3-(-1-(4,6-dimethyl-2-pyrimidinylimino)methyl-2-napthol, to Mn(II), Co(II), Ni(II), Mn(II), Zn(II), Cu(II) and Pd(II) ions with N_2O_2 chromophores resulted in tetrahedral/square planar geometry for the complexes. The complex, $[PdL_2]2H_2O$ had the best anticancer activities against HL 60 (Leukaemia) and Melanoma (518A2) carcinomas while $[CuL_2]$ and $[ZnL_2]H_2O$ had broad-spectrum activity similar to gentamycin against the bacteria used, although much lower.

ACKNOWLEDGEMENT

AAO thanks the Alexander von Humboldt (AvH) Foundation for a Georg Forster fellowship.

REFERENCES

Abd El-Wahab, ZH. 2008. Complexation of 4- amino -1,3 dimethyl-2,6-pyrimidinedione derivatives with cobalt(II) and nickel(II) ions: synthesis, spectral, thermal and antimicrobial studies. J. Coord. Chem. 61(11):1696-1709.

Atkins, M., Jones, CA. and Kirkpatrick P. 2006. Sunitinib maleate. Nat. Rev. Drug Discov. 5:279-280.

Bassett, J., Denney, RC., Jeffery, GH. and Mendham, J. 1978. Vogel's Textbook of Quantitative Inorganic Analysis. ELBS. London. 325-361.

Bolos, CA., Nikolov, G St., Ekateriniadour, L., Kortsaris, A. and Kyriakidis, DA. 1998. Structure-activity relationships for some diamine, triamine and Schiff base derivatives and their Cu(II) complexes. Metal based drugs. 5 (6):323-332.

Chohan, ZH. 2001. Synthesis, characterization and biological properties of bivalent transition metal complexes of Co(II), Cu(II), Ni(II) and Zn(II) with some acylhydrazine derived from furanyl and thienyl ONO and SNO donor Schiff base ligands. Synth. React. Inorg. Met.-Org. Chem. 31 (1):1-16.

Earnshaw, A. 1980. The Introduction to Magneto-chemistry. Academic Press. London. 80-88.

Gorneva, GA. and Golovinsky, E. 2003. Comparative study of the apoptogenic effect of fluoro pyrimidines on murine leukaemia cells. Nova Acta Leopoldina. 87 (329):183-189.

Harris, PA., Boloor, A., Cheung, M., Kumar, R., Crosby, RM., Davis-Ward, RG., Expertly, AH., Hinkle, KW., Hunter, RN., Johnson, JH., Knick, VB., Lindeman, CP., Luttrell, DK., Mooch, RA., Nolte, RT., Rudolph, SK., Szewczyk, JR., Truesdale, AT., Veal, JM., Wang, L. and Stafford, JA. 2008. Discovery of 5-[4-[(2,3-

dimethyl-2H-indazol-6-yl)methylamino]-2-pyrimidinyl]-amino]-2-methyl-benzenesulfonamide (Pazopanib), a novel and potent vascular endothelial growth factor receptor inhibitor. J. Med. Chem. 51: 4632-4640.

Kwiatkowski, E. and Kwiatkowski, M. 1980. Unsymmetrical Schiff base complexes of Ni(II) and Pd(II). Inorg. Chim. Acta. 47 (2):197-202.

Lever ABP. 1980. Inorganic Electronic Spectroscopy. (4th ed.) Elsevier. London. 481-579.

Osowole, AA, Kolawole GA. and Fagade, OE. 2005. Synthesis, Physicochemical and Biological Properties of Ni(II), Cu(II) and Zn(II) Complexes of an Unsymmetrical Tetradentate Schiff-base and their Adducts. Synth. React. Inorg. Met. Org. Chem. & Nano-Met. Chem. 35:829-836.

Osowole, AA., Kolawole, GA. and Fagade, OE. 2008. Synthesis, Characterization and Biological Studies on unsymmetrical Schiff-base Complexes of Ni(II), Cu(II), Zn(II) and Adducts with 2, 2'-Dipyridyl and 1,10-phenanthroline. J. Coord. Chem. 61(7):1046-1055.

Osowole, AA., Kolawole, GA., Kempe, R. and Fagade, OE. 2009. Spectroscopic, magnetic and biological studies on some metal(II) complexes of 3-(4,6-dimethyl-2-pyrimidinylamino)-1-phenyl-2-butenone and their adducts with 2,2'-bipyridine and 1,10-phenanthroline. Synth. React. Inorg. Met. Org. Chem .& Nano-Met. Chem. 39:165-174.

Pelczar, MJ Jr., Chan, ECS. and Krieg, NR.. 1996. Microbiology. McGraw-Hill. New York, USA. 469-510.

Ramaling, S. and Belani, CP. 2007. Role of bevacizumab for the treatment of non-small-cell lung cancer. Future oncology. 3:131-139.

Sharma, VK. and Srivastava, S. 2006. Template synthesis and structural characterisation of Homo Binuclear Cr(III), Mn(II), Fe(III), Co(III) and Ru(III) complexes with octamacrocyclic ligands. Turk J. Chem. 30:755-767.

Shreelekha, A., Vivek, B., Di, C., Fakhara, A., Ping Dou, Q., Subhash, P. and Fazlul, HS. 2006. Novel Schiff Base Copper Complexes of Quinoline-2-Carboxaldehyde as Proteasome Inhibitors in Human Prostate Cancer Cells. J. Med. Chem., 49 (24):7242 -7246.

Singh, KN., Singh, DK. and Singh, SB. 2001. Synthesis, characterization and biological studies on Co(II), Ni(II), Cu(II) and Zn(II) complexes with N-picolinoyl-N-thiobenzoyl hydrazine. Synth. React. Inorg. Met.-Org. Chem. 32 (4):703-720.

Soenmez, M., Levent, A. and Sekerci, M. 2004. Synthesis, characterization, and thermal investigation of some metal complexes containing polydentate ONO-donor heterocyclic Schiff base Ligand. Russian J. Coord. Chem. 30 (9):655-659.

Sonmez, M. and Haciyusufoglu, ME. 2006. Synthesis and characterization of Co(II), Ni(II), Cu(II) and Zn(II) Schiff base complexes derived from acetylacetone with 1- amino -5-benzoyl-4-phenyl-1H pyrimidine -2-one. Asian J. Chem. 18(3):2032-2036.

Thangadurai, TD. and Natarajan, K. 2001. Mixed ligand complexes of ruthenium(II) containing α,β-unsaturated-β-ketoamines and their antibacterial activity. Trans. Met. Chem. 26: 500–504.

Wilhelm, S., Carter, C., Lynch, M., Lowinger, T., Dumas, J., Smith, RA., Schwartz, B., Simantov, R. and Kelley, S. 2006. Discovery and development of sorafenib: a multikinase inhibitor for treating cancer 1. Nat. Rev. Drug Discov. 5(10):835-844.

Zhaohua, H., Zhaoliang, L. and Huang, J. 2001. A novel kind of antitumor drugs using sulfonamide as parent compound. Eur. J. Med. Chem. 36 (11-12):863-867.

Zhong, X., Yi, J., Sun, J., Wei, HL., Liu, WS. and Yu, KB. 2006. Synthesis and crystal structure of some transition metal complexes with a novel bis-Schiff base ligand and their antitumor activities. Eur. J. Med. Chem. 41 (9):1090-1092.

Received: April 10, 2010; Accepted: May 29, 2010

SENRA Academic Publishers, Burnaby, British Columbia
Vol. 4, No. 2, pp. 1179-1185, June 2010
ISSN: 1715-9997

Canadian Journal of pure&applied sciences

HISTOLOGICAL STUDIES OF BREWERY SPENT GRAINS IN DIETARY PROTEIN FORMULATION IN DONRYU RATS

*Ajanaku, K O[1], Dawodu, F A[2], James, O O[1], Ogunniran, K O[1], Ajani, O O[1] and Nwinyi, O C[3]
[1]Department of Chemistry, College of Science and Technology, Covenant University
PMB. 1023, Ota, Ogun State
[2]Department of Chemistry, Faculty of Science, University of Ibadan, Oyo State
[3]Department of Biological Sciences, College of Science and Technology, Covenant University
P.M.B. 1023, Ota, Ogun State, Nigeria.

ABSTRACT

The increasing production of large tonnage of products in brewing industries continually generates lots of solid waste which includes spent grains, surplus yeast, malt sprout and cullet. The disposal of spent grains is often a problem and poses major health and environmental challenges, thereby making it imminently necessary to explore alternatives for its management. This paper focuses on investigating the effects of Brewery Spent Grain formulated diet on haematological, biochemical, histological and growth performance of Donryu rats. The rats were allocated into six dietary treatment groups and fed on a short-term study with diet containing graded levels of spent grains from 0, 3, 6, 9, 12 and 100% weight/weight. The outcome demonstrated that formulated diet had a positive effect on the growth performance of the rats up to levels of 6% inclusions, while the haematological and biochemical evaluation revealed that threshold limit should not exceed 9% of the grain. However, the histological study on the liver indicated a limit of 3% inclusion in feed without serious adverse effect. Thus invariably showing that blend between ranges 1-3% is appropriate for the utilization of the waste in human food without adverse effect on the liver organ. The economic advantage accruing from this waste conversion process not only solves problem of waste disposal but also handle issues of malnutrition in feeding ration.

Keywords: Brewery spent grains, waste utilization, donryu rats, dietary treatment.

INTRODUCTION

Brewery Spent Grains (BSG) is one of the voluminous solid residuals that remain after the mashing process. It has received little attention as a marketable commodity apart from being used primarily as ruminant feed and its disposal is often a problem. Its present disposal methods which include dumping, use as animal feed and biomass are no longer sustainable for the environment with devastating level of pollution. Nutritionally, the grain is far from spent since the residual protein level is in the range of 26-30% and crude fibre content up to 13% (Qzturk *et al*., 2002). BSG is a safe feed when it is used fresh or properly stored. The wet grain spoils quickly and should be used fresh or stored in an air tight compartment. However, BSG may vary with barley variety, time of harvest, characteristics of hops and other adjunct added as well as brewing technology. The waste management problems then require developing new ways to use the spent grains considering the adverse impacts on environment and health.

There have been advances on the importance of fibre in diets as well as protein being used as supplements in food (Trowell *et al*. (1975). Other researches Bays (1977); Tacon and Ferms (1978); Ahn (1979); Enweremade *et al*. (2008); and Bi-Yu *et al*. (1998) also focused on alternative uses of brewery by – products and waste minimization from brewery processes. There was also a growing interest in the use of BSG in human foods such as flour mixes, bread and meat product (Morgan *et al*., 1984; Chiou *et al*., 1995; Kellems and Church, 1998; Finley and Hanamoto, 1980). However not much has been carried out in the area of histopathological effect in human foods when used as protein supplement. In the light of the above findings, this study has been undertaken to determine the effect of using BSG as dietary feed and the histological effect it will have on human organs if utilized.

*Corresponding author email: kolatooyin@yahoo.com

MATERIALS AND METHODS

Chemicals and Reagents

All chemicals and reagents were of analytical grade.

Sources of Materials

Brewery Spent Grains was obtained from Nigerian Breweries Plc, Ibadan, Nigeria. The spent grain was a mixture of sorghum and barley. Maize, soyabean meal, wheat offal, fish meal, bone meal, salt, lysine, methionine and premix (Growers) were obtained from International Institute of Tropical Agriculture (IITA) Ibadan, Nigeria to

prepare the rats feed. The rats for the experiment were obtained from the animal farm of Cocoa Research Institute (CRIN) Ibadan having life average weight range of 49.92 ± 5.69g. The rats were in the family of Donryu species and were four weeks old before the commencement of the experiments. The ethnic use of the animals was also obtained from the Institute.

Treatment of Brewery Spent Grains Sample

The BSG samples were collected in wet form, sundried and later dried at 40^{o}C for six hours in an electric oven. It was then stored in an airtight container till the time of use. The dried BSG was milled to increase the surface area. The moisture content, ash content, crude fat, crude protein, crude fibre and the nitrogen-free extract of the BSG were determined. The BSG were mixed with rats feed at levels of 0, 3, 6, 9, 12 and 100% w/w. The 0% was the control, while the 100% serves as the extreme use of BSG alone.

Treatment of Animals

The thirty six (Donryu) rats were allocated into six dietary treatment groups of six rats each and confined into individual cages during the experimental period. The animals were free from externals and internal parasites. The study was conducted during the rainy season and the cages were built for easy collection of the faeces and urine. They were weighed at the beginning of the experiment as zero (0) day; fed according to their group levels with the BSG compounded feeds and subsequently weighed at daily intervals in a short time study of fifteen days.

Preparation of Blood Samples

On the sixteenth day of the experiment, the rats were humanely slaughtered using cervical dislocation method of Euthanasia Klaunberg *et al.* (2004). Their blood samples were collected into two heparinized tubes for the studies; one tube contains ethylene diaminetetracetic acid (EDTA) with calcium serving as anticoagulant in the blood samples for the haematology tests while the second tubes, which did not contain EDTA, were stored at -20^{o}C for the biochemical studies. The internal organs of the rats (liver, heart and kidney) were collected and weighed. The microscopic slide of the liver organs were then prepared and observed.

Analysis of Heamatological and Biochemical Parameters

Red blood Cell (RBC) and white blood cell (WBC) counts were determined using Neubauer haemocytometer. Packed cell volume (PVC) was determined using haematocrit centrifuge. Haemoglobin was determined by cyanmethemoglobin method (MCH), Mean Corpuscular Haemoglobin (MCH) and Mean Corpuscular Haemoglobin Concentration (MCHC) were determined according to the methods of Jain (1986). Glutamate Pyruvate Transaminose (GPT), Glutamate Oxaloacetate Transaminase (GOT), Globulin (GLB), Albumin (ALB) and Alkaline Phosphatase (ALP) were analysed spectrophotometrically by using commercially available diagnostic kits.

STATISTICAL ANALYSIS

The data collected were subjected to statistical analysis of variance and means compared by the Duncan's Multiple Range Test (Steel and Torrie, 1980).

RESULT AND DISCUSSION

The proximate analysis of the Brewery Spent Grains (BSG) samples is presented in table 1. The carbohydrate level was high with value of 51.38% and coupled with the 38% of nitrogen-free extract and crude protein of 23.19% gives a clue of a balanced formulation if the BSG is compounded as feed blends. The high protein values observed in the sample was due to the protein rest and washing operation of the grains during the brewing process.

Table 1. Proximate Analysis of the Brewery Spent Grains (BSG) Samples.

Analysis	Percentage Mean Amount (%)
Crude Protein	23.20
Crude Fibre	12.85
Crude Fat	2.79
Moisture Content	6.14
Ash Content	16.99
Carbohydrate	51.39
Total Nitrogen	3.71
Nitrogen – Free Extract	38.03

The ration formulation for the feed diet is shown in table 2 while the effect of spent grains on the weight of the rats and the average weights of the rats are shown in tables 3 and 4. The effect of BSG blend on the weight of the rats was commendable. The 3 and 6% BSG blends gave an average daily weight gain of 3.810 and 3.520g respectively, which was higher than the value of 3.706g obtained for the control (0% BSG). There was significance increase ($p < 0.05$) in the average weight gained by the rats fed in all the groupings except in the 100% group. This implied a high feed-efficiency due to increased level of blending of the spent grains. The statistical analysis shows that the results fits a linear model of 0.532024 - 0.154247 x Weight Gain in order to describe the relationship between the feed-efficiency and weight gain. This also revealed 84.58% of the variability in feed-efficiency while the correlation coefficient indicated a strong relationship between the variables. Since the p-value is < 0.05, there is a statistically

Table 2. Ration formulation of the treatment feed diets (g/100g).

Ingredients	Diets					
	1	2	3	4	5	6
	% BSG inclusion in diets					
	0%	3%	6%	9%	12%	15%
Maize	2.64	2.57	2.49	2.41	2.33	2.25
BSG	0.00	0.07	0.15	0.23	0.31	0.39
Soybean Meal	1.20	1.20	1.20	1.20	1.20	1.20
Palm Kernel Cake / Wheat offal	1.60	1.60	1.60	1.60	1.60	1.60
Blood meal	0.4	0.4	0.4	0.4	0.4	0.4
Bone meal	0.04	0.04	0.04	0.04	0.04	0.04
Salt	0.04	0.04	0.04	0.04	0.04	0.04
Lysine	0.03	0.03	0.03	0.03	0.03	0.03
Methionine	0.03	0.03	0.03	0.03	0.03	0.03
Premix[1]	0.02	0.02	0.02	0.02	0.02	0.02
Total (g)	6.00	6.00	6.00	6.00	6.00	6.00

[1]Contained vitamins A (10,000,000iu); D (2,000,000iu); E (35000iu); K (1900mg); B_{12} (19mg); Riboflavin (7,000mg); Pyridoxine (3800mg); Thiamine (2,200mg); D pantothenic acid (11,000mg); Nicotinic acid (45,000mg); Folic acid (1400mg); Biotin (113mg); and trace elements as Cu (8000mg); Mn (64,000mg); Zn (40,000mg); Fe (32,000mg); Se (160mg); I_2 (800mg); and other items as Co (400mg); Choline (475,000mg); Methionine (50,000mg); BHT (5,000mg) and Spiramycin (5,000mg) per 2.5kg

Table 3. Mean body weight of Rats for each day (Grammes).

Days/Blends	0%	3%	6%	9%	12%	15%	100%
0 day (g)	52.55 ±2.250	55.50 ±2.700	49.55±3.350	49.15 ±4.351	44.10 ±3.900	42.29 ±2.100	48.65 ±4.110
1st (g)	52.95 ±4.751	55.75 ±3.851	51.00 ±5.201	51.40 ±3.901	45.45 ±5.020	42.13 ±3.220	46.00 ±3.951
2nd (g)	52.35 ±3.150	56.45 ±3.551	55.85 ±4.251	54.10 ±6.001	46.35 ±5.651	43.26 ±2.510	41.80 ±3.751
3rd (g)	55.85 ±1.850	57.93 ±3.826	60.00 ±4.101	59.65 ±5.751	47.05 ±6.451	43.12 ±4.280	38.35 ±3.301
4th (g)	58.55 ±0.6501	70.80 ±4.201	63.80 ±4.301	61.75 ±6.051	48.30 ±4.801	43.64 ±2.110	37.35 ±4.601
5th (g)	63.30 ±2.20	83.15 ±5.51	68.50 ±4.301	64.25 ±5.051	50.55 ±4.551	44.32 ±3.320	34.90 ±4.351
6th (g)	66.10 ±2.50	86.30 ±3.001	71.10 ±4.801	68.10 ±4.301	51.35 ±5.051	44.24 ±4.110	32.70 ±3.351
7th (g)	69.95 ±3.050	90.15 ±3.751	74.25 ±4.351	70.90 ±4.701	51.40 ±5.801	45.13 ±4.350	29.60 ±3.751
8th (g)	75.50 ±4.001	93.95 ±3.451	75.80 ±4.801	74.70 ±4.001	52.60 ±4.401	45.35 ±2.600	30.00 ±3.751
9th (g)	80.30 ±4.101	95.70 ±3.501	83.05 ±3.451	78.45 ±3.351	52.55 ±4.751	45.68 ±3.140	26.10 ±3.651
10th (g)	84.50 ±5.101	98.65 ±4.451	85.15 ±3.151	79.15 ±2.150	53.45 ±4.851	46.32 ±2.101	25.20 ±3.851
11th (g)	88.50 ±5.351	99.15 ±4.451	90.30 ±2.10	81.85 ±0.850	54.50 ±4.101	47.01 ±5.210	22.95 ±3.001
12th (g)	93.65 ±4.951	105.25 ±3.051	94.00 ±2.700	83.70 ±3.101	55.20 ±4.501	48.15 ±2.130	20.35 ±3.401
13th (g)	99.70 ±6.201	108.65 ±3.051	95.90 ±0.90	84.25 ±3.451	55.45 ±3.651	48.98 ±3.323	17.85 ±2.701
14th (g)	102.10 ±4.701	112.60 ±1.10	97.70 ±2.30	84.90 ±2.50	56.15 ±2.350	49.32 ±2.220	17.50 ±2.951
15th (g)	108.15 ±4.551	112.65 ±1.750	102.40 ±2.70	85.15 ±2.550	57.70 ±2.40	49.71 ±3.170	17.45 ±2.901

significant relationship between feed-efficiency and weight gained at the 95.0% confidence level. It was observed that increasing levels of BSG in the diet resulted in decreased body weight with threshold limit in the range of 9% (Fig. 1).

The rats in the 100% BSG group experienced daily weight loss of -2.080 g per day, and their metabolic wastes concentration was very high and toxic to inhale. The loss in the body weight might be due to low level of crude fat (2.79%) in the feed. These findings agreed with the reports of Ironkwo and Oruwari (2004) who reported that fat supplementation significantly improve feed conversion efficiently. The acceptable limit is in the range of 1% to 6% w/w of the blends. For obese patient, the range between 9-12% is a good recommendation. The statistical significance of the mean body weight of the rats ($p<0.01$) when compared with the control (0%) in all groupings was significantly difference at the 0.01 level (2-tailed). Therefore their body weights are different from each other from the descriptive statistics.

Table 4. Weight gain by rats for each feed formulation per day.

Feeding	Weight at 0 day (g)	Weight at 15th day (g)	Weight difference (g)	Weight gain/day
0%	52.55 ±2.250	108.15 ±4.551	55.60	3.706
3%	55.50 ±2.700	112.65 ±1.750	57.15	3.810
6%	49.55 ±3.350	102.40 ±2.70	52.85	3.520
9%	49.15 ±4.351	85.15 ±2.550	36.00	2.400
12%	44.10 ±3.900	57.70 ±2.400	13.6	0.907
15%	42.29 ±2.100	49.71 ±3.170	7.42	0.495
100% BSG	48.65 ±4.100	17.45 ±2.901	-31.20	2.080*

* Weight loss

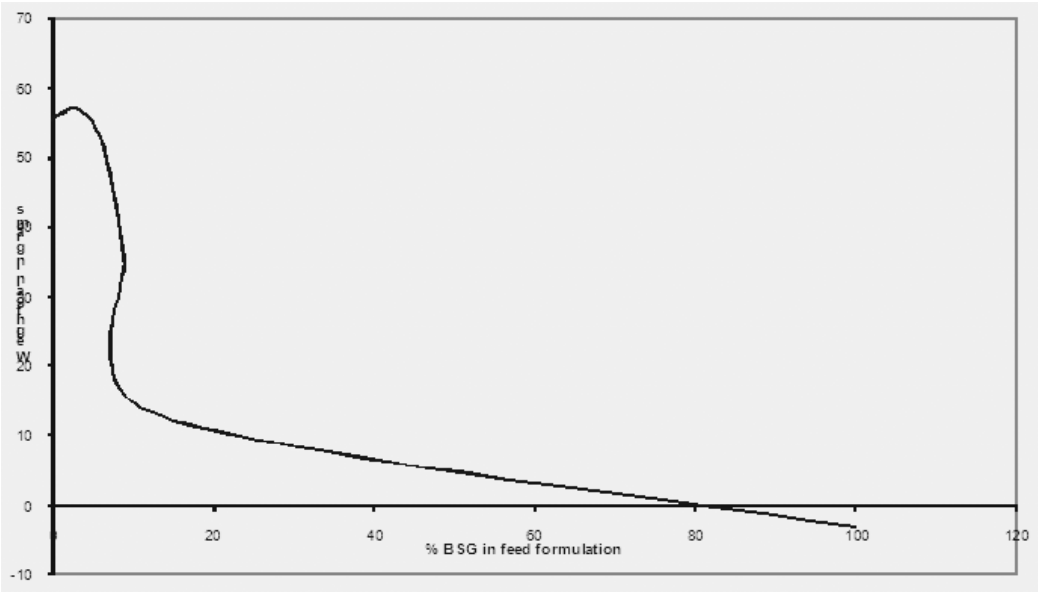

Fig. 1: Graph showing weight gain by rat against % BSG in the feed formulation.

Table 5. Mean internal organ weight (grammes) of the rats.

Blends	Internal organs			
	Liver	Kidneys	Lungs	Heart
	weight (g)	weight (g)	weight (g)	weight (g)
0%	5.41 ±0.11	0.970 ±0.05	0.86 ±0.060	0.53 ±0.025
3%	4.54 ±0.06	0.75 ±0.01	0.80 ±0.01	0.46 ±0.035
6%	5.01 ±0.59	0.91 ±0.04	1.30 ±0.13	0.42 ±0.005
9%	4.87 ±0.035	0.91 ±0.07	1.09 ±0.01	0.51 ±0.01
12%	5.11 ±0.685	0.75 ±0.255	1.03 ±0.175	0.51 ±0.005
15%	4.42 ±0.535	0.77 ±0.450	1.10 ±0.295	0.39 ±0.710
100% BSG	2.01 ±0.685	0.69 ±0.090	0.52 ±0.030	0.25 ±0.035

The result of the mean internal organs weight of the rats fed with the blends is presented in table 5. The mean liver weight for the control group was 5.41 ± 0.11 g, while those fed with only BSG dropped to 2.01 ± 0.685 g. The same was observed for the mean kidney weights, while others were within the range of the control 0.970 ± 0.05 g. Those fed in 100% BSG have their kidney weight reduced to 0.69 ± 0.09 g. Generally, the rats fed with 100% BSG have their liver, kidneys, lungs and heart weight reduced when compared with the control and other groups, because of the absence of enrichment that could sustain the blend. This implies that, if the blend is appropriately enriched, there could be a positive response as it was observed in the other groupings.

In tables 6 and 7, the heamatological and the biochemical studies of the rats used for the experiment were respectively presented. The normal packed cell volume

Table 6. Haematological studies of BSG blended feed in Rats.

Parameter / Blends	0% BSG	3% BSG	6% BSG	9% BSG	12% BSG	15% BSG	Normal Value
Hb (g%)	10.90 ± 0.2	13.8 ± 0.6	13.80 ± 0.2	7.60 ± 0.3	11.60 ± 0.4	12.8 ± 0.1	16.1 ± 0.4
PCV (%)	31.70 ± 1.22	39.00 ± 1.18	38.00 ± 2.17	30.00 ± 1.11	24.00 ± 1.42	30.70 ± 2.23	40.6 ± 0.27
RBC ($x10^6/mm^3$)	3.68 ± 0.42	5.52 ± 0.22	4.78 ± 0.45	3.80 ± 0.34	4.50 ± 0.23	3.85 ± 0.54	8.21 ± 0.14
MCV (U^3)	95.00 ± 6.10	87.00 ± 4.20	83.00 ± 3.02	82.00 ± 5.40	85.00 ± 3.25	91.00 ± 2.50	56.2 ± 0.6
MCH (Ug)	33.00 ± 1.22	32.00 ± 3.10	29.00 ± 3.12	27.00 ± 1.12	30.00 ± 2.72	32.00 ± 1.11	14.7 - 15.9
MCHC (%)	33.00 ± 2.10	37.00 ± 2.11	36.00 ± 1.10	35.00 ± 3.11	34.00 ± 3.40	34.20 ± 3.25	32.4 ± 0.4
Neutro (%)	6.00 ± 0.15	20.00 ± 0.55	2.00 ± 0.18	4.00 ± 0.10	26.00 ± 0.49	12.00 ± 1.20	10 – 55
Lympho (%)	94.00 ± 5.35	80.00 ± 6.82	98.00 ± 6.82	96.00 ± 4.57	74.00 ± 3.45	88.00 ± 5.10	40 – 90
Eosino (%)	0	0	0	0	0	0	0
Mono (%)	0	0	0	0	0	0	0
Baso (%)	0	0	0	0	0	0	0
Platelets ($x10^3/mm^3$)	155.00 ± 11.20	198.00 ± 10.30	210.00 ± 12.32	180.00 ± 13.16	184.00 ± 10.10	168.00 ± 11.12	54.5 ± 13.6
WBC ($x10^3/mm^3$)	5.00 ± 0.11	7.20 ± 0.14	6.60 ± 0.17	7.10 ± 0.26	5.20 ± 0.13	6.20 ± 0.10	5.3 ± 0.5

Platelets($10^3/mm^3$), Neutrophil (%) Eosinophil (%); Lymphocytes (%); Monocytes (%); Basophil (%) Hb = Haemoglobin, concerntration (g%); PCV = Packed cell volume (%), RBC = Red Blood Cell Counts ($x10^6/mm^3$), WBC = White Blood cell count ($x10^3/mm^3$), MCV = Mean Corpuscular Volume (U^3) , MCH = Mean corpuscular Haemoglobin (UUg); MCHC = Mean Corpuscular Haemoglobin Concentration (%). IU/L = International unit per litre;

Table 7. Biochemical studies of BSG blended feed in Rats.

Parameter/ Blends	0%	3%	6%	9%	12%	15%	Normal Value
ALP (IU/L)	250.00 ± 35.10	302.00 ± 30.12	300.00 ± 12.20	298.00 ± 16.30	275.00 ± 28.20	213.00 ± 30.11	43.2 ± 0.38
GOT (IU/L)	66.00 ± 5.40	72.00 ± 4.90	71.00 ± 3.20	70.00 ± 2.50	68.00 ± 4.50	57.00 ± 3.11	7.3 ± 0.4
GPT (IU/L)	46.00 ± 4.22	36.00 ± 3.61	44.00 ± 1.84	46.00 ± 2.61	48.00 ± 2.22	46.00 ± 2.62	NA
AP (g/dL)	65.00 ± 4.80	68.00 ± 2.56	67.00 ± 1.68	66.00 ± 3.22	59.00 ± 3.81	62.00 ± 1.12	NA
TP (g/dL)	7.30 ± 0.57	6.60 ± 0.77	6.90 ± 0.83	6.40 ± 0.10	6.50 ± 0.22	7.10 ± 0.45	0.65 ± 0.02
ALB (g/dL)	3.90 ± 0.71	4.30 ± 0.90	4.10 ± 0.21	4.00 ± 1.00	3.80 ± 0.51	3.80 ± 0.60	0.43 ± 0.02
GLB (g/dL)	3.40 ± 0.55	2.30 ± 0.11	2.80 ± 0.30	2.40 ± 0.41	2.70 ± 0.12	3.30 ± 0.45	NA
ALB/GLB RATIO	1.15 ± 0.01	1.87 ± 0.12	1.46 ± 0.11	1.67 ± 0.55	1.41 ± 0.31	1.15 ± 0.50	

ALP = Alkaline phosphatase (IU/L); g/dL = gramme per deciliter; GOT = Glutamate Oxalacetate Transaminase (IU/L); ALB = Albumin (g/dL); GLB = Globulin (g/dL); ALB/GLB = Albumin – Globulin ratio; GPT = Glutamate Pyrovate Transaminase (IU/L); TP = Total Protein (g/dL); AP = Acid Phosphatase (IU/L).

(PCV) of the Donryu rat was in the range of 36 – 54 %. The lower end of the range is normal in juveniles, but not in adult rats. The rats fed with 3% and 6% BSG blends experienced a significant increase in haemoglobin concentration of 13.8 ± 0.6 and 13.8 ± 0.2 g% respectively. The observed value for packed cell volume (PCV), 39.00 ± 1.18% for 3% blend and 38.00 ± 2.17% for 6% blend; red blood cell counts (RBC) was 4.78 ± 0.45 $10^6/mm^3$ as against the control 3.68 ± 0.42 $10^6/mm^3$; white blood cell counts (WBC) was in the range of 7.20 – 7.10 $10^3/mm^3$ in 3% to 9% respectively.

Platelets had the highest value of 210 ± 12.32 $10^6/mm^3$ in 6% as against 155.00 ± 11.20 $10^6/mm^3$ observed in the control. Mean corpuscular haemoglobin concentration (MCHC) of the entire group was higher than the control group. Alkaline phosphatase (ALP), glutamate oxalacetate transminase (GOT), acid phosphatase (AP), and albumin (ALB) also showed significant increase as compared with the 0% BSG blend. The resistance of the body system to infection in 3% and 6% rats' blood was high because there are direct actions of antibodies attacking the antigenic invaders, due to antibodies or anti infection properties that is present in the blood. Blood of the rats fed with 9% BSG blend had a reduced haemoglobin concentration, packed cell volume, but there was high value in WBC, lymphocytes, platelets, alkaline phosphates and albumin, compared with the 0% blend.

Table 8. Histopathology result of rats' liver.

Formulation	Histology	
	Sinusoids	Central Vein
0%	Normal	No visible lesions
3%	Normal	Mild periportal lymphocytic infiltrates
6%	Widening	Epithelia lining affected
9%	Almost disappeared	Epithelia lining affected
12%	Inflammatory	Hepatitis
15%	Compacted	Hepatitis

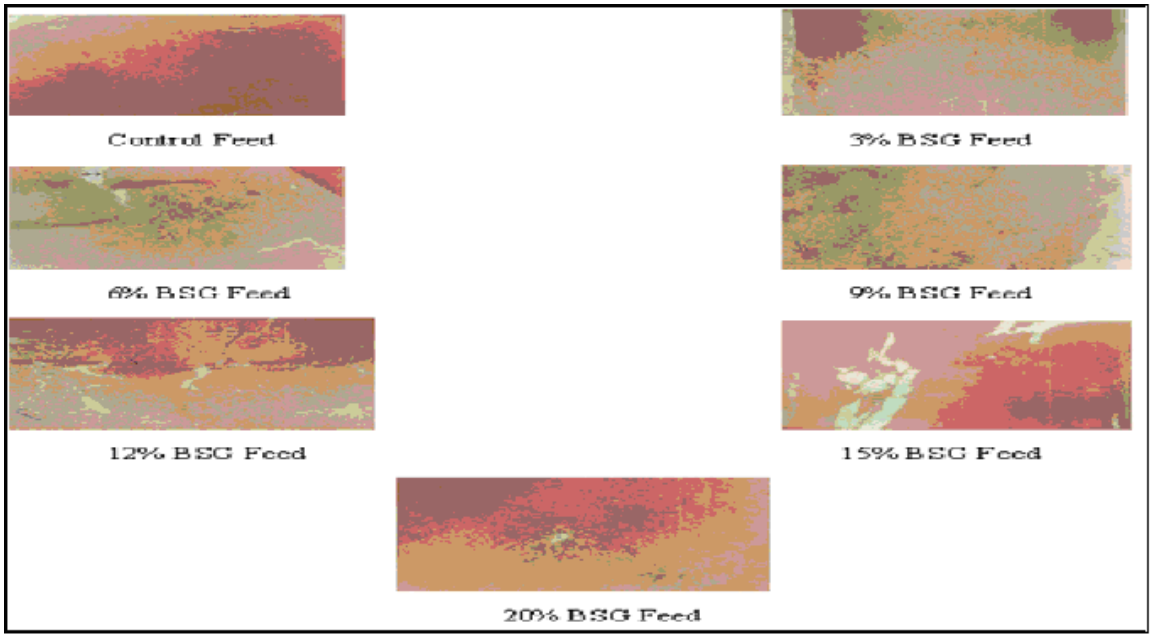

Plate 1. Microscopic view of rats' liver fed with BSG compounded feeds.

The rats fed with 12% blend had a low value in PCV, MCV, MCH, lymphocytes, AP, but increased value in ALP, Hb, RBC and WBC in comparison with the control. The 15% blends had a reduced MCV, MCH, ALP and lymphocytes values but an increased PCV, Hb, RBC, MCHC, WBC and platelets values. This result revealed that BSG presence activates oxygen in the blood cell thereby making the haemoglobin in the red blood cell inactive, a state which is termed hypoxia, and this enhances increase in the production of red blood cell counts and haemoglobin stimulating synthesis. It was observed that the histopathology result varies with the weather, climate, and region under which the experiment was carried out. The temperate and tropical region may have slight difference from each other in their blood result. In spite of this, it was observed that the rats fed with high concentration was adversely affected, hence low concentration of the blend is appropriate without side effects. Eosinophils count, monocytes and basophils counts are not significantly different in the blood of the rats, hence no significant change. The statistical significance of the histophatology on blood of the different blends at the 0.01 level (2-tailed) of 99% confidence interval showed significant difference, but they are not significantly different at 0.05 level (2-tailed) at 95% confidence interval, $p<0.05$, when compared with the control.

The histopathology study of the liver of the rats used as experimental model is shown in Plate 1 and Table 8. This revealed that the control blend cell looks normal, the central vein was seen and there was no visible lesion, the sinusoids were normal and the epithelium lining remained. In the 3% blend; the cell appeared normal but the sinusoids became larger and the space between sinusoids was bigger when compared to the control. There were mild periportal lymphocytic infiltrates noticed in the central vein. In 6% blend, the sinusoids became widened which encloses the central vein and the epithelia lining was affected too. The sinusoids almost disappeared and the hepatic cells were affected when the 9% blend was observed. For 12% blend, the central vein was seen and

the sinusoids experienced a hepatitis alteration. The sinusoid was more compacted and there was serum hepatitis in the central vein in the categories of 15% blend. The histological study of the kidney also showed that the kidneys of the control, 3, 6, 9 and 12% are all normal, while the kidney of 100% blend had a nephrotoxic effect, which is fatty degradation in the cellular tubules and glomerular region. This could be attributed to high protein, though the basis was not understood and the phenomenon that it was due to high protein was not confirmed. It could be due to some other substances that are present in BSG. The summary of the histopathology result suggest that the use up to 3% concentration will not have adverse effect on human liver and that the concentration of the blend should be kept minimal.

CONCLUSION

In this study, it has been shown that blends from 1-3% BSG could be used as protein supplement with 3% BSG as the threshold limit by virtue of the histological effect on rats liver. Thus invariably showing that blend between ranges 1-3% is appropriate for the utilization of the waste in human food without adverse effect on the liver organ. These levels of incorporation will reduce the number of people suffering from micronutrient deficiency related disease in developing nations as well as propose an additional utilization alternative to the disposal of brewery spent grains worldwide.

REFERENCES

Ahn, BH. 1979. Studies on the Nutritive Value of Brewery Activated Sludge: Animal Science. 21:411-414.

Bays, JD. 1977. Waste Activated Sludge: A new brewery by-products. MBAA Teach Quart. 14:47-49.

Bi-Yu, Chen-Chaoven. and Chiou-Wenshy. 1998. Wet Brewer's Grain or Bean Curd Pomance as Partial Replacement of Soya bean meals lactating cows. J. Animal Feed Science and Technology. 5:120-128.

Chiou, PWS., Chen, KJ., Kuo, KS., Hsu, JC. and Yu, B. 1995. Studies on the protein degradabilities of feedstuffs in Taiwan. Anim. Feed Sci. Technol. 55:215-226.

Enweremade, CC., Waheed, MA., Adekunle, AA. and Adeola, A. 2008. The energy potential of Brewer's Spent Grain for Breweries in Nigeria, Journal of Engineering and Applied Sciences. 3(2):175-177.

Finley, JW. and Hanamoto, MM. 1980. Milling and baking properties of dried brewer's spent grains. Cereal Chem. 57(3):166-168.

Ironkwo, MO. and Oruwari, BM. 2004. Influence of the dietary Palm oil, Groundnut oil and Corn meal on Performance of the Rabbit. Proceedings of the 29th Annual Conference of the Nigerian Society for Animal Production. 29:176-178.

Jain, NC. 1986. Schalms Veterinary Haematology 4th Edition. Lea and Febiger. Philadelphia, USA.

Kellems, RO. and Church, DC. 1998. Livestock Feeds and Feeding (4th Edit.) Simon and Schuster, New Jersey, USA. pp. 59-61.

Klaunberg, BA., O'Malley J., Clark, T. and Davis, JA. 2004. Euthanasia of Mouse Fetuses and Neonates. Contemp. Top. Lab. Anim. Sc. 43(5):29-34.

Morgan, PJ., Smith, WC. And Jones, KAC. 1984. Preliminary observations on the use of rats as a model for the pig in the determination of apparent digestibility of dietary proteins. New Zealand J.Agric. 27(4):509-512.

Ozturk, S., Ozboy, O., Cavidogly, I. and Koksel, H. 2002. Effect of Brewer's Spent grain on the Quality and Dietary Fibre Content of Cookies. Journal of the Institute of Brewing. 108(1):23-27.

Steel, RGD. And Torrie, JH. 1980. Principles and Procedures of Statistics. A Biometrical Approach (2nd Edit. McGraw-Hill Book Co. New York.

Tacon, ACJ. and Ferns, PN. 1978. Activated Sludge: A potential Animal Food Stuff I. Proximate and Mineral Content. Seasonal Variation Agric, Environ. 4:257-269.

Received: Aug 5, 2009; Accepted: April 19, 2010

SENRA Academic Publishers, Burnaby, British Columbia
Vol. 4, No. 2, pp. 1187-1197, June 2010
ISSN: 1715-9997

Canadian Journal of pure&applied sciences

ESTIMATING GEOMAGNETICALLY INDUCED CURRENTS AT SUBAURORAL AND LOW LATITUDES TO ASSESS THEIR EFFECTS ON POWER SYSTEMS

Falayi EO and Beloff, N.
Space Science Centre, University of Sussex, Falmer, East Sussex, BN1 9QJ, UK

ABSTRACT

During large magnetic storm the geomagnetically induced current has a negative impact on ground conducting technology systems. The time derivative of the horizontal component of the geomagnetic field (dH/dt) is greater than 30nT/min for induced currents causing undesirable consequence in power grids. Multiple regression analyses were developed to predict the level of geomagnetic disturbance using time derivatives of the horizontal geomagnetic field, east and north components of the geoelectric field, auroral electrojet and disturbance storm times from 1994-2007 at low and subauroral latitudes. The statistical test RMSE (Root Mean Square Error) and MBE (Mean Bias Error) were employed to evaluate the accuracy of the geomagnetic disturbance. Different variables have been used to develop different types of models. Values of the correlation coefficient and the coefficient of determination were high, which indicates that the results are good. The equations produced the best correlations at subauroral and low latitudes, and the best correlation was obtained with low values of RMSE and MBE.

Keywords: Time derivatives of the geomagnetic field, geomagnetically induced current, latitudes.

INTRODUCTION

Grounds based technologies especially electric power, are susceptible to geomagnetic storms and geomagnetically induced current. This arises from the changes in the Earth's magnetic field, caused by high energy particle streams from the Sun. It creates voltage between grounding points in the grid, which in turn induces a small, irregular dc current to flow along electric power lines and into transformers. Both space-borne and ground-based technology can experience problems due to space weather (Pirjola *et al*., 2005).

Geomagnetically induced current (GIC) are directly related to the horizontal time derivatives of the geomagnetic field strength produced by the changing of electrical current in the ionosphere and magnetosphere. These changes in the geomagnetic field in turn produce an electrical current that flows around the Earth's surface. Disturbances in power grid systems are directly related to geomagnetic storms and are caused by voltages induced at ground level by variations in ionospheric and magnetosphere currents. The magnetosphere and ionospheric electric current induces changes in the magnetic field and varying voltage in the crust of the Earth and this in turn drives a direct current through transformers, called (GIC). These GIC can harm power equipment and even cause a collapse of the power system (Coles *et al*., 1992; Makinen, 1993; Viljanen, 1998, 2001; Kappenman, 2006). Observations also confirmed that geomagnetic field disturbances usually associated with equatorial region current intensification can be a source of large magnitude and long duration GIC in power grids in low and equatorial regions (Erinmez *et al*., 2002). Kappenman (2005) established the fact that GIC studied during an October 2003 storm that caused geomagnetic disturbance in low and equatorial areas were due to ring current intensification that served as a source for GIC in the mid latitude regions.

The fundamental principle of the flow of GIC in ground based technology is well understood using the Faraday law of induction. Electric fields drive current in ground technology networks. The geomagnetic variation and the geoelectric field observed at the Earth's surfaces which primarily depend on the magnetosphere and ionospheric current, determine the space weather conditions in the Earth's environment. Also, surface fields are affected by the current and charges induced in the Earth (Viljanen, 1997; Trichtchenko and Boteler, 2006). The geomagnetic field variations are associated with geoelectric field variation at the surface of the Earth which is influenced by the conductivities of different structures of the Earth's interior. The induced electric field is directly related to the rate of change of the geomagnetic field, which implies that many researchers have used time derivatives of the geomagnetic field as a measure of GIC strength. Boteler *et al*. (2000) concluded that geomagnetic disturbances are

*Corresponding author email: olukayodefalayi@yahoo.com

directly related to auroral electrojet and an assessment of the effects on the ground based technological systems requires that appropriate models of the electrojet are available. In the predicted levels of geomagnetically induced currents in power systems, it is significant that the electrojet model allows rapid calculations of the Earth-surface electric fields.

The geomagnetic disturbance that triggered the Hydro-Quebec collapse during the March 13, 1989, storm reached an intensity of 479nT/min. Power pools serving the entire north-eastern of Canada also came perilously close to a comparable calamity, with similar cascading system failures, during the same geomagnetic storm; its intensity ranged between 300 and 600nT/min. Malmo in Sweden experienced GIC problems leaving 50,000 customers with power blackouts on October 30, 2003, which lasted between 20 and 50 minutes. In South Africa, it was observed that the October and November 2003 geomagnetic disturbance damaged transformers (Campbell, 2003; Wik *et al*., 2008; Kappenman, 2006; Poppe and Jordan, 2006). In Africa and South America the GIC effect was also observed at low and mid latitudes (Barkers and Skinner, 1980; Ogunade, 1986; Osella and Favetto 1999; Vodjannikov *et al*., 2007). Koen and Gaunt (2002) carried out dH/dt measurement simultaneously with GIC records in the South African power grid. Comparison of GIC and dH/dt has shown that when dH/dt >30 nT/min, the induced current has an effect on the power grid.

Most of the ground technological systems located in higher latitude areas are prone to GIC effects. Pirjola (2004) reported that equatorial regions are affected by the equatorial electrojet current, and GIC investigation has been performed in Kenya, Nigeria and Argentina.

This paper presents the significance of GIC by measuring variation of the horizontal time derivatives of the geomagnetic field, at the threshold of dH/dt > 30nT/min at mid and low latitude. Multi regression analysis was also performed between the variables used.

METHODS

Data analysis

We used Dst and AE indices obtained from http://isgi.cetp.ipsl.fr and http://swdcwww.kugi.kyoto-u.ac.jp/index.html to define the substorms events from -90 up to -1800nT. The geomagnetic field parameters and telluric electric field (Ex and Ey) are obtained from the Canadian magnetic observatory for subauroral zones, and geomagnetic fields for low latitudes were obtained from INTERMAGNET. Table 1 gives the geographic and geomagnetic corrected coordinates (IGRF model http://www.iugg.org/IAGA/iaga_pages/pubs/igrf.htm) for the 6 observatories selected for this study which are: Ottawa, Victoria, St John, Addis Ababa, Bangui and M'bour. Ottawa, Victoria and St John are in the subauroral zone in the American longitude sector, M'bour is in tropical zone and Addis Ababa and Bangui are in the equatorial zone of the African longitude sector. The data used in this study covers the disturbed periods from 1994 -2007. We have taken a value as a threshold for the definition of total time of existence in the power grids of the selected geomagnetic observatories of the appreciable induced current, when dH/dt values are greater than 30nT/min, which appears to be significant in South Africa. Table 1 lists geographic and geomagnetic corrected coordinates.

A regression and correlation analyses were carried out between the time derivatives of the horizontal geomagnetic field (dH/dt), AE magnetic index related to auroral electrojets, Dst magnetic index related to the storm development, and North and East components of the geoelectric field (Ex and Ey). The regression values and correlation coefficients are reported in table 2 (a, b, c) and 2 (d, e, and f). The accuracy of the estimated values was tested by calculating the RMSE (Root Mean Square Error) and MBE (Mean Bias Error) for the variables.

$$RMSE = \left\{\left[\sum\left(dH/dt_{pred} - dH/dt_{obs}\right)^2\right]/n\right\}^{1/2} \quad (1)$$

$$MBE = \left[\sum\left(dH/dt_{pred} - dH/dt_{obs}\right)\right]/n \quad (2)$$

Table 1. Lists of geographic and geomagnetic corrected coordinates.

Abbreviation	Name	Geographic Latitude (N)	Geographic Longitude (E)	Geomagnetic Latitude (N)	Geomagnetic Longitude (E)
AAE	Addis Ababa	9.0	38.8	5.28	111.79
BNG	Bangui	4.3	18.6	4.16	91.14
MBO	Mbour	14.4	343.0	20.13	57.44
OTT	Ottawa	45.4	284.5	55.63	355.38
STJ	St John	47.6	307.3	57.15	23.98
VIC	Victoria	48.5	236.6	54.12	297.6

Mid latitude

Table 2a. Shows equation, correlation coefficient, correlation of determination, MBE and RMSE.

Equations (Number)	Equations **(Ottawa)**	r	R^2	MBE	RMSE
4	dH/dt=-3.179- 0.197E_x+0.366E_y+0.00378AE-0.136Dst	0.959	0.920	1.416E-15	13.171
5	dH/dt=3.064- 0.0017Ex +0.256Ey+0.0012AE	0.953	0.908	-3.64E-15	12.963
6	dH/dt=4.233 +0.095Ex+0.263Ey	0.947	0.897	2.1E-5	13.759
7	AE=92.422+ 9.74Ex+0.567Ey	0.926	0.857	-5.507E-14	397.7
8	Dst=-51.639 -1.876Ex+0.777Ey	0.906	0.821	2.344E-13	45.278

Table 2b. Shows equation, correlation coefficient, correlation of determination, MBE and RMSE.

Equations (Number)	Equations **(Victoria**)	r	R^2	MBE	RMSE
9	dH/dt=6.479+0.335E_x+0.302E_y+0.0021AE-0.096Dst	0.966	0.933	1.200E-15	6.175
10	dH/dt=3.80+0.4027 Ex -0.1322Ey+0.00254AE	0.958	0.917	-2.387E-15	6.866
11	dH/dt=3.803 +0.4007Ex+0.129Ey	0.960	0.92	-2.609E-15	6.867
12	AE=-11.15+ 8.057Ex+13.15Ey	0.909	0.825	-7.240E-14	479.3
13	Dst=-27.59 +0.502Ex-2.089Ey	0.950	0.903	2.575E-14	33.35

Table2 c. Shows equation, correlation coefficient, correlation of determination, MBE and RMSE.

Equations (Number)	Equations **(St John)**	r	R^2	MBE	RMSE
14	dH/dt=-1.66+0.1286E_x+0.1109E_y+0.00092AE-0.0189Dst	0.989	0.977	-6.106E-16	4.194
15	dH/dt=-0.863+0.1386 Ex +0.1284Ey+0.0094AE	0.988	0.970	4.441E-16	4.26
16	dH/dt=0.95 +0.22Ex+0.208Ey	0.980	0.960	7.216E-16	5.44
17	AE=193.45+ 8.71Ex+8.54Ey	0.950	0.900	5.684E-14	360.94
18	Dst=-43.084-0.566Ex-0.966Ey	0.925	0.856	1.0658E-14	40.65

Low latitudes

Table 2d. Shows equation, correlation coefficient, correlation of determination, MBE and RMSE.

Equations (Number)	Equations **(Addis Ababa)**	r	R^2	MBE	RMSE
19	dH/dt= -1.42054 +0.0070AE -0.0286Dst	0.859	0.739	-2.498E-15	6.493
20	dH/dt= 0.489 +0.00934AE	0.853	0.727	11.703	6.633

RMSE and MBE are statistical instruments used to compare the models of geomagnetic distribution prediction. Low values of RMSE are desirable, but a few errors in the sum can produce a significant increase in the indicator. Low values of MBE are also desirable. It is also possible to have large RMSE values at the same time as a small MBE or vice versa.

Distribution of time derivatives of the horizontal magnetic field (dH/dt)

The large scale auroral ionospheric electric currents flow mainly in an east- west direction thus mostly affecting the X- Z components. Horizontal currents of small scales and amplitudes and field aligned currents also contribute to Y. The distribution of dH/dt provides a strong indication that the occurrence of large value time derivatives is strongly coupled with the occurrence of great magnetic storms.

Figure 1 illustrates the distributions of dH/dt for 4 intervals, in the 3 observatories Ottawa, Victoria and St John. It was observed that the power lines disruption which occurred when the geomagnetic rate of change exceeded 30nT/min posed a serious threat to high voltage power line circuits. Between 1994 and 2007, mid latitudes percentages of the horizontal component of time derivatives of the geomagnetic field (dH/dt) which were greater than 30nT/min were: 78.48 %(Ottawa); 64.56 %(Victoria); and 38.75 %(St John).

Table2 e. Shows equation, correlation coefficient, correlation of determination, MBE and RMSE.

Equations (Number)	Equations **(Bangui)**	r	R^2	MBE	RMSE
21	dH/dt= -2.051 -1.1E-06AE -0.0495Dst	0.952	0.907	3.60	1.641
22	dH/dt= 1.1306 +0.0031AE	0.791	0.626	-4.545	3.28

Table 2f. Shows equation, correlation coefficient, correlation of determination, MBE and RMSE.

Equations (Number)	Equations **(Mbour)**	r	R^2	MBE	RMSE
23	dH/dt= 0.6232 +0.004AE +0.0012Dst	0.917	0.841	8.327E-16	2.488
24	dH/dt= 1.072 +0.0050AE	0.912	0.832	5.274E-16	2.555

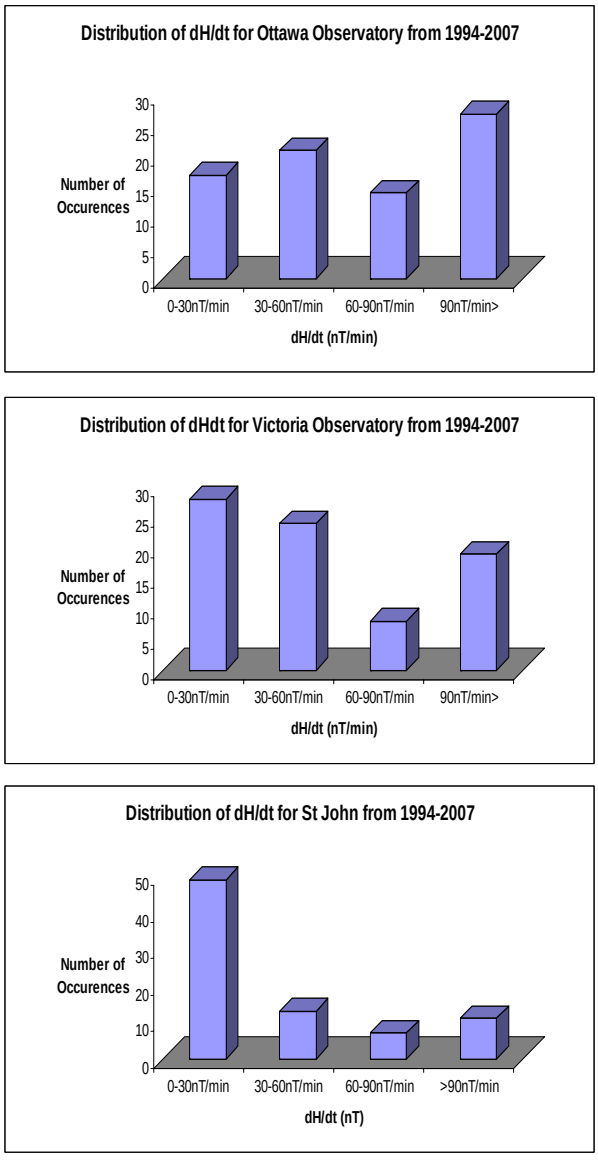

Fig. 1. Distributions of dH/dt at mid latitude of Ottawa, Victoria, and St John geomagnetic field Observatories.

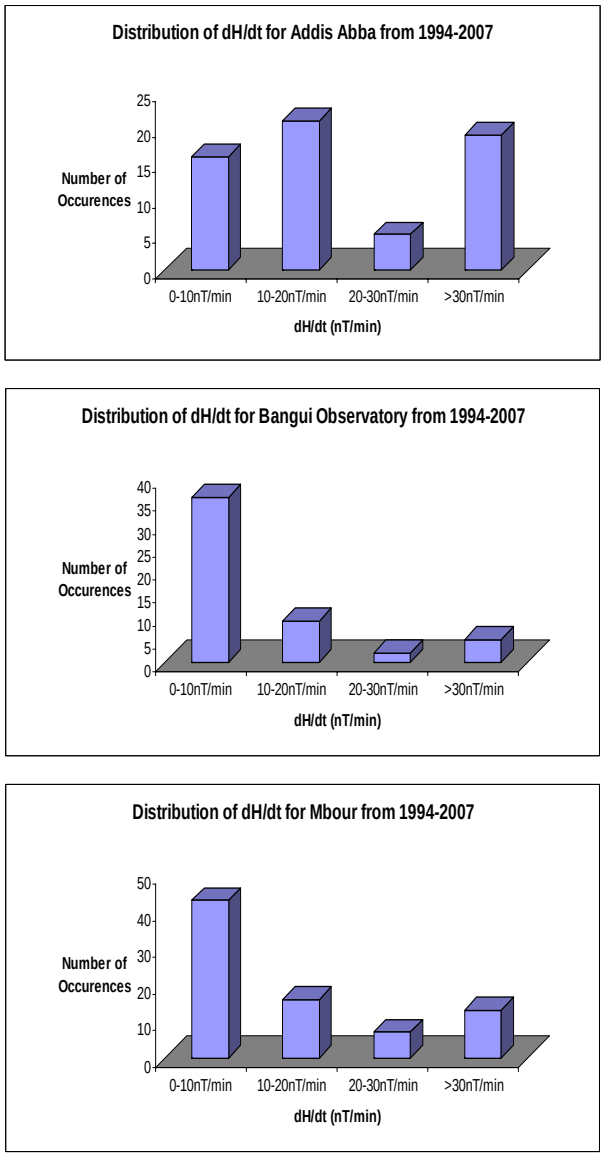

Fig. 2. Distributions of dH/dt at mid latitude of Bangui, Mbour and Addis Ababa geomagnetic field observatories.

Figure 2 is similar to Figure 1, for the observatories of the low latitudes in the African longitude sector and illustrates the data recorded at Bangui, M'bour and Addis Ababa. From figure 2, the geomagnetic disturbances are not significant in value at Bangui and M'bour; they more significant at low latitude in Addis Ababa. Between 1994 and 2007, low latitudes percentages of the horizontal component of time derivatives of the geomagnetic field (dH/dt) which were greater than 30nT/min were: 9.6 %(Bangui); 24.2 %(M'bour); and 45.2 %(Addis Ababa). Figures 3-8, further illustrate the comparison between observed and predicted values of the correlation coefficient.

Figure 3 illustrates the comparison between observed and predicted values of the correlation coefficient at Ottawa. For equations (4/ Table 2a), a correlation coefficient of 0.959 exists between time derivatives of the horizontal geomagnetic field, north and east components of the geoelectric field, auroral electrojet and disturbance storm time. The coefficient of determination of 0.920 which implies 92.0% of time derivatives of the horizontal geomagnetic field can be accounted for using the auroral electrojet index, disturbance storm time, and north and east components of the geoelectric field.

Ottawa

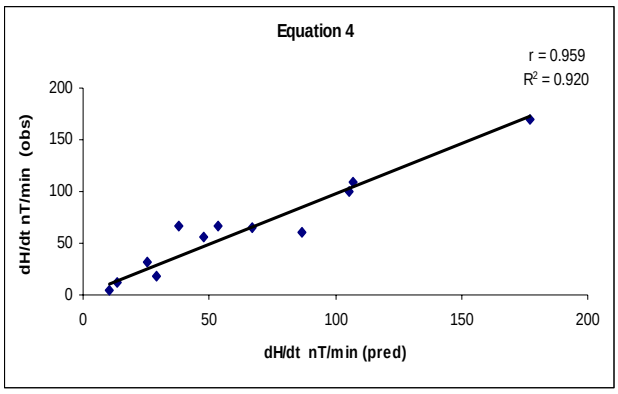

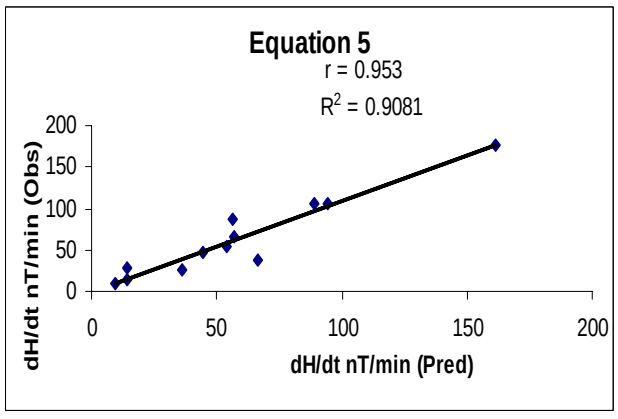

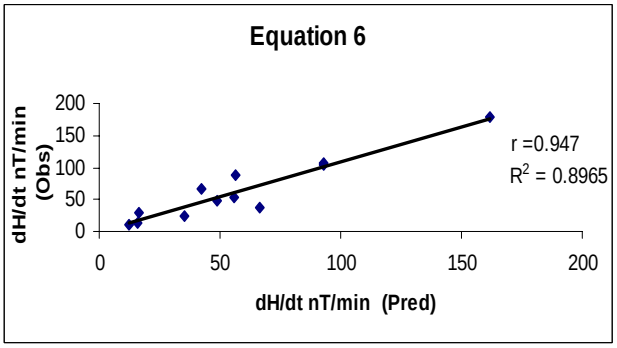

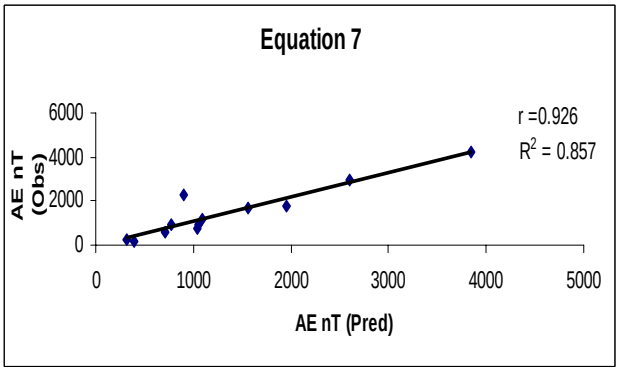

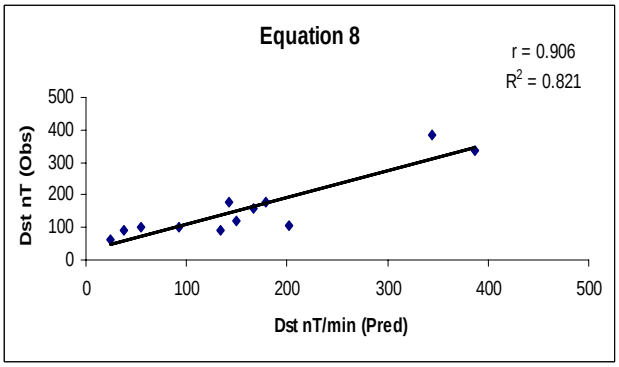

Fig. 3. Comparison between observed and predicted values of the correlation coefficient at Ottawa.

Figure 4 is devoted to the comparison between observed and predicted values of the correlation coefficient at Victoria. Equation (9/ Table 2b) shows the correlation coefficient of 0.966 that exists between time derivatives of the horizontal geomagnetic field, north and east components of the geoelectric field, the auroral electrojet and disturbance storm time. The coefficient of determination of 0.933 which implies 93.3% of time derivatives of the horizontal geomagnetic field can be accounted for using the auroral electrojet index, disturbance storm time, and north and east components of the geoelectric field.

Victoria

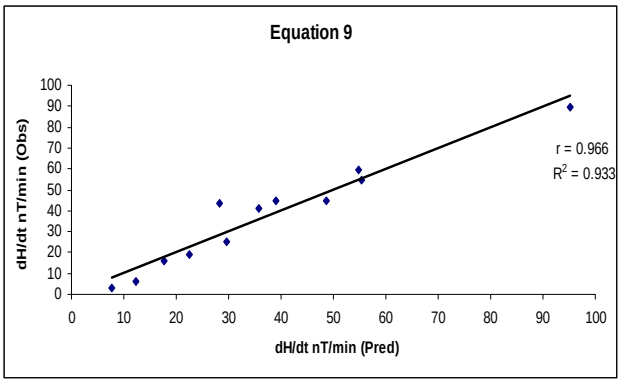

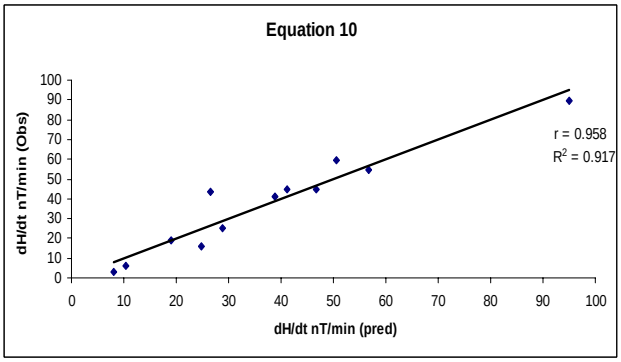

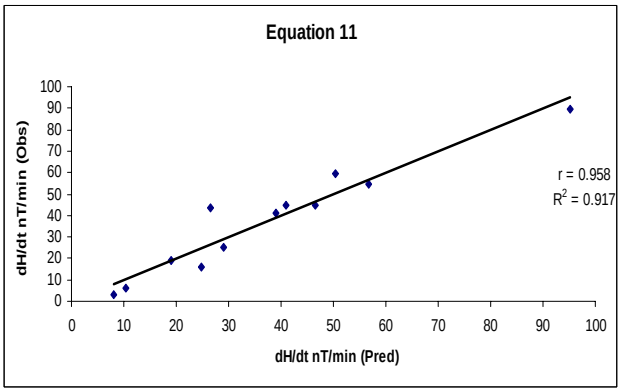

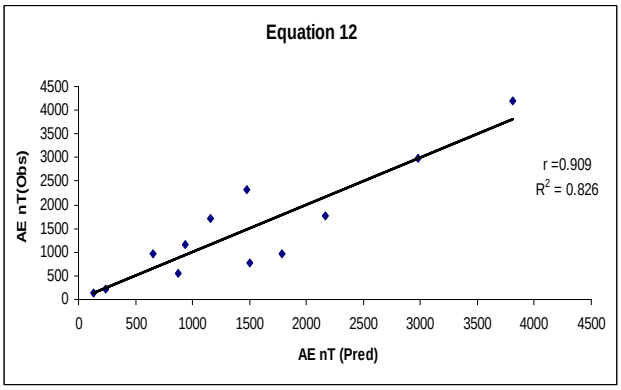

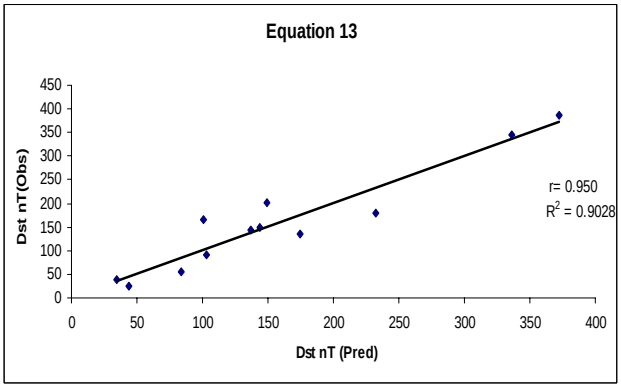

Fig. 4. Comparison between observed and predicted values of the correlation coefficient at Victoria.

Figure 5 shows the comparison between observed and predicted values of the correlation coefficient at St John. Equation (14/ Table 2c) shows a correlation coefficient of 0.988 that exists between time derivatives of the horizontal geomagnetic field, north and east components of the geoelectric field, auroral electrojet and disturbance storm time. The coefficient of determination of 0.977 which implies 97.7% of time derivatives of the horizontal geomagnetic field can be accounted for by using the auroral electrojet index, disturbance storm time, and the north and east components of the geoelectric field.

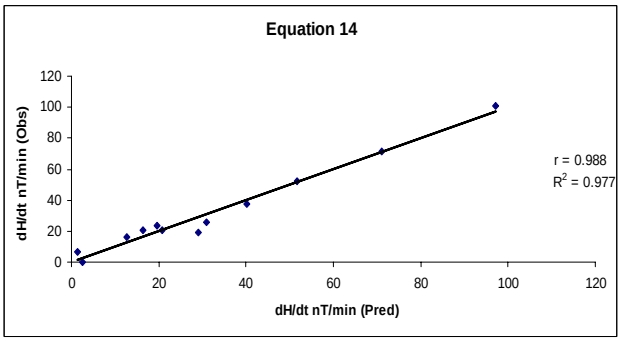

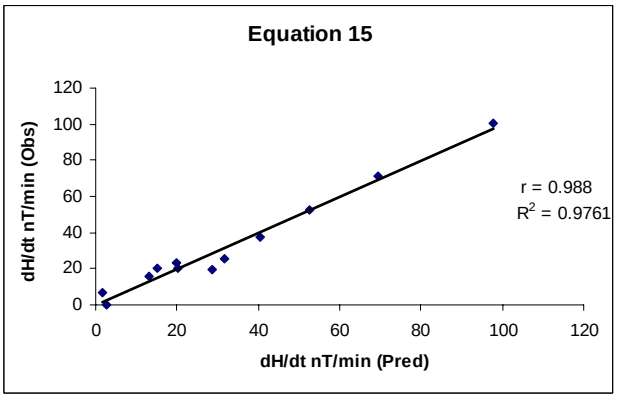

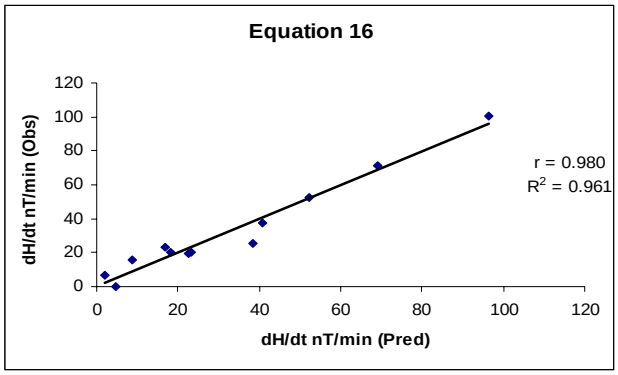

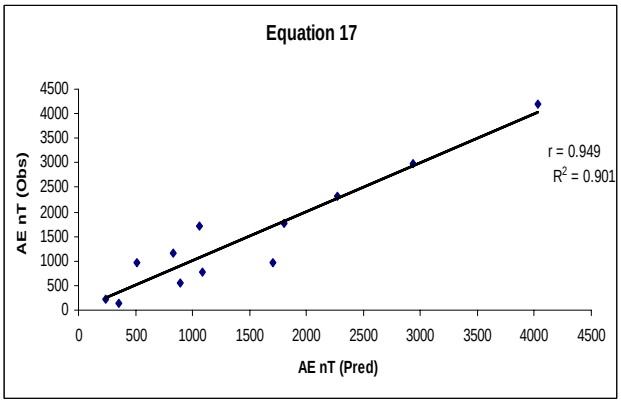

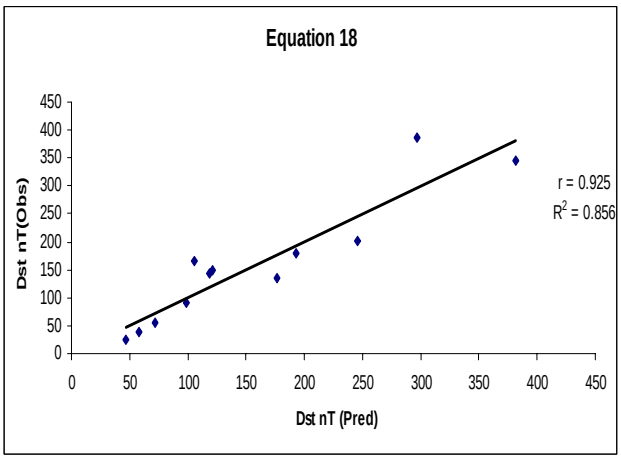

Fig. 5. Comparison between observed and predicted values of the correlation coefficient at St John.

Figure 6 illustrates the comparison between observed and predicted values of the correlation coefficient at Addis Ababa. From equation (19/ Table 2d) a correlation coefficient of 0.859 exists between time derivatives of the horizontal geomagnetic field, the auroral electrojet and disturbance storm time. The coefficient of determination of 0.739 implies 73.9 % of time derivatives of the horizontal magnetic field can be accounted for by using the auroral electrojet and disturbance storm time.

Addis Ababa

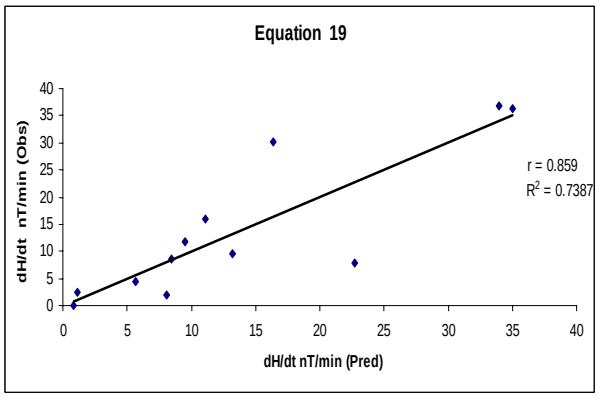

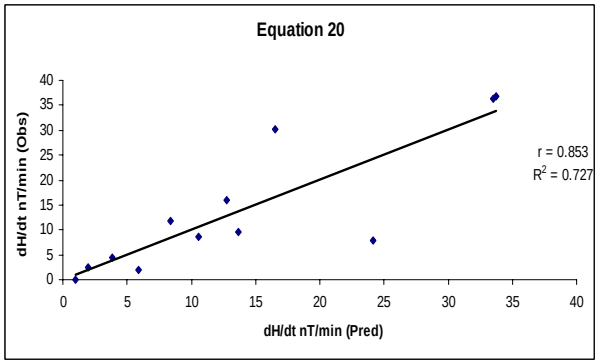

Fig. 6. Comparison between observed and predicted values of the correlation coefficient at Addis Ababa.

Figure 7 shows the comparison between observed and predicted values of the correlation coefficient at Bangui. Equation (21/ Table 2e) shows a correlation coefficient of 0.952 that exists between time derivatives of the horizontal geomagnetic field, the auroral electrojet and disturbance storm time. The coefficient of determination of 0.907 implies 90.7% of time derivatives of the horizontal magnetic field can be accounted for by the using auroral electrojet and disturbance storm time.

Bangui

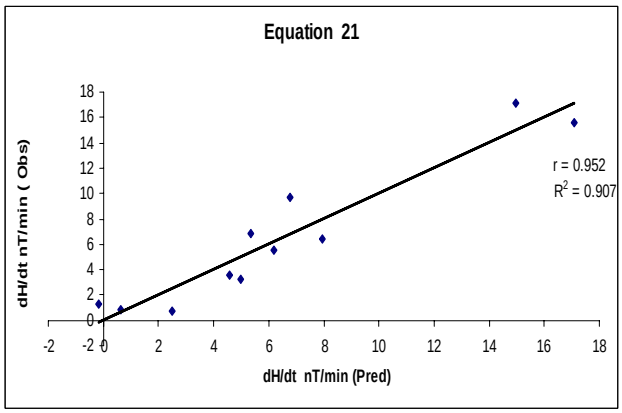

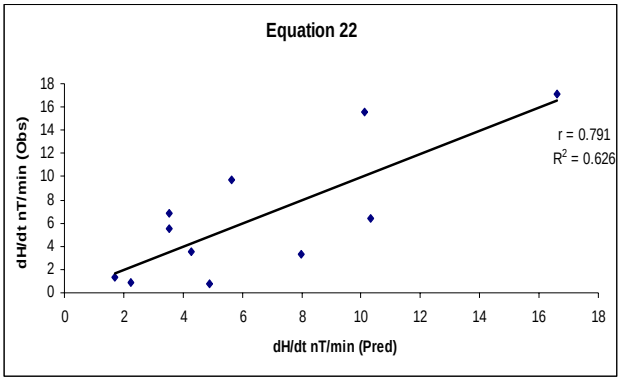

Fig. 7. Comparison between observed and predicted values of the correlation coefficient at Bangui.

Figure 8 is devoted to the comparison between observed and predicted values of the correlation coefficient at Mbour. Equation (23/ Table 2f) shows a correlation coefficient of 0.917 that exists between time derivatives of the horizontal geomagnetic field, auroral electrojet and disturbance storm time. The coefficient of determination of 0.841 implies 84.1% of time derivatives of the horizontal magnetic field can be accounted for by using the auroral electrojet and disturbance storm time.

M'bour

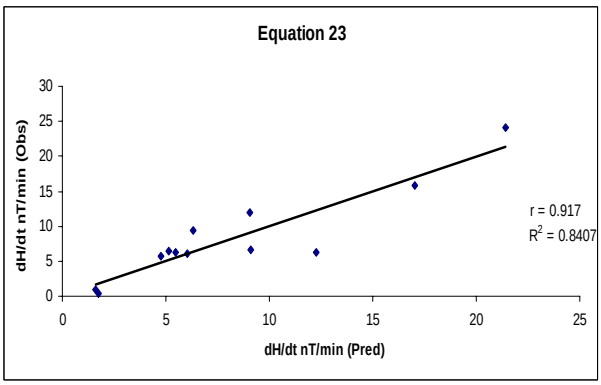

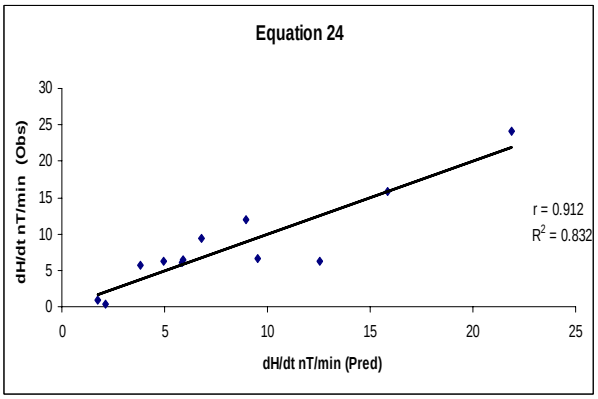

Fig. 8. Comparison between observed and predicted values of the correlation coefficient at Mbour.

The statistical tests, RMSE and MBE were used to evaluate the accuracy of the predicted time derivatives of the geomagnetic fields. They provide the long and short term performances of an equation. The smaller the values, the better the equation.

RESULTS AND DISCUSSION

During geomagnetic activity periods, the amplitude of auroral electrojets flowing along the auroral oval increases and the auroral oval can extend toward and usually reach subauroral zones. Sometimes during very strong magnetic storms the auroral oval extends toward middle and equatorial latitudes, occasionally becoming visible from tropical latitudes. Many physical processes are involved in auroral zones: the precipitation of particles which increase the electric conductivities in the E region, the field aligned currents which close magnetospheric electric currents and the dawn dusk potential drop imposed by the solar wind flowing around the magnetosphere. All these processes contribute to an increase in the electric currents flowing in the ionosphere (Kikuchi *et al*., 1996; Abduet *et al*., 1998; Kobea *et al*., 1998).

As the geomagnetic storm is intense the edge of the auroral boundary moves to a lower geographical latitude. Geomagnetic activity, even when there is not a big storm, affects the whole Earth from auroral to low latitudes. Kobea *et al*. (2000), shows the latitudinal profile of a magnetic disturbance observed on May 27, 1993 (Fig. 4 of the paper). The amplitude of this disturbance is ~ 150-200nT at auroral latitudes ~ 80-100nT (half) at subauroral latitudes and still ~30nT at equatorial latitudes. Kappenman (1996, 2005) reported that the power grids are seriously affected by geomagnetic storms at high latitude due to large impulsive geomagnetic disturbance driven by auroral intensification, but there are signs that space weather poses significant risks to ground technology at low latitude (Addis Ababa) and subauroral latitudes (Ottawa and Victoria); it is reported in our investigation that when the rate of change of geomagnetic disturbance exceeded 30nT/min it posed a threat to power grids. Vanhamaki *et al*. (2005) established that changes in ionospheric current will give rise to induction current in the conducting ground which can significantly contribute to magnetic and electric fields. It has been reported that auroral electrojet, substorm onsets, geomagnetic pulsation and sudden impulses are responsible for large GIC (Boteler, 2001; Lam *et al*., 2002; Kappenman, 2003; Pulkkinen *et al*., 2003, 2005; Viljanen *et al*., 2006). Recently, Watari *et al*. (2009) confirmed that GIC associated with substorms were detected in Japan over a 2 year GIC measurement period, during the solar minimum although intense GIC do occur mostly during geomagnetic storms.

Tables 2 (a-f) contain summaries of various linear regression analyses. It is clear that the correlation coefficient r, correlation of determination R^2, MBE (nT/min), and RMSE (nT/min) vary from one variable to another. Generally, correlation coefficients (0.990 - 0.779) are high for all the variables. This implies relationships between the time derivatives of the horizontal geomagnetic field (dH/dt), auroral electrojet (AE) index, disturbance storm time (Dst), and north and east components of the geoelectric field (Ex and Ey). This is further demonstrated by high values of the coefficient of determination R^2 (0.980 - 0.607) across the variables. There is a significant relationship between ionospheric response and ground based parameters.

Comparing the output, we can see that all regressions give good results. For better analysis we considered high values of the correlation coefficient and coefficient of determination and a low value of RMSE. The following equations produced the best subauroral correlations: Eq. 4 (Table 2a, Ottawa), Eq. 9, (Table 2b, Victoria) and Eq. 14 (Table 2c, St John). At low latitude: Eq. 19 (Table 2d, Addis Ababa), Eq. 21 (Table 2e, Bangui), and Eq. 23 (Table 2f, M'bour) were considered the best correlations with low values of RMSE and MBE.

Our result has demonstrated that temporal variation of time derivatives of the horizontal geomagnetic field shows high correlation with the geoelectric field and ionospheric response (AE and Dst indices) at different stations in mid and low altitudes. The variation in correlation coefficient may be a result of geographical orientation of the power grids and also Earth conductivities.

Pulkkinen *et al.* (2006) suggested that GIC magnitudes also depend on grid topology, configuration and resistances and vary greatly from site to site in a network. Pulkkinen *et al.* (2001) reported that GIC flow in the pipeline responds differently for the east-west and north-south geoelectric fields in association with temporal changes of the magnetic field. Also Pirjola (2000) recommended that power grids should be aligned as close to north-south as possible rather than east–west direction. This is because of the auroral electrojet which is significant in connection with magnetic disturbance inducing GIC in an east-west direction. Our analysis has shown that geomagnetic storm effects were not so strong at St John (subauroral), M'bour and Bangui (low latitude), and the effect on consumers was small during weak and mild geomagnetic disturbance.

CONCLUSION

Kataoka and Pulkkienen (2008) reported that the horizontal geomagnetic field (dH/dt) is an excellent indicator of GIC and the relationship between the GIC and dH/dt is always the same in a very large dynamic range of about three orders of magnitude. This study examined the possibility of geomagnetic induced current (GIC) using time derivatives of the horizontal geomagnetic field (dH/dt) at the threshold of 30nT/min at mid and low latitude. When the rate of change of geomagnetic disturbance exceeded 30nT/min it posed a serious threat for power grids. Strong relationships between time derivatives of the horizontal magnetic field (dH/dt), auroral electrojet (AE) index, disturbance storm time (Dst), and the geoelectric field (Ex and Ey) led to the conclusion that auroral activity influences GIC down to low latitudes.

An interesting phenomenon was also detected in the Addis Ababa region, which showed much higher GIC activity when compared to other typical low latitude regions (Bangui and M'bour). This may be due to current moving at equator called equatorial electrojet. Ionospheric current systems exist which can occasionally affect equatorial electrojet. This current is generated at high latitudes in the vicinity of the auroral zones as a result of motions in the magnetosphere (Onwumechilli and Ogbuechi, 1967). During magnetically disturbed conditions this current system may undergo considerable enhancement and may extend to equatorial latitudes. Akasofu and Chapman (1963) showed that polar geomagnetic storms can greatly enhance the equatorial electrojet current and Rastogi (1977) suggested that when there is fluctuation in the magnetic field during SSC at low latitude station are due to the imposition of electric field over the equatorial ionosphere leading to equatorial electrojet. Kappenman (2003) showed that during the global burst (the sudden beginning of a magnetic storm), the intensity of the geomagnetic field can be a reason of significant GIC at all geomagnetic latitudes, including the equatorial region.

The results obtained in this paper are applicable to the estimation of geomagnetically induced currents GIC using time derivatives of the horizontal geomagnetic field in connection with research of space weather effects.

ACKNOWLEDGEMENTS

The authors acknowledge World Data Centre (WDC) for geomagnetism, Space Physics Interactive Data Resources (SPIDR) for Dst and AE indices data, Canadian magnetic observatory and INTERMAGNET for geomagnetic fields. We also thank Christine Amory Mazaudier of CEPT for her valuable comments.

REFERENCES

Abdu, MA., Sastri, JH., Liihr, H., Tachihara, H., Kitamura, T., Trivedi, NB. and Sobral, JHA 1998. DP 2 electric field fluctuations in the dusk-time dip equatorial ionosphere, Geophys. Res. Left. 25:1511-1514.

Akasofu, S. I and Chapman, S. 1963. The lower limit of latitude (US sector) of northern quiet auroral arcs, and its relation to Dst (H), J. Atmos. Terr. Phys. 25**:**9-12.

Barker, RH. and Skinner, NJ. 1980. Flow of electric current of telluric origin in a long metallic pipeline and their effect in relation to corrosion control, Mater. Performance. 19(2):25-28.

Boteler, DH., Pirjola, R. and Trichtchenko, L. 2000. On calculating the electric and magnetic fields produced in technological systems at the Earth's surface by a wide electrojet. Journal of Atmospheric and Solar terrestrial Physics. 62:1311-1315.

Boteler, DH. 2001. Space weather effects on power systems. In: Space Weather, Geophys. Monogr. (vol. 125). Eds. Song, P., Singer, H. and Siscoe, G. pp. 347--352, AGU, Washington, DC, USA.

Campbell, WH. 2000. Introduction to geomagnetic fields. Cambridge University Press, (2nd ed). 235-236.

Coles, RL., Thompson, K. and Jansen van Beek, G. 1992. A comparison between the rate of change of the geomagnetic field and geomagnetically induced currents in a power transmission system, Proc. EPRI Conf. Geomagnetically Induced Currents, Burlingame, Ca., 8–10 Nov. 1989, EPRI TR-100450. 15:1-8.

Erinmez, I.A., Majithia, S., Rogers, C., Yasuhiro, T., Ogawa, S., Swahn, H. and Kappenman, JG. 2002. Application of Modeling Techniques to Assess Geomagnetically Induced Current Risks on the NGC Transmission System, CIGRE Paper 39-304.

Kataoka, R. and Pulkkinen, A. 2008. Geomagnetically induced currents during intense storms driven by coronal mass ejections and corotating interacting regions. Journal of geophysical research. 113, A03S12, doi:10.1029/2007JA012487.

Kappenman, JG. 1996. Geomagnetic Storms and Their Impact on Power Systems, IEEE Power Engineering Review.

Kappenman, J.G. 2005. An overview of the impulsive geomagnetic field disturbance and power grid impacts associated with violent Sun -Earth connection events of 29-31 October 2003 and a comparative evaluation with other contemporary storms, Space Weather. 3. S08C01,doi.1029/2004SW000128.

Kappenman, JG. 2006. Great geomagnetic storms and extreme impulsive geomagnetic field disturbance events – An analysis of observational evidence including the great storm of May 1921. Advances in Space Research. 38:188-199.

Kappenman, JG. 2003. Storm sudden commencement events and associated geomagnetically induced current risks to ground-based systems at low-latitude and mid-latitude locations, Space weather 1, 3, 1016, doi: 10.1029/2003SW000009.

Kikuchi, T., Lfihr, H., Kitamura, T., Saka, O. and Schlegel, K. 1996. Direct penetration of the polar electric field to the equator during a DP2 event as detected by the auroral and equatorial magnetometer chains and the EISCAT radar, J. Geophys. Rest. 101(17):161-173.

Kobea, AT., Mazaudier, CA., Do, JM., Luhr, H., Houngninou, E., Vassal, J., Blanc, E. and Curto, JJ. 1998. Equatorial electrojet as part of the global circuit: A case study from the IEEY, Ann. Geophys. 16:698-710.

Kobea, A., Richmond, A., Emery, BA., Peymirat, C., Lürh, H., Moretto, T., Hairston, M. and Amory-Mazaudier, C. 2000. Electrodynamic coupling of high and low latitudes observations on May, 27, 1993, Journal of Geophys. Res. 105, A 10:22979-22989.

Koen, J. and Gaunt, CT. 2002. Geomagnetically Induced currents at mid latitudes, Abs. The 27th General Assembly of URSI, 17-24 August, Netherlands, Maastricht. 177.

Lam, HL., Boteler, DH. and Trichtchenko, L. 2002. Case studies of space weather events from their launching on the Sun to their impacts on power systems on the Earth, Ann. Geophys. 20:1073-1079.

Makinen, T. 1993. Geomagnetically induced currents in the Finnish power transmission system, Finn. Meteorol. Inst. Geophys. Publ. 32, 101.

Onwumechilli, A. and Ogbuechi, A. 1967. Daily variation and secular variation of the geomagnetic field. Journal atmospheric and terrestrial physics. 29:149.

Ogunade, S. 1986. Induced electromagnetic field in oil pipelines under electrojet current sources, Phys. Earth Planet. 43:307-315.

Osella, A. and Favetto, A. 1999. Numerical simulation of current induced by geomagnetic storms on buried pipelines. An application to the Tierra del Fuego, Argentina, Gas Transmission Route, IEET. Geosci.Remote. 37:614.

Pirjola, R., Kauristie, K., Lappalainen, H. and Pulkkinen, A. 2005. Space weather risk. AGU Space Weather. 3,S02A02, doi:10.1029/2004SW000112.

Pirjola, R. 2004. Effects of space weather on high-latitude ground systems. Advances in Space Research. 36:2231-2240.

Pirjola, R. 2000. Geomagnetically induced current during magnetic storms. IEE Transactions on Plasma Science. 28:1867-1872.

Poppe, B.B. and Jordan, KP. 2006. Sentinels of the Sun: Forecasting space weather. Johnson, Boulder, Colo. pp196.

Pulkkinen, A., Viljanen, A., Pajunpaa, K. and Pirjola, R. 2001. Recordings and occurrence of geomagnetically induced currents in the Finnish natural gas pipeline network, J. Appl. Geophys. 48:219-231.

Pulkkinen, A., Thomson, A., Clarke, E. and McKay, A. 2003. April 2000 storm: ionospheric drivers of large geomagnetically induced currents, Ann. Geophys. 21:709-717.

Pulkkinen, A., Lindahl, S., Viljanen, A. and Pirjola, R. 2005. Geomagnetic storm of 29–31 October 2003: Geomagnetically induced currents and their relation to problems in the Swedish high-voltage power transmission system, Space Weather. 3, S08C03, doi:10.1029/

2004SW000123.

Pulkkinen, A., Viljanen, A. and Pirjola, R. 2006. Estimation of geomagnetically induced current levels from different input data. Space Weather. 4, doi:10.1029/2006SW000229.

Rastogi, RG. 1977. Geomagnetic storms and electric fields in the equatorial ionosphere. Nature. 268:422-424.

Trichtchenko, L. and Boteler, DH. 2006. Response of power systems to the temporal characteristic of geomagnetic storms. IEE, CCECE/CCGEI, Ottawa.

Viljanen, A. 1998. Relation of Geomagnetically Induced Currents and Local Geomagnetic Variations, IEEE Trans. Power Delivery. 13:1285-1290.

Vanhamäki, H., Viljanen, A. and Amm, O. 2005. Induction effects on ionospheric electric and magnetic fields, Ann. Geophys. 23, 1735.

Viljanen, A. 1997. The relation between geomagnetic variation and their time derivatives and implication for estimation of induction risks. Journal of geophysical research letter. 24: 631- 634.

Viljanen, A., Nevanlinna, H., Pajunpaa, K. and Pulkkinen, A. 2001. Time derivative of the horizontal geomagnetic field as an activity indicator. Annales Geophysicae. 19:1107–1118.

Viljanen, A., Taskanen, E.I and Pulkkinen, A. 2006. Relation between substorm characteristics and rapid temporal variations of the ground magnetic field, Ann. Geophys., 24:725-733.

Vodjanikov, VV., Gordienko, GI., Nechaev, SA., Sokolova, OI., Homutov, SJ. and

Yakovets, AF. 2007. Study of geomagnetically induced current from time derivatives of the

Earth's magnetic field. PUBLS. INST. GEOPHYS. POL. ACAD. SC. C-99 (398).

Watari, S., Kunitake, M., Kitamura, K., Hori, T ., Kikuchi, T., Shiokawa, K., Nishitani, N., Kataoka, R ., Kamide, Y., Aso, T., Watanabe, Y. and Tsuneta, Y. 2009. Measurements of geomagnetically induced current in a power grid in Hokkaido, Japan. Space Weather. 7, S03002, doi:10.1029/2008SW000417.

Wik, M., Viljanen, A., Pirjola, R., Pulkkinen, A., Wintoft, P. and Lundstedt, H. 2008. Calculation of geomagnetically induced currents in the 400 kV power grid in southern Sweden. Journal of Space weather. 6, doi:10.1029/2007SW000343.

Received: April 18, 2010; Accepted: May 29, 2010

SENRA Academic Publishers, Burnaby, British Columbia
Vol. 4, No. 2, pp. 1199-1206, June 2010
ISSN: 1715-9997

Canadian Journal of pure&applied sciences

STUDY OF INTERANNUAL AND INTRA-SEASONAL VARIABILITY OF SUMMER MONSOON CIRCULATION OVER INDIA

*Bhanu Kumar, O S R U, S Ramalingeswara Rao and S S Raju
Department of Meteorology and Oceanography, Andhra University, Visakhapatnam, India

ABSTRACT

In this study satellite derived Outgoing Long wave Radiation (OLR) and National Centre for Environmental Prediction (NCEP) reanalysis zonal wind (U-850 and U-200 hPa levels) datasets for 27-years are used to examine important and unique characteristics of summer monsoon circulation variability across India. Among mean 73 pentads of annual cycles for OLR and zonal wind components, large scale monsoon convective activity, monsoon westerlies at 850 hPa and strengthening of easterlies at 200 hPa levels are conspicuously represented by P-30 to P-55 pentads over India. More details of monsoon circulation change are inspected in spatial distribution of OLR and wind fields for the climatological annual cycles. The OLR field is inversely related with U-850 hPa, while it is directly related with U-200 hPa levels; both are statistically significant at 0.1% level in this study. Annual cycles of the OLR and wind fields (anomaly) reveal striking interannual monsoon circulation variability in El Nino (2002) and La Nina (1998) years. The monsoon seasonal circulation changes in above contrasting years are highlighted and they reveal that U-850 hPa is almost a mirror image of U-200 hPa distribution of wind fields over the monsoon region. Finally the strength of ISO index in terms of Monsoon Hadley Index (MHI) and Madden and Julian Oscillation (MJO) index are evaluated to study year-to-year monsoon variability across India. Above ISO indices are related with Indian summer monsoon rainfall and the relationships are statistically significant.

Keywords: Convective activity, circulation changes, variability.

INTRODUCTION

The interannual variability of combined atmosphere-ocean system is manifest in changes of the atmospheric, oceanic circulations and extreme events like monsoon rainfall in the regional climate. Strong seasonality in terms of rainfall over the tropical monsoon region is observed due to interannual variability in the form of the mean annual cycle (Mooley and Parthasarathy, 1984). Goswami (1997) opined that modulation of the Intra-Seasonal Oscillations (ISO) by the annual cycle could give rise to an internal quasi-biennial oscillation in the tropical atmosphere. It is well documented that the most dominant feature in the tropics is the ISO, which is a naturally occurring component of both coupled ocean-atmospheric phenomenon. ISOs represent an entire cycle of 30-50 days and fluctuations in tropical rainfall, which is driven by internal feedback mechanism between convection and dynamics (Madden and Julian, 1971). It is also called as Madden-Julian Oscillation (MJO) or 40-day wave. They have originated from western Indian Ocean, which propagate quite vigorously in eastward or northward direction and exhibits remarkable interannual and intra-seasonal variability of rainfall (Ramamurthy, 1969). The ISO moves northward across India resulting in wet and dry spells within the Indian monsoon season, which is known as active and break monsoon conditions. It is, however, varied its activity from year-to-year over Southeast Asia in general and India in particular. Northward propagation of ISO using convective fields during Indian summer monsoon is studied by (Yasunari, 1979 and 1980; Sikka and Gadgil, 1980) with a limited data. Singh and Kripalani (1990) and Singh *et al*. (1992) used long records of daily rainfall data over the Indian continent and examined the 30-50 day oscillation. They, however, could not come to a clear conclusion regarding relationship between the ISOs and the interannual variability of the Indian summer monsoon rainfall. Fenessey and Shukla (1994) showed that the spatial structures of the interannual variability and intraseasonal variability are quite similar, while Goswami (1994) proposed a conceptual model of how the ISOs influence the seasonal mean and interannual variability of the Indian monsoon. Later Annamalai *et al*. (1999) examined the relationship between intraseasonal oscillations and interannual variability using NCEP and European Centre for Medium range Weather Forecast (ECMWF) reanalysis and they concluded that there was not a common mode that described the intraseasonal and interannual variability. Apart from the above, several studies have indicated that the 30-50 day oscillation is a dominant phenomenon in the interannual variability of Indian summer monsoon rainfall (Julian and Madden, 1981; Krishnamurthi *et al*., 1985; Wang and Rui, 1990; Goswami and Mohan, 2001; Annamalai and Slingo, 2001; Kemball-Cook and Wang, 2001; Goswami *et al*., 2003; Rao and Sikka, 2007; Susmitha *et al*., 2008; Bhanu Kumar *et al*., 2008). Several modeling studies showed

*Corresponding author email: osrubhanukumar@yahoo.com

that a significant fraction of the interannual variability of the seasonal mean Indian summer monsoon is governed by internal chaotic dynamics (Goswami, 1998; Hazarallah and Sadourny, 1995; Rowell *et al*., 1995; Stern and Miyakoda, 1995). Most of these studies, however, do not provide any detailed insight regarding the origin of the internally generated interannual variability. Recently a few studies of course made use of MJO and Monsoon Indices to express Asian monsoon circulation variability with limited data (Webster and Yang, 1992; Degtyarev *et al*., 2007; Manoel *et al*., 2006; Goswami *et al*., 1999; Li and Zeng, 2002). So far there are no detailed studies to explain variability of monsoon circulation based on convection, circulation changes and above said indices. Hence the aim of this paper is to investigate interannual and intra-seasonal monsoon variability over India.

MATERIALS AND METHODS

We know that marked interannual and intra-seasonal variations of the atmosphere-ocean system are an essential characteristic of tropical climate. In this study satellite derived daily OLR and NCEP zonal wind fields (2.5°x2.5°) at 850 and 200 hPa levels are downloaded from the NOAA website (www.cdc.noaa.gov) to study interannual and intra-seasonal variability of Indian monsoon circulation changes for the period, 1979-2005 and the study region (50°-100°E and 0°-38°N) is shown in figure 1. These datasets are used to prepare mean 73 pentads in order to examine climatological annual cycles in the form of histograms and spatial distribution formats over the study region. Anomaly annual cycles of OLR and wind fields are also prepared for El Nino (2002) and La Nina (1998) years to find out contrasting convection and circulation changes if any. Mean convective and circulation changes over study region during monsoon season (June-September) are also prepared for above contrasting years. The MJO index is obtained from the Climate Prediction Centre (http://www.cpc.noaa.gov) at 70°E, 80°E and 100°E longitudes for the monsoon period, which is evaluated from pentad velocity potential at 200 hPa level using extended empirical orthogonal function analysis across Indian longitudes for intra-seasonal variations. And mean MJO index variations are calculated for the study period and related with monsoon rainfall. Similarly MHI is evaluated by taking the difference between U-850 and U-200 hPa wind flow over the study region during the monsoon season and above indices are related with monsoon rainfall, which is downloaded from IITM website for the study period. The connection between them is promising. To find out the relationship between any two variables used in this study is correlation and regression analyses.

RESULTS AND DISCUSSIONS

Study of climatological annual cycle

The mechanisms of interannual variability of circulation and climate are related to the functioning of the annual cycle and the annual cycle over a region has a significant year-to-year variations. Anomaly climatological annual cycle of large scale organized convection in 73 pentads from 27-year mean is presented in figure 2a. The most salient features of the mean annual pentad OLR march of convection shows extrema of annual OLR cycle reached minimum in August and maximum in February. Out of these 73 pentads, P-30 to P-55 pentads show large scale monsoon convective activity, which relates to Indian monsoon rainfall. Similarly figures 2b and 2c represent anomalous annual cycle of winds at U-850 and U-200 hPa levels respectively. They depict that trade winds are replaced by monsoon westerlies (850 hPa) and got strengthened from pentad P-25 to P-55, while easterlies (jet stream) at 200 hPa have attained maximum strength during the above period. Further OLR field is inversely related with the U-850 hPa, while it is positively related with U-200 hPa levels for the study period. Both are statistically significant. Thus OLR field has profound influence on wind fields to relate mean interannual variability of monsoon circulation.

To further examine climatological annual cycle of convection and circulation features across India, the OLR and wind fields for typical pentads of P-1 (3^{rd}-7^{th} January), P-26 (8^{th}-12^{th}May), P-31 (2^{nd}-6^{th}June), P-55 (30^{th} Sept.- 4^{th} Oct.) P-60 (4^{th}-8^{th} Nov.) and P-72 (24^{th}-28^{th} Dec.) are presented (Fig. 3a-c). Details of convection and circulation changes are discussed as follows. Pentad (P-1) in figure 3a shows a maximum OLR of about 280W/m^2, which is centered over central India. This is the slowly emerging part of annual cycle of monsoon circulation. Later there is a dramatic change in convective activity in the pentad P-26 and this is the beginning of fast intra-seasonal cycle of Indian summer monsoon, which coincides with the Onset of monsoon over Kerala in extreme south India. Above intense convective activity continued till the pentad P-55 due to planetary scale monsoon activity over study region. The value of OLR of P-26 to P-55 is negatively correlated with rainfall during June through September over India and it amounts to -0.6 and hence OLR is a good proxy for monsoon rainfall. Next pentads, P-56 to P-68 represent the post-monsoon season with low OLR field due to seasonal disturbances like tropical cyclones and easterly waves etc. In December, the climatological annual cycle of OLR fields again represents 280 W/m^2. Thus the convective activity is very interesting in climatological annual cycle, which reveals both summer and post-monsoon convection across India. As OLR is related with zonal wind, climatological annual circulation changes at U-850 and U-200 hPa levels are discussed. The figure 3b represents pentads of mean annual cycle of circulation changes at U-850 hPa. Pentad, P-1 of above figure shows a strong anti-cyclonic circulation over central India with a dominant easterly component over India. There is a spectacular change in circulation changes by migrating above anti-cyclone at the end of May/early June (P-26) by the appearance of strong southwesterlies. Somali jet is also appeared over

the Arabian Sea and maintained its strength till the end of September (P-31 to P-55). Later southwesterlies are replaced gradually by northeasterlies with a commencement of post-monsoon from the Siberian high (P-60). At the end of the mean annual cycle these easterlies are weakened and conditions are favourable for the formation of anti-cyclone over central India (P-72). The figure 3c shows corresponding circulation changes at U-200 hPa for the above pentads. Pentad P-1 of above figure reveals the axis of Sub-Tropical Ridge (STR) at 10°N and westerly jet stream (28°N). Later easterly jet stream is fully established rather abruptly over south Bay of Bengal and south India by early June (P-31), while existing westerly jet stream disappeared. In September (P-55), the axis of STR shifts southwards (15°N) and week low level easterlies begin to appear over north Bay, which is a beginning of post-monsoon season. Later easterly jet stream has disappeared in P-60 and P-72 with the weakening of easterlies and the STR is shifted towards south. Thus above studies conclude that the climatological interannual variability in the tropics is dominated by changes in cloudiness and circulation changes caused by the Indian monsoon.

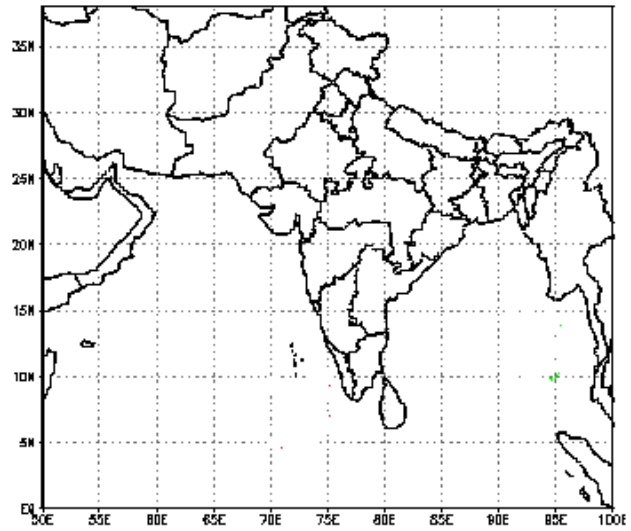

Fig. 1. Study region (0°-38°N and 50°-100°E).

Anomaly annual circulation changes over India

In tropics extreme atmospheric circulation changes are generally attributed with El Nino and its counter part La Nina episodes through Walker circulation. So it is of interest to know how monsoon convective activity and its related circulation changes are varying during anomaly annual cycles using OLR and wind datasets instead of precipitation criteria in this study. Figure 4a depicts composite annual cycle of OLR for El Nino (2002) and La Nina (1998) years, when monsoon rainfall amounts received were 81% and 108% respectively over India. Negative OLR anomalies were highly dominant over the most parts of Arabian Sea, Indian sub-continent and the Bay of Bengal in La Nina period, while reverse convection was observed in El Nino period during June through September in composite annual cycle (not shown). Thus there is a striking contrast in monsoon convection in El Nino and La Nina periods, but there is no change noticed in the pre-monsoon period in the above two cases. During active phase of the Indian monsoon, typically there is more rain over central India and a stronger monsoon trough. Thus the variations of Indian summer monsoon convection are better seen in the anomaly annual cycles of above contrasting years.

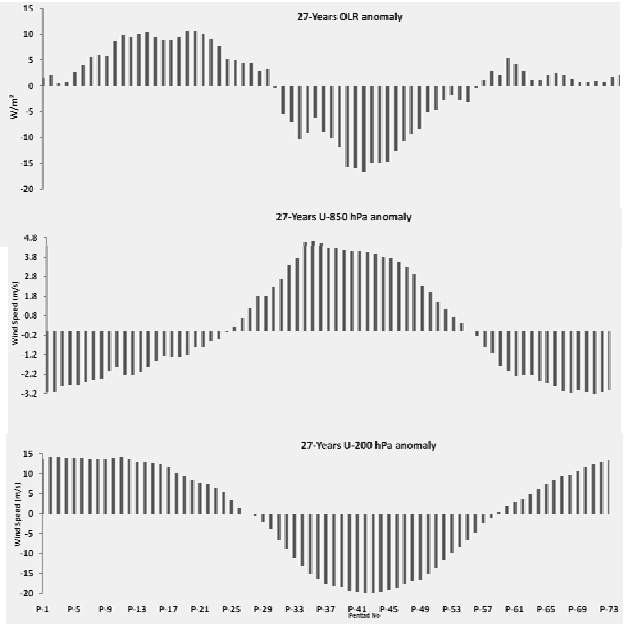

Fig. 2. Anomaly annual cycles of (a) large scale organized cumulus convention (OLR); (b) zonal wind at 850 hPa; (c) Zonal wind at 200 hPa over the study region during 1979 -2005 in 73 pentads.

Similarly interannual monsoon variability in El Nino and La Nina years are also examined through a composite anomaly annual cycle of zonal wind at 850 and 200 hPa levels (Fig. 4b) and curves indicate variation of zonal wind in terms of direction and speed. At the time of Indian summer monsoon though both the low level westerlies and upper level easterlies are considerably strong in both contrasting years. However there is a striking difference in strength of winds at 850 and 200 hPa levels in the above years. This figure also explains that the signal associated with El Nino and La Nina years extends backward some seasons before an anomalous monsoon. Thus this study explains that significant variations may be due to ISOs during Indian monsoon season.

Above interannual monsoon variability studies have clearly indicated that OLR and circulation changes are more predominant during the Indian summer monsoon due to ISOs. And the variations in convective activity and circulation changes for the monsoon period of above El

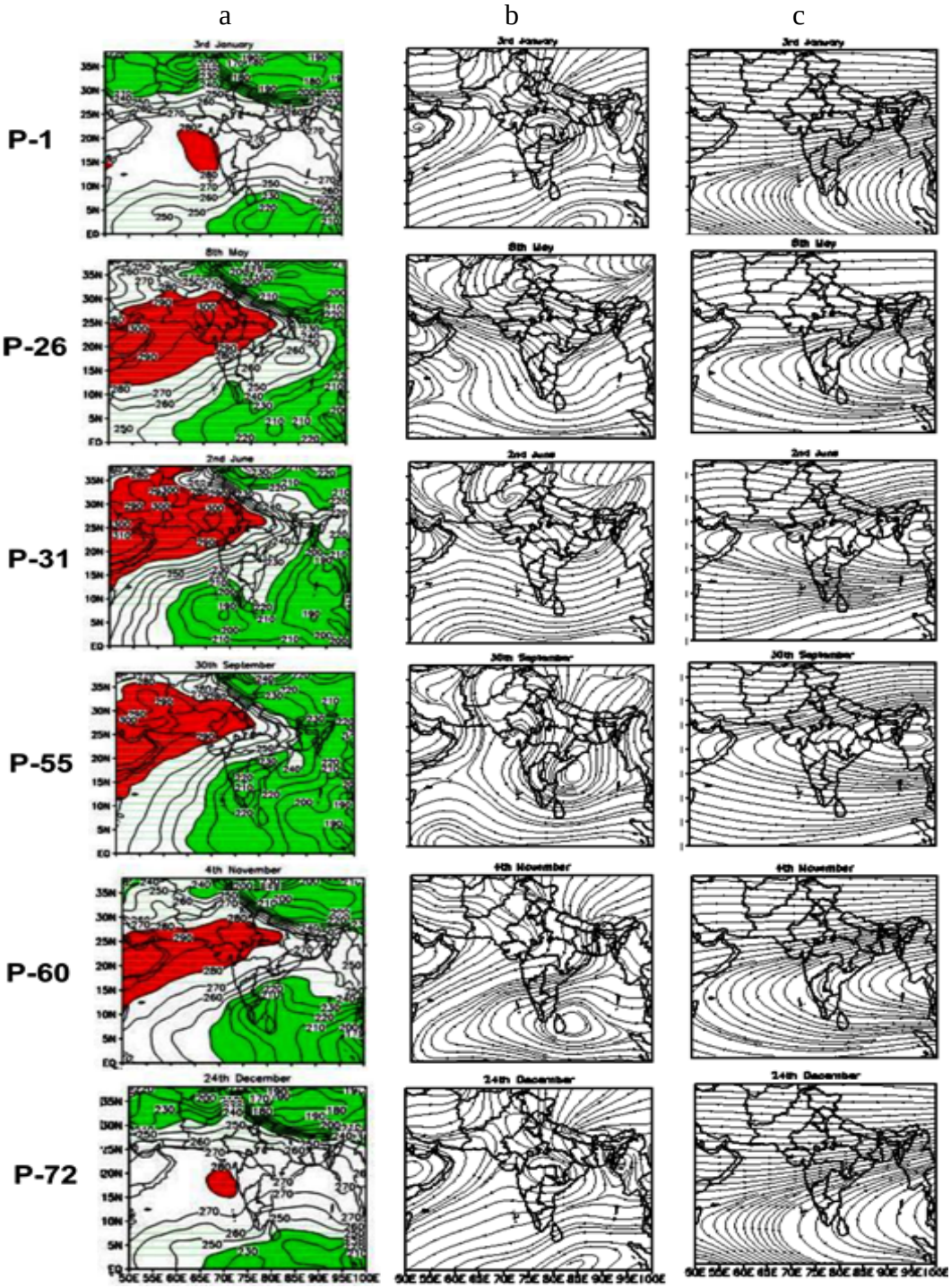

Fig. 3. Mean annual cycles of (a) OLR and wind at (b) U-850 hPa (c) U-200 hPa levels in typical pentads.

Nino and La Nina periods are also discussed in detail (Figs. 5a & b). The large scale phenomenon are often associated with changes with atmospheric circulation that encompass areas for larger than a particular affected region. There is a distinct pattern of low level and upper-level atmospheric anomalies, which accompany ISO related pattern of monsoon rainfall. In this study figure 5 a & b shows composite anomaly OLR and wind fields at U-850 hPa and U-200 hPa levels relative in 1998 and 2002 respectively for the monsoon period. The strength of OLR is different in 1998 and 2002 in terms of large scale cumulus convection. Negative OLR anomalies lie over most of the Indian sub-continent, central Arabian Sea and southeast Bay of Bengal, which extends across the

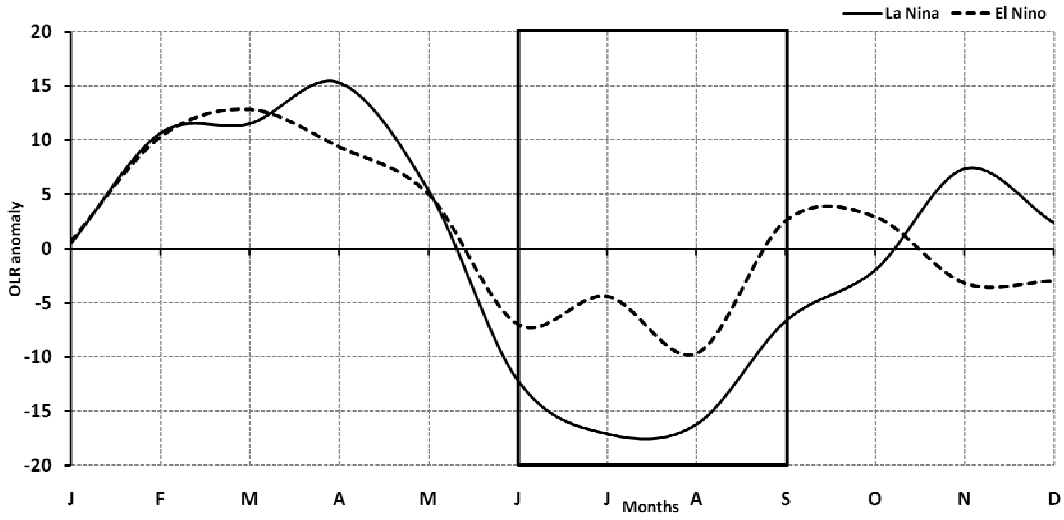

Fig. 4a. Interannual variation of the anomalous OLR relative to El Nino and La Nina years.

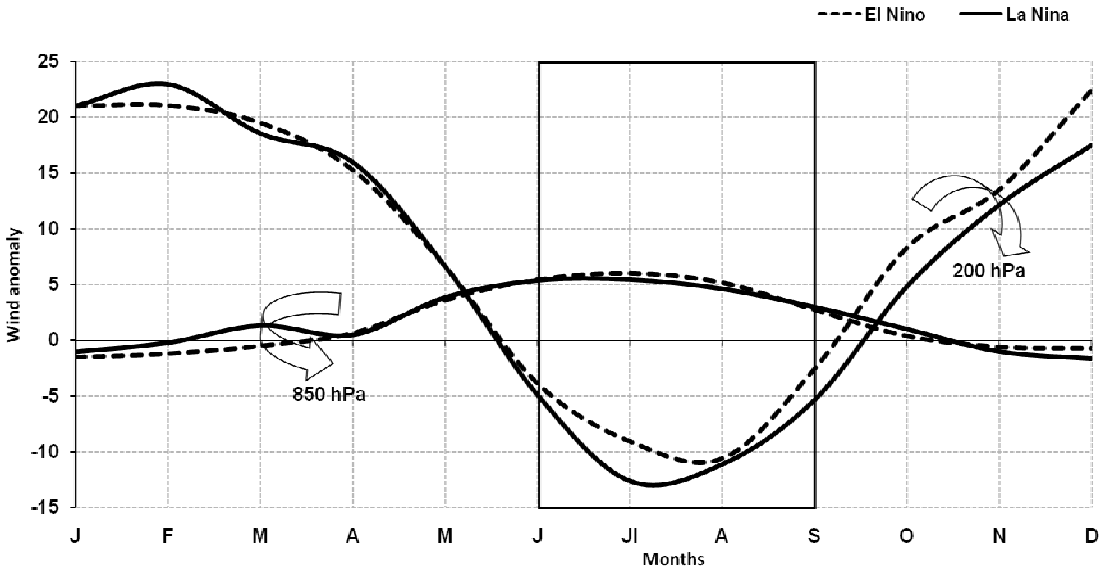

Fig. 4b. Same as above figure except for zonal wind at 850 hPa and 200 hPa levels.

equator in 1998, while in 2002 reverse situation is shown. Thus there is a spectacular contrast in the enhanced and depressed convection during La Nina and El Nino periods respectively. Next the wind strength at U-850 hPa shows much stronger (2 m/s) in 1998, while the wind strength was relatively weak in 2002. Similar differences are also observed at the anomaly wind at U-200 hPa in terms of strength of easterly jet stream. Anomalous easterly wind speed of -1.5 m/s is observed in the region of tropical easterly jet in 1998, while relatively weak wind appeared in the year 2002. Over the monsoon region, U-850 hPa is almost a mirror image of U-200 hPa distribution of wind fields. Thus these circulation changes clearly indicate that stronger monsoon westerlies in the La Nina period influence Indian monsoon rainfall through Walker circulation.

Influence of ISOs on monsoon circulation

Above studies indicate that OLR and wind fields are very potential to examine interannual circulation variability and spectacular changes due to ISOs in monsoon season. The strength of ISO is determined in terms of MJO index, which is positively related with OLR (r = 0.54) and MJO index is also statistically related (r = -0.5) with monsoon rainfall in this study. Year-to-year variation of mean MJO index (June-September) clearly shows El Nino, La Nina and neutral periods (Fig. 6a). There are six El Nino (1979, 1982, 1987, 1992, 1997 and 2002) and five La Nina

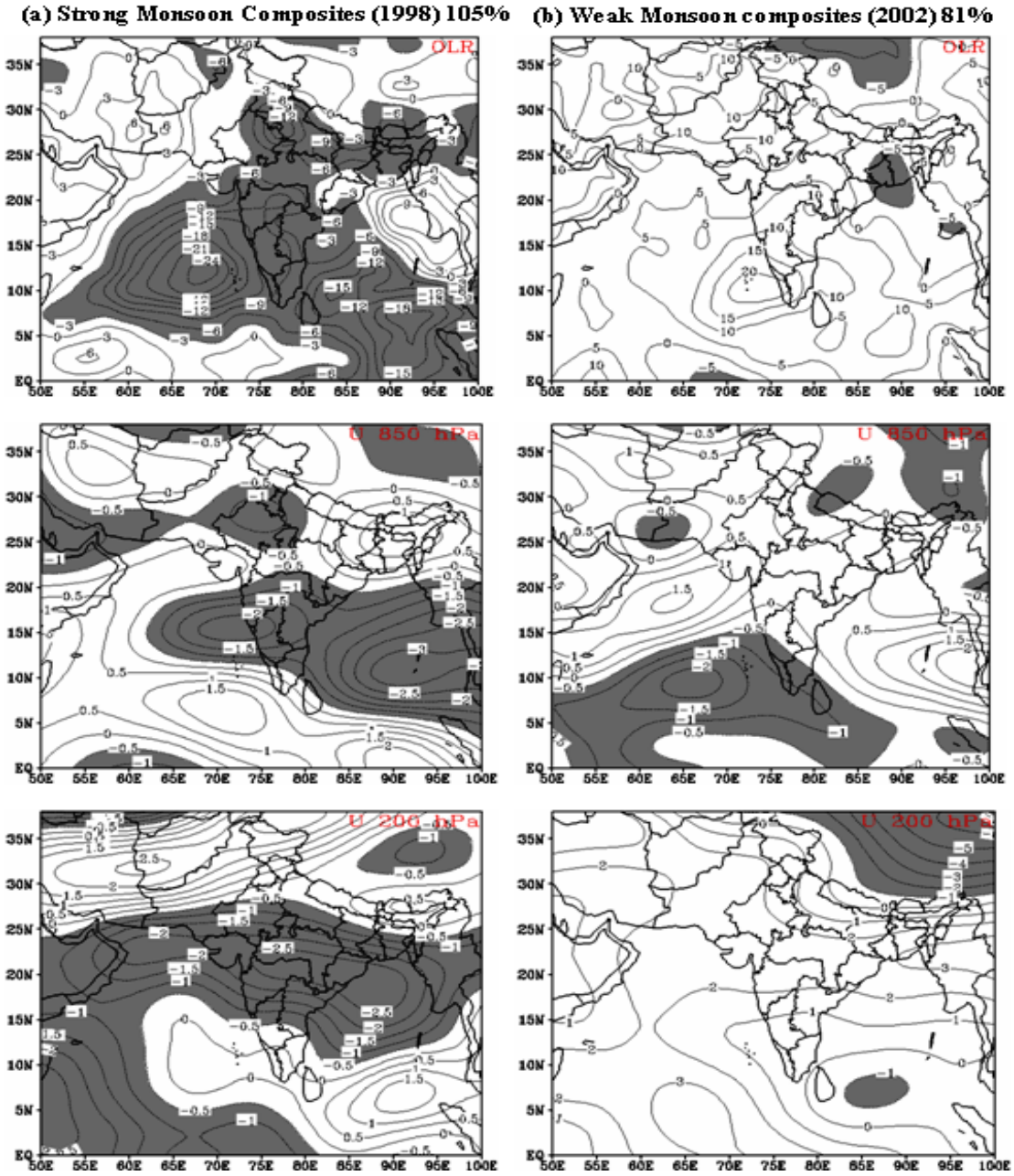

Fig. 5. a & b. Composite anomaly OLR and zonal wind fields for (a) La Nina (1998) and (b) El Nino (2002) monsoon years (shaded regions represent negative anomalies; percentage denote all India rainfall).

periods (1981, 1984, 1991, 1998 and 2005). Similarly monsoon Hadley index is also evaluated to define the strength of ISO, which also represents the same El Nino and La Nina periods (Fig. 6b). The relationship between MHI and monsoon rainfall is 0.6. In the year 2002, MJO and MHI are 0.31 and -1.2 respectively, while in 1998 they are -0.91 and 0.26. Thus year-to-year variability of Indian summer monsoon activity (rainfall) can be identified using above indices.

CONCLUSIONS

The analysis of datasets of satellite derived OLR and NCEP winds over the study region for 27-years reveals some interesting facts of variability of Indian monsoon.

The mean annual cycle of OLR in the tropics is dominated by changes in cloudiness caused by the Indian monsoon. Out of 73 pentads, P-30 to P-55 pentads show marked large scale monsoon convective activity. Mean

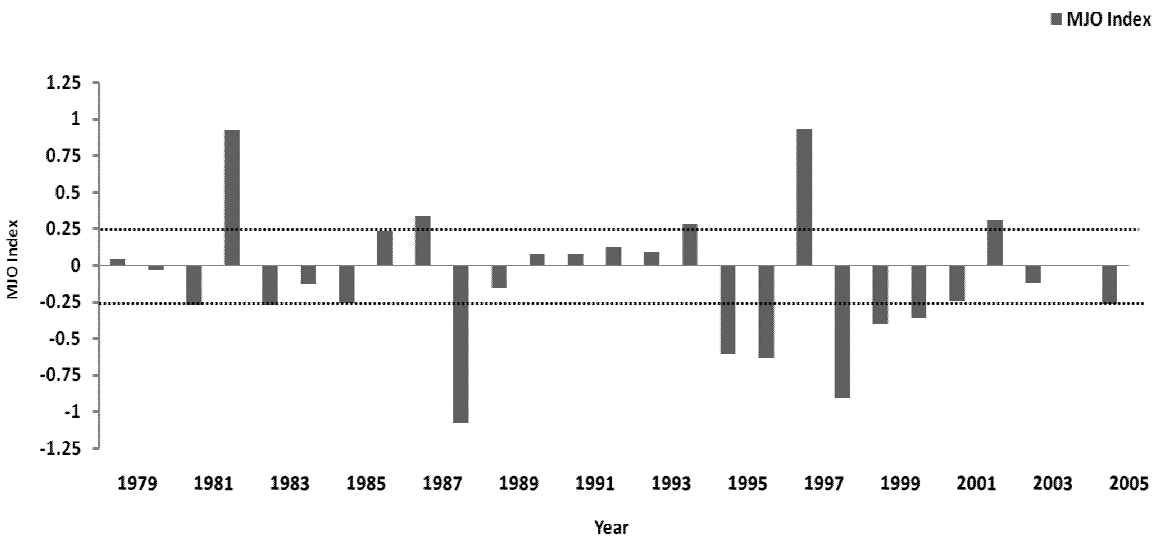

Fig. 6a. Inter annual variation of MJO Index during 1979-2005.

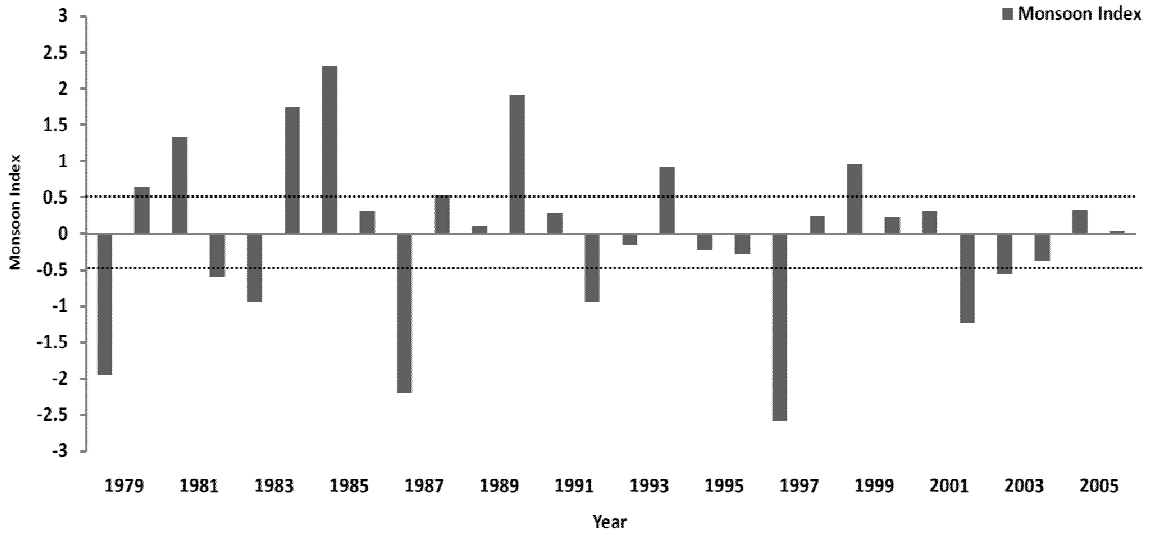

Fig. 6b. Inter annual variation of monsoon Hadley index during 1979-2005.

annual cycle of wind field supported above monsoon variability. The Interannual variability of ISO is partly linked to ENSO cycle. Strong ISO activity is often observed with La Nina.

Indices of MJO and monsoon indicate year-to-year variation of summer monsoon rainfall.

ACKNOWLEDGEMENTS

The authors are thankful to Ministry of Earth System Sciences, Government of India, New Delhi for financial support through a research project (11/MRDF/1/41/P/08). The authors are also thankful to NCEP/NCAR and NOAA team for providing data.

REFERENCES

Annamalai, H., Slingo, JM, Sperber, KR, and Hodges, K. 1999. The mean evolution and variability of the Asian summer monsoon: Comparison of ECMWF and NCEP-NCAR reanalysis. Mon. Wea. Rev. 127:1157-1186.

Annamalai, H. and Slingo, JM. 2001. Active/break cycles: Diagnosis of the intraseasonal variability over the Asian summer monsoon. Climate Dynamics. 18: 85-102.

Bhanu Kumar, OSRU., Muni Krishna, K. and Ramalingeswara Rao, S. 2008. Simulation of environmental heavy rainfall episodes during June and July 2006 - A case study, Canadian Journal of Pure and Applied Sciences. 2(1):211-220.

Degtyarev, AI, Smirnova, TG. and Degtyareva, NV. 2007. Indices of Monsoon Circulation, Russian Meteorology and Hydrology. 32:28-34.

Fenessy, M. and Shukla, J. 1994. GCM simulations of active and break monsoon periods. Proc. Int. Conf. on Monsoon Variability and Prediciton. Trieste, Italy, WMO/TD 619, WCRP-84. 2:576-585.

Goswami, BN. 1994. Dynamical predictability of seasonal monsoon rainfall: Problems and prospects. Proc. Indian Nat. Sci. Acad. 60A:101-120.

Goswami, BN. 1997. Chaos and predictability of the Indian summer monsoon. Pramana, 48, 719-736.

Goswami, BN. 1998. Inter-annual variations of Indian monsoon in a GCM: External conditions versus internal feedbacks. J. Climate. 11:501-522.

Goswami, BN, Krishnamurthy, V. and Annamalai, HA. 1999. broad scale circulation index for the interannual of the Indian summer monsoon, Quarterly Journal of the Royal Meteorologìcal Society. 125(55a):611-633.

Goswami, BN. and Mohan, RSA. 2001. Intraseasonal oscillations and interannual variability of the Indian summer monsoon. J. Climate. 14:1180-1198.

Goswami, BN., Ajaymohan, RS., Prince, KX. and Sengupta, D. 2003. Clustering of synoptic activity by Indian summer monsoon intraseasonal oscillations. Geo. Res. Lett. 30 (8):1431-1435.

Hazarallah, A and Sadourny, R. 1995. Internal versus SST forced atmospheric variability simulated by an atmospheric general circulation model. J. Climate. 8:474-495.

Julian, PR. and Madden, RA. 1981. A quasi-stationary appearance of a 30 to 40 day period in the cloudiness fluctuations during the summer monsoon over India, J. Meteor. Soc. Japan. 59:435-437.

Kemball-Cook, S. and Wang, B. 2001. Equatorial waves and air–sea interaction in the boreal summer intraseasonal oscillation. J. Climat. 14:2923-2942.

Krishnamurti, TN., Jayakumar, PK., Sheng, J., Surgi, N. and Kumar, A. 1985. Divergent circulations on the 30-50 day time-scale. J. Atmos. Sci. 42:364-375.

Li, J. and Zeng, QA. 2002. Unified monsoon index. Geophy Res Let. 29. 10.1029/2001GL013874.

Madden, RA. and Julian, PR. 1971. Detection of 40-50 day oscillation in the zonal wind in the tropical Pacific. J. Atmos. Sci. 28:702-708.

Manoel, AG., Rao, VB. and Marley, CLM. 2006. South American monsoon indices. Atmos. Sci. Let. 6:219-223.

Mooely, DA. and Parthasarathy, B. 1984. Fluctuations in Indian summer monsoon rainfall during 1871-1978. Climate Change. 6:286-301.

Ramamurthy, R. 1969. Monsoons of India: Some aspects of the break in the southwest monsoon during July-August. Forcasting manual. Part IV, No. 18.3, India Meteor. Dept., Pune, India.

Rowell, D., Folland, CK, Maskell, K. and Ward, MN. 1995. Variability of summer monsoon rainfall over tropical north Africa (1906-1992): Observations and modeling. Quart. J.Roy. Meteor.Soc. 121:669-704.

Rao Sanjeeva, P. and Sikka, DR. 2007. Interactive aspects of the Indian and the African summer monsoon systems. Pure and Applied Geophysics. 164:1699-1716.

Sikka, DR. and Sulochana, G. 1980. On the maximum cloud zone and the ITCZ over India longitude during the southwest monsoon; Mon. Weather Rev. 108**:**1840-1853.

Singh, SV. and Kripalani, RH. 1990. Low frequency intraseasonal oscillations in Indian rainfall and outgoing long wave radiation. Mausam. 41:217-222.

Singh, SV., Kripalani, RH. and Sikka, DR. 1992. Interannual variability of the Madden-Julian oscillation in the Indian summer monsoon rainfall. J.Climate. 5:973-978.

Stern, W. and Miyakoda, K. 1995. The feasibility of seasonal forecasts inferred from multiple GCM simulation. J. Climate. 8:1071-1085.

Susmitha, J., Sahai, AK. and Goswami, BN. 2008. Eastward propagating MJO during boreal summer and Indian monsoon droughts. Climate Dynamics. DOI 10.1007/s00382.

Wang, B. and Rui. 1990. Synoptic climatology of transient tropical intraseasonal convection anomalies, 1975-1985. Meteorol. Atmos. Phys. 44**:**43-61.

Webster, PJ. and Yang, S. 1992. Monsoon and ENSO: Selective interactive systems. Quart. J. Roy. Meteor. Soc. 118:877-926.

Yasunari, T. 1979. Cloudiness fluctuations associated with the northern hemisphere summer monsoon. J. Meteorol. Soc. Japan. 57:227-242.

Yasunari, Y. 1980. A quasi-stationary appearance of 30-40 day period in the cloudiness fluctuations during the summer monsoon over India. J. Met. Soc. Japan. 58:225-229.

Yu, JY. and Janiga, MA. 2007. Changes in the in-phase relationship between the Indian and subsequent Australian summer monsoons during the past five decades. Ann. Geophys. 25:1929-1933.

Received: Aug 5, 2009; Revised: April 14, 2010; Accepted: May 26, 2010

SENRA Academic Publishers, Burnaby, British Columbia
Vol. 4, No. 2, pp. 1207-1216, June 2010
ISSN: 1715-9997

Canadian Journal of pure&applied sciences

ENZYMATIC SURFACE HYDROLYSIS OF POLY(ETHYLENETEREPHTHALATE) BY LIPASE ENZYME AND ITS PRODUCTION

*Magda A El-Bendary [1], Samiha M Abo El-Ola[2] and Maysa E. Moharam[1]
[1]Microbial Chemistry Department, National Research Center, Dokki, Giza
[2]Proteinic and Synthetic Fiber Department National Research Center, Dokki, Giza, Egypt

ABSTRACT

In this study, hydrolysis of the surface of poly(ethyleneterephthalate) (PET) fabric by *Bacillus* isolate 5W and 6C lipases was confirmed by improved hydrophilic property which tested by wetability and staining with basic dyes, scanning electron microscope, and FTIR measurements. Lipase treated PET fabrics showed good physical and mechanical properties. It was observed that the retained strength of lipase treated PET was 96-98% and pilling and static charges were reduced. *Bacillus* isolate 5W was chosen for economic production of PET surface modifying lipase enzyme in 14 agro-industrial by-products. The most suitable substrate for the highest lipase production was cotton seed meal at 6% and initial pH 7.5 (90U/ml). Effect of volume of the medium in the flask, inoculums size and incubation period were investigated and 25 ml of the medium, 25 x 10^6 CFU/ml, and 24h, respectively were the optimal. Addition of peptone to cotton seed meal medium enhanced the lipase production 22.5% (130.7 U/ml). The results of this article focuses on production of lipase enzyme that hydrolyze PET under feasible and economic conditions for replacing harsh chemical processes currently used for hydrophilization.

Keywords: Lipase production, Poly(ethyleneterephthalate), surface modification, *Bacillus*, agro-industrial by-products.

INTRODUCTION

In the last few years there has been increasing interest in enzymatic surface modification of poly(ethyleneterephthalate) (PET), a synthetic polymer which widely used in the textile industry with an annual production of 36 million tons (Alisch-Mark *et al*., 2004; Fischer-Colbrie *et al*., 2004; Vertommen *et al*., 2005; Alisch-Mark *et al*., 2006; Heumann *et al*., 2006; Kim and Song, 2006; Silva *et al*., 2007; Guebitz and Cavaco-Paulo, 2008). PET produced from purified terephthalic acid or alternatively dimethyl terephthalate and ethylene glycol. PET has become very successful within the fashion industry due to its chemical resistance, wrinkle resistance and quick-drying properties. However it has a moisture regain of 0.4% (measured at 20°C and 65% relative humidity), this means that PET is extremely hydrophobic. Therefore, the use of PET in textile applications such as sportswear, underwear and bedding is restricted due to a relatively low level of comfort, as moisture is not absorbed nor drawn away from the skin. Additionally, PET exhibits static problems such as cling during wear and difficulty in cutting and sewing.

Consequently, increasing its hydrophilicity is essential for many applications ranging from textiles to medical and electronics (Guebitz and Cavaco-Paulo, 2008). Alkaline treatment is used to increase hydrophilicity of PET based textile materials (Shalaby *et al*., 2007). However, it leads to the deterioration of the fiber properties such as formation of pit-like structure as a result of high weight loss and reduction of fiber strength (Shalaby *et al*., 2007).

Recent studies clearly indicate that the modification of synthetic and natural polymers with enzymes is an environmentally friendly alternative to chemical methods using harsh conditions. Potential of microbial enzymes for the targeted surface functionalization of synthetic fibers has recently been assessed (Fischer-Colbrie *et al*., 2003). The major advantages of enzymes in polymer modification compared to the chemical methods are milder reaction conditions and easier control, environmental friendlier process, and specific non-destructive transformations on polymer surfaces (Matama *et al*., 2006).

Enzymes like lipases (EC. 3.1.1) and cutinase (EC. 3.1.1.74) may potentially hydrolyze the surface ester bonds of PET resulting in superficial formation of hydroxyl and carboxyl groups (Killis *et al*., 2001; Gubitz and Cavaco-Paulo, 2003; Silva and Cavaco-Paulo, 2004; Hasan *et al*., 2006). Due to the size of enzymes and the insoluble nature of PET fiber in an aqueous medium, the enzymes are merely active at the surface so that the bulk characteristics of fibers remain unchanged.

Recently attempts to isolate microorganisms that produce lipase enzyme which used for surface modification of textile gain a special interest.

*Corresponding author email: tasnim41@.yahoo.com

The purpose of the present study is selection of a novel *Bacillus* isolate that is capable of producing lipase enzyme that has the ability to modify PET surface without losing its strength. In addition, production of this enzyme by using industrial by-products as cost effective method for feasible application in textile industry. The results of this work support the research for potential utilization of lipase as a hydrolytic source for modification of PET.

MATERIALS AND METHODS

MATERIALS

p-nitrophenyl-acetate (*P*-NPA) was from Sigma, sodium dihydrogen phosphate, disodium hydrogen phosphate, non-ionic detergent Hostpal CVL-EL from Clarient, glacial acetic acid purchased from El-Naser Pharmaceutical Chemical Company.

Basic dyes (C.I Basic Red 18 and C.I Basic Yellow 28) kindly supplied by European Colour Plc, Stockport, England, however, Methylene Blue was from Merck. All other used chemicals were of analytical grade.

Polyester 100% fabric was provided by Hosam Textile Company, Bourge El-Arab, Alexandria, Egypt. Specification of woven fabric is 22 ends/inch, 20 picks/inch and 177g/m^2 fabric weight.

Agro-industrial byproducts were from Oil Extraction Unit and Animal Nutrition Department at National Research Center. These Agro-industrial byproducts were sugar beet pulp, potato peels, orange peels, pea peels, beans peels, banana peels, carrots pomace, jojoba meal, cress meal coconut meal, linen meal, sesame meal, wheat germ meal, and cotton seed meal.

METHODS

Screening of lypolytic bacilli

Ninety one *Bacillus* isolates were screened for lipase production by plating on tributyrin agar medium. These isolates were isolated from underground sand of underground spring, sands carried by winds during spring season in Cairo, sands and plant roots from the Egyptian desert, and sugar cane roots from upper Egypt. The bacterial isolates producing maximum clear zone were selected, subcultured, and stored on nutrient yeast agar slants at 4°C.

Media used

Nutrient yeast broth (NYB) contains per liter, 5g peptone, 3g beef extract and 5g yeast extract. For solidification, 20g agar is added.

Tributyrin agar medium (TBA) contains per liter, 5g peptone, 3g yeast extract, 10ml tributyrin, and 20g agar.

Agro-industrial by-products media contained 60g of agro-industrial wastes in 1 liter tap water.

Growth conditions and Preparation of cell free extracts

The isolates were grown in 25ml NYB medium in Erlenmeyer conical flask (250ml) for 3 days at 30°C and 150rpm on an orbital shaker. The cultures were harvested by centrifugation at 10000 x g for 10min. The supernatant was examined for lipase activity.

Lipase activity assay

Lipase activity was assayed according to Meghwanshi *et al*. (2006) and Chen *et al*. (2007) with some modifications. Lipase activity was determined using *p*-nitrophenyl acetate (*p*-NPA) as substrate. The substrate solution was prepared by dissolving *p*-NPA in isopropanol. The mixture of 880µl of 50mM phosphate buffer (pH 8), 20µl of substrate solution and 100µl of suitably diluted enzyme solution was incubated at the tested temperature for 30min. The reaction was terminated by the addition of 0.2ml of 100mM $CaCl_2$ solution (at 0°C) and keeping it on ice. The reaction mixture was centrifuged to clarify the solution and the absorbance of the yellow color of the supernatant was read at 410nm.

One unit of enzyme activity was defined as a 0.1 increase in OD_{410} under the standard assay conditions.

Enzymatic treatments of textile

Enzymatic treatments of textile were according to (O 'Neil, 2007). All fabric samples were washed to remove the impurities. The fabric was washed with 10g/l hostapal at 65°C for 1 h, followed by rinsing several times with tap water then the fabric was washed in aqueous solution contain 2g/l sodium carbonate for 1h at 65 °C, followed by rinsing several times with tap water. Finally, the fabrics gently squeezed and air dried. Two sets of experiments were performed. One gram of the fabric was incubated in a glass vessel containing a solution of 0.05 M sodium phosphate buffer (pH 8) using the same amount of crude enzyme (4%), the liquor ratio was 50:1. One set of experiment was incubated at 50°C for 8 h and the other set was incubated at 37°C for 24h on an orbital shaker at 150rpm. After enzymatic treatments, all samples were washed several times with tap water then with 2g/l sodium carbonate for 1h at 50°C followed by washing with distilled water for 1h at 50°C. Finally, the samples were washed with running tap water for 5 min and allowed to dry in open air.

Staining the fabrics

The staining was carried out below the glass temperature (Tg) of PET (at 50°C for 90 min) as described by O 'Neil (2007). After enzymatic treatments, the fabric samples were stained together in the same sealed glass vessel (500ml) on shaking water bath at proper pH. The dyeing was performed with 0.5 % shade owf, liquor ratio 50:1 and at 200rpm agitation. After dyeing process, samples

were washed with aqueous solution containing 2g/l non ionic detergent at 55°C for 1h then, washed with tap water and dried in oven at 50°C for 6h.

Wetability test
A water drop test was applied to lipase treated fabric and control samples according to AATCC standard method.

Colour Measurement
The K⁄S percentage increments after the enzymatic treatments and staining of the fabric samples were measured in order to detect differences in reactive groups formed on the surface according to Matama *et al*. (2006) and Silva *et al*. (2007). The colourimetric data K⁄S of the dyed samples was collected using Mini Scan XE integrated with Hunter lab universal software at maximum absorption, as an average of three readings. The relative K⁄S of enzymatic treated samples was calculated as follow:

$$\% \text{ Relative K/S} = \{(K/S)_{treated} - (K/S)_{control}\}/(K/S)_{control} * 100$$

Scanning electron microscope (SEM)
Changes of the fiber surface morphology due to enzymatic treatment were followed by SEM model JEOL JXA-84OH Electron Prope Microanalyzer, Japan operating at 19 KV. A thin coating film (~10 nm) of gold was deposited onto the samples, before examination by SEM.

FTIR measurements
To investigate the effect of enzymatic treatment on structure of the PET fabrics surface, the fabrics were analyzed by FTIR spectroscopy using Nicolet 380 spectrophotometer in the spectral range 4000-650 cm^{-1}, with a resolution of 4 cm^{-1} and a number of scans of 128. Fabrics were measured by "Smart Performer ATR" unit accessory with zinc selenide crystal.

Transfer printing
Transfer printing was done by using two disperse dyes, C.I Disperse blue 56 and C.I Disperse Red 60.

Weight loss
Weight loss, was evaluated according to the following equation

$$\text{Weight loss } \% = (W_1 - W_2)/W_1 * 100$$

Where W_1, W_2 are the weight before and weight after enzymatic hydrolysis, respectively.

Oily Stain resistance
Oily stain release was measured according to AATCC Test method 130-1992.

Pilling resistance
Pilling resistance of PET fabrics was measured according to ASTM 4966/4970 (2002) using Martindale Abrasion and Piling Testers (M235 Martindale SDL ATLAB, England).

Air permeability
Air permeability was measured according to ASTM D 737 (96).

Static charge
Static charge was measured using electricity collect type Potentiometer Type KS- 525 KASUGA, DENKJ, Inc., Tokyo, Japan.

Tensile strength
Tensile strength of PET fabrics was measured according to ASTM D3822-01 by INSTRON, USA. Tensile strength results are the arithmetic means of three tests per sample.

Morphological and biochemical identification of isolated *Bacillus*
Bacillus isolate which produce high lipase enzyme, and showed good PET surface modification was identified using standard morphological and biochemical procedures according to Gordan (1974), Claus and Berkeley (1986) and Stukus (1997).

Optimization of the medium conditions for lipase production
1. A group of locally available agro-industrial by-products were tested as possible media for lipase production.
2. Effect of the best agro-industrial byproduct concentrations on lipase production was studied.
3. Effect of initial pH of the medium was studied by buffering the medium with 0.05M phosphate buffer at pH values ranging between 5.5 and 9.0.
4. Effect of aeration level was tested by varying the volume of the medium in the experimental flasks between 6-100ml.
5. Effect of inoculum size was studied by varying the inoculum size between 5 $x10^6$ and $25x10^7$ CFU/ml.
6. Effect of incubation period was investigated by incubation for varying periods up to five days.
7. Effect of supplementation of the medium with additional nutrient sources at 2% final concentration was studied.

RESULTS AND DISCUSSION

Screening of *Bacillus* isolates for lipase production.
Thirty one of the tested *Bacillus* isolates showed high lypolytic activity as clear zone around their colonies on TBA medium.

Quantitative screening for lipase activity by *P*-NPA showed that 19 *Bacillus* isolates (2U, 1W, 2W, 5W, 6C, 8C, 12C, 14C, 11P, 16P, 18P, 19P, 20P, 21P, 22P, 36P, 38P, 41P and 45P) were the most lypolytic isolates at 37°C. Most of them showed promising activities at 50°C (data not shown).

The literature reported that several *Bacillus* species isolated from several diverse environments produced lipase enzyme (Sharma *et al*., 2001; Kumar *et al*., 2005; Hasan *et al*., 2006; Deive *et al*., 2007).

Lipase enzymes produced by the above 19 *Bacillus* isolates were examined for hydrolysis of PET fabrics.

Wetability of lipase treated PET fabrics

The results of wetability of PET fabrics treated with lipase of *Bacillus* isolates 2U, 5W, 6C, 16P and 22P at 37°C for 24h were more effective than at 50°C for 8h as proved by the decrement of the time for water drop absorption as shown in table 1. This revealed that they are promising lipase producers for improving surface wetability of PET fabrics. These results indicated that the amount of hydrophilic groups (OH and COOH) at the surface of PET increased as a result of lipase treatment. Hsieh and Cram (1998) reported that, the surface wetability of enzyme treated substrates is associated with hydrolytic action rate.

Cationic Dye Binding

Significant increase in K/S values were observed for stained lipase treated PET fabrics. The results supported that the enzymatic treatment increased adhesion of cationic compounds probably by creating carboxyl groups on the surface of the treated fabrics. The staining degree of lipase treated PET fabrics varies according to the basic dye used which may be attributed to the size of dye molecule and the pore size created on the fabric surface as a result of enzymatic hydrolysis. PET fabrics treated with lipase enzyme produced by *Bacillus* isolates 5W and 6C at 37°C for 24 h showed promising increase in K/S percentage after staining by Methylene Blue, C.I. Basic Yellow 28 and C.I. Basic Red 18 as shown in table 2.

Transfer Printing

The impact of lipase treatment on transfer printing of PET using two different disperse dyes, C.I Disperse Blue 56 and C.I Disperse Red 60 was shown in table 3. The results revealed that a significant improvement of color strength of printed modified PET fabrics. Lipase enzyme produced by *Bacillus* isolate 5W enhanced the relative color strength to large extent.

Physical and Mechanical properties

Table 4 illustrates the effect of lipase treatment on some physical and mechanical properties of PET fabrics. Based on these data, it was observed that breaking strength of PET decreased with treatment of the fabrics with lipase enzymes produced by *Bacillus* isolates 5W and 6C to a limited extent and 96-98% of the strength of the fabric was retained. The decrease in breaking strength may be due to the formation of pits on the surface which probably

Table 1. Wetability of PET fabrics treated with lipase produced by *Bacillus* isolates

Bacillus isolate	Lipase activity (U/ml) at		Wetting time (min) of lipase treated PET at 37 °C for 24 h	Wetting time (min) of lipase treated PET at 50°C for 8 h
	37°C	50°C		
2U	39.6	29.4	0.22	1.6
5W	39.8	32.4	0.23	1.2
6C	19.2	21.0	0.28	3.8
16P	30.7	21.2	0.43	5.37
22P	30.2	20.9	0.33	2.37
Control (buffer)	-	-	6.3	3.3

Table 2. Relative K/S of dyed PET fabric treated with lipase enzyme produced by *Bacillus* isolates.

Lipase produced by *Bacillus* isolate	% Relative K/S of PET treated with lipase enzyme at 37 °C for 24h or 50°C for 8h and stained by					
	Methylene blue λ_{max} 650 pH 9.5		C.I. Basic yellow 28 λ_{max} 460 pH 4.5		C.I. Basic Red 18 λ_{max} 520 pH 4.5	
	37°C for 24 h	50°C for 8 h	37°C for 24 h	50°C for 8 h	37°C for 24 h	50°C for 8 h
2U	-13.6	5.7	18.4	3.16	6.3	-2.1
5W	28	9.49	18.4	17.6	84	-27.3
6C	18.4	5.13	65.9	18.35	56.3	32.87
16P	12.4	3.8	22.09	-24.05	12.8	2.8
22P	-3.23	5.13	1.58	7.6	27.3	5.87

-ve value means that K/S of control is more than K/S of treated samples.

act as weak points when the fabric is elongated under stress. In addition, the amount of static charge decreased as a result of lipase treatment of PET. This may be attributed to the creation of hydroxyl and carboxyl groups consequently enhanced the moisture regain and the amount of static charge decreased. Improvement of pilling resistance and dissipation of electrostatic charge soil release resistance were noticed. Lipase pretreatment of PET also reduced the susceptibility of the fabric to stain by corn oil in comparison to the control. Presumably enzymatic hydrolysis of PET and formation of hydroxyl and carboxyl groups decrease hydrophobicity and attraction for oily soil thereby enabling the easier removal of the corn oil stain.

Scanning Electron Microscope

The physical modification of lipase treated PET fabrics was examined by SEM. As shown in figure 1, a significant modification of the fiber surface was observed. The surface of PET fabrics treated with buffer was smooth however, the enzymatic treated fabrics gained heterogeneous appearance such as cracks, pits, pores, and rough surfaces.

FTIR measurements

Infrared spectra for PET fabric samples are shown in figure 2. Different spectra were obtained for control (denaturated enzyme) and lipase treated samples. There is intensity differences in some bands between lipase treated and untreated fabrics. The selected region used for comparison is from 1350-1150 cm^{-1}, where the peak of C-O is located at 1241cm^{-1}. The spectra reveal an increase in the absorbance of C-O vibration for the lipase treated samples as compared to the control. This may be attributed to the formation of carboxyl groups (COOH) due to lipase hydrolysis of the ester linkages in PET producing polar carboxyl and hydroxyl groups.

Table 3. Effect of Lipase treatment of PET fabric on transfer printing.

Lipase produced by *Bacillus* isolate	Relative K/S		% Increase in K/S	
	C.I Disperse Blue 56	C.I Disperse Red 60	C.I Disperse Blue 56	C.I Disperse Red 60
5W	0.82	4.331	148.5	305.5
6C	0.4	1.1242	21.2	5.24
Control (buffer)	0.33	1.068	-	-

Table 4. Effect of lipase treatment of PET fabric on physical and mechanical properties.

Lipase produced by *Bacillus* isolate	Weight loss (%)	Breaking strength (Kg)	Retained strength (%)	Elongation (%)	Static charge (KV)	Pilling resistance	Soil release
5W	0.35	108	95.57	24.1	6.6	3-4	3
6C	0.3	111	98.2	26.1	7.66	3-4	2-3
Control (buffer)	0.31	113	100	23.3	8	2	1

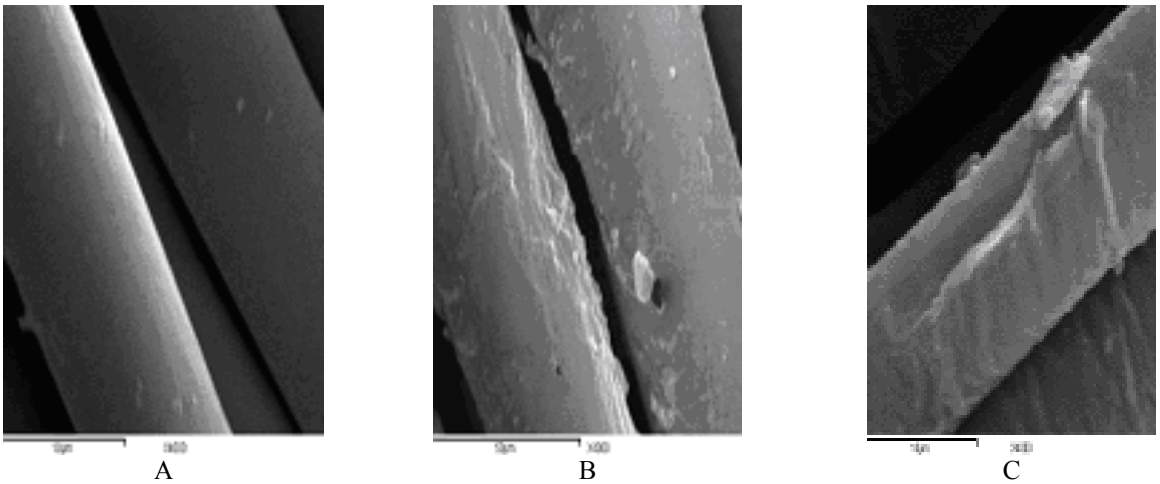

A B C

Fig.1. SEM of PET fabric treated with buffer solution (A) and lipases of *Bacillus* isolate 5W and 6C (B and C, respectively).

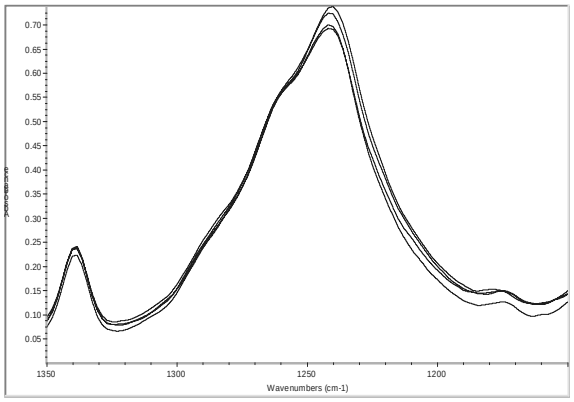

Fig. 2. FTIR spectra of PET fabric treated with (from bottom to top) denaturated enzyme of *Bacillus* isolate 5W, denaturated enzyme of *Bacillus* isolate 6C, lipase enzyme of *Bacillus* isolate 6C and lipase enzyme of *Bacillus* isolate 5W showing increase in the absorbance of the C-O vibrations (1241 cm^{-1}) as a result of lipase treatment.

Production of lipase by *Bacillus* isolate 5W on agro-industrial by-products.

Bacillus isolate 5W produced higher lipase activity and PET fabrics treated with this lipase showed good wetability, staining, physical and mechanical properties. These results supported by SEM and FTIR studies, which proved the modification of PET surfaces. Therefore, this isolate was selected for further studies. It was identified according to the morphological and biochemical tests as *Bacillus subtilis.*

Fourteen agro-industrial residues were studied for production of lipase by *Bacillus* isolate 5W without pretreatment under submerged fermentation conditions. As shown in table 5 nine substrates enhanced the lipase production by the tested isolate as or more than NYB medium. The most efficient media were cotton seed meal, banana peels, wheat germ meal, and cress meal. The maximum production (52.8U/ml) was obtained with cotton seed meal (CSM) medium. Concentrations of CSM was tested and maximum lipase yield was at 6%.

Haba *et al*. (2000) used frying oils wastes for production of lipase by 47 strains of bacteria and yeasts. They reported that the genera *Pseudomonas*, *Bacillus*, *Candida*, *Rhodococcus* and *Staphylococcus* grew on the waste oil and produced high lypolytic activity. Rohit *et al*. (2001) and Mohan *et al*. (2008) reported that high levels of lipase activity were obtained by *Bacillus* strains grown in olive oil as a medium. Ertugrul *et al*. (2007) found that 20% whey with 1% triolein gave the highest lipase activity by *Bacillus* sp. Souissi *et al*. (2009) produced lipase by *Staphylococcus simulans* grown on sardinella hydrolyzates and peptone. Lin *et al*. (1996) reported an extracellular alkaline lipase produced by *Pseudomonas alcaligenes* F-111 in a medium that contained soybean meal, peptone and yeast extract. Kumar *et al*. (2005) produced lipase by *Bacillus coagulans* BTS-3 with refined mustard oil, peptone and yeast extract.

Table 5. Production of lipase by *Bacillus* isolate 5W on agro-industrial by-products.

Industrial by-products	Final pH	Lipase activity (U/ml)
Sugar beet pulp	6.16	5.25
Potato peels	7.25	24.6
Orange peels	5.74	0.0
Pea peels	7.47	36.0
Bean peels	6.25	30.8
Banana peels	6.65	44.6
Carrot pomace	7.65	33.1
Jojoba meal	7.32	17.8
Cress meal	8.4	40.1
Coconut meal	5.94	5.25
Linen meal	8.32	32.4
Sesame meal	7.25	31.4
Wheat germ meal	8.16	43.1
Cotton seed meal	8.41	52.8
NYB	8.18	34.5

Effect of initial pH of the medium

Effect of initial pH of the medium on lipase production by *Bacillus* isolate 5W is shown in figure 3. There is an increase in the lipase production with increasing the pH between 5.5 and 7.5. Increasing the pH of the medium more than 7.5 has destructive effect on the lipase production by the tested organism. These results are in consistence with that reported by Achamma *et al*. (2003) and Deive *et al*. (2007). They found that lipase production by *Bacillus* sp. and *Pseudomonas aeruginosa* MB was the maximum at neutral pH. However Ertugrul *et al*. (2007) reported that the optimal pH for lipase production by *Bacillus* sp was 6. Although bacteria prefer pH around 7 for best lipase production, maximum activity at higher pH values were also reported in the literature (Kumar *et al*., 2005).

Effect of aeration level on lipase production

The enzyme levels formed at different aeration levels under shaking conditions are shown in figure 4. The maximum lipase production (91.2U/ml) was at 25ml medium in 250ml flask (10% of the flask volume).

Effect of inoculum size

Lipase activity of *Bacillus* isolate 5W reached its maximum value (109.3 U/ml) upon using approximately $25x10^6$ CFU/ml as shown in figure 5. However, further increase in inoculum size lead to a dramatic decrease in lipase production.

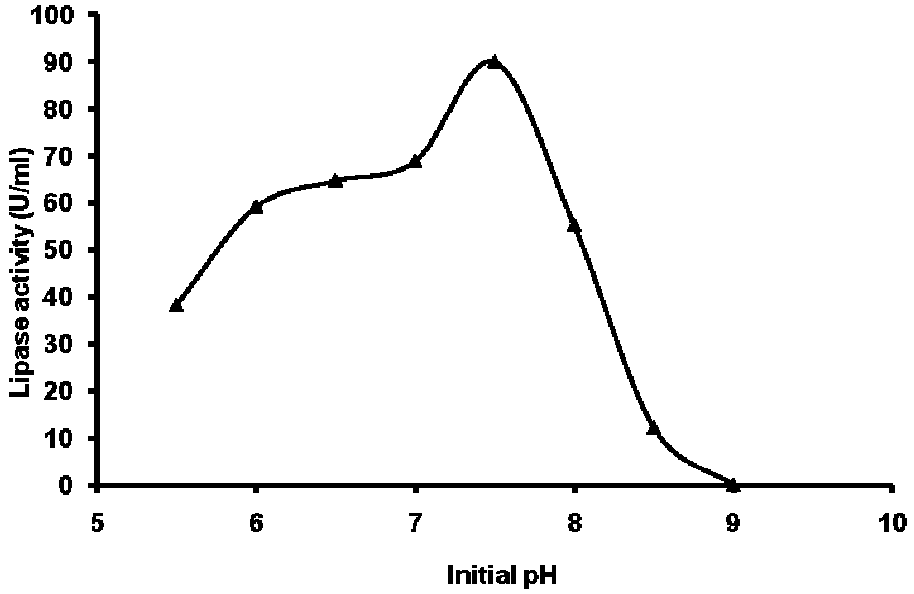

Fig. 3. Effect of initial pH of the medium on lipase production by *Bacillus* isolate 5W.

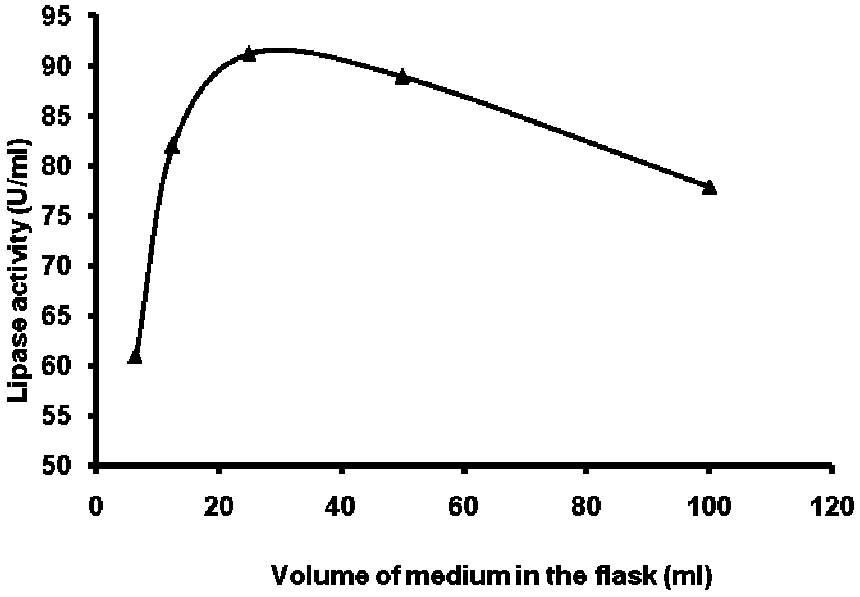

Fig. 4. Effect of aeration level on lipase production by *Bacillus* isolate 5W.

Effect of incubation period

Lipase production by *Bacillus* isolate 5W grown for extended incubation periods up to 96h. The highest lipase production was obtained after 24h of incubation and no significant variations could be observed in activity with the increment of the incubation period up to 96h. Kumar *et al*. (2005) and Ertugrul *et al*. (2007) reported that the time course for the maximum intracellular lipase production by *Bacillus* was 48 and 63h, respectively.

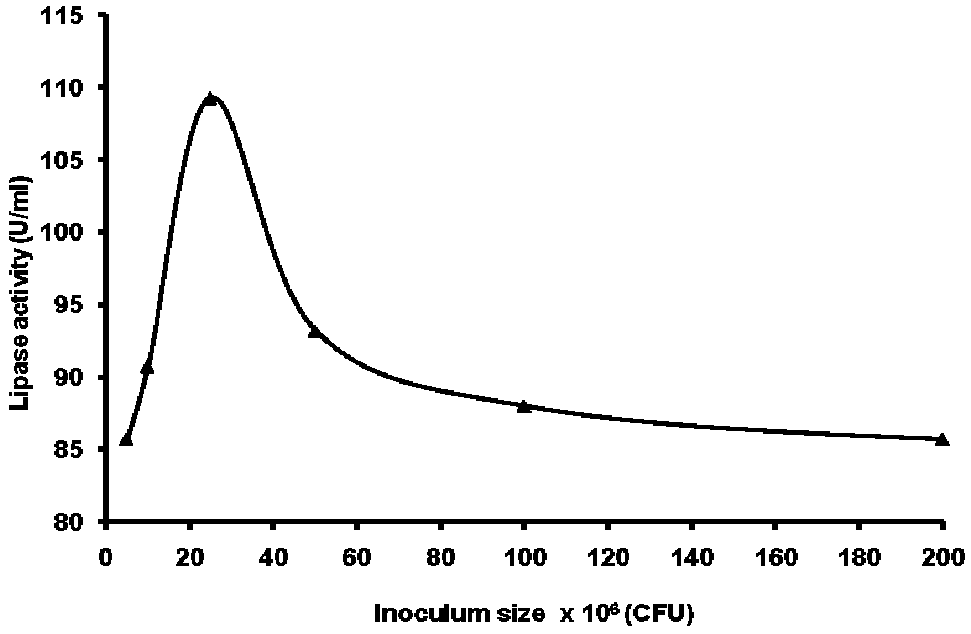

Fig. 5. Effect of inoculum size on lipase production by *Bacillus* isolate 5W.

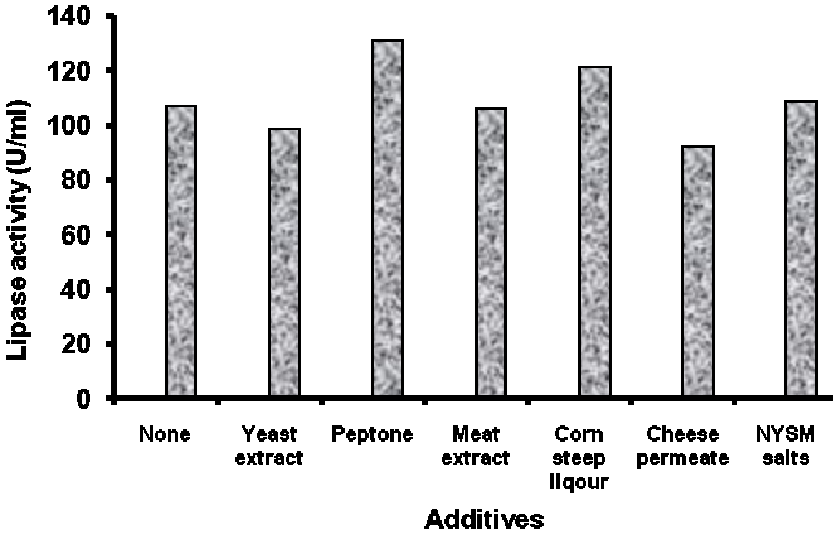

Fig. 6. Effect of additives on the lipase production by *Bacillus* isolate 5W.

Effect of supplementation of CSM with additional nutritional sources

Selected nutritional sources were incorporated as supplements to CSM medium for further enrichment of the growth medium. As shown in figure 6. Peptone and corn steep liquor at 2% enhanced the lipase production about 22.5% (130.7 U/ml) and 9% (121.1U/ml), respectively. Lin *et al*. (1996); Kumar *et al*. (2005) and Souissi *et al*. (2009) added peptone to their media for production of lipase by *Pseudomonas alcaligenes* F-111, *Bacillus coagulans* BTS-3 and *Staphylococcus simulans*, respectively. Corn steep liquor was an optimal nitrogen

source for intracellular and extracellular lipase production by the fungus *Rhizopium oryzae* as reported by Essamri *et al*. (1998) and Hiol *et al*. (2000), respectively.

Effect of metal ions

A group of metal ions (Ca^{2+}, Mg^{2+}, Na^{+}, Co^{2+}, Cu^{2+}, Fe^{2+}, K^{+}, Mn^{2+}, Mo^{2+} , and Zn^{2+}) were added to the medium separately as lipase enhancer but they did not enhance the lipase production with exception of Zn^{2+} which enhanced its production by 8%.

REFERENCES

Achamma, T., Manoj, MK., Valsa, A., Mohan, S. and Manjula, R. 2003. Optimization of growth condition for the production of extracellular lipase by *Bacillus mycoides*. Indian Journal of Microbiology. 43:67-69.

Alisch-Mark, M., Feuerhack, A., Muller, H., Mensak, B., Andreaus, J. and Zimmermann, W. 2004. Biocatalytic modification of polyethylene terephthalate fibers by esterases from actinomycete isolates. Biocatalysis and Biotransformation. 22:347-351.

Alisch-Mark, M., Herrmann, A. and Zimmermann,W. 2006. Increase of the hydrophilicity of polyethylene terephthalate fibers by hydrolases from *Thermomonospora fusca* and *Fusarium solani* f sp pisi. Biotechnology Letter. 28: 681-685.

Chen, A., Qian, L. and Shi, B. 2007. Purification and properties of enantioselective lipase from a newly isolated *Bacillus cereus* C71. Process Biochemistry. 42: 988-994.

Claus, D. and Berkeley, RCW. 1986. Genus Bacillus Cohn 1872. In Bergey's Manual of Systematic Bacteriology (vol. 2nd) Ed. Sneath, PHA. Baltimore, Williams and Wilkins. Pp. 1105-1141.

Deive, FJ., Sanroman, MA., and Longo, MA. 2007. Lipase production by a newly isolated *Bacillus thermomylovorans* strain. Journal of Biotechnology. 131:S238-S239.

Ertugrul, S., Donmez, G. and Takac, S. 2007. Isolation of lipase producing *Bacillus* sp from olive mill wastewater and improving its enzyme activity. Hazardous Materials. 149: 720-724.

Essamri, M., Valerie, D. and Louis, C. 1998. Optimization of lipase production by *Rhizopus oryzae* and study on the stability of lipase activity in organic solvents. Journal of Biotechnology. 60:97-103.

Fischer-Colbrie, G., Heumann, S., Cavaco-Paulo, A. and Gubitz, GM. 2003. Enzymatic modification of synthetic fiber. 225th ACS National Meeting, Mar 23-27, New Orleans, USA.

Fischer-Colbrie, G., Heumann, S., Liebminger, S., Almansa, E., Cavaco-Paulo, A. and Gubitz, GM. 2004. New enzymes with potential for PET surface modification. Biocatalysis and Biotransformation. 22:341-346.

Gordon, RE. 1974. The genus *Bacillus*: In handbook of microbiology (vol. 1) (organisms microbiology). Eds. Laskin, AI and Lechevalie, HA. Rutgers University, New Brunswick, New Jersey.

Guebitz, GM and Cavaco-Paulo, A. 2008. Enzymes go big: surface hydrolysis and functionalization of synthetic polymers. Trends in Biotechnology. 26:32-38.

Guebitz, GM. and Cavaco-Paulo, A. 2003. New substrates for reliable enzymes: enzymatic modification of polymers. Current Opinion in Biotechnology. 14:577-582.

Haba, E., Bresco, O., Ferrer, C., Marques, A., Busquets, M. and Manresa, A. 2000. Isolation of lipase-secreting bacteria by deploying used frying oil as selective substrate. Enzyme and Microbial Technology. 26:40-44.

Hasan, F., Shah, AA. and Hameed, A. 2006. Industrial applications of microbial lipases. Enzyme and Microbial Technology. 39: 235-251.

Heumann, S., Eberl, A., Pobeheim, H., Liebminger, S., Fischer-Colbrie, G., Almansa, E., Cavaco-Paulo,A. and Gubitz, GM. 2006. New model substrates for enzymes hydrolyzing polyethyleneterephthalate and polyamide fibers. Journal of Biochemical and Biophysical Methods. 69:89-99.

Hiol, A., Jonzo, MD., Rugani, N., Druet, D., Sarda, L. and Comeau, LC. 2000. Purification and characterization of an extracellular lipase from a thermophilic *Rhizopus oriza* strain isolated from fruit. Enzyme and Microbial Technology. 26:421-430.

Hsieh, Y-L. and Cram, LA. 1998. Enzymatic hydrolysis to improved wetabilitty and absorbency of polyester fabrics, Textile Research Journal. 68:311-319.

Killis, J., James, T., Ayrookran, PJ. and Yoon, M-Y. 2001. Enzymatic modification of the surface of a polyester fiber. US patent 6254645.

Kim, HR. and Song, WS. 2006. Lipase treatment of polyester fabrics. Fibers Polymers 7:339-343.

Kumar, S., Kikon, K., Upadhyay, A., Kanwar, SS. and Gupta, R. 2005. Production, purification and characterization of lipase from thermophilic and alkalophilic *Bacillus Coagulans* BTS-3. Protein Expression and Purification. 41:38-44.

Lin, SF., Chiou, CM., Yeh, C. and Tsai, YC. 1996. Purification and partial characterization of an alkaline lipase from *Pseudomonas pseudoalkaligenes* F-111. Applied and Environmental Microbiology. 62:1093-1095.

Matama, T., Vaz, F., Gubitz, GM. and Cavaco-Paulo, A. 2006. The effect of additives and mechanical agitation in

surface modification of acrylic fibers by cutinase and esterase. Biotechnology Journal. 7:842-879.

Meghwanshi, GK., Agarwal, L., Dutt, K. and Saxena, RK. 2006. Characterization of 1,3-regiospecific lipase from new *Pseudomonas* and *Bacillus* isolates. Journal of Molecular Catalysis. B: Enzyme 40:127-131.

Mohan, ST., Palavesan, A. and Immanvel, G. 2008. Isolation and characterization of lipase-producing *Bacillus* strains from oil mill waste. African Journal of Biotechnology. 7:2728-2735.

O'Neill, A., Araújo, R., Casal, M., Guebitz, G. and Cavaco Paulo, A. 2007. Effect of the agitation on the adsorption and hydrolytic efficiency of cutinase on polyethylene terephthalate fibers. Enzyme and Microbial Technology. 40:1801-1805.

Rohit, S., Yusuf, C. and Ullamchand, B. 2001. Production, purification, characterization and application of lipases. Biotechnology Advances. 19:627-662.

Shalaby, SE., El-Balacosy NG. and Abo El Ola, SM. 2007**.** Alkaline treatment of polyethylene glycol modified poly(ethyleneterephthalate) fabrics. Journal of Textile Association. May-June 31-38.

Sharma, R., Chisti, Y. and Banerjee, UC. 2001. Production, purification, characterization, and applications of lipase. Biotechnology Advances. 19:627-662.

Silva, C. and Cavaco-Paulo, A. 2004. Monitoring biotransformations in polyamide fibers. Biocatalysis and Biotransformation. 22:357-360.

Silva, C., Araujo, R., Casal, M., Gubitz, GM. and Cavaco-Paulo, A. 2007. Influence of mechanical agitation on cutinases and protease activity towards polyamide substrates. Enzyme and Microbial Technology. 40:1678-1685.

Souissi, N., Bougatat, A., Triki-ellouz, Y. and Nasri, M. 2009. production of lipase and biomass by *Staphylococcus simulans* grown on sardinella (*Sardinella aurita*) hydrolysates and peptone. African Journal of Microbiology. 8:451-457.

Stukus, PE. 1997. Investigating microbiology: A laboratory manual for general microbiology. Saunders College Publishing, New York. pp. 143-209.

Vertommen, MAME., Nierstrasz, VA., van der Veer, M. and Warmoeskerken, MMCG. 2005. Enzymatic surface modification of poly(ethyleneterephthalate). Journal of Biotechnology. 120:376-386.

Received: April 3, 2010; Accepted: May 26, 2010

SENRA Academic Publishers, Burnaby, British Columbia
Vol. 4, No. 2, pp. 1217-1219, June 2010
ISSN: 1715-9997

Canadian Journal of pure&applied sciences

ON SUBMANIFOLDS OF INDEFINITE COMPLEX SPACE FORM

Augustus Nzomo Wali
Department of Applied Mathematics
Kigali Institute of Science and Technology, B. P. 3900, Kigali, Rwanda

ABSTRACT

Sun (1994) showed that if M is a maximal spacelike submanifold of $\bar{M}_n^n(c)$ then either M is totally geodesic $(n \geq 2, c \geq 0)$ or $0 \leq S \leq -\frac{c}{4}n(n-1), (n \geq 2, c < 0)$. The purpose of this paper is to study the geometry of an n-dimensional compact totally real maximal spacelike submanifold M immersed in an indefinite complex space form $\bar{M}_p^{n+p}(c)$. In this manuscript we have shown that either the square of the length of second fundamental form S=0, implying M is totally geodesic for $c \geq 0, n > 1$ or $S \leq \frac{(1-n)(n+2p)}{4}c$ for $c < 0, n > 1$ and thus generalized Sun (1994) result.

Keywords: Totally real submanifold, complex space form, totally geodesic.

INTRODUCTION

Among all submanifolds of a Kaehler manifold there are two classes; the class of totally real submanifolds and the class of holomorphic submanifolds. A submanifold of a Kaehler manifold is called totally real (resp. holomorphic) if each tangent space of the submanifold is mapped into the normal space (resp. itself) by the almost complex structure of the Kaehler manifold, Chen and Ogiue (1974). A Kaehler manifold of constant holomorphic sectional curvature is called a complex space form, Wali (2005).

Let M be an n-dimensional totally real maximal spacelike submanifold isometrically immersed in a 2(n+p)-dimensional indefinite complex space form $\bar{M}_p^{n+p}(c)$ of holomorphic sectional curvature c and index 2p. We call M a spacelike submanifold if the induced metric on M from that of the ambient space is positive definite, Ishihara (1988). Let J be the almost complex structure of $\bar{M}_p^{n+p}(c)$. An n-dimensional Riemannian manifold M isometrically immersed in $\bar{M}_p^{n+p}(c)$ is called a totally real submanifold of $\bar{M}_p^{n+p}(c)$ if each tangent space of M is mapped into the normal space by the almost complex structure, Yano and Kon (1976).

Let h be the second fundamental form of M in $\bar{M}_p^{n+p}(c)$ and denote by S the square of the length of the second fundamental form h.

Sun (1994), proved that if M is a maximal spacelike submanifold of $\bar{M}_n^n(c)$ then either M is totally geodesic $(n \geq 2, c \geq 0)$ or $0 \leq S \leq -\frac{c}{4}n(n-1), (n \geq 2, c < 0)$. The purpose of this paper is to study an n-dimensional compact totally real maximal spacelike submanifold M immersed in an indefinite complex space form $\bar{M}_p^{n+p}(c)$.

Our main result is:

Theorem: Let M be an n-dimensional compact totally real maximal spacelike submanifold of $\bar{M}_p^{n+p}(c)$. Then either S=0, implying M is totally geodesic for $c \geq 0, n > 1$ or $S \leq \frac{(1-n)(n+2p)}{4}c$ for $c < 0, n > 1$.

LOCAL FORMULAS

Let $\bar{M}_p^{n+p}(c)$ be an indefinite complex space form of holomorphic sectional curvature c, dimension 2(n+p), $p \neq 0$ and index 2p. Let M be an n-dimensional totally real maximal spacelike submanifold isometrically immersed in $\bar{M}_p^{n+p}(c)$. We choose a local field of orthonormal frames

*Corresponding author email: tabnzo@yahoo.co.in

$\left\{e_1,...,e_n;e_{n+1},...,e_{n+p};e_{1^*}=Je_1,...,e_{n^*}=Je_n;e_{(n+1)^*}=Je_{n+1},...,e_{(n+p)^*}=Je_{n+p}\right\}$

in $\bar{M}_p^{n+p}(c)$ such that restricted to M, the vectors $\{e_1,...,e_n\}$ are tangent to M and the rest are normal to M. With respect to this frame field of $\bar{M}_p^{n+p}(c)$, let $\omega^1,...,\omega^n;\omega^{n+1},...,\omega^{n+p};\omega^{1^*},...,\omega^{n^*};\omega^{(n+1)^*},...,\omega^{(n+p)^*}$ be the field of dual frames.

Unless otherwise stated, we shall make use of the following convention on the ranges of indices: $1\le A,B,C,D\le n+p;\quad 1\le i,j,k,l,m\le n;$ $n+1\le\alpha,\beta,\gamma\le n+p;$ and when a letter appears in any term as a subscript or a superscript, it is understood that this letter is summed over its range. Besides

$\varepsilon_i=g(e_i,e_i)=g(Je_i,Je_i)=1$, when $1\le i\le n$

$\varepsilon_\alpha=g(e_\alpha,e_\alpha)=g(Je_\alpha,Je_\alpha)=-1$, when $n+1\le\alpha\le n+p$.

Then the structure equations of $\bar{M}_p^{n+p}(c)$ are;

$d\omega^A+\sum\varepsilon_B\omega_B^A\wedge\omega^B=0,\ \omega_B^A+\omega_A^B=0,\ \omega_j^i=\omega_{j^*}^{i^*},$

$\omega_j^{i^*}=\omega_i^{j^*},$

$$d\omega_B^A+\sum_C\varepsilon_C\omega_C^A\wedge\omega_B^C=\frac{1}{2}\sum_{CD}\varepsilon_C\varepsilon_D\bar{R}_{ABCD}\omega^C\wedge\omega^D,$$

$$\bar{R}_{ABCD}=\frac{c}{4}\varepsilon_C\varepsilon_D\left(\delta_{AC}\delta_{BD}-\delta_{AD}\delta_{BC}+J_{AC}J_{BD}-J_{AD}J_{BC}+2J_{AB}J_{CD}\right)$$

where $\bar{R}_{ABCD}$ denote the components of the curvature tensor $\bar{R}$ on $\bar{M}_p^{n+p}(c)$.

Restricting these forms to M we have;

$\omega^\alpha=0,\ \omega_i^\alpha=\sum_i h_{ij}^\alpha\omega^i,\ h_{ij}^\alpha=h_{ji}^\alpha,\ d\omega^i=-\sum\omega_j^i\wedge\omega^j,$

$\omega_j^i+\omega_i^j=0,$

$$d\omega_j^i=-\sum\omega_k^i\wedge\omega_j^k+\frac{1}{2}\sum_{kl}R_{ijkl}\omega^k\wedge\omega^l,$$

$$R_{ijkl}=\bar{R}_{ijkl}-\sum_\alpha\left(h_{ik}^\alpha h_{jl}^\alpha-h_{il}^\alpha h_{jk}^\alpha\right),$$

$$d\omega^\alpha=-\sum_\beta\omega_\beta^\alpha\wedge\omega_\beta,$$

$$d\omega_\beta^\alpha=-\sum_\gamma\omega_\gamma^\alpha\wedge\omega_\beta^\gamma+\frac{1}{2}R_{\alpha\beta ij}\omega^i\wedge\omega^j,$$

$$R_{\alpha\beta ij}=\sum_k\left(h_{ik}^\alpha h_{jl}^\beta-h_{il}^\alpha h_{jk}^\beta\right)\qquad(2.1)$$

From the condition on the dimensions of M and $\bar{M}_p^{n+p}(c)$ it follows that $e_{1^*},...,e_{n^*}$ is a frame for $T^\perp(M)$. Noticing this, we see that

$$R_{ijkl}=\frac{c}{4}\left(\delta_{ik}\delta_{jl}-\delta_{il}\delta_{jk}\right)-\sum_\alpha\left(h_{ik}^\alpha h_{jl}^\alpha-h_{il}^\alpha h_{jk}^\alpha\right)\qquad(2.2)$$

We call $H=\frac{1}{n}\sum_\alpha trh^\alpha$ the mean curvature of M and $S=\sum_{ij\alpha}\left(h_{ij}^\alpha\right)^2$ the square of the length of the second fundamental form. If H is identically zero then M is said to be maximal. M is totally geodesic if h=0.

From (2.2) we have the Ricci tensor R_{ij} given by

$$R_{ij}=\sum_k R_{ikjk}=\frac{(n-1)}{4}c\delta_{ij}+\sum_{\alpha k}h_{ik}^\alpha h_{kj}^\alpha\qquad(2.3)$$

Thus the Ricci curvature R is

$$R=R_{ii}=\frac{c}{4}(n-1)+S\qquad(2.4)$$

From (2.3) the scalar curvature is given by

$$\rho=\sum_j R_{jj}=\frac{n(n-1)}{4}c+S\qquad(2.5)$$

Let h_{ijk}^α denote the covariant derivative of h_{ij}^α. Then we define h_{ijk}^α by

$$\sum_k h_{ijk}^\alpha\omega^k=dh_{ij}^\alpha+\sum_k h_{kj}^\alpha\omega_i^k+\sum_k h_{ik}^\alpha\omega_j^k+\sum_\beta h_{ij}^\beta\omega_\alpha^\beta\qquad(2.6)$$

and $h_{ijk}^\alpha=h_{ikj}^\alpha$. Taking the exterior derivative of (2.6) we define the second covariant derivative of h_{ij}^α by

$$\sum_l h_{ijkl}^\alpha\omega^l=dh_{ijk}^\alpha+\sum_l h_{ljk}^\alpha\omega_i^l+\sum_l h_{ilk}^\alpha\omega_j^l+\sum_l h_{ijl}^\alpha\omega_k^l+\sum_\beta h_{ijk}^\beta\omega_\alpha^\beta\qquad(2.7)$$

Using (2.7) we obtain the Ricci formula

$$h_{ijkl}^\alpha-h_{ijlk}^\alpha=\sum_m h_{mj}^\alpha R_{mikl}+\sum_m h_{im}^\alpha R_{mjkl}+\sum_\beta h_{ij}^\beta R_{\beta\alpha kl}\qquad(2.8)$$

The Laplacian Δh_{ij}^α of the second fundamental form h_{ij}^α is defined as $\Delta h_{ij}^\alpha=\sum_k h_{ijkk}^\alpha$.

Therefore,

$$\Delta h_{ij}^\alpha=\frac{c}{4}(n-1)\sum h_{ij}^\alpha+\sum_{\beta mk}h_{mi}^\alpha h_{mk}^\beta h_{kj}^\beta+\sum_{\beta mk}h_{km}^\alpha h_{mk}^\beta h_{ij}^\beta\qquad(2.9)$$

$$+\sum_{\beta mk}h_{ki}^\beta h_{jm}^\alpha h_{mk}^\beta-2\sum_{\beta mk}h_{ki}^\beta h_{mk}^\alpha h_{mj}^\beta$$

From $\frac{1}{2}\Delta\sum_{\alpha ij}\left(h_{ij}^{\alpha}\right)^2=\sum_{\alpha ijk}\left(h_{ijk}^{\alpha}\right)^2+\sum_{\alpha ij}h_{ij}^{\alpha}\Delta h_{ij}^{\alpha}$ we obtain,

$$\frac{1}{2}\Delta\sum_{\alpha ij}\left(h_{ij}^{\alpha}\right)^2=\sum_{\alpha ijk}\left(h_{ijk}^{\alpha}\right)^2+\frac{c}{4}(n-1)\sum_{\alpha ij}\left(h_{ij}^{\alpha}\right)^2+\sum_{\alpha\beta ijkl}h_{ij}^{\alpha}h_{kl}^{\alpha}h_{lk}^{\beta}h_{ij}^{\beta} \tag{2.10}$$

$$+\sum_{\alpha\beta ijkl}\left(h_{li}^{\alpha}h_{lj}^{\beta}-h_{li}^{\beta}h_{lj}^{\alpha}\right)\left(h_{ki}^{\alpha}h_{kj}^{\beta}-h_{ki}^{\beta}h_{kj}^{\alpha}\right)$$

PROOF OF THE THEOREM

Let M be an n-dimensional compact totally real maximal spacelike submanifold isometrically immersed in $\bar{M}_p^{n+p}(c)$. For each α let H_α denote the symmetric matrix $\left(h_{ij}^{\alpha}\right)$ and let $S_{\alpha\beta}=\sum_{ij}h_{ij}^{\alpha}h_{ij}^{\beta}$. Then the (n+2p)×(n+2p)-matrix $\left(S_{\alpha\beta}\right)$ is symmetric and can be assumed to be diagonal for a suitable choice of $e_{n+1},\ldots,e_{n+p}$. Setting $S_\alpha=S_{\alpha\alpha}=trH_\alpha^2$ and $S=\sum_\alpha S_\alpha$, equation (2.10) can be rewritten as

$$\frac{1}{2}\Delta S=\sum_{\alpha ijk}\left(h_{ijk}^{\alpha}\right)^2+\frac{c}{4}(n-1)S+\sum_{\alpha}S_\alpha^2+\sum_{\alpha\beta}tr\left(H_\alpha H_\beta-H_\beta H_\alpha\right)^2 \tag{3.1}$$

$$=\sum_{\alpha ijk}\left(h_{ijk}^{\alpha}\right)^2+\frac{c}{4}(n-1)S+\sum_{\alpha}S_\alpha^2+\frac{1}{n+2p}S^2$$

$$+\frac{1}{n+2p}\sum_{\alpha>\beta}\left(S_\alpha-S_\beta\right)^2+\sum_{\alpha\beta}tr\left(H_\alpha H_\beta-H_\beta H_\alpha\right)^2$$

$$=\sum_{\alpha ijk}\left(h_{ijk}^{\alpha}\right)^2+\left(\frac{c}{4}(n-1)+\frac{1}{n+2p}S\right)S+\frac{1}{n+2p}\sum_{\alpha>\beta}\left(S_\alpha-S_\beta\right)^2$$

$$+\sum_{\alpha\beta}tr\left(H_\alpha H_\beta-H_\beta H_\alpha\right)^2$$

From (3.1) we see that $\int_M\frac{1}{2}\Delta S dv\geq\int_M\sum_{\alpha ijk}\left(h_{ijk}^{\alpha}\right)^2dv+\int_M\left(\frac{c}{4}(n-1)+\frac{1}{n+2p}S\right)Sdv$

where dv is the volume element of M.

By the well known theorem of Hopf (1950), $\Delta S=0$.

Therefore,

$$0\geq\int_M\sum_{\alpha ijk}\left(h_{ijk}^{\alpha}\right)^2dv+\int_M\left(\frac{c}{4}(n-1)+\frac{1}{n+2p}S\right)Sdv$$

which implies that

$$\int_M\left(\frac{c}{4}(n-1)+\frac{1}{n+2p}S\right)Sdv\leq 0 \tag{3.2}$$

Thus either S=0 implying M is totally geodesic or $S\leq\frac{(1-n)(n+2p)}{4}c$. This shows that M is totally geodesic for $c\geq 0, n>1$ or $0\leq S\leq\frac{(1-n)(n+2p)}{4}c$ for $c<0, n>1$. This proves our theorem.

CONCLUSION

In this paper we studied the geometry of an n-dimensional compact totally real maximal spacelike submanifold M immersed in an indefinite complex space form $\bar{M}_p^{n+p}(c)$ by computing the square of the length of the second fundamental form. In conclusion, we have shown that either the square of the length of second fundamental form S=0, implying M is totally geodesic for $c\geq 0, n>1$ or $S\leq\frac{(1-n)(n+2p)}{4}c$ for $c<0, n>1$. This generalizes the result by Sun (1994).

REFERENCES

Chen, BY. and Ogiue, K. 1974. On totally real submanifolds. Transactions of the American Mathematical Society. 193:257-266.

Hopf, E. 1950. A theorem on the accessibility of boundary parts of an open point set. Proceedings of the American Mathematical Society. 1:76-79.

Ishihara, T. 1988. Maximal spacelike submanifolds of a Pseudoriemannian space of constant curvature. Michigan Mathematical Journal. 35:345-352.

Sun, H. 1994. Totally real maximal spacelike submanifolds in indefinite complex space form. Journal of Northeastern University. 15:547-550.

Wali, AN. 2005. On bounds of holomorphic sectional curvature. East African Journal of Physical Sciences. 6(1):49-53.

Yano, K. and Kon, M. 1976. Totally real submanifolds of complex space forms II. Kodai Mathematical Seminar Reports. 27:385-399.

Received: Nov 13, 2009; Revised: Feb 15, 2010; May 14, 2010

SENRA Academic Publishers, Burnaby, British Columbia
Vol. 4, No. 2, pp. 1221-1225, June 2010
ISSN: 1715-9997

Canadian Journal of pure&applied sciences

EXPERIMENTAL STUDY ON THE REDUCTION OF PRESSURE DROP OF FLOWING WATER IN HORIZONTAL PIPES USING PADDY HUSK FIBERS

*Hayder A Abdul Bari, Mohd Azimie Ahmad and Rosli Bin Mohd Yunus
Faculty of Chemical and Natural Resources Engineering, University Malaysia Pahang
Lebuhraya Tun Razak-26300 Gambang, Kuantan, Pahang Darul Makmur, Malaysia

ABSTRACT

Abundant of waste from rice production in Malaysia have become the trigger for this investigation. Paddy husk are the waste from the rice production. Utilization of this waste in transportation of fluid can reduce the pressure drop in pipelines. Several studies have shown that addition of minute quantities of fiber additives can reduce the drag in pipe and maintain the pressure drop along the pipelines. Experimental works have been conducted in the laboratory in order to test paddy husk fibers in a closed loop of turbulence water flowing system. Flow tests were conducted using water as the transport liquid. The experimental work starts by pumping water from reservoir tank that had mixed with paddy husk fibers was pumped with six different flow rates in same pipe diameters a (0.025m ID). The types of pipe used are galvanized iron pipe. The testing length of this flow system is 1.0m. The pressure drop and drag reduction were measured in the flow varying concentrations of fiber (paddy husk). After adding the fibers to the water, the results have shown that the percentage drag reduction (Dr%) of 32% at the first flow rate setting and become depleted in term of the reading after travel at larger flow rate setting, but still there was drag reduction involve during transportation of the water.The results have shown that the fibers (paddy husk) have an effect on the pressure drop. In addition to this, we point out that the paddy husk fiber is available as drag reducing agent.

Keywords: Waste, paddy husk fiber, closed loop, galvanized iron pipe, reduce drag.

INTRODUCTION

The addition of minute amounts of additives such as surfactants, polymers or rigid particles can result in important drag reduction effects in many types of flows. Most of the existing literature dealing with drag reduction by additives has focused on wall-bounded flows such as pipe flows, due to their importance in many technological processes. For this class of flows, there was a special interest in the use of high molecular weight surfactants to reduce pressure drops and friction effects, and there are a large number of experimental and numerical studies that document the effects of surfactant additives on such flows (Pinho and Whitelaw, 1990; Tiederman, 1990). On the other hand, the use of fibre additives as drag-reducing agents remains limited. There are, however, few experimental studies that show the great potential of these additives, and drag reduction effects of up to 60% in pipe flows have been reported by Arranaga (1970) and other authors. Depending on the flow geometry, the particle size and the importance of viscous effects versus inertial effects, the addition of fibres to a flow can have either a stabilizing (Vaseleski and Metzner, 1974) or a destabilizing effect (Pilipenko *et al*., 1981). In general, where particle additives tend to stabilize the flow, it has been observed that the stabilizing effect increases with the particle aspect-ratio and concentration (Vaseleski and Metzner, 1974).

There are much less studies devoted to the effects of fibre additives on the mechanisms of instability and transition to turbulence in free shear flows. The flow visualizations reported by Filipsson *et al*. (1977) represent one of the few available experiments on this subject. In this study, the authors presented results for a jet flow of viscoelastic (Polyox WSR-301), fibre suspension (chrysotile fibres), and Newtonian (water) fluids at high Reynolds numbers.

The addition of a small amount of either surfactant or fibres led to similar trends towards an enhancement of the large-scale turbulent structures and a modulation of the turbulence by the suppression of small-scale structures. In spite of the well-documented experimental and theoretical evidence for drag reduction by surfactant and solid particle additives, the physical mechanisms responsible for these phenomena are still not well understood and are subject to debate.

Later, the usage of the suspended solid (insoluble in liquid media) as Drag Reducer opened the wide door for more research to examine the availability of the solubility condition in the drag reduction phenomena (Hideo *et al*., 2000; Toorman, 2002; Mawla and Naderi, 2006).

*Corresponding author email: mohdazimie@gmail.com

The aim of this study is to formulate and to test the efficiency of paddy husk fiber as drag reducer agent on transport of water in pipes; different sizes of fiber (500 µm and 800µm) were used. Six different concentrations were used in the purpose to investigate the concentration effect. The efficiency of fiber was tested using clear water.

MATERIALS AND METHOD

Liquid Circulation System

Figure 1 shows a schematic diagram of a build up liquid circulation system used in the present investigation. Generally, this system consists of reservoir tank, pipes, valves, pumps, flow meter and pressure gauge. The reservoir tank was supported with two exit pipes connected to centrifugal pumps. The first exit pipe with was connected to the main centrifugal pump which delivers the fluid to the testing sections. The other exit is connected to the other centrifugal pump for deliver excess solvent to reservoir tank.

Three galvanized iron pipes of various inside diameters 0.015 (C), 0.025 (B) and 0.038 (A) m ID were used in constructing the flow system. A complete closed loop piping system was build. Piping starts from the reservoir tank through the pump, reaching a connection that splits the pipe into two sections. The first section returns to the reservoir tank, build up as bypass and the other splits into three sections with different pipe diameters at testing section. The testing sections were 1.0m long, 0.025m ID and it was located about 50 times of pipe diameter to ensure the turbulent flows are fully developed before the testing point. Two sets of Baumer Differential Pressure Gauge were used to detect the pressure drop in pipelines with maximum differential pressure reading up to 0.10 and 0.20 bars for both. In order to measure the flow rate of fluid in pipelines, Ultraflux Portable Flow Meter Minisonic P has been used. This ultrasonic flow meter measurement was sensitive with small changes in flow rate as low as 0.001 ms^{-1} can be detected.

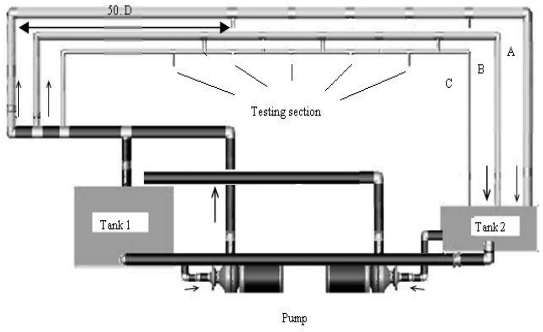

Fig. 1. Schematic of the flow system.

Materials Investigated

Paddy Husk Fibers

Paddy husk is obtained from Bernas Sdn. Bhd. at Jitra, Kedah. The paddy husk was dried by the oven overnight at temperature of 100°C. Once dry, the fibers is graded into fibers by using grinder then sample was sieve using a screen into two sizes which are 500 and 800µm. Physical properties of the paddy husk were determined by using pycnometer. The results are as shown in table 1.

Table 1. Physical properties of paddy husk fibers.

Paddy husk size (µm)	Fibers Density (gcm^{-3})
500	2.0811
800	1.2538

Transported Liquid

The transported liquid used in the present investigation was water. The physical properties of water are shown in table 2.

Table 2. Physical properties of water.

Water properties @ 25°C	
Viscosity ($\mu_{water\ @\ 25°C}$)	0.8973 x 10^{-3} Pa.s
Density ($\rho_{water\ @\ 25°C}$)	997.08 kg/m^3

Experimental Procedure

All the experiments were carried in a constructed liquid circulation system, testing different variables, which are:

- Paddy husk fibers concentration (100, 300 and 500ppm)
- Paddy husk sizes (500µm and 800µm)
- Pipe diameter (0.025m)
- Solution flow rates (2.5, 3.0, 3.5, 4.0, 4.5 and 5.0 m^3/hr)

The experimental procedure starts by testing every additive concentration and pipe diameter, the operation begins when the pump starts delivering the solution through the testing section. The solution flow rate is fixed at the certain value by controlling it from the bypass section. Pressure readings are taken to this flow rate. By changing the solution flow rate to another fixed point, pressure readings are taken again until finishing the six desired values of flow rates. This procedure is repeated for each fibers concentrations and sizes to test its effect on the drag reduction operation.

Experimental Calculation

(a) Velocity and Reynolds number calculations

The average velocity (V) and Reynolds number (Re) were calculated using the solution volumetric flow rate

readings (Q), density (ρ), viscosity (μ) and pipe diameter (D), for each run as follows:

$$Re = \frac{\rho.V.D}{\mu} \quad \textbf{(1)}$$

(b) Percentage Drag Reduction calculations
Pressure drop readings through testing sections before and after drag reducer addition, were needed to calculate the percentage drag reduction %Dr as follows (Virk, 1975)

$$\%Dr = \frac{\Delta P_b - \Delta P_a}{\Delta P_b} \quad \textbf{(2)}$$

RESULTS AND DISCUSSIONS

Effect of Fluid Velocity (Re)

Figures 2 and 3 shows the behaviour of the transported water velocity on the percentage drag reduction (Dr%). The velocity (V) was represented by the Reynolds number (Re). Figures 2 and 3 shows the effect of (Re) on Dr% for water transported with paddy husk fibers (500 and 800 μm) with different addition concentrations.

From figure 2, it can be noticed that the Dr% reaching maximum value 32% power saving with 500ppm addition concentration of 500μm in Re number ranges (35363 to 70726) in the 0.025m ID pipe. Further increase of Re resulted decreasing in the Dr% compared with maximum value.

Meanwhile, in figure 3, it was shown that the Dr% reaching maximum value of 25% power saving with 100ppm addition concentration of 800μm fibers size before decreasing slowly after Re are above 40000.

These phenomenons may be caused by the particle momentum generated from paddy husk fibers drive the eddy to flow straight along the pipe because the momentum of the particle is larger from the energy to form turbulence eddies.

Effect of Solid Particles Concentration

The results of analysis of paddy husks drag reduction performances as a function of fibers concentration and Re which is from 100 to 500ppm in the range of 35363 to 70726 are shown in figure 4. Note that the profile pattern of each concentration is similar but varies in its value. As shown in figure 4, the maximum drag reduction values of 32 % in 500ppm of concentration occur when the Re at

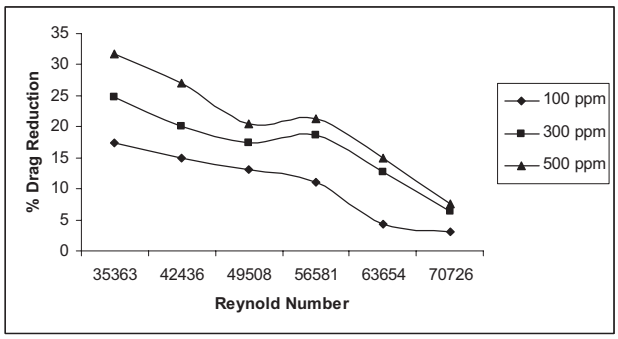

Fig. 2. Effect of Re on Dr% for transported water with Paddy husk fibers (500μm) with different addition concentrations.

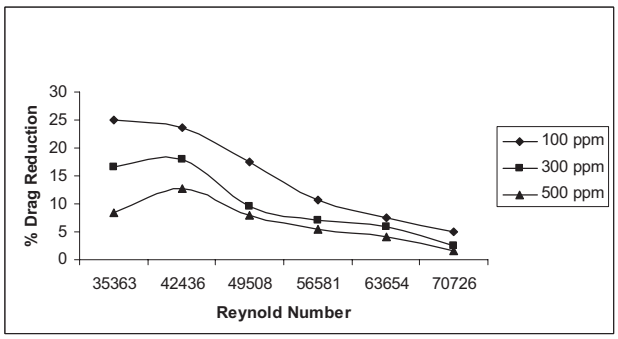

Fig. 3. Effect of Re on Dr% for transported water with Paddy husk fibers (800μm) with different addition concentrations.

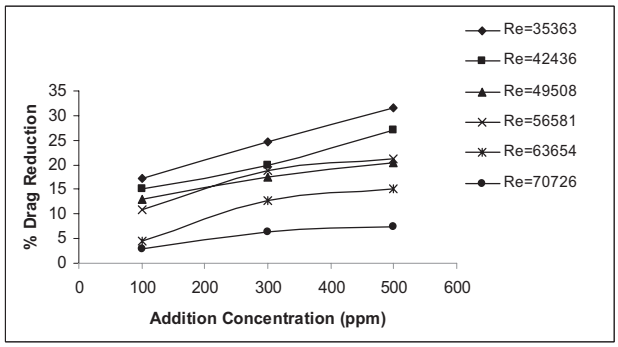

Fig. 4. Effect of fibers concentration on Dr% for transported water with Paddy husk fibers (500μm) with different flowrates (Re).

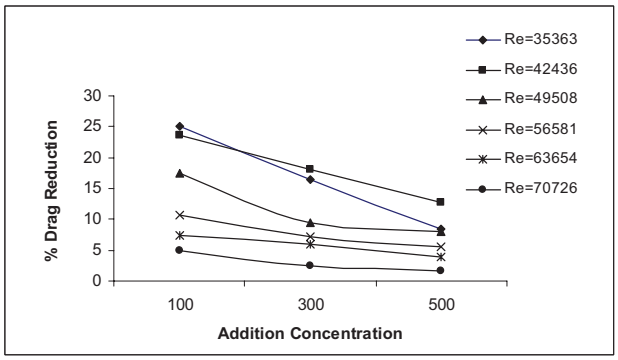

Fig. 5. Effect of fibers concentration on Dr% for transported water with Paddy husk fibers (800μm) with different flowrates (Re).

35363. In general based on the experiments conducted, all concentration showed a drastic reduction of drag reduction at 35363 to 70726 of Re which the drag reduction values ranged between 3 and 27%. These results showed that the optimum performance of the fibers additive investigated is limited to the degree of turbulence, that by increasing the flow the degree off turbulence will increase also which will provide more suitable environment for the drag reducer to perform. Further increase in the flow will cause the reduction in the additive efficiency due to the decrease of the additive concentration to degree of turbulence ration. In another words, the reduction of drag as obtained in this experiment shows that the paddy husk capable to act as drag reducing agent at 500µm size of fibers.

Figure 5 shows the performance of drag reduction as a function of fibers concentration and Re which is from 100 to 500ppm in the range of 35363 to 70726. The profile pattern of each concentration is similar but different in values. As shown, the highest drag reduction occurs at 100 ppm concentration of 800µm fibers size with 25%. Further increase of fibers concentration shows decrease in drag reduction but still reduction of flow still occur. The lowest drag reduction was obtained in 500ppm of paddy husk fibers that is 2%. These phenomena probably can be defined as the result of the diameter effect towards the flexibility of the fibers to acts as drag reducer. By increasing the diameter of the fibers lead to the decrease of flexibility. In order fibers to act as drag reducer agent, basic criteria such as flexibility and surface roughness should be fulfilled (Singh, 1990). Singh proven that drag reduction of fibers with small diameter is higher than drag reduction cause by the fibers with larger diameter because fibers with small diameter can improved the flexibility of fibers in flow system. These results are consistent with the findings in a few literatures, in which the drag reduction increase as addition concentration is increases.

Effect of Particle Size

There were two sizes of paddy husk fibers that were used to investigate drag reduction in this present research (500 and 800µm). Figure 6 shows a selected sample of fibers size effect data. These results clearly shows that the DR% of the paddy husk with the size 500 µm is larger than the paddy husk with the size of 800µm.

This may be due to the small momentum needed in order to transport smaller particles that make these particles easily been drag by the turbulent flow in pipe. Small diameter of fiber material increases the flexibility. Flexibility is the important for fibers to act as drag reducer. From this condition, there was a decreasing effect in the spectrum of turbulence causing the drag reduction higher at this smaller particles size.

Normally, during fibers are travelled in pipe, the fibers was torn into pieces due to an eddy during turbulence flow. In this case, smaller size of fibers has become great impact to make larger eddies to break up to smaller eddies which as the result, an increment of the Dr%.

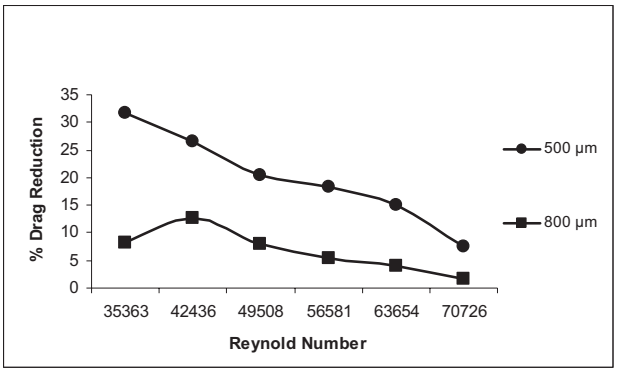

Fig. 6. Effect of changing the particle diameter (500 to 800µm) on the Dr% for transported water with paddy husk fibers with different Re at 500ppm.

CONCLUSIONS

Paddy husk fibers were found to behave as good drag reducing agent at 500µm of sizes and 500ppm of concentrations. Drag reduction for fibers materials was found to increase by smaller fibers size used as drag reducer.

ACKNOWLEDGMENTS

I wish to express my deepest gratitude to my supervisor Dr. Hayder A. Abdul Bari and co-supervisor Prof. Dr. Rosli Bin Mohd Yunus for their guidance, advice, criticism, encouragements and insight throughout the research.

REFERENCES

Arranaga, AB. 1970. Friction reduction characteristics of fibrous and colloidal substances. Nature. 225:447-449.

Filipsson, LGR., Torgny, JH., Lagerstedt. and Bark, FH. 1977. A note on the analogous behaviour of turbulent jets of dilute surfactant solutions and fibre suspensions, J. non-Newtonian Fluid Mech. 3:97-103.

Hideo, I., Naoto, H. and Akihiko, H. 2000. Flow drag and heat transfer reduction of flowing water containing fibrous material in straight pipe. Int. J. Thermal Sci. 39:18-29.

Mowla, D. and Naderi, A. 2006. Experimental study of drag reduction by a polymeric additive in slug two-phase

flow of crude oil and air in horizontal pipes. Chem. Eng. Sci. 61:1549-1554.

Pinho, FT. and Whitelaw, JH. 1990. Flow of non-Newtonian fluids in a pipe, J. non-Newtonian Fluid Mech. 34:129-144.

Pilipenko, VN., Kalinichenko, NM. and Lemak, AS. 1981. Stability of the flow of a fibre suspension in the gap between coaxial cylinders, Sov. Phys. Dokl. 26:646-648.

Singh, RD. 1990. Encyclopedia of Fluid Dynamics, Gulf Publishing Co., Houston, Texas, Chapt. 9. 14:425-480.

Tiederman, WG. 1990. The Effect of Dilute Surfactant Solution on Viscous Drag and Turbulent Structure. In: A. Gyr (Ed.), Structure of Turbulence and Drag Reduction, IUTAM Symp. Springer, Berlin. 187-200.

Toorman, EA. 2002, Modelling of turbulent flow with suspended cohesive sediment. Proc. Mar. Sci. 5:155-169.

Vaseleski, RC. and Metzner, AB. 1974. Drag reduction in the turbulent flow of fibre suspensions, AICHE J. 20: 301-306.

Vaseleski, RC. and Metzner, AB. 1974. Drag reduction in the turbulent flow of fibre suspensions. AICHE J. 20:301–306.

Received: Dec 29, 2009; Accepted: April 20, 2010.

SENRA Academic Publishers, Burnaby, British Columbia
Vol. 4, No. 2, pp. 1227-1231, June 2010
ISSN: 1715-9997

Canadian Journal of pure&applied sciences

EFFECTIVENESS OF ACCESSIBILITY AND USABILITY OF GOVERNMENT WEBSITES IN SAUDI ARABIA

Muhammad Asif Khan and Khalid Abdulmohsen Buragga
Computer Sciences and Information Technology, King Faisal University, Al Ahsa, Saudi Arabia

ABSTRACT

In today's rapidly changing world, information technology has significant impact in almost all sectors of daily life. With greater internet penetration among individuals and organizations use of online services is becoming indispensable. The increasing demand of electronic services has forced governments all around the world to provide online services to their citizens and residents. The government of Saudi Arabia has also realized the need of such services and it is working on an accelerating pace to provide excellent electronic services infrastructure to its citizens. Internet is an exciting technological tool that requires innovative design in order to be accessible to everyone. The purpose of this paper is to examine and evaluate accessibility and usability of e-government websites of Saudi Arabia. A subjective assessments method has been used to carryout the study. The results of the study have been compared with web accessibility tools. This study investigates the issues that are required to make a website accessible and examines accessibility guidelines. It also evaluates the Saudi government websites in context of W3C Web Content Accessibility Guidelines. The present study also presents some suggestions for improving e-government web sites to be more effective and beneficial to general public.

Keywords: E-government, usability, Saudi e-government, accessibility, Saudi Arabia.

INTRODUCTION

Information and Communication Technology (ICT) has revolutionized the way individuals and organizations used to work. Now internet has become an essential tool that is used for information dissemination. People around the world use Internet mainly for email, product or organization information and health information (Goodman et al., 2003). With greater Internet penetration in society organizations started offering their services online so that customers access them whenever and wherever they want. People would like to use Internet as a transaction tool and now more people are using electronic transactions in different areas of their daily life (e.g. banking, shopping) due to less effort and quick service. Governments also have realized the significance of Internet and seem to be undergoing transformation to use Internet to deliver services and information according to these time and effort expectations (Abdulkarim, 2003). More than 160 countries worldwide have started e-government project, creating a major market for IT vendors and service providers that facilitate public organizations in adoption of technology (Qureshi, 2005).

E-government has been defined by some researchers in terms of specific actions (e.g. obtaining documents, accessing information, creating a sharing database) or simply as the automation of services. E-government concepts introduced in public administration in late 1990s (Moon, 2002). There are issues involve in e-government such as security and privacy, diverse educational background of users, accessibility issues, prioritization of e-government over basic functions of government, building citizen confidence in e-government whether certain forms of government do better with e-government than others (Jagear, 2003). E-government has been thought as a best tool for serving citizens in a country and almost all countries have been trying to design and implement e-government. The government of Saudi Arabia has realized the effects of information technology in the economy and therefore special attention has been given to information technology that has brought a huge change in the last forty years.

Governments around the world especially in Gulf region are providing funds to the e-government projects in order to meet their society's increasing cyber skills. In every part of world from industrialized countries to developing ones governments is putting information online to provide better services for citizens (Chircu *et al*., 2005). Currently Saudi ARAMCO, Saudi Arabia Basic Industries (SABIC), Saudi Telecommunication (STC), Saudi Arabian Airlines and banks are using stat-of-the-art technologies in their applications. The government of Saudi Arabia has also realized the significance of e-government and to achieve the aim of e-government a program called YESSER has been initiated that is a user-centric and it focuses on governments services to be provided to individuals and businesses. The user-centric vision for Saudi Arabia's e-government initiative is

*Corresponding author email: asifkhan@kfu.edu.sa

summarized as 'By the end of 2010, everyone in the Kingdom will be able to enjoy- from anywhere and at anytime – world class government services offered in a seamless, user friendly and secure way by utilizing a variety of electronic means (www.yesser.gov.sa/english).

As the Internet is fast becoming a major source of information and services, a well designed e-government website has become an essential so that citizens can access public information and improve their participation. Government websites can serve as a tool for both communication and public relations for the general public. Information and data can easily be shared with and transferred to external stakeholders (Moon, 2002).

The Web Accessibility Initiative (WAI) was established by World Web Consortium (W3C) in 1997. The W3C publishes Web Content Accessibility Guidelines (WCAG), which provide a series of checkpoints for web content development. These checkpoints are broken down into three priorities depending on their impact on accessibilities. Table 1 shows each priority with its description

Table 1. Web Content Accessibility Guidelines (WCAG) Priorities

Priority	Description
Priority 1	A web content developer must satisfy this checkpoint. Satisfying this checkpoint is a basic requirement for some groups to be able to use web documents
Priority 2	A web content developer should satisfy this checkpoint. Satisfying this checkpoint will remove significant barriers to accessing web documents
Priority 3	A web content developer may address this checkpoint. Satisfying this checkpoint will improve access to web documents

The W3C has been promoting web accessibility and according to it a web accessibility in general term is defined as "people with disabilities can use the Web… more specifically [they] can perceive, understand, navigate and interact with the Web" (Henry, 2006). Accessibility is considered as a subset of usability where problems related to usability may affect to all users equally apart from ability or disability (Thatcher *et al*., 2003). Accessibility can be dealt with as a part of usability evaluations process. Usability is defined by the International Standards Organizations (ISO) as 'the effectiveness, efficiency and satisfaction with which specified users achieve specified goals in particular environment' (ISO, 2000; ISO, 1998). There is a possibility that some accessibility problems may affect non-disabled users. However, all usability problems are within the scope of accessibility meaning that people with disabilities encounter all the same problems that people without disabilities encounter. The ISO has defined accessibility as 'the usability of a product, service, environment or facility by people with the widest range of capabilities' (ISO, 2003).

Methodology

There are various methods to evaluate web accessibility that include standards review, user testing, subjective assessments and barrier walkthrough. These methods differ in terms of their usefulness, efficiency and effectiveness (Branjik, 2006). Standards review also called expert or conformance review is an analytic method based on evaluator's opinions. This method depends on chosen checklist that range from standards issued by international bodies such as W3C, IBM or SUN. This method is costly and requires experienced evaluators. Several studies of usability evaluation methods have shown that user testing methods may fail in yielding consistent results when performed by different evaluators (Hertzum *et al*., 2001).

Subjective assessments method has various benefits that include low cost and its ability to be performed remotely. This method does not require experienced evaluators and any specific criteria of pages being tested. In the present study we have assessed the usability of the government web sites that include effectiveness and efficiency and satisfaction thoroughly by users without any disability even such as color vision.

In the present study subjective assessments method has provided an opportunity to gain experience of general evaluators who had no experience of website evaluation.

We selected two websites for evaluation purpose i.e. Saudi Railways (www.saudirailways.org) and Saudi Post (www.sp.com.sa). The reason for selecting both of these websites was an increasing accessibility and usefulness among citizens (www.arabnews.com). Another reason for selecting the two websites was being in complete dual versions (i.e Arabic and English) which we could not find in other websites at the time of decision. It was confirmed by the participants that they never had visited the websites before this study. Participants were given common tasks for evaluation purpose in different places. All participants were asked to rate the severity of problems on four point scale based on Nielsen's heuristic evaluation method i.e. Cosmetic, Minor, Major or Catastrophic problem (Nielsen, 1994).

We asked 250 evaluators and provided them with 12 features to be evaluated manually in the websites that include logo of the company, office phone, address, email, contents, foreign language version, other link,

online payment option, links to other government sites, search option, subject index and audio/video clips. We received positive and complete response from 173 participants. Among the participants were 102 males and 71 females with a median age of 32 and varied education background from high school to research institutions/universities. Table 2 shows participants' computer literacy, use of internet, website knowledge and time consumption on computer.

Table 2. Participants Computer and Internet Skills.

Skill	Median	
	Male (1-5)	Female (1-5)
Computer Literate	5	4
Internet User	5	5
Website Knowledge	5	3
Internet Usage	3	2

Computer Literate - 1 = never; 2 = somehow; 3 = average; 4 = often; 5 = very often
Internet User - 1 = never; 2 = somehow; 3 = average; 4 = often; 5 = very often
Web Site knowledge - 1 = never; 2 = somehow; 3 = average; 4 = good; 5 = very good
Hours per day on internet - 1 = up-to 1; 2 = 2 to 4; 3 = 5 to 7; 4 = 8 to 10; 5 = more than 10

The results obtained by the evaluators were analyzed carefully and then it was decided to use well known tools available online to compare the outcomes of this manual evaluation with the available tools. We used EvalAccess 2.0 and CynthiaSays tools for evaluation of the websites. We also used W3C MarkUp Validator, Link Checker and CSS Validator tools to compare the conformance of web pages with the guidelines provided by W3C. EvalAccess evaluates web pages based on WAI and WCAG. The implemented web service for accessibility evaluation can process a web page from its URL or its HTML mark-up. The result of the evaluation process is formatted in XML following a predefined XML schema. CynthiaSays is a web content accessibility validation tool that has been designed based on WCAG guidelines. The MarkUp Validator is also known as HTML Validator that assists in checking web documents in formats like HTML, XHTML, SVG and MathML. The Link Checker checks the anchors (hyperlinks) in HTML/XHTML documents while CSS Validator tool validates CSS stylesheets or documents using CSS Validator.

RESULTS AND DISCUSSION

All participants were provided with the clear instructions about the 12 features to be evaluated and they were told to use their internet browsing experience and aesthetic features during the evaluation of the websites. There was a significant difference of evaluation of the websites between male and female participants. We found the participants rated the severity of problems differently, for example, 81% male participants considered a page 'not found' as a catastrophic problem while 53% female participants rated the same page 'not found' as a general problem. Likewise, 77% female participants have given more consideration to the aesthetic features of the website over the contents while 42% male participants focused more on contents than aesthetic features. Since the website has English language version as well, therefore, participants evaluated both the versions. Table 3A shows the summary of the results of Saudi railways website.

Table 3. Web page and Problems Statistics in Saudi Railway Website.

Version	Mean	Male	Female	Standard Deviation
English	Number of pages visited	50.0	48.0	1.414214
	Number of pages with problems	7.0	6.0	0.707107
	Number of pages with severity	1.25	0.86	0.275772
Arabic	Number of pages visited	50.0	48.0	1.414214
	Number of pages with problems	3.0	2.0	0.707107
	Number of pages with severity	0.5	0.15	0.247487

For the Saudi Post website all the participants evaluated the above stated features and their findings are summarized in the table 3B:

Table 3b. Web Pages and Problems Statistics In Saudi Post Website.

Version	Mean	Male	Female	Standard Deviation
English	Number of pages visited	70.0	67.0	2.12132
	Number of pages with problems	3.0	4.0	0.707107
	Number of pages with severity	0.73	0.82	0.06364
Arabic	Number of pages visited	68.0	65.0	2.12132
	Number of pages with problems	0.65	0.34	0.219203
	Number of pages with severity	0.17	0.04	0.091924

Evaluation by EvalAccess 2.0 and CynthiaSays Tools
Following analyzing results of the manual evaluation of both websites, we used online tools for accessibility evaluation. Following table IVA shows the results for Saudi Railways website obtained by using EvalAccess 2.0 that evaluates automatically the accessibility of web pages using the WCAG 1.0 from the W3C:

Table 4a. Web Pages Accessibility Results for Saudi Railways Website.

	Priority 1	**Priority 2**	**Priority 3**
Errors	2	47	23
Warnings	110	178	208
General Warnings	5	7	9

It is evident from the table 4A above that the website has two errors of priority 1 that must satisfy the basic requirement for some groups to be able to use web documents. Likewise, Priority 2 shows that there are some significant barriers that should be removed to access the web pages. Priority 3 shows that there are some areas which require attention for improving the website. Following table 4B shows the results for Saudi Post website using the same EvalAccess 2.0 tool

Table 4b. Web Pages Accessibility Results for Saudi Post Website.

	Priority 1	**Priority 2**	**Priority 3**
Errors	6	5	2
Warnings	27	13	4
General Warnings	5	7	9

The table 4B above shows there are six errors of Priority 1 that must satisfy the basic requirements for some groups to be able to use web document. However, there are less significant barriers and areas of improvement in the website as depicted by Priority 2 and Priority 3.

We also used CynthiaSays tool to evaluate both the websites and found that the Saudi Railways website could not pass the Priority 1, Priority 2 and Priority 3 checkpoints. The same tool passed the Saudi Post website the Priority 1, Priority 2 with 2 warnings and Priority 3 with 1 warning.

Evaluation by MarkUp Validator, Link Checker and CSS Validator
We used different online tools to evaluate the web accessibility of the websites and following Table 4C shows the results:

Table 4c. Web Accessibility Evaluation by Different Tools.

Website	**MarkUp Validator**	**Link Checker**	**CSS Validator**
Saudi Railways	73 Errors, 1 Warning, Doctype: XHTML 1.0 Transitional	Invalid 13 links, valid 4 anchors	File not found
Saudi Post	6 Errors, 5 Warnings, Doctype: HTML 4.01 Transitional	Valid links, Valid anchors	No error found Validates as CSS Level 2.1

The above table 4C depicts that Saudi Railways web pages have significant number of errors in XHTML pages that were evaluated by MarkUp Validator. Also, there are various invalid links found by Link Checker. The CSS Validator tool could not find any CSS file on this website. However, it is evident that Saudi Post website has less number of error pages, all valid links and CSS level 2.1 files evaluated by the above stated tools.

CONCLUSION

The present study has investigated the accessibility and usability of the two government websites. We have evaluated the websites manually and the results obtained were compared with the results obtained by using different tools. We found that the manual results are more or less same as of the results we obtained by using different tools. In the research it has been found that Saudi Railways (SR) website has more severity problems than Saudi Post (SP) website. We found that authorities of the websites are not well equipped to provide services electronically that are required to the Saudi citizens and residents. The authorities of the websites should ensure basic compliance with legal HTML, XHTML and CSS standards. This would entail regular validating and correcting code, but would mean that files could then be compatible with different browsers and platforms. To make the websites usable to all users the competent authorities need to take measures immediately in order to provide appropriate services electronically that are in compliance with W3C guidelines. Although disabled users have not participated in the present study but as Thatcher *et al.* (2003) have proposed that usability problems affect all users regardless of ability or disability.

This study also suggests that government should improve their websites in terms of providing necessary information in both English and Arabic versions equally so that all residents in the country are served effectively and efficiently. The evaluation of the two more familiar

websites indicates the plight of government websites that need to be developed according to W3C standards.

REFERENCES

Abdulkarim, MR. 2003. Technology and Improved Service Delivery: Learning Points from the Malaysian Experience, International Review of Administrative Sciences. 69:191-204.

Brajnik, G. 2006. Web Accessibility Testing: When the Method is the Culprit. 1ICCHP 2006, 10th International Conference on Computers Helping People with Special Needs. Lecture Notes in Computer Science. Linz, Austria. 4061.

Chircu, M. and Lee, Hae-Dong. 2005. E-government: Key Success Factors for Value Discovery and Realization. Electronic Government. 2(1):11-24.

Goodman, J., Syme, A. and Eisma, R. 2003. Older adults' use of Computers: A survey. Proceedings of HCI Bath, UK.

Henry, SL. 2006. Introduction to Web Accessibility. www.w3.org/WAI/intro/accessibility.php.

Hertzum, M. and N. Jacobsen. 2001. The Evaluator Effect: A Chilling Fact about Usability Evaluation Methods. Int. Journal of Human-Computer Interaction. 1(4):421-443.

Jagear, P. 2003. The Endless Wire: E-government as a Global Phenomenon. Government Information Quarterly. 20:323-331.

Moon, J. 2002. The Evolution of E-government among muncipilaties: Rhetoric or Reality? Public Admin Rev. 62, No 4.

Nielsen, J. 1994. Heuristic evaluation. In: Usability inspection methods. Eds. Nielsen, J. and Mack, RL. John Wiley and Sons, New York.

Qureshi, S. 2005. E-Government and IT Policy: Choices for Government Outreach and Policy Making: In Information Technology for Development. Wiley Periodicals. 11(2): 101-103.

Thatcher, J., Waddell, CD., Henry, SL., Swierenga, S., Urban, MD., Burks, M., Regan, B. and Bohman, P. 2009. Constructing accessible web sites. Glasshaus, San Francisco. www.yesser.gov.sa/english.

International Standard Organization. 1992-2000. Standard 9241: Ergonomic requirements for office work with visual display terminals.www.iso.org

International Standards Organization. 1998. ISO 9241-11:guidance on usability.

International Standards Organization. 2003. ISO/TS 16071:ergonomics of human-system interaction – guidance on accessibility for human-computer interfaces.

Received: Feb 22, 2010; Revised: May 21, 2010; Accepted: May 29, 2010